MEMBRANE TRAFFICKING IN NEURONS REGULATED BY NEW SYNTAXIN 13-INTERACTING PROTEINS

THÈSE N° 3091 (2004)

PRÉSENTÉE À LA FACULTÉ SCIENCES DE LA VIE

Institut des neurosciences

SECTION DES SCIENCES DU VIVANT

ÉCOLE POLYTECHNIQUE FÉDÉRALE DE LAUSANNE

POUR L'OBTENTION DU GRADE DE DOCTEUR ÈS SCIENCES

PAR

Pascal STEINER

biologiste diplômé de l'Université de Lausanne
de nationalité suisse et originaire de Belmont-sur-Lausanne

acceptée sur proposition du jury:

Prof. S. Catsicas, Dr H. Hirling directeurs de thèse
Prof. R. Luthi-Carter, rapporteur
Dr A. Malgaroli, rapporteur
Prof. R. Regazzi, rapporteur

Lausanne, EPFL
2004

La vérité ne brille, ni n'étincelle.

C. Palahniuk

CONTENTS

SUMMARY

Recently, it has been shown that correct trafficking of neuronal plasma membrane receptors along the endosomal pathway is directly implicated in molecular mechanisms underlying synaptic plasticity and is fundamental for proper neuronal communication. To understand the molecular mechanisms that regulate neuronal trafficking through endosomes, we used syntaxin 13, an endosomal protein that we had previously characterized, as a bait to immunopurify protein complexes. Among the 5 new syntaxin 13-interacting proteins that we identified, my thesis work has focused on the characterization of 2 of them, Neuron-Enriched Endosomal Protein of 21 kDa (NEEP21) and Reticulon1-C (RTN1-C).

NEEP21. Our work revealed that NEEP21 is expressed by neurons in their somatodendritic compartments, where it is mainly found in Rab4-positive subdomains of early endosomes. This domain has been implicated in the sorting of internalized surface receptors. We demonstrated that NEEP21 suppression strongly retards recycling of receptors including AMPA-type glutamate receptors. We recently identified a molecular link between NEEP21 and AMPA-receptor trafficking. NEEP21 is present in a complex with GRIP, a scaffold protein for GluR2, and GluR2, a subunit of AMPA receptors. Overexpression of the NEEP21 binding site for GRIP causes a retraction of dendrites, an effect partially compensated by GluR2 overexpression. In addition, expression of this fragment inhibits AMPA receptor recycling. Based on the recent findings of the importance of AMPA receptor trafficking between endosomes and the cell membrane during synaptic structural and functional plasticity, we postulate that NEEP21 modulates synaptic strength.

RTN1-C. The second identified syntaxin 13-associated protein is RTN1-C. Reticulons constitute a family of membrane proteins localized primarily to the endoplasmic reticulum (ER). So far the cellular function of reticulons is little undertsood. We found that RTN1-C interacts with several SNARE proteins. In addition, we showed that overexpression of the RTN1-C binding site for syntaxin 1 significantly enhanced regulated secretion. Based on these findings, we hypothesized that RTN1-C could be a key actor in the regulation of SNARE-dependent membrane fusion processes.

Together, our studies contribute to the elucidation of the roles of NEEP21 and RTN1-C in neurons and the molecular mechanisms of membrane protein trafficking that are at fundamental for synaptic plasticity.

RESUME

Il a récemment été démontré que le trafic des récepteurs des neurones à travers la voie endosomale, était un des événement s« clés » de l'expression de la plasticité synaptique et de la transmission de l'information entre neurones. Afin d'élucider les mécanismes moléculaires du traffic endosomal des neurones, nous avons immunopurifié les complexes protéiques contenant syntaxin 13, une protéine des endosomes fortement exprimée dans le cerveau que nous avons récemment caractérisée. Parmi les 5 nouveaux partenaires de synatxin 13 que nous avons isolé d'extrait de cerveau correspondant au stade de maturation des synapses, mon travail de thèse s'est focalisé sur 2 d'entre eux, NEEP21 (Neuron-Enriched Endosomal Protein of 21 kDa) et RTN1-C (Reticulon1-C).

NEEP21. Notre travail a montré que la protéine NEEP21 est exprimé dans le compartiment somatodendritic des neurones, où elle est majoritairment localisée dans un sous-domaine des endosomes précoces contenant Rab4. Ce domaine est impliqué dans l'adressage de la destination future des lipides et protéines membranaires. De plus, NEEP21 est essentiel pour le recyclage des récepteurs de surface internalisés. Nous avons démontré que la suppression de l'expression de NEEP21 retarde fortement le recyclage des récepteurs et notamment une classe de récepteurs au glutamate, les récepteurs AMPA. Nous avons récemment identifié un lien moléculaire entre NEEP21 et le trafic des récepteurs AMPA. NEEP21 est présent dans un complexe contenant la protéine GRIP, qui intéragit avec GluR2, et GluR2 elle-même qui est une des 4 sous-unités des récepteurs AMPA. L'expression du site d'interaction de NEEP21 pour GRIP cause la retraction des dendrites, un effet partiellement compensé par la surexpression de GluR2. La surexpression de ce fragment provoque aussi l'inhibition du recyclage des récepteurs AMPA. Sur la base de la récente découverte de l'importance du trafic des récepteurs AMPA entre la voie endosomale et la membrane cellulaire durant la plasticité synaptique fonctionnelle et structurale, nous postulons que NEEP21 est un modulateur de l'activité synaptique.

RTN1-C. Le second partenaire de syntaxin 13 identifié est la protéine RTN1-C. Les réticulons constituent une famille de protéines membranaires localisées majoritairement sur le réticulum endoplasmique (RE). Cependant, la fonction des réticulons reste jusqu'à présent extrêmement mal comprise. Nous avons découvert que RTN1-C intéragit avec plusieurs protéines SNARE. De plus, nous avons montré que la surexpression du site d'intéraction de RTN1-C pour syntaxin 1 augmente de manière significative la sécrétion régulée. Sur la base de nos

découvertes nous postulons que RTN1-C pourrait être un acteur clé dans la régulation des processus de fusion dépendents des SNAREs.

Nos études contribuent à l'élucidation du rôle de NEEP21 et RTN1-C dans les neurones et à la compréhension des mécanismes moléculaires du trafic de protéines, une des bases de la plasticité synaptique.

REMERCIEMENTS

Je veux tout d'abord remercier mon directeur de thèse, le Prof. Stefan Catsicas pour tout le soutien qu'il m'a apporté durant ces années de doctorat. C'est lui, le premier, qui a su me communiquer son enthousiasme pour les Neurosciences et m'a donné l'envie de persévérer dans cette direction . Je lui suis également redevable de m'avoir donner l'opportunité de toucher du bout des doigts le monde fascinants de la biophysique, de ses AFMologistes et de ses SNOMologistes.

Je tiens à exprimer ma gratitude la plus sincère envers le Dr Harald Hirling. C'est lui qui m'a donné la passion de l'expérimentation et m'a virtuellement tout appris dans les domaines de la biochimie et de la biologie cellulaire. Je le remercie donc pour ses qualités scientifiques, parce qu'il a su diriger ce projet d'une manière magistrale, et pour la quantité phénoménale de science qu'il m'a transmise. Je le remercie aussi pour ses qualités humaines, sa gentillesse et sa patience face à mon impatience et mes « excentricités », pour avoir rendu la période de ma thèse exceptionnelle et pour le soin qu'il a mis à ne pas me faire regretter une seule seconde passée au sein de son groupe de recherche.

Un merci tout particulier à Liliane Glauser, Lili pour les intimes, qui a pris soin de moi pendant ces 5 dernières années et qui me remettait sur le droit chemin lorsque je m'égarais dans les voies tortueuse de la recherche. Je la remercie pour m'avoir initier au monde des neurones, les vrais, pour toute l'aide précieuse et inestimable qu'elle m'a apporté, sans laquelle cette thèse ne serait pas ce qu'elle est aujourd'hui. Je la remercie aussi pour tous les rires et bons moments que nous avons partagés ensemble et qui ont contribué à me faire me lever chaque matin avec entrain et bonne humeur. Tu vas me manquer Lili...

Je remercie également Sarah Magnin, qui a aussi contribué d'une manière significative à l'aboutissement de ce travail et pour tous les coups de main apporté spontanément. Sarah, qui m'a fait découvrir de nouveaux horizons de la langue « vaudoise » qui resteront à jamais gravé dans ma mémoire et qui me rendront toujours nostalgique de cette période doctorale quand je serai parti sur un autre continent.

Comment poursuivre ce texte sans mentionner Floyd Sarria, l'homme des Images, mon consultant préféré, celui qui m'a ouvert les yeux au monde de la fluorescence. Floyd, mon

voisin de paillasse, mon frère de confocal, qui a égayé mon existence de thésard de par sa bonne humeur et de tous ces moments partagés ensemble. Floyd, celui qui traitait mes images que je retournais en statistiques et enfin, celui qui personnifie ce qu'il y a de meilleur dans mon travail, la découverte, la découverte d'une nouvelle amitié.

Et puis, il y aussi les AFMologistes. Tout d'abord Sandor Kasas, qui a toujours su me faire rire par ses mille et une plaisanteries parfois douteuses et tenté de m'introduire aux mondes des vérités « vraies », après lesquelles courent désespérément la Science. Et évidement, Alexandre Yersin, l'autre « physicobiologiste » qui a essayé de faire de moi un « biologicophysicien ». Je le remercie d'avoir partagé avec moi toutes ces parties d'AFM et de golfs et su m'écouter et me conseiller dans certains de mes choix de vie scientifiques et plus...personnels.

Je remercie aussi la nouvellement Dr Florence Morgenthaler, pour tous ces instants agréables passés sur les bancs de l'IBCM à discuter et pour tout ce que nous avons partagé durant nos années de thèse à l'IBCM.

Je tiens également à remercier Karina Kulangara, celle qui me suit et me précède, pour toutes les discussions enrichissantes et les « quelques verres » que nous avons partagé ensemble. Je la remercie pour son enthousiasme et son pragmatisme qui ont su à maintes reprises redonner de l'élan à mon travail.

Merci aussi aux « nouveaux », la relève, le sang frais, Michel et Charles qui assurent la pérennité de nos projets.

Parmi les personnes de l'IBCM, qui m'ont aidé au cours de ce projet, il y a Catherine Chevalley, qui a suivie et dirigée mes tous premiers pas dans la biochimie, le Prof. Romano Regazzi, qui m'a appris à extraire la substantifique sécrétion des PC12, Robert Marsault, mon ancien « papa » et Thierry Coppola, les 2 inséparables franchouillards qui m'ont montré entre autre les joies du séquençage. Je remercie infiniment le Prof. Egbert Welker et son équipe pour m'avoir donné la possibilité de découvrir le monde fabuleux de la physiologie « des moustaches » et merci à Charles Quairiaux pour tous ces « tonneaux » partagés au labo et au bistrot.

Je remercie aussi tous les membres de la Faculté des Sciences de la Vie, en particulier le groupe du Prof. Henry Markram et Patrick Aebischer, pour leur collaboration et leur amitié.

J'aimerais pouvoir remercier chaleureusement tous mes amis, qui de loin ou de près m'ont aidé durant ce travail. Merci à mes parents Eliane et Jean-Claude et ma famille qui m'ont permis d'une certaine manière d'être ce que je suis et sans qui je n'arriverais pas à ma cheville. Merci aussi à Evelyne pour m'avoir « supporté » par vents et marées et avoir toujours su faire preuve d'attention à mon égard.

Enfin, je tiens à remercier les membres du Jury de Thèse, en particulier les Prof. Ruth Luthi-Carter, Antonio Margaroli, Romano Regazzi et le Dr William Pralong, pour accepter de considérer mon travail.

ABBREVIATIONS

AA	amino acid
ADP	adenosine diphosphate
AFM	atomic force microscope
AMPA	alpha-amino-3-hydroxy-5-methyl-4-isoxazolepropionate
AMPAR	AMPA receptor
APV	D(-)-2-amino-5-phosphonovaleric acid
ATP	adenosine triphosphate
AS	antisense
BDNF	brain-derived neurotrophic factor
BFA	brefeldin A
CAM	Cell adhesion molecule
cAMP	cyclic adenosine 3',5'-monophosphate
CCD	coupled-charged device
CNS	central nervous system
Cy	cyan
DIC	differential interference contrast
DMP	dimethylpimelimidate
DNA	deoxyribonucleic acid
DTT	dithiotheitol
EDTA	ethylene diamine tetraacetic acid
EGTA	ethylene bis(oxyethylenenitrilo) tetraacetic acid
ELISA	enzyme-linked-immunosorbent serologic assay
Eph	ephrin
EPSP	excitatory postsynaptic potential
ER	endoplasmic reticulum
ERGIC	ER-Golgi intermediate compartment
FCS	foetal calf serum
FITC	fluorescein isothiocyanate
GDP	guanosine diphosphate
GFP	green fluorence protein
GH	growth hormone

GIT	GRKs interactor1
GRASP	GRIP-associated protein-1
GRIP	glutamate receptor intercating protein
GRK	G-protein-coupled receptor kinase
GTP	guanosine triphosphate
HEPES	2-[4-(2-hydroxyethyl)-1-piperazine]ethanesulfonic acid
hGH	human growth hormone
hTfR	human transferrin recptor
IF	immunofluorescence
Ig	immuglobulin
IgG	immunoglobuline G
LBPA	lysobiphosphatidic acid
LC3	light chain 3
LTD	long term depression
LTP	long term potentiation
MES	4-morpholinoethanesulfonic acid
mIgG	mouse IgG
mRNA	messenger RNA
NEEP21	neuron-enriched endosomal protein of 21 kDa
NGF	nerve growth factor
NIPSNAP1	4-nitrophenylphosphatase synaptosomal associated protein
NMDA	*N*-methyl-D-aspartate
NSF	N-ethylmaleimide-sensitive factor
NSP	Neuroendocrine-Specific Protein
NT-3	neurotrophin-3
NT-4/5	neurotrophin-4/5 (NT-4/5)
OD	optical density
PAGE	polyacrilamide gel electrophoresis
PC12	pheocromocytoma cell 12
PDZ	PSD-95/Discs-large/ZO-1
PICK1	Protein Interacting with C Kinase 1
PBS	phosphate buffer
PKA	cAMP-dependent protein kinase A
PKC§	protein kinase C

PCR	polymerase chain reaction
PMSF	phenylmethylicsulfonic fluor
PMT	photomultiplier tube
PSD	postsynaptic density
Rab	Ras superfamily of GTPases
rIgG	rabbit IgG
RNA	ribonucleic acid
RT	room temperature
RTN	reticulon
SAP97	synapse associated protein of 97 kDa
SDS	sodium dodecyl sulfate
SERCA	smooth ER calcium ATPase
α/β/γ-SNAP	soluble NSF attachement protein
SNAP-25	synaptosomal associated protein 25, Mr 25 kDa
SNARE	soluble-NSF-attachement-protein receptor
SV	synaptic vesicle
SV2	synaptic vesicle protein 2
TGN	trans-Golgi network
Tf	transferrin
Tris	tris(hydroxymethyl) aminoethane
TfR	transferrin receptor
TRITC	tetramethyl rhodamine isothiocyanate
TrkA	tyrosine receptor kinase A
TTX	tetrodotoxin
VAMP	vesicle associated membrane protein
Wnt	weaver and meander tail

I Introduction

The human brain consists of a vast network of more than 10^{11} nerve cells that communicate with each other through more than 10^{15} specialized cell junctions called synaspes. The pattern of synaptic connections supports all aspects of brain function, from sensory perception and movement to learning and memory. The complexity of brain architecture is intimately associated with the inherent heterogeneous nature of neurons, since they can be classified into perhaps as many as 10'000 different types. Differences in their structure, but also in their molecular content, allow the generation of very different patterns of activity responsible for brain function. Understanding the development of neuron-neuron synapses is crucial to understand development of the nervous system abnormalities which underlie neurological and behavioural disorders. Moreover, because the adult brain is constantly reorganizing itself in response to experience, it is probable that at least some developmental mechanisms will be replayed during long-term modifications in the mature nervous system.

I.1 Neuron Doctrine

The current view of nerve cells, the brain, and behavior have emerged over the last century from the coalescence of five experimental traditions : anatomy, embryology, physiology, pharmacology, and psychology.

The anatomical complexity of nervous tissue was not appreciated before the invention of the compound microscope. Until the 18th century nervous tissue was thought to be glandular in function an idea that was based on Galen's proposal that nerves are ducts conveying fluid secreted by the brain and the spinal cord to the periphery of the body. Toward the end of the 19th century, the histology of the nervous system became a more precise science, culminating in the investigations of Camillo Golgi and Santiago Ramon y Cajal. Golgi developed the chrome silver method that allows microscopic visualization of the anatomy of the whole neuron, including the cell body and its 2 major processes : the axon, that transmits information away from the cell body, and the dendrites, that receive information from other neurons and conduct it toward the cell body. Ramon y Cajal used this staining technique to label individual cells, thus showing that the nervous system is not a syncitium, as it was proposed by Golgi, but an intricate network of discrete cells. In the course of this work Ramon y Cajal developed some of the key conceptual insights and much of the early empirical support for the *neuron doctrine* -the principle that the nervous system is made up of

individual signaling elements, the neurons, which contact one another only at specialized points of interaction, called synapses. In addition to providing the critical evidence for the neuron doctrine, Cajal also outlined 2 other rules that governed the functioning of nerve cells. First, he restated the *principle of dynamic polarization*. According to this principle signaling within a neuron flows in a single, predictable direction from the dendritres and the cell body, that receive inputs from other neurons to the axon and from there to the presynaptic terminals, which contact yet other neurons or effector cells. Second, he outlined the *principle of connectional specificity*, according to which nerve cells do not connect indiscriminately with one another or form a random networks. Rather, each cell communicates only with certain postsynaptic targets, but not with others, and always at special points of synaptic contact. Taken together, the principles of dynamic polarization and connectional specificity form the cellular basis for the modern connectionist approach to the brain.

I.2 Synapses

The introduction of the term synapse marked the beginning of a new area in the study of the nervous system. In 1897, Charles Sherrington, who was convinced by Ramon y Cajal's work, accepted the idea that it was difficult to conceive how specific neural functions could be executed if the central nervous system was an elaborate syncitium, while neuroanatomical studies argued for the view that neurons are morphologically distinct entities. On this basis, he introduced the term « synapse » (from the Greek « clasp ») to point out the sites at which axons make functional contacts with their target cells and definitely settled the neuron doctrine.

Synapses are specialized intercellular junctions between neurons or between neurons and other excitable cells where signals are propagated from one cell to another. Synapses are defined as electrical or chemical depending upon whether transmission occurs via direct propagation of the electrical stimulus in the presynaptic process or via chemical intermediate. Electrical synapses are gap junctions between neurons, which allow bidirectional propagation of the signal and play a role in synchronizing neuronal activity (Bennett, 2000). However, most synapses are chemical synapses, sites of discontinuity of the neuronal network where propagation of the signal is highly regulated. At chemical synapses, refered to as synapses, the presynaptic electrical signal is converted into a secretory response, leading to the release of chemical intermediates, the neurotransmittters, into the synaptic cleft. This chemical message

is then reconverted postsynaptically into an electrical signal along dendrites. Thus chemical synapses are fundamentally asymetric, although some retrograde, feedback signaling does occur (Goda and Davis, 2003). The basic feature of a synapse is a close apposition of specialized regions of the plasma membranes of the 2 participating cells to form the synaptic interface. On the presynaptic side a cluster of neurotransmitter-filled synaptic vesicles is associated with the presynaptic plasma membrane. On the postsynaptic membrane an accumulation of neurotransmitter receptors is marked by a thickening of the membrane and by the presence of a submembranous electron-dense scaffold, enriched in specific proteins (Figure 1). In the mammalian brain, the majority of chemical synapses are excitatory and use glutamate as neurotransmitter. However, there is a great diversity of neurotransmitters which can lead to either an excitation or an inhibition of the postsynaptic cell (Cowan, 2001). The presynaptic specialization can contact directly the shaft of the dendrites to make a synapse ; however, in mammals most excitatory synapses form onto small, bulbous cellular compartments called dendritic spines consisting of a head (volume 0.01-1μm^3) connected to the parent dendrite by a thin (diameter o.1μm) spine neck. Each spine is biochemically isolated (Sabatini et al., 2001) and contains components of many signaling pathways necessary for synaptic plasticity (Kennedy, 2000). Spines provide a closed compartment that allows rapid change in the concentrations of signalling molecules, such as calcium, and therefore make possible efficient response to input (Nimchinsky et al., 2002).

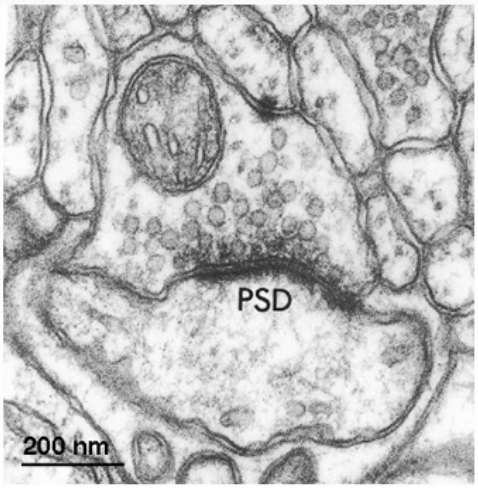

Figure 1. Ultrastructure of the synapse. Electron micrograph of a synapse between a parallel fiber axon terminal and a Purkinje cell dendritic spine in the rat cerebral cortex. Docked vesicles surrounded by a dense matrix are present at the presynaptic plasma membrane. Other vesicles are clustered behind these « front row vesicles » A thick membrane undercoat, the postsynaptic density (PSD), is present postsynaptically. Image from Cowan (2001).

I.3 Developmental Mechanisms of Synapse Assembly

Synapse development and formation (synaptogenesis) involves a series of very gradual structural, functional, and molecular changes. The very early steps during brain development, consist of neuron production, neuron migration and axonal and dendritic outgrowth. Connections are formed in 3 phases : (1) establishment of a first physical contact ; (2) a maturation process, during which each connection acquires its characteristic properties ; and (3) a stabilization phase, during which only « robust » connections will be maintained (Goodman and Shatz, 1993; Tessier-Lavigne and Goodman, 1996). The first 2 processes, which are involved in establishing the early formation of circuitry, are mostly activity-independent, while developmental and activity-dependent changes in synaptic strength are associated with the refinement of functional synaptic connectivity.

I.3.1 Filopodial Contact : the First Physical Contact

In the CNS, synapse assembly begins when axons approach their target and establish contact with dendritic arbor or soma of their target neurons. Axons are guided by a variety of extracellular cues that direct movement of a motile structure at the end of the growing axon known as the axonal growth cone. These cues are recognized by recognition molecules on the surface membrane of the growth cone (Huber et al., 2003). Initial contacts between synaptic partners are frequently established by axonal and dendritic filopodia (Figure 2A), which have been proposed to play an inductive role in synapse formation (Jontes and Smith, 2000). Imaging of fluorescently labeled neurons revealed that dendritic filopodia initiate contacts with nearby axons that could results in the formation of functional presynaptic boutons (Ziv and Smith, 1996). This implies that the action of the dendrites is deterministic for synapse assembly. Compatible with such a proposal, conditions that are thought to culminate in new synapse formation by postsynaptic triggering of long-term synaptic plasticity, induce active filopodial formation from dendrite shafts (Maletic-Savatic et al., 1999). Axons can also modulate synapse formation. In hippocampal neurons in culture, axonal filopodia that remain in contact with the postsynaptic target are stabilized and thought to be correlated with synapse formation (Tashiro et al., 2003). Preventing physical contact between inappropriate partners by repulsive signals or promoting interactions with the appropriate target cells should provide a mechanism that promotes specific synapse formation at a very early stage (Tessier-Lavigne and Goodman, 1996).

While the growth of axons and dendrites is independent of activity, filopodial motility is promoted by glutamate or electrical stimulation. Indeed, presynaptic electrical activity, by exocytic glutamate release stimulates dendritic filopodial motility during synaptogenesis (Lendvai et al., 2000). Moreover, like dendritic filopodia, the motility of axonal filopodia is enhanced by activation of kainate (Tashiro et al., 2003) and AMPA receptors (De Paola et al., 2003). Coordinate enhancement of the dendritic and axonal filopodial motility by localized release of glutamate from exocytic hot spots would thus increase the chances of axo-dendritic contact.

In addition to neurotransmitter several other diffusible factors that may provide general early synaptogenic signals have been identified. Members of the neurotrophin family of secreted growth factors, including nerve growth factor (NGF), brain-derived neurotrophic factor (BDNF), neurotrophin-3 (NT-3), and neurotrophin-4/5 (NT-4/5), promote synapse formation. For example, BDNF has been demonstrated to promote dendrite and axonal arborization and to increase synapse number, thereby facilitating the development and maturation of excitatory and inhibitory synaptic circuits in cultured neurons (McAllister et al., 1999). Secreted Wnt proteins and their related signaling pathway has also been shown to promote synaptogenesis either positively or negatively. Moreover, they seem to act on the pre-and postsynaptic parts of synapses (Salinas, 2003). Thus a number of different factors seem thus to be necessary for controlling synapse formation between different cell combinations.

I.3.2 Maturation Process

(a) Specification of Synaptic Adhesion

After formation of initial contacts, cell adhesion molecules present at the cell surface of dendrites and axons trigger the assembly of synaptic specialization and promote synapse stabilization through their adhesive properties (Scheiffele, 2003) (Figure 2B). The molecular diversity of some of the synaptic adhesion molecules satisfies the requisite specificity of synaptic connections in various regions of the brain, and the *trans*-synaptic link could be used to reciprocally coordinate the differentiation and alignment of pre- and postsynaptic terminals.

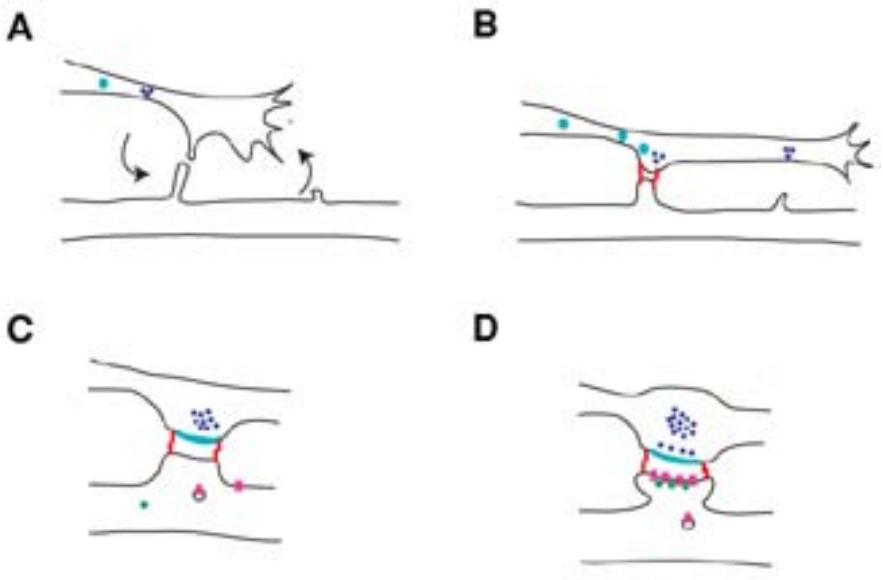

Figure 2. Model of excitatory central synapse formation. (A) Motile filopodia search for potential partners. Secreted signals from the axonal and dendritic neurites act as guiding molecules. Transport packets containing active zone molecules are transported along axonal neurites (light blue circles). Neurotransmitters are released from exocytic hot spots where small clusters of synaptic vesicles are formed (dark blue circles). (B) Presynaptic transport packets and synaptic vesicles accumulate at the initial contacts made by filopodia. Cell adhesion molecules stabilize them (red rectangles). (C) Assembly of the presynaptic zone is made by the accumulation of presynaptic transport packets and synaptic vesicles. Postsynaptic terminal assembly follows the presynaptic assembly by recruiting neurotransmitter receptors (purple ellipses) and postsynaptic scaffold proteins (green octogones). (D) In the assembled synapse, the presynaptic terminal has docked and possesses a reserve pool of synaptic vesicles and the postsynaptic terminal show neurotransmitter receptors embedded with the scaffold proteins. Modified from Goda and Davis (2003).

These molecules include members of the Immunoglobulin (Ig) superfamily such as N-CAM, L1, nectin, and SynCAM, Ca^{2+}-dependent homophilic cell adhesion proteins such as N-cadherin and protocadherin, the heterophilic cell adhesion proteins such as neurexins and neuroligins, the ephrin B and EphB tyrosine kinase receptor system and proteoglycans such as syndecans (Goda and Davis, 2003; Sytnyk et al., 2004). Interfering with their *trans*-synaptic interactions affects synapse formation. For example, studies in heterogenotypic co-culture of neurons lacking NCAM with wild-type neurons indicate that N-CAM-deficient cells form fewer synapses (Dityatev et al., 2000). The heterophilic adhesion interaction between β-neurexins and neuroligins provides a potential synaptogenic cell surface interaction that satisfies the necessary asymmetry of pre-and postsynaptic differentiation. Ectopic expression

of neuroligin in nonneuronal cells was reported to induce presynaptic assembly in contacting axons in vitro. The synaptogenic activity of neuroligins was blocked by overexpression of exogenous β-neurexins, suggesting that β-neurexins on the axonal plasma membrane mediate presynaptic differentiation. Their action could be mediated through intracellular interactions with CASK and syntenin, 2 proteins known to be involved in the formation and the organization of presynaptic molecular scaffolds (Scheiffele et al., 2000).

(b) Specialized Transport Packets of Synaptic Components

Time-lapse studies of synapses have shown that synapse assembly can occur within 1 to 2 hours of initial axo-dendritic contacts (Friedman et al., 2000; Okabe et al., 2001; Washbourne et al., 2002). Such speed of synapse assembly is possible by a rapid recruitement of pre-assembled synaptic components to the sites of contact, thereby obviating the building of a new synapse from scratch. The pre- and postsynaptic transport carriers travel along neurites at remarkable speeds, up to several micrometers per minute (Ahmari et al., 2000; Washbourne et al., 2002). Several minutes after the first contact between axon and dendrite, these organelles accumulate at the contact site (Ahmari et al., 2000; Sytnyk et al., 2002; Washbourne et al., 2002). This suggests that signals from the pre- and postsynaptic membranes are required to tell carriers when and where the apposing membranes meet (Figure 2C). Mobile cytoplasmic transport packets containing some synaptic vesicle proteins like VAMP2 and active zone components, including piccolo, bassoon, N-cadherin and a Ca^{2+} channel subunit, have been reported to be highly mobile along growing axons but are promptly immobilized at nascent synapses to participate in synapse construction. They could thus deliver active zone components prior to the appearence of synaptic vesicle proteins required for exocytosis (Ahmari et al., 2000; Friedman et al., 2000). This would provide a scaffold for the recruitment of competent synaptic vesicles or de novo formation of synaptic vesicle clusters at the site of the active zone (Ahmari et al., 2000; Friedman et al., 2000; Okabe et al., 2001).

On the dendritic side, the assembly of the postsynaptic specialization lags behind that of the presynaptic specialization. The timing difference of pre- and postsynaptic assembly is thought to depend on reciprocal signaling that begins with retrograde activation of the axon by the motile dendritic filopodia, followed by an anterograde signal from the presumptive presynaptic locus that induces postsynaptic differentiation. (Friedman et al., 2000; Okabe et al., 2001). Golgi-related structures were shown to be present in dendrites and different types of membranous carriers also exist postsynaptically (Horton and Ehlers, 2003a; Sytnyk et al.,

2002). For example, the rapid recruitment of PSD-95, a scaffold protein necessary for NMDA receptor clustering into nascent synapses, is detectable as soon as 20 minutes after axon-dendrite contact (Okabe et al., 2001). Morover, the existentce of non-synaptic clusters of PSD-95 (Marrs et al., 2001) are consistent with the idea that prefabricated complexes are used to assemble the PSD, analogous to presynaptic differentiation. However, it is not known whether the non-synaptic clusters of PSD-95 represent packets of PSD proteins in transit. NMDA receptors are probably not components of this complex, as non-synaptic NMDA receptor puncta only partially colocalize with PSD-95 (Washbourne et al., 2002). Although some synaptic PSD-95 clusters might be derived from translocation of pre-existing non-synaptic PSD-95, the de novo accumulation of PSD-95 clusters at nascent synapses seems to occur mostly from diffuse cytoplasmic pools of PSD-95 protein (Marrs et al., 2001). In addition, time-lapse imaging revealed the presence of glutamate NMDA receptors subunit NR1 and glutamate AMPA receptor subunit GluR1 in largely non-overlapping mobile clusters present before synaptogenesis occurs with NMDA receptors being recruited more rapidly to sites of axon-dendrite contacts than AMPA receptors (Washbourne et al., 2002). It is also uncertain whether these glutamate receptor clusters represent prefabricated packets of PSD proteins, or just reflect the presence of multiple glutamate receptors in transport vesicles. The non-overlap of mobile AMPA- and NMDA-receptor clusters and the differential kinetics of their recruitments to synapses indicate that AMPA and NMDA receptors clusters are distinctly regulated during synapse formation. Indeed, the cytoplasmic domains of AMPA and NMDA receptor subunits bind to different sets of regulatory, scaffolding and trafficking proteins (Barry and Ziff, 2002; Sheng and Sala, 2001). At steady-sate the concentration of AMPA receptors in synapses seems to depend on the interaction of its subunits with PDZ-domain proteins such as GRIP (glutamate-receptor-interacting protein) and PICK1 (protein that interacts with C-kinase alpha 1) (Barry and Ziff, 2002). However it has not been yet established whether these PDZ proteins are necessary for the correct assembly of postsynaptic membrane molecular machinery during synaptogenesis. Moreover, established synapses sometimes lack AMPA receptors (see below), so AMPA receptor incorporation is not required for synapse formation and seems to be a relatively late event in synapse development.

(c) Transformation of Initial Contact Complexes to Synapses

Accumulation of transport carriers is followed by transformation of the contact sites into a functional synapse (Ahmari et al., 2000; Sytnyk et al., 2002; Washbourne et al., 2002; Zhai et al., 2001) (Figure 2D). This probably includes fusion of the carriers with the synaptic plasma membrane, that inserts membrane proteins such as Ca^{2+} channels, and NMDA/AMPA receptors into the pre- and postsynaptic membranes. Insertion of synaptic constituents to build a functional synapse occurs mainly by constitutive exocytosis early in development. However it has also been reported that regulated exocytosis occurs both in axons and in dendrites. This is apparently activated by external stimuli, such as membrane depolarization, that elevate the intracellular Ca^{2+} concentration. Regulated exocytosis replaces the constitutive one in mature synapses and plays important role in the regulation of synaptic strength (Maletic-Savatic and Malinow, 1998; Sytnyk et al., 2002).

In addition to the contact-dependent formation of presynaptic assemblies mediated by synaptic adhesion molecules like β-neurexins, several molecules that are capable of organizing the postsynaptic assemblies at excitatory CNS synapses have been identified. For example, EphB receptor tyrosine kinases bind to and cluster NMDA receptors when activated by their ephrinB ligand in cultured neurons (Dalva et al., 2000). The ability of ephrinB-EphB receptor interaction to reorganize NMDA receptors suggests that EphB receptors have direct effects on synapse assembly, maturation and modification. Another protein that displays postsynaptic receptor clustering is Narp, a member of the pentraxin family. Narp is a secreted protein that triggers the clustering of AMPA receptors and increases the number of excitatory synapses when overexpressed in cultured spinal neurons (O'Brien et al., 2002; O'Brien et al., 1999; Tsui et al., 1996).

Following inital assembly, the synapse expands in size, alters its morphology and grows in strength. On the presynaptic side in the rat visual cortex, the mean number of synaptic vesicles per synapse increases fourfold during the first month of postnatal development (Blue and Parnavelas, 1983a; Blue and Parnavelas, 1983b). The other major structural change in developing central synapses is the morphology of the postsynaptic element at excitatory synapses. It has been proposed that dendritic filopodia that initiate synaptic contacts, contribute to the generation of synapses on dendritic shafts or can serve as precursors of spines (spinogenesis). In the latter case dendritic filopodia become stabilized by transforming into spines. However it is not clear whether postsynaptic morphology changes from filopodia to shaft to spine (Fiala et al., 1998) or directly from filopodia to spine (Ziv and Smith, 1996).

I.3.3 Stabilization Phase

Following the initial formation of synaptic connections, many developing circuits undergo a period of refinement, through which some connections are eliminated while others are strengthened (Goodman and Shatz, 1993; Katz and Shatz, 1996). This precise rewiring of connectivity is thought to depend on the pattern of electrical activity in the circuit and involves cooperative and competitive interactions between converging inputs on the postsynaptic cell. The first steps of synapse assembly may thus occur in the absence of neurotransmission (Craig and Boudin, 2001; Verhage et al., 2000). Indeed, genetic deletion of Munc18, a neuron-specific protein essential for synaptic vesicle docking and neurotransmitter release from presynaptic terminals, completely abolishes neurotransmitter secretion and synaptic transmission, yet apparently normal structural synapses and neuronal circuits form in these knock-out mice (Verhage et al., 2000). This confirms that activity may not be required for initial aspects of synaptogenesis. However, numerous studies support the notion that some aspects of synapse maturation require activity (see above). As synapses mature, synaptic activity exerts a stabilizing action on the existing dendrites by reducing spine motility through membrane depolarization (Cline, 2001) or glutamate receptor activation (McKinney et al., 1999). It seems that the level of synaptic activity, mediated through Ca^{2+}-calmodulin-dependent kinase II (CaMKII), is responsible for a switch of the role of the activity from growth promotion to arbor stabilization (Cline, 2001). Morover, studies of synapse maturation in the developing tectum and cortex have provided insights into the involvement of synaptic activity in the maturation of central excitatory synapses. Newly formed glutamatergic synapses communicate through NMDA receptors and more synapses acquire AMPA receptors as the neuron matures (Isaac et al., 1997; Wu et al., 1996). The immature synapses may be « silent » unless sufficient depolarization is provided. The depolarization may result in the recruitment of AMPA receptors to the synapse in a manner similar to that found in the induction of long term potentiation (LTP) in the CA1 region of the hippocampus (Liao et al., 1995; Shi et al., 2003). The parallel between developmental maturation of synapses and LTP is further supported by the finding that delivery of AMPA receptors to synapses occurs early in development, is activity-dependent and shares some, but not all, features with LTP (Zhu et al., 2000). Thus, synapse maturation may require a tight correlation between a robust NMDA receptor activation and afferent activity, similar to that required for the induction of LTP, whereas low-level NMDA receptor activation prevents maturation in a manner similar to that found in long-term synaptic depression (LTD). Besides the effects on functional maturation,

the early NMDA receptor activity in the postsynaptic neuron also helps to stabilize dendritic arbors, through the activation of CaMKII (Cline, 2001). Thus, there is an intricate interplay between functional and structural maturation during synaptogenesis.

Hebb postulated many years ago that strengthening of a synapse might be achieved by repetitive presynaptic activation that leads to postsynaptic firing (Hebb, 1949). Hebb's postulate was later transformed into a simple correlation rule : coincident pre- and postsynaptic activity leads to synapse strengthening. Hebb's rule was extended by assuming that noncoincident pre- and postsynaptic activity leads to synapse weakening. A strong evidence for the validity of these assumptions came from studies made on the visual and somatosensory systems. Repetitive visual stimuli can induce NMDA receptor-dependent LTP of retinotectal synapse, suggesting that natural experience-driven activity is capable of inducing LTP-like synaptic modification (Zhang et al., 2000). Furthermore, the composition of NMDA receptors undergoes experience-dependent developmental regulation in the visual system (Philpot et al., 2001) and there is a correlation between the susceptibility of developing synapses to the induction of LTP/LTD and the susceptibility of the developing circuits to refinement during the critical period (Feldman, 2000; Kirkwood et al., 1996).

I.4 Synaptic Plasticity

The strength of the connection between a presynaptic and a postsynaptic neuron often exhibits a remarkable degree of plasticity. Synaptic transmission can be either enhanced or depressed, and these alterations can last from a transient few milliseconds to days, weeks, or perhaps longer. Such changes in efficacy of synaptic transmission are likely to be important for a number of aspects of neural function. Transient modifications have been associated with short-term adaptation to sensory inputs, changes in behavioral states associated with arousal, and short-term memory. More lasting changes have been associated with neuronal development in the immature nervous system, as described above, and with long-term memory in the mature nervous system. In this context, I will principally consider one form of synaptic plasticity that has been implicated in learning and memory (Martin et al., 2000b) : long-term potentiation (LTP) in the mammalian hippocampus.

I.4.1 Long Term Potentiation : An Intensively Studied Model of Synaptic Plasticity

It is widely believed that a long-lasting change in synaptic function is the cellular basis of learning and memory (Hebb, 1949; Kandel, 2001). The most thoroughly described examples of such synaptic plasticity in the mammalian nervous system are long-term potentiation (LTP) and long-term depression (LTD). LTP was first described at excitatory synapses in the dentate gyrus of the hipocampus in vivo by Bliss and his collegues in the early 1970s (Bliss and Gardner-Medwin, 1973; Bliss and Lomo, 1973). LTP and LTD consist of an activity-dependent persistent change of synaptic strength has been observed at virtually every excitatory synapse in the mammalian brain that has been studied. Thus, LTP appears to be a ubiquitous property of mammalian excitatory synapses and may subserve a variety of functions. LTP can be induced experimentally by stimulating afferents at high frequency (25-100 Hz) or by directly depolarizing the postsynaptic cell with current injection while maintaining low-frequency afferent stimulation. This leads to a stable increase in the postsynaptic response. In the opposite situation, low-frequency stimulation of a presynaptic terminal reduces the frequency of presynaptic bursts and decreases the postsynaptic response in a lasting manner. This phenomenon is called long term depression (LTD) (Stevens and Sullivan, 1998). These activity-dependent changes in synaptic function are believed to be the cellular correlate of learning and memory (Stevens, 1998). There are at least 2 temporally distinct phases of LTP, analogous to memory storage : the early phase of LTP (short-term memory) lasting minutes and the late phase of LTP (long-term memory) lasting days or longer. These 2 phases differ not only in their time course, but also in their molecular mechanisms : the late phase of LTP, but not the early phase, requires the synthesis of new proteins (Martin et al., 2000a). Short-term synaptic changes involve modification of pre-existing proteins, like their state of phosphorylation or trafficking, leading to modification of pre-existing connections (functional plasticity), whereas the long-term synaptic changes involve activation of gene expression, mRNA translation and the formation or elimination of connections (structural plasticity) (Kandel, 2001).

I.4.2 Molecular Mechanisms of LTP

In most cases, triggering of LTP requires the synaptic activation of postsynaptic NMDA receptors. This activation requires depolarization of the postsynaptic cell. During low-

frequency synaptic transmission, the neurotransmitter glutamate binds to 2 different subtypes of receptors that are often, but not always, colocalized on individual dendritic spines. The first one is the AMPA receptor, that is a channel permeable to monovalent cations (mainly Na^+ and K^+) and that provides the majority of inward current for generating synaptic responses when the cell is close to its resting membrane potential. The second is the NMDA receptor, that exhibits a profound voltage dependence because of the blocking of its channel by extracellular Mg^{2+}, such that it contributes little to the basal postsynaptic response during low-frequency synaptic transmission. However, when the postsynaptic cell is depolarized during induction of LTP, Mg^{2+} dissociates from its binding site within the NMDA receptors channel, allowing Ca^{2+} as well as Na^+ to enter the dendritic spine. The NMDA receptor is thus a coincidence detector : it only passes Ca^{2+} when presynaptic activity and postsynaptic activity coincide. The consequent rise of intracellular Ca^{2+} is the critical trigger for LTP. This local source of Ca^{2+} within the dendritic spine accounts for the input specificity of LTP. Associativity occurs because strong activation of one set of synapses depolarizes adjacent regions of the dendritic tree (Malenka and Nicoll, 1999).

Alterations in synaptic strength and increase of local intracellular Ca^{2+} concentration seems to activate a large number of different transduction pathways, resulting in changes in gene expression, differential targeting of newly synthesized proteins and posttranslational modification. One of the key component of the molecular machinery of LTP is α-calcium-calmodulin-dependent protein kinase II (α-CaMKII). α-CaMKII is found in high concentrations in the postsynaptic density of dentritic spines that also contains the glutamate receptor that mediates synaptic transmission. Postsynaptic injection of inhibitors of α-CaMKII blocks the ability to generate LTP (Malenka et al., 1989). Morover, it has been shown that α-CaMKII can directly phosphorylate the AMPA receptor subunit GluR1, in situ, and this has been shown to occur following the generation of LTP and is correlated with the increase of responsiveness of AMPA receptors after LTP induction (Barria et al., 1997). In addition, α-CaMKII has the interesting biochemical property that, when autophosphorylated on threonine 286, its activity is no longer dependent on calcium-calmodulin, thus allowing its activity to outlast the Ca^{2+} signal that originally activated the enzyme (Braun and Schulman, 1995). Several other protein kinases including protein kinase C (PKC), cyclic adenosine 3',5'-monophosphate (cAMP)-dependent protein kinase A (PKA), have also been suggested to contribute to LTP, by phosphorylation of membrane receptors such as AMPA receptors (Malinow and Malenka, 2002).

Another potentially important class of signaling molecules that may play important roles in LTP are retrograde messengers. These are substances that are produced in the postsynaptic cell and diffuse across the synaptic cleft to modify presynaptic function. Molecules with such characteristics include nitric oxide (NO), carbon monoxide, arachidonic acid, and platelet-activating factor (Malenka and Nicoll, 1999).

Finally, neurotrophins have emerged recently as potent synaptic modulators (Lu, 2003). Studies have focused attention on the role of BDNF in synaptic transmission and plasticity in the hippocampus. At hippocampal CA1 synapses, substantial evidence indicates that BDNF acutely facilitates LTP (Korte et al., 1995; Lu, 2003). This effect is caused primarily by a presynaptic mechanism and has been atttributed to a potentiation of synaptic responses to tetanic stimulation and an enhancement of synaptic vesicle docking, possibly through changes in protein phosphorylation (Jovanovic et al., 2000). Postsynaptic effects of BDNF on dentate LTP in hippocampal slices and on NMDA receptors in cultured hippocampal neurons have also been reported (Kovalchuk et al., 2002; Levine et al., 1998). BDNF and other neurotrophins could thus represent a new class of neuromodulators that regulate neuronal connectivity and synaptic efficacy.

I.4.3 Silent Synapse Hypothesis

Over the past decade, no question concerning LTP has generated more confusion or contreversy than the seemingly simple issue of whether LTP is due primarily to pre- or a postsynaptic modifications. Indeed, many components, both pre- and postsynaptic, are potential target for changes in synaptic strength resulting in LTP. Changing the probability of neurotransmitter release or increasing the quantity of neurotransmitter per vesicle could be potential presynaptic modifications. At the same time, changing the number of neurotransmitter receptors or their biophysical properties and function would be the simplest postsynaptic modification. Although many studies suggested primarily postsynaptic modifications, a decrease in the proportion of synaptic failures during LTP (Kullmann and Siegelbaum, 1995) were also widely reported. Because synaptic failure were assumed to be due to failure to neurotransmitter release, these results were in contradiction.

A resolution arrived with the finding that synaptically released glutamate activated more synapses containing NMDA receptors than synapses containing AMPA receptors. The simplest explanation for this observation is that some synapses express only NMDA receptors

whereas others express both AMPA and NMDA receptors. Synapses with only NMDA receptors would be functionally silent at hyperpolarized membrane potentials ; thus when transmitter is released from the corresponding presynaptic bouton, they would not yield a response. However, LTP at such « silent » synapses could occur if there was activity-induced expression of AMPA receptors (Malinow and Malenka, 2002). Thus, at resting potentials NMDA receptors are minimally opened, and transmitter release at such synapses is recorded as a failure. The appearance of an AMPA response at such synapses during LTP , with no change in the NMDA response, strongly supports a postsynaptic modification consisting of a functional recruitment of AMPA receptors (Liao et al., 1995). One potential mechanism consists of the rapid delivery of AMPA receptors from nonsynaptic sites to the synapse, via a mechanism analogous to the exocytosis of presynaptic vesicles during transmitter release. Two recent studies support that postsynaptic exocytosis occur during LTP. One study showed that LTP is blocked by loading postsynaptic neurons in hippocampal slice with toxins that inhibit membrane fusion (Lledo et al., 1998). The other demonstrated the existence of a dendritic exocytosis that is CaMKII activity-dependent (Maletic-Savatic et al., 1998). Another evidence to support the silent synapse hypothesis came from electron microscopic analysis using immunogold labeling that fails to detect AMPA receptor at significant proportions of synapses in developing hippocampus and hippocampal cultures, whereas all synapses contain NMDA receptors (Liao et al., 1999; Petralia et al., 1999). AMPA receptor trafficking seems thus an important mechanim underlying the generation of LTP.

I.4.4 LTP/LTD and AMPA Receptor Trafficking

AMPA receptors are hetero-oligomeric proteins made of the subunits GluR1 to GluR4 (also known as GluRA-D). Each receptor complex is thought to contain 4 subunits. In the adult hippocampus 2 different species of AMPA receptors appear to predominate : receptors made of GluR1 and GluR2 (GluR1/2) and those made of GluR2 and GluR3 (GluR2/3) subunits (Wenthold et al., 1996). AMPA receptor subunits contain an extracellular region and transmembrane regions that are very similar, while their intracellular cytoplasmic domains are distinct. GluR1, GluR4 and an alternative splice form of GluR2 (GluR2L) have longer cytoplasmic tails and are homologous. In contrast, GluR2 and GluR3 have a shorter, homologous cytoplasmic tail. These cytoplasmic tails are responsible for their interactions with cytoplasmic proteins that are crucial in the control of their targeting, trafficking and

clustering. Most AMPA receptor-interacting proteins have single or multiple PDZ domains that interact with the extreme C-terminal tails of AMPA receptor subunits (Sheng and Sala, 2001).

AMPA receptor insertion and removal are closely coupled to synaptic strengthening and depression, respectively. Recent works revealed 2 general mechanisms of synaptic insertion and removal of AMPA receptors, depending strongly on the subunit composition. In one elegant study, Malinow and collegues used homomeric GluR1 or mutant GluR2 receptors with inwardly rectifiying currents (« electrophysiologically tagged » AMPA receptors) to monitor synaptic targeting of receptor subunits expressed in hippocampal slice cultures. These studies showed that synaptic accumulation of homomeric GluR1 receptors depends on NMDA receptor stimulation and activation of CaMKII, correlating with LTP (Hayashi et al., 2000; Shi et al., 1999). On the other hand, GluR2 incorporates into the synapse independently of activity, but causes no change in synaptic strength (Shi et al., 2001), suggesting that GluR2 exchanges constitutively with existing synaptic AMPA receptors. The synaptic expression of homomeric GluR2 receptors depends on its C-terminal PDZ binding motif, suggesting the involvement of PDZ proteins (Shi et al., 2001). The GluR1 subunit appears to govern the trafficking behavior of heteromeric GluR1/2 receptors, preventing constitutive exchange and conferring inducible delivery of heteromers (Shi et al., 2001). This is no longer dependent of the C-terminal PDZ binding motif of GluR2, again emphasizing the « dominance » of GluR1 (Figure 3).

Using a thrombin cleavage assay to isolate AMPA receptor exocytosis, Sheng and collegues showed that GluR2 homomer insertion is rapid and constitutive, whereas GluR1 insertion is slow but inducible in hippocampal cultures. The GluR1 phenotype is dominant in heteromers. Activation of NMDA receptors enhanced the rate of exocytosis of GluR1 but not of GluR2 homomers. GluR2 accumulated more immediately in synapses, whereas GluR1 accumulated in nonsynaptic locations (Passafaro et al., 2001) before diffusing into the synapse. Thus both the subunit composition of the incoming receptor and the prior synaptic content appear to govern synaptic receptor insertion. In addition, LTP is absent in adult mice lacking the GluR1 subunit, consistent with the dependence of de novo insertion and LTP upon GluR1 (Zamanillo et al., 1999). In mice lacking GluR2, LTP is enhanced,which is consistent with the present view that de novo insertion of AMPA receptors is independent of GluR2 (Jia et al., 1996). Interestingly, a GluR1-independent form of LTP has been reported in the developing hippocampus that slowly decreases during the maturation of the hippocampus while the GluR1-dependent form increases and becomes dominant in the adult brain (Jensen et al.,

2003). In addition, the recent findings that the GluR2L splice variant expression declines between P14 and P42 and that recombinant expression of the C-terminal domain of GluR2L in hippocampal slices from juvenile GluR1-deficient mice reduce LTP expression would make GluR2L an attractive alternative to GluR1 in mediating activity dependent synaptic AMPA receptor insertion for LTP expression (Kolleker et al., 2003).

The C-terminal domains of AMPA receptors subunit contribute to trafficking through subunit-specific interactions with cytosolic proteins. They may engage the trafficking machinery by an unknown mechanism, anchor receptors at membranes, or regulate receptor-binding protein interactions. GluR1 C-terminal domain binds via a class I PDZ domain interaction to SAP97 (synapse-associated protein 97 kDa). GluR2 and GluR3 bind group II PDZ ligands, consisting in the glutamate receptor interacting protein (GRIP) and the protein interacting with C kinase 1 (PICK1). In addition GluR2 C-terminal domain binds N-ethylmaleimide sensitive factor (NSF) (Nishimune et al., 1998; Osten et al., 1998; Song et al., 1998).

These different AMPA receptor-binding proteins have been suggested to modulate the trafficking of AMPA receptors between the plasma membrane and intracellular stores, which may be a critical step in determining the number of synaptic AMPA receptors during synaptic plasticity (Barry and Ziff, 2002; Malinow and Malenka, 2002).

AMPA receptor cycling between the plasma membrane and internal stores is crucial during modulation of synaptic strength. As described above, insertion of AMPA receptors from an internal store to the synapse sustains the expression of LTP. Conversely, rapid loss of synaptic AMPA receptors has been observed following low-frequency synaptic stimulation with subsequent induction of LTD (Carroll et al., 1999b) or with exogenous application of glutamate (Lissin et al., 1999) or insulin (Man et al., 2000). Again, PDZ proteins have been identified that are important for receptor internalization, stabilization or membrane trafficking through intracellular compartments, the endosomes. Regarding the latter, regulation of AMPA receptor-mediated synaptic transmission and synaptic plasticity by exocytosis and endocytosis (Lledo et al., 1998; Luscher et al., 1999; Man et al., 2000) and clathrin-dependent endocytosis of AMPA receptors emphasize this view (Carroll et al., 1999a; Man et al., 2000). Moreover, it has been shown that after internalization, AMPA receptors traffick along the endosomal pathway and can follow different pathways depending on the stimulus, i.e. NMDA receptor or AMPA receptor activation or GluR subunits phosphorylation (Ehlers, 2000).

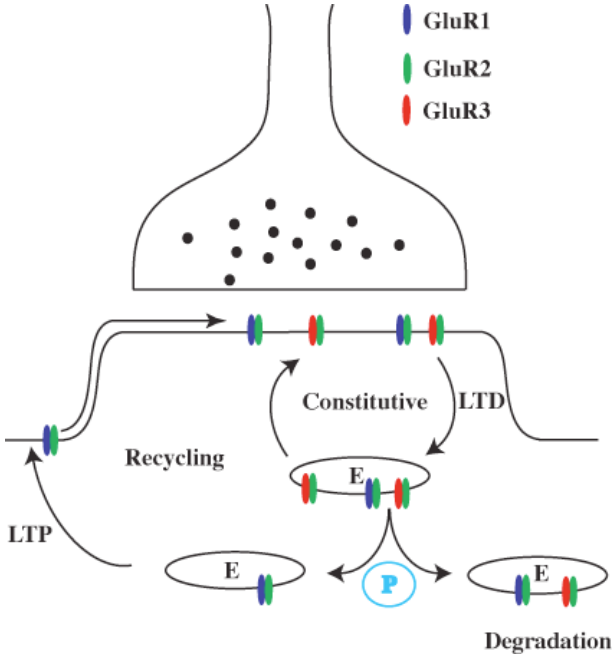

Figure 3. Model of synaptic AMPA receptor trafficking in LTP and LTD. AMPA receptors containing GluR2/3 subunits do not require synaptic activity to cycle between the synaptic plasma membrane and endosomal pathway (E). In opposite, delivery of AMPA receptor composed of GluR1/2 subunits require activity for delivery to synapse. A number of evidence suggest that the receptors may be initially inserted extrasynaptically by exocytosis and then shuttled laterally to the synapse. Phosphorylation/dephosphorylation (P) of AMPA subunits may control their entry in the recycling or degradation pathway.

Following NMDA receptor activation, AMPA receptors are dephosphorylated, traffick through the endosomes and are then recycled to the plasma membrane. In contrast, when endocytosis is stimulated by AMPA receptor activation, dephosphorylation does not take place and the receptors are transported to the degradation pathway where they are eliminated (Ehlers, 2000). However the molecular mechanisms and important actors involved in AMPA receptor trafficking are largely unknown.

Changes in the presynaptic nerve terminal leading to the long-term synaptic plasticity can not be excluded. For example, another form of LTP that occurs at mossy fiber-CA3 synapses has a presynaptic locus and is NMDA receptor activity-independent (Nicoll and Malenka, 1995). A similar form of LTP also appears to occur in the cerebellum at synapses between parallel fibers and Purkinje cells (Salin et al., 1996). There is also evidence that the « silent synapse » hypothesis could be due to a « silent presynaptic mechanism » due to a low level of glutamate release (Voronin and Cherubini, 2003). Delayed modifications in postsynaptic receptors matched with transmitter release changes underlie structural alterations associated with late

LTP phases. In conclusion, the synapse is a structural unit with important protein-protein interactions occcuring between and within pre- and postsynaptic elements. Thus it seems likely that long-lasting synaptic modifications will involve functional and structural (see below) alterations both in the pre- and postsynaptic part of the synapse.

I.4.5 Morphological Changes during LTP

There is strong evidence for the idea that creation of stable, persistent long term changes in synaptic strength, underlying learning and memory mechanisms like LTP/LTD, requires gene expression and the resultant synthesis of new proteins (Kandel, 2001). However, molecular changes are transient and so, on their own, are insufficient to explain long-term memory. Therefore, it is generally believed that changes in synaptic morphology are also necessary. These changes might occur either consequent to protein synthesis or in parallel with it. This is known as « structural plasticity ».

Modulation of the number of dendritic spines and/or their morphology has been proposed to contribute to alterations in excitatory synaptic transmission during learning (Nimchinsky et al., 2002). Indeed, there is evidence that induction of synaptic plasticity (LTP induction or memory formation) leads to changes in the number or the shape of spines (Nikonenko et al., 2002). For example it has been shown that induction of LTP in hippocampal slice cultures leads to the formation of new spines, and that inhibition of LTP with APV, a NMDA blocker, prevents this structural change (Engert and Bonhoeffer, 1999). Changes in morphology and number of spines has also been reported after learning in several brain areas using histological methods. For example, an increase in spine density has been detected in the hippocampus 24h after trace eyeblink conditioning, and these changes were blocked by NMDA antagonists (Leuner et al., 2003). In addition, it is important to note that recent studies have provided evidence, that structural plasticity of spine morphology and spine number exhibit a high degree of plasticity that enables sensory experience-dependent synapse formation (Grutzendler et al., 2002; Knott et al., 2002; Trachtenberg et al., 2002).

Long-term changes in spine morphology could contribute to the modulation of synaptic transmission that occurs after learning or LTP. Shortening or widening the neck of a spine affects calcium influx into dendrites and therefore might affect biochemical events in spines. It has been shown that glutamate sensitivity is correlated with spine shape, sensitivity being highest at spines with larger heads (Matsuzaki et al., 2001). In addition, polyribosomes are

preferentially translocated to large spines during synapse plasticity, an event that might facilitate the incorporation of a local protein synthesis machinery (Ostroff et al., 2002)

The AMPA receptors have been found to stabilize spine morphology (Fischer et al., 2000). Actin-based spine motility is inhibited by applying AMPA receptor antagonist in hippocampal neuron cultures. While NMDA receptors might be important in the initial phase of spine motility and formation, AMPA receptors mediate the following stabilization phase. Enduring changes in AMPA receptor transmission could therefore contribute to long-lasting spine stability. In this sense, it has been shown that blocking activity-dependent release of glutamate with TTX had no effect on spine density, whereas blocking both activity-dependent glutamate release and activity-independent glutamate release, by blocking vesicular glutamate release using botulinum toxin A or C, resulted in marked loss of spines (Luthi et al., 2001; McKinney et al., 1999). This means that AMPA receptor activation by spontaneous synaptic release is sufficient to maintain dendritic spines. Moreover, since AMPA receptor levels in spines increase after LTP induction or learning experiences, it has been postulated that an increase in AMPA receptors in spines could contribute to enduring spine stability and memory persistence (Bredt and Nicoll, 2003). This is strengthened by the fact that AMPA receptor insertion is a key event in LTP induction, as discussed above (Malinow and Malenka, 2002).

Modulations in spine morphology thus correlate well with synaptic plasticity and memory formation. These alterations last for many hours and even for days and could contribute to enduring changes in synaptic transmission. While modulation of spine structure is correlative to synaptic plasticity, morphological changes might have a key role in the maintenance of plastic changes in synaptic transmission.

I.5 SNAREs

Both AMPA receptor trafficking and synaptic vesicle exocytosis between the plasma membrane and internal neuronal compartments requires a vesicular transport and fusion mechanism between donor vesicles and target membranes. This is called the « vesicular transport hypothesis » postulated by George Palade and colleagues in the middle of the 70s. It states that the transfer of cargo molecules between organelles of the secretory pathway is mediated by shuttling transport vesicles. According to these hypothesis, vesicles bud from a « donor » compartment by a process that allows selective incorporation of cargo into the forming vesicles while retaining proteins in the donor compartments. The vesicles are

subsequently targeted to a specific acceptor compartment into which they unload their cargo upon fusion of their limiting membranes. To balance this forward movement of cargo, organelle homeostasis requires the retrieval of transport machinery components from the accceptor compartments back to the corresponding donor compartments, a process that is also proposed to occur by vesicular transport (Palade, 1975).

I.5.1 SNAREs and Membrane Fusion

Many proteins of this ubiquitous transport mechanism have been decribed like members of the Rab GTPases, and of the Soluble-N-ethylmaleimide-sensitive-factor-Attachment-protein-REceptors (SNAREs) (Jahn et al., 2003). The latter are essential proteins on donor vesicles and target membranes for correct vesicle fusion (Jahn et al., 2003; Rothman, 1994; Scheller, 1995). SNAREs are composed of 3 different families of proteins, SNAP-25 and its related isoforms, and the VAMP and the syntaxin families. These have previously been identified as components of the molecular machinery that promotes fusion of synaptic vesicles with the presynaptic plasma membrane of synapses (synaptic vesicle exocytosis). One of these proteins, known as VAMP2/synaptobrevin 2, was known to be associated with synaptic vesicles, whereas the other 2 proteins, syntaxin 1 and SNAP-25 has been localized to the presynaptic plasma membrane. It is currently known that synaptic vesicle exocytosis is mechanistically related to other vesicular transport steps. VAMP2, syntaxin 1 and SNAP-25 fom a complex known as the « SNARE complex ». It is generated by the pairing of a cognate v- and t-SNARE in a very stable 4-helix bundle, with one α-helix contributed by the monomeric v-SNARE (VAMP2) and the other 3 α-helices contributed by the oligomeric t-SNARE (syntaxin 1 and SNAP-25) (Figure 4A).

A major finding from structural analysis of the SNARE complex was that v- and t-SNAREs pair in parallel fashion (Lin and Scheller, 1997). v- and t-SNAREs in separate membrane pair thus to form a *trans*-SNARE complex, or v- and t-SNAREs in the same membrane pair to form a cis-SNARE complex. A *trans*-SNARE complex persists throughtout the fusion reaction to become a *cis*-SNARE complex in the fused membrane. Disassembly of the cis-SNARE complex is then promoted by 2 proteins α-SNAP and the ATPase NSF possibly by exerting rotational force to untwist the 4-helix bundle (Yu et al., 1999) (Figure 4B).

SNAREs seem to perform 2 major functions : one function is to promote the fusion itself. In all transport reactions that have been examined, the formation of *trans*-SNARE complexes is

essential for fusion. Assembly of the four-helix bundle is thought to supply the free energy needed to bring apposing membranes close enough to fuse (Chen and Scheller, 2001).

Moreover, in an elegant study, Rothman and colleagues recently demonstrated that the fusion of natural biological membranes can be driven by SNAREs in the absence of accessory proteins. Cells were engineered to produce “flipped” SNAREs that faced the outside of the cell rather than the cytoplasm. When cells containing a flipped v-SNARE were mixed with cells containing the cognate flipped t-SNARE, efficient fusion occurred. The combined data leave little doubt that SNAREs form the conserved, essential core of the fusion machinery (Hu et al., 2003).

The second major function of SNAREs is to help ensuring the specificity of membrane fusion. The discovery that cells contain various SNAREs that localize to different intracellular compartments leads to the « SNARE hypothesis » that proposed that each type of transport vesicle carries a specific v-SNARE that binds to a cognate t-SNARE on the target membrane (Rothman, 1994). In this sense it has been demonstrated that the formation of productive trans-SNARE complexes was almost exclusively restricted to physiologically relevant v- and t-SNARE combinations (McNew et al., 2000).

I.5.2 SNAREs and the Development of the Nervous System

In addition to their role in membrane fusion along the secretory pathway, it has been postulated that SNAREs could be implicated in nervous system development during neurite outgrowth and synaptogenesis. It is well established that SNARE proteins are present in mature adult neurons, where they participate in neurotransmission and the distribution of these proteins is widespread throughout all brain region. In addition, SNAREs have also been identified in the developping nervous system (Catsicas et al., 1991; Shirasu et al., 2000) and several lines of evidence showed that SNARE proteins are involved in neurite outgrowth, both in the central and peripheral nervous systems. Indeed, axonal growth is inhibited by SNAP-25 antisense oligonulcleotides in rat cortical neurons and PC12 cells in vitro and in amacrine cells of the developing chick retina in vivo (Osen-Sand et al., 1993). Similar effects have also been observed using botulic neurotoxins that specifically cleave SNAREs.

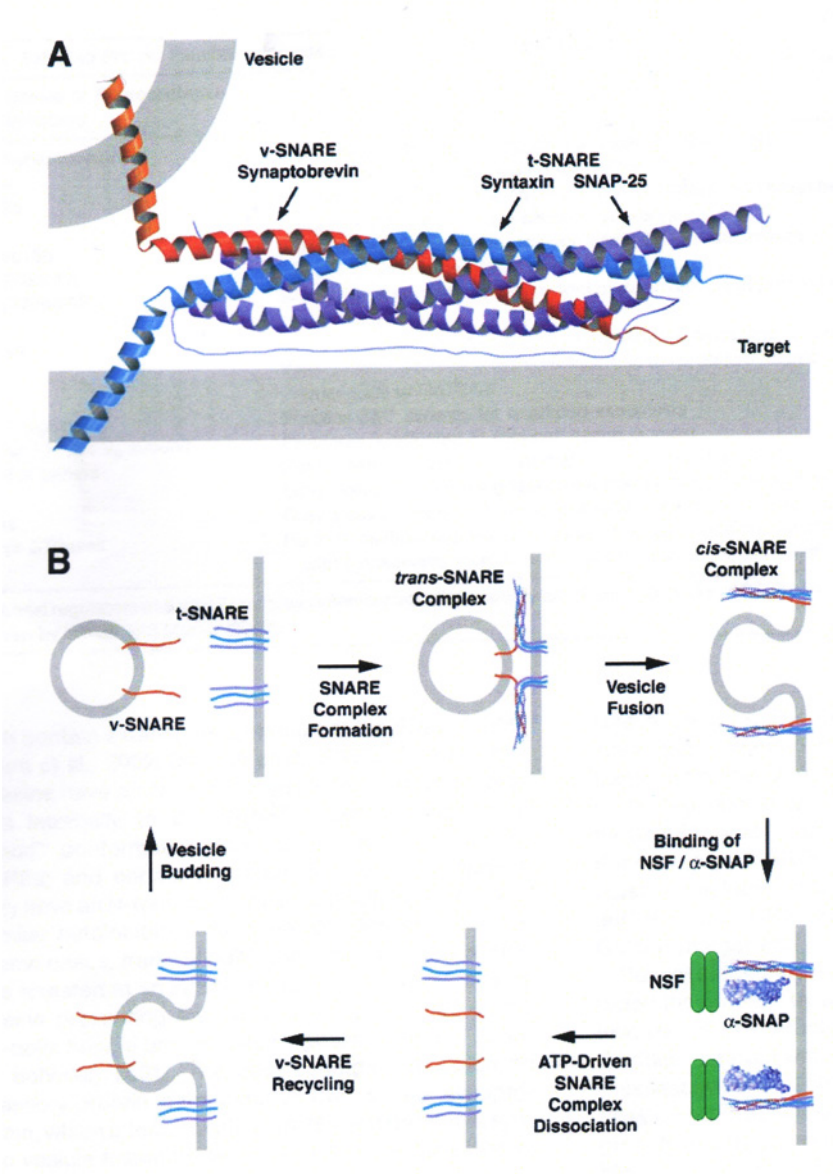

Figure 4. Structure and model of membrane fusion mediated by SNAREs. (A) Crystal structure of synaptic trans-SNARE complex drawn after Sutton et al. (1998). (B) The SNAREs cycle during membrane fusion. A trans-SNARE complex assembles when a monomeric v-SNARE on the vesicle binds to an oligomeric t-SNARE on the target membrane, forming a stable four-helix bundle that promote fusion. The result is a cis-SNARE complex in the fused membrane. α-SNAP binds to this complex and recruits NSF, that hydrolyzes ATP to dissociate the complex. Unpaired v-SNAREs can then be packaged again into vesicles. The depictions are from Bonifacino and Glick (2004).

However, not all the SNAREs seem to be equally involved in axonal growth. The cleavage of VAMP2 by Tetanus toxin impairs neurotransmitter release, but appears to have no effect on axonal growth (Osen-Sand et al., 1996). In addition, overexpression of Munc-18, a syntaxin 1-binding protein proposed to regulate SNARE complex formation in neurotransmitter

release, has been found to enhance axonal sprouting by increasing the number of axonal branch points in hippocampal cultures (Steiner et al., 2002b).

Several developmental studies have shown that SNARE protein expression can be dramatically modified at the time of the establishment of neurotransmission. SNAP-25 is markedly upregulated in the brain and a shift in localization from cell bodies to neurites and presynaptic terminals has been observed during development that seems to coincide with synaptogenesis (Catsicas et al., 1991; Oyler et al., 1991). Recent work demonstrates that depolarization of PC12 cells increases SNAP-25 levels, suggesting that electrical activity could be responsible for the control of SNAP-25 expression during synaptogenesis (Hepp and Langley, 2001). It has also been shown that certain regions of the adult brain, like the olfactory bulb and the hippocampus, continue to express the major form of SNAP-25 that is expressed during brain development, SNAP-25a, in adult (Boschert et al., 1996), supporting the function of SNAP-25 in membrane remodelling.

Taken together, it may be concluded that the SNARE machinery involved in axonal growth is similar to that associated with neurotransmitter release in neurons, since many proteins are common to both processes (Hepp and Langley, 2001).

Recently, syntaxin 13 that belongs to the syntaxin family and is implicated in early endosomal trafficking (see below) has been shown to be enriched in the developing brain and in the growth cone of differentiated neuroendocrine PC12 cells as well as primary cortical neurons. Moreover, overexperession of syntaxin 13 enhanced neurite outgrowth in NGF-stimulated PC12, while it has no effect on regulated secretion (Hirling et al., 2000). This suggests that syntaxin 13-endosomal trafficking step plays a limiting role in membrane expansion during neuronal development.

I.6 Endosomal Pathway

Internalization, insertion and degradation of membrane proteins in a temporally and spatially ordered manner is extremely important during neuronal differentiation and in adult neuron. The key organelles involved in protein and lipid trafficking are endosomes. Receptors and lipids present at the plasma membrane are internalized into the cell through the formation of clathrin-coated vesicles. A key event in this process is the recruitment of cytosolic clathrin to the membrane where it associates with protein complexes called adaptor proteins. Many of the membrane receptors for extracellular ligands become highly concentrated in clathrin-

coated vesicles. After endocytosis, internalized proteins, lipids,and solutes are recycled back to the cell surface or routed to the degradative pathway. The membrane trafficking decisions and sorting events take place in the endosomes (Gruenberg, 2001; Gruenberg and Maxfield, 1995). Separation of proteins to be recycled from proteins destined for lysosomal degradation takes place, at least in part, in the sorting endosomes, also known as early endosomes, located in the periphery of the cell (Mayor et al., 1993; Sonnichsen et al., 2000). The sorting endosome is a compartment comprised of 2 general domains, a vacuolar domain adjacent to a network of tubules and vesicles that can be dispersed throughout the cytoplasm. Proteins selected for recycling enter these tubular extensions via clathrin-coated vesicles. The vacuolar domain, on the other hand, contains proteins destined for degradation and either directly matures into late endosomes and lysosomes, or shuttles these proteins to these organelles through endosomal carrier vesicles (Gruenberg, 2001). From the sorting endosomes, recycled proteins can be rapidly shuttled back to the plasma membrane or enter tubulovesicular organelles located in the pericentriolar region of cell, known as recycling endosomes (Tooze and Hollinshead, 1991) (Figure 5).

The importance of protein recycling for signal transduction during development has been shown in a number of cases. One example is the neural cell adhesion L1 that is critical for axon growth in vitro and for the formation of major axonal tracts in vivo. During axonal growth, it has been shown that L1 is internalized in the centre part of the growth cone and recycled in its periphery through the endosomal pathway. Blocking its internal trafficking provokes the inhibition of axonal growth cone motility (Kamiguchi and Lemmon, 2000). NGF causes internalization of its high-affinity receptor TrkA upon ligand binding. Retrograde transport of TrkA-containing endosomes from the axon tip to the cell body is thought to be the mechanism of NGF signal integration (Delcroix et al., 2003; Grimes et al., 1996)

Likewise, GABA-A receptor, the principal receptor that mediates synaptic inhibition in the CNS, translocates rapidly from internal compartments during insulin stimulation in adult neurons, leading to an increase in the amplitude of the GABA(A)-receptor-mediated miniature inhibitory postsynaptic currents (Wan et al., 1997). Moreover, recent findings has demonstrated that AMPA receptor trafficking through endosomes during synaptic transmission is a potential key mechanism in the regulation of functional and structural synaptic plasticity at excitatory synapses (Beattie et al., 2000; Carroll et al., 1999b; Ehlers, 2000; Lin et al., 2000).

These results all indicate that stores of receptors are maintained intracellularly in endosomes capable of a rapid delivery to the synapse. Therefore, it is important to understand the

mechanisms that regulate the communication between endosomes and the synaptic plasma membrane (Bredt and Nicoll, 2003; Malenka and Nicoll, 1999; Malinow and Malenka, 2002). However, the molecular actors of such a mechanism are largely unknown.

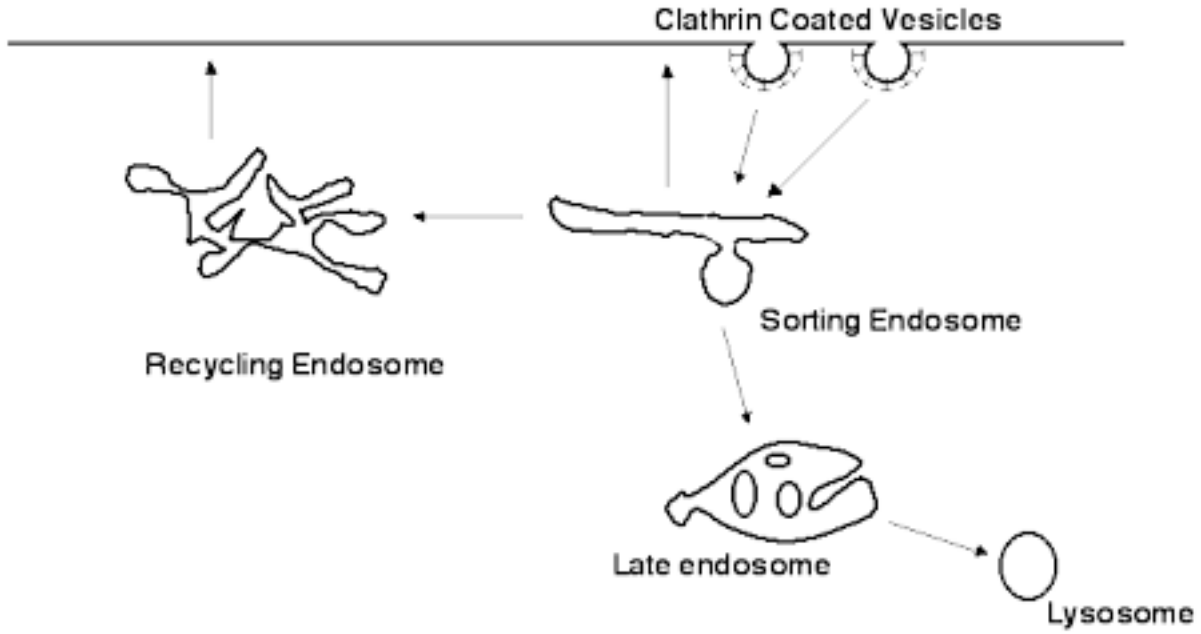

Figure 5. Model of the endosomal pathway. Lipids and transmembrane proteins are internalized into clathrin-coated vesicles. The latter fuses with the sorting endosome. There, the sorting decision is taken. Internalized lipids and proteins are directed either to the late endosome and then to the lysosome for degradation, or are recycled back to the plasma membrane via a direct route or indirectly through tubular vesicular recycling endosomes.

A number of inherited diseases have recently been associated with mutations that cause an impairment of proper cell surface targeting of plasma membrane proteins. Examples are the cyclic nucleotide-gated channel (CNGA1) in Retinis Pigmentosis (Trudeau and Zagotta, 2002), the epithelial sodium channel in Liddle's syndrome (Firsov et al., 1996) or GABA receptor γ2 subunit in familial epilepsy (Bianchi et al., 2002). Huntingtin, a protein modified by polyglutamine expansion in Huntington's disease is associated with endosomes and its defect could cause an impairment in axonal protein trafficking (Lee et al., 2004). These examples demonstrate again the importance of understanding the intracellular mechanisms of membrane protein internalization and recycling through the endosomal pathway.

In neuronal cells, endosomal trafficking is particularly complex, since neurons are composed of the cell body, and dendritic and axonal subdomains. Nevertheless, endosomal compartments have been clearly identified in neurons and their distribution is particularly

well described in dendrites and dendritic spines. Endosomal tubules have been identified in spine heads and postulated to be involved in local recycling near synapses. In addition, sorting endosomes have also been observed at the spine origin. However, the frequency of sorting endosomes per spine was relatively low, around one sorting endosome per spine, suggesting that spines contain a very local reservoir for receptor in their self-contained (Cooney et al., 2002). Instead, it has been proposed that receptors are recycled among a pool of synapses along the length of dendrite. Since AMPA receptor trafficking clearly goes through the endosomal pathway, it has been suggested that their rapid insertion at synapse accompaning LTP may rely on receptors garnered from a pool of neighboring synapses. This mechanism could also contribute to the depression of neighboring synaspes after LTP (Bi and Poo, 2001). Despite the morphological characterization of endosomes in neurons and their crucial importance in receptor cycling, little is known about specific proteins involved in this process. Nevertheless, one of them, the recently identified syntaxin 13, is of particular interest in the neuronal context. Syntaxin 13 is a SNARE protein that localized to the recycling endosomes (Hirling et al., 2000; Prekeris et al., 1998; Tang et al., 1998). Antibody blocking of syntaxin 13 in permeabilized PC12 cells inhibited receptor recycling (Prekeris et al., 1998). Such antibodies also inhibited in vitro endosome fusion, and syntaxin 13 has been found to form a complex with the Rab5 effector EEA1 and rabaptin-5, that are necessary for the control of endosomal fusion (McBride et al., 1999). This supports the view that syntaxin 13 is an essential player in the recycling processus of receptor along the endosomal pathway. The strong expression of syntaxin 13 during brain development and its outgrowth-enhancing effect (Hirling et al., 2000) suggest, that it could take part in molecular mechanisms, that are largely unknown, implicated in membrane protein cycling necessary for the establishment of correct brain connectivity.

I.7 Aim of the Thesis

The discovery that trafficking of membrane proteins through the endosomal pathway is implicated in brain development and synaptic plasticity prompted to investigate and characterize the role of the endosomal machinery in these processes. To this purpose, we used syntaxin 13 as a bait to identify endosomal protein complexes at a brain development stage that is characteristic for synapse maturation. This will increase our understanding of the

neuronal trafficking implicated in the molecular aspects of brain development and adult synaptic plasticity.

II Materials and Methods

II.1 Biochemistry

II.1.1 Antibodies

Antibodies against the following antigens were used: (a) polyclonal, GluR1 (immunofluorescence (IF) 1:10; Oncogene); GluR1 (Western blot (W) 1:500; Chemicon); GluR2/3 (W 1:1000; Chemicon); L1 (IF 1:4000; a gift of Dr V. Lemmon, USA); NEEP21 (IF 1:300, W 1:6000; developed in our laboratory (see II.1.5 antibody purification protocol); RTN1-C (IF 1:300, W 1:6000; developed in our laboratory (see II.1.5 antibody purification protocol) ; syntaxin 13 (IF 1: 200, W 1.6000; (Hirling et al., 2000); syntaxin 7 (W 1:2000; provided by Dr. W. Hong, Singapore), TGN38 (IF 1:500; a gift of Dr. G. Banting, UK); VAMP3/cellubrevin (W 1:500; provided by Dr P. DeCamilli, USA); VAMP1 (W 1:1000; provided by Dr. C. Montecucco, Italy); synaptophysin (W 1:100; Zymed); (b) monclonal, αSNAP (W 1:500; a gift of Dr R. Jahn Göttingen); EE-tag (supernatant; IF 1:40; W 1:2000; (Grussenmeyer et al., 1985); EEA1 (IF 1:300; Transduction Labs); GluR2 (IF 1:250, Chemicon); GRIP (IF 1:300, W 1: 2000, Transduction laboratories); HA-tag (IF 1:1000 myc-tag, Covance); Myc-tag (9E10 hybridoma supernatant; IF 1:20; W 1:10); MAP2 (IF 1:300; Sigma); Na/K-ATPase (W 1:100; clone a6F, developed by Dr. Farmbrough, obtained from DSHB); Rab4, Rab11 (IF 1:300; Transduction Labs); rat TfR (IF 1:500; Chemicon); SAP97 (IF 1:100, W 1:2000, Stressgen) SERCA2 (IF 1:100; Calbiochem) SNAP25 (W 1:2000; Sernberger Monoclonals); SV2 (IF 1:500; W 1:5000; developed by Dr K. Buckley, obtained from Developmental Studies Hybridoma Bank); syntaxin 1A (IF 1:500; W 1:2000; clone HPC1; Sigma) ; Tau (supernatant; IF 1:10; gift of Dr. Riederer USA); VAMP2 (IF 1:750; W 1:5000; clone 69.1, provided by Dr. R. Jahn, Göttingen); we also used: peroxidase-conjugated secondary anti-rabbit and anti-mouse IgG (W 1:2000; Calbiochem), and Cy3-, Cy5-coupled (IF 1:200; Jackson Immunoresearch) and Oregon-Green-coupled (IF 1:200; Molecular Probes secondary anti-mouse and anti-rabbit IgG.

II.1.2 Antibody Crosslinking

1 mg of antibodies was crosslinked to 2 mg of protein-G-sepharose (G-beads) for crosslink of monoclonal antibodies or protein A-sepharose (A-beads) (Pharmacia) for crosslink of polyclonal antibodies. G-beads and A-beads were first resuspended in H_2O for 10 min, then washed 3 times with H_2O and once with 100 mM Na_2HPO_4 for G-beads and PBS 1X for A-beads. Antibodies were added to the beads and agitated for 1h at RT. After centrifugation at 1000 g, beads were resuspended and washed 2 times in 200 mM $Na_2B_4O_7$-$10H_2O$ pH 9. 1/25 of the totality of the beads was removed and mixed with an equal volume of loading buffer 2X (see western blot protocol) for SDS-PAGE analysis (see below). Beads and antibodies were then covalently crosslinked with 20 mM DMP dissolved in 10 volumes of $Na_2B_4O_7$-$10H_2O$ for 25 min. Antibody-bead complexes were then washed 3 times with 10 volumes of 200 mM Ethanolamine pH 8. 1/25 of the totality of the beads was removed and mixed with an equal volume of loading buffer 2X (see section II.1.6 western blotting). Bead samples taken before and after the crosslinking step were separated on a 12% SDS-PAGE, stained by Coomassie Blue and destained with the destain solution. One band corresponding to the heavy chain (50kDa) and one band corresponding to the light chain of the antibody (25kDa) appeared on the gel. Comparing the intensity of these bands that corresponds either to the step before or after the addition of the crosslinker, showed the quantity of antibody which was covalently crosslinked to the beads (not present on the gel). The efficiency of the crosslinking was estimated to be at least 50%. During this time, beads were incubated and agitated for 2h in 200 mM Ethanolamine at RT, to quench all free amino termini. After incubation, beads were washed 3 times with PBS 1X and kept in PBS-0.005% merthiolate at 4°C.

II.1.3 Immunopurification

Immunocomplexes were isolated as follows. Brains were prepared and quick frozen from adult rats killed with CO2 and from postnatal day 3 (P3) rats killed by decapitation. Brains were homogenized in 8 volumes of ice-cold buffer A (320 mM sucrose, 10 mM HEPES/KOH pH 7.4), containing the protease inhibitors 0.3 mM PMSF, 2 mg/ml aprotinin, 2 mg/ml leupeptin, 0.7 mg/ml, by 10 strokes at 800 rpm in a motor-driven Teflon-glass homogenizer. After centrifugation at 1000 g for 15 min, the postnuclear supernatant was centrifuged at 100 000 g for 40 min and the pellet was extracted with 6 volumes of buffer B (20 mM HEPES/KOH pH 7.4, 2 mM EDTA, 2 mM EGTA, 1 mM DTT) containing 1M KCl (K).

After a second centrifugation at 100 000 g the membrane pellet was lysed for 40 min in buffer B containing 0.1M K, 1% Triton X-100 (T), and 10 mM Taxol to reduce tubulin content. Membrane protein extract was recovered by centrifugation at 100000 g. 250 μl of anti-syntaxin 13 (1 mg/ml) polyclonal antibody or control rabbit IgG beads were covalently crosslinked (see section II.1.2) and transferred into columns which were washed with 10 column volumes of PBS, 0.5 volume of 100 mM Glycine pH 2.5, 2 volumes 1 M Tris pH 8, 5 volumes PBS 1X, 2 volumes buffer B containing 100 mM KCl. Membrane protein extract was batch-loaded on IgG column for 1 h. Flow-through was collected and loaded in batches on the anti-syntaxin 13 column for 1 h. After collection of a second flow-through, both columns were washed as follows: 20 volumes of buffer B, 1% T, 100 mM K, 2 volumes of buffer B, 0.2% T, 100 mM K, 2 volumes of buffer B, 0.2% T, 500 mM K, 1 volume of buffer B, 0.2% T, 1 M K, and 1 volume of buffer B/0.2% T, 100 mM K. Bound proteins were eluted by 6 x 300 ml 100 mM glycine pH 2.5 and neutralized with 30 ml 1 M Tris pH 10.3. Regeneration of both columns was done by washing with 2 volumes of 1 M Tris pH 8 and 10 volumes of PBS 1X. Concentration of proteins was done in Centricon 10 by centrifugation at 1000 g (Milllipore). Immunocomplexes were analysed on 12% SDS-PAGE stained with Coomassie Blue. Purification from 21 g of adult and P3 brains were pooled and separated on a12% SDS-PAGE stained overnight with 0.03% amido black. 3 bands appearing predominantly only in the P3 membrane extract purification and one appearing in both purifications were cut out from the gel, dried in a speed vac and sent for trypsin digestion, HPLC analysis and peptide sequencing to the Protein Microsequencing Laboratory at the Institut Pasteur, Paris. Sequencing of 5 single peaks revealed the following peptide sequences: (1) SVSPWMSV corresponds to a brain specific clone 1A75/p21 (Sutcliffe et al., 1983); (2) AYLELEIT corresponds with reticulon 1/neuroendocrine-specific protein (NSP)/reticulon 1 (Roebroek et al., 1993); the isoform RTN1-C/NSP-C has been reported to be 23 kD in size, similar to the size of our sequenced protein band; (3) SYQLRPGTMI corresponds to 4-nitrophenylphosphatase synaptosomal associated protein 1 (NIPSNAP1) (Seroussi et al., 1998); (4) FLVPDHVN corresponds to microtubule-associated protein 1 light chain 3 (LC3) (Mann and Hammarback, 1994); (5) NRLDYHIS corresponds to ATP synthase b chain mitochondrial precursor (ATPF) (Tsurumi et al., 1990).

II.1.4 Brain Extract Immunoprecipitation

Postnatal day 3 (P3) brain extracts were prepared as described before, but without the extraction step with buffer B/1 M K and without taxol during lysis of the extract. P3 extracts were incubated with antibodies covalently crosslinked to 10 μl A- or G-beads at 4°C for 4 h-5 h. Beads were then washed once with 1 ml buffer B, 100 mM K, 1% T, twice with 1 ml buffer B, 100 mM K, 0.5% T and immunoprecipitated protein complexes were eluted as previously described. Elutions were analysed by Western blot.

II.1.5 Antibody Purification

A polyclonal antiserum was raised against a peptide spanning aa 7-23 of NEEP21 (Eurogentec) and affinity purified using Affigel 15 beads (Biorad Laboratories). The choice of the peptide sequence was made by searching hydrophilic regions along the protein sequence, which had a high probability to be present on the external part of the protein. 600 μl Affigel 15 beads in poly-prep column (Biorad Laboratories) were washed with 10 volumes H_2O, 3 volumes 100 mM MOPS pH 7.5, and then crosslinked with 4 μg of peptide, reconstituted in H_2O (pI = 4.14), one volume 100 mM MOPS pH 7.5 during 4 h at 4°C. Peptide-bead complexes were washed twice with 10 volumes 100 mM MOPS pH 7.5, 5 volumes PBS 1X, 1 volume 100 mM glycne pH 2.5, 1 volume 1 M Tris pH 8, 1 volume PBS 1X. For antibody purification, the final bleed was diluted with 2 volumes of 10 mM Tris pH 7.5 and centrifuged at 1500 g for 5 min at 4°C. Supernatant was passed 4 times on the column which was equilibrated with 10 volumes 10 mM Tris pH 7.5. The column was then washed with 10 volumesof 10 mM Tris pH 7.5, 10 volumes 10 mM Tris pH 7.5, 500 mM NaCl, and 5 volumes 10 mM Tris pH 7.5. Antibodies were eluted by 8 times 1 volume 100 mM glycine pH 2.5 into tubes containing 50 μl 1 M Tris pH 10.5. Reconstitution of the column was made by 1 volume 1 M Tris pH 8, 2 volumes 10 mM Tris pH 7.5, 1 volume 1 M Tris pH 7.5, 5 volumes PBS 1X, 0.01% merthiolate. 2 μl of each fraction was loaded on12% SDS-PAGE and coloured by Coomassie Blue to determine the concentration of the antibody per fraction. The antibody was then concentrated by centrifugation at 1000 g in centricon 10 until a concentration of > 0.8 mg/ml was reached.

For anti-RTN1-C purification, polyclonal antiserum was raised against a peptide coresponding to amino acid 5 to 20 of RTN1-C, which was purified using Affigel 10 (Biorad). The beads were washed with H_2O and with 3 volumes 100 mM MES pH 5.8. 3.6 mg of

peptide (pI 6.02) was then crosslinked to 600 μl beads with one volume of 100 mM MES pH 5.8 for 4h at 4°C. Purification of the antibody was then performed as decribed before.

II.1.6 SDS-PAGE and Western Blotting

All samples submitted to SDS-PAGE separation or western blotting analysis were diluted in an equal volume of 2X loading buffer (1 M Tris pH 6.8, 10% Glycerol, 2% SDS, 5% β-mercaptoethanol, 5 mg Bromophenol Blue), heated at 100°C during 10 min and separated by SDS-PAGE. In-gel staining of proteins was done by incubating the gel in Coomassie Blue 0.25%, methanol 30%, acetic acid 10% during 30 min. The gel was then destained in destain solution consisting in methanol 30%, acetic acid 10% for 30-60 min. For western blot analysis, proteins on the gel were transferred by electrophoresis to Protran BA 83 nitrocellulose membrane (Schleicher and Schuel). Immunoblots were then immersed in blocking solution consisting of 5% milk powder, 150 mM NaCl, 50 mM Tris pH 8, 0.1% Tween-20 for 30 min. Blots were subsequently incubated with primary antibodies diluted in blocking solution overnight and signals were detected using the ECL Western blotting kit (Pharmacia, Uppsala, Sweden).

II.1.7 NEEP21 Expression During Development

For the analysis of NEEP21 levels at different developmental stages, postnuclear supernatants were prepared as described above. Cortical neurons were lysed in PBS 1X/0.5% T. Protein concentrations were determined by the Bradford technique and Coomassie blue-stained 12% SDS-PAGE. Detection of NEEP21 in the different extracts was made by Western blot.

II.1.8 GST-binding Assay

II.1.8.1 Bacterial Expression of GST-fusion proteins

GST fusion proteins were expressed in Escherichia Coli DH5α (GibcoBRL). Each recombinant protein was tested before producing it at large scale. Bacteria from glycerol stock expressing a GST fusion protein were plated on LB-agar (GibcoBRL) plates, 50 μg/ml ampicillin and allow to grow ovenight at 37°C. The next day one colony was picked and grown up in 5 ml LB, 50 μg/ml ampicillin under agitation at 37°C for 2h. Induction of

recombinant protein was achieved with 100 mM IPTG for 4 h. Bacteria were then centrifuged at 1000 g at 4°C for 10 min and washed once with 1 ml TE pH 7.5 (40m M tris-HCl, 1 mM EDTA pH 8). Bacteria were then centrifuged at 3000 g for 1 min, lyzed with 200 μl lysozyme solution (1 mg/ml lysozyme, 4% sucrose, 30 mM Tris pH 8.0) and left on ice for 10 min. Triton X-100 was added to a final concentration of 0.3% and left again on ice for 2 min. Bacterial lysate was centrifuged at 30 000 g for 1 min and supernant was incubated with 10 μl of gluthatione sepharose beads (Sigma) prepared as described in section II.1.8.2. Beads were then washed once with 1 ml lysozyme solution without lysozyme. Control of the production of recombinant proteins was achieved by separating the recombinant proteins linked to the beads by electrophoresis on a SDS-12% PAGE.

For production of recombinant protein at large scale, a colony was picked as before and let grown up in 50 ml LB medium, 50 μg/ml ampicillin at 37°C overnight. Next day, the culture was diluted 1:10 and OD 600 was measured after about 1 h until it reached 0.8. Then, production of recombinant proteins was induced by 100 mM IPTG at 37°C during 4h. The culture was then centrifuged at 1000 g at 4°C during 10 min (tubes which contained the culture was cooled before use). The pellet was then resuspended in french press buffer consisting in PBS 1X, 1 mM EDTA, 0.1% β-mercaptoethanol, 300 mM PMSF, 0.05% Tween 20. Bacteria suspension was then passed twice through the French Pressure (Thermospectronic) cell to lyse the Bacteria and centrifuged at 10·000 g at 4°C for 10 min. Supernatant was then either frozen or used directly for binding assay.

II.1.8.2 Binding Assay

20 µl of glutathione sepharose beads for each GST fusion protein were incubated in H_2O on ice for 30 min. Beads were washed 3 times with 1 ml H_2O and twice with 1 ml french press buffer. After removal of supernatant, beads were incubated and rolled with 250 μl of each GST-recombinant protein at 4°C for 1 h. Beads were then washed 3 times with 1 ml french press buffer and twice with 1 ml buffer B (see section II.1.3)/1% T. After the last washing, beads were resuspended in 1 volume (20 μl) of buffer B/1% T and 2μl were removed to be loaded and separated on a 12% SDS-PAGE to evaluate the quantity of GST fusion proteins linked to the beads. 1-2 μg of each GST fusion proteins were used typically for binding assay. 2-4 mg of P11 brain extract were incubated on the beads at 4°C for 2 h (if the brain extract was not prepared fresh, it was centrifuged at 10·000g at 4°C for 10 min before to use). Beads

were then washed 3 times with buffer B/1% T and complexes of proteins linked to the GST fusion proteins were analysed by western blot.

II.2 DNA Constructs

II.2.1 NEEP21

Standard DNA procedures were performed according to Sambrook, 1989. We amplified by PCR a full-length mouse clone using oligo-dT-primed mouse brain cDNA, (a gift of Dr Lavery, IBCM, Lausanne, Switzerland). To express tagged protein, the myc-his-coding sequence between XbaI and PmeI of pcDNA3.1/myc-his.B (Invitrogen) was replaced by GAGTACATGCCCATGGAGTGA coding for the EE-tag EYMPMEstop (Grussenmeyer et al., 1985). The cDNA of full-length or deleted mouse 1A75 (NH_2-terminus, aa 1-106 and COOH terminus, aa 77-185), which we propose to name NEEP21, was subcloned by PCR into EcoRI/XhoI upstream of the EE tag. To express NEEP21 antisense RNA, its cDNA was subcloned by PCR in the reverse direction into pcDNA3 between BamHI and EcoRI, downstream of the GFP cDNA and additional stop codons (herein called NEEP21-antisense). The dominant negative mutant used in the recycling assay and in the outgrowth experiments (herein called N129-165) was constructed by subcloning the cDNA that contains the putative interacting domain of NEEP21 with GRIP (129-165), into pcDNA3, downstream of the GFP openr reading frame, between BamHI and EcoRI. For live imaging, we generated NEEP21-YFP and NEEP21-CFP. The full length cDNA of NEEP21 was subcloned by PCR between BamHI and EcoRI upstream YFP in the pEYFP vector or upstream of CFP into the eCFP vector (Clontech Laboratories).

II.2.2 RTN1-C

We amplified by PCR from a mouse cDNA a fragment encoding full-length RTN1-C, which was subcloned between EcoRI and XbaI into the modified vector pcDNA3.1.B-EE upstream the EE-tag.

II.2.3 Syntaxin 13

Amino-terminal myc tagged expresssion constructs were made by amplifying the mouse syntaxin 13 cDNA encoding aa 1-274 for wildtype syntaxin 13 by PCR. The syntaxin 13 fragment was subcloned into the BamHI/EcoRI sites of pcDNA3.1/myc-his.B. For live imaging, we subcloned by PCR the cDNA of syntaxin 13 between BamHI and EcoRI upstream YFP in the pEYFP vector or upstream CFP into the eCFP vector.

II.2.4 GST-fusion proteins

Constructs corresponding to the different NEEP21-fragments were produced by Sarah Magnin, an excellent technician of our group. Briefly, the different DNA fragments were subcloned into the following restriction sites of the pGex-KG vector: NEEP21-amino acid (aa) 104-185, NEEP21-aa104-134, NEEP21-aa129-164 between the EcoRI and XhoI sites, NEEP21-aa104-164 between the EcoRI and NcoI sites, NEEP21-aa167-185 between the NcoI and XhoI sites, and NEEP21-aa129-185 between the BamHI and XhoI sites.

II.2.5 Human Transferrin Receptor

The cDNA of human transferrin receptor was kindly provided by Dr. Lukas Kuhn (Epalinges, Switzerland) and cloned into the EcoRV and XbaI sites of pcDNA3.

II.2.6 Rab5-wild type and Rab5-Q79L

The cDNA of Rab5-wild type and Rab5-Q79L, kindly provided by Dr. R. Regazzi (IBCM, Lausanne, Switzerland) were subcloned by PCR as BamHI/EcoRI fragments downstream of a myc-tag in pcDNA3.

II.3 Cell Cultures

II.3.1 COS-7 Cell Culture, Transfection and Immunoprecipitation

COS-7 cells were grown in a humidified incubator at 37°C and 5% CO_2 in full medium (DMEM,NUT MIX F-12 without Glutamine/10% FCS/2 mM L-Glutamine/25 units Penicillin/Streptomycin (GibcoBRL). Transient transfections were achieved using Fugene

reagent (Roche) or the Calcium Phosphate method. 100'000 to 150'000 cells per 35 mm dish were plated the day before transfection. The next day, DMEM and Fugene was mixed and incubated during 10 min. 1-1.2μg of DNA was added to the mixture and incubated at RT during 30 min. The DNA-fugene complex was then added to the cells. Six h laters cells were washed and grown in fresh medium. For Calcium Phosphate transfection, 500'000 to 1 million cell per 9 cm dish were plated the day before transfection. The next day, fresh medium was added to the cells one hour prior to transfection. Six μg of DNA was mixed with H_2O and 31.5 μl of 2.5 M $CaCl_2$ (final concentration of 250 mM) for a final volume of 250 μl and which was then added dropwise to HBS 2X, pH7.12 (280 mM NaCl, 50 mM HEPES (base), 1.5 mM Na_2HPO_4). The complex DNA-Phosphate-Calcium was incubated 40 min at RT and was then added onto the cells. Six hours later, cells were washed once with full medium and replaced then by fresh medium.

For immunoprecipitation, 2 wells per condition containing cells transfected by the Fugene method were lysed with 100 μl of buffer B, 100 mM K, 1% T (section II.1.3). After centrifugation at 20 000 g at 4°C for 10 min the supernatant was incubated with antibodies crosslinked to 10 μl A- or G-beads at 4°C during 4 h. Beads were washed once with 1 ml buffer B, 100 mM K, 1% T, and twice with 1 ml Buffer B, 100 mM K, 0.5% T. Complexes were then eluted with twice 10 μl of 100 mM glycine pH2.5 in tubes containing 2 μl 1 M Tris pH 10.5. Analyses of immunoprecipitation products were performed by Western blot.

II.3.2 PC12 Cell Culture and Transfection

The pheochromocytoma cell line PC12 (clone ES) (Greene and Tischler, 1976) was cultured in medium of DMEM (GibcoBRL) with 6% fetal calf serum, 6% horse serum and 25 U/ml Penicillin/Streptomycin, on polystyrene dishes (Becton-Dickinson) in humidified 37°C incubator with 7.5% CO_2. Cells were electroporated (Biorad, Gene Pulser system) at 0.26 kV and 925 mF (2 pulses) in serum-free medium containing 50 U/ml Penicillin/Streptomycin (wash medium). We estimated that the transfection efficiency consistently ranged between 10% and 30%. For immunofluorescence, cells were grown on 200 mg/ml poly-D-lysine and 30 mg/ml laminin-coated borosilicate coverslips and induced to differentiate by DMEM with 1% horse serum and 50 ng/ml nerve growth factor (NGF; Promega) for 2 days. For trypsin digestion experiments, PC12 cells were directly plated on 35-mm plastic dishes.

II.3.3 Neuron Cell Cultures and Transfection

All the primary neuronal cultures were kindly prepared by our excellent technician, Liliane Glauser. Cortex or hippocampi without dentate gyri were removed from newborn rat pups (P0) cut in small pieces and in dissociated medium containing 200 units of papain (Sigma) for 30 min at 34°C. The enzyme was neutralized by incubation with trypsin inhibitor (Sigma) for 15 min at RT. The tissue was then triturated with a glass pipette until a suspension of single cells was obtained. Cells were centrifuged at 400 g for 2 min at 20°C. For immunostaining and live imaging, 80 000 cells were plated on 35-mm dishes containing 12-mm and 24-mm poly-D-lysine (200 mg/ml) and laminin (33.2 mg/ml)-coated borosilicate coverslips in MEM (with Earle's salt, without glutamine, (GibcoBRL)), 10% horse serum, 0.5 mM Glutamine, 20 mM glucose, 100 U/ml Penicillin and 100 mg/ml Streptomycin. Medium was changed after 2 h to Neurobasal, 1 :50 B27, 0.5 mM glutamine, 100 U/ml penicillin and 100 mg/ml streptomycin. 10 mM ara-C was added 2 days after plating to arrest growth of glial cells. For biochemistry, hippocampal neurons were prepared slightly differently: 220 000 cells were plated directly into 35-mm dishes coated with poly-D-lysin and laminin. Drug treatment experiments were carried out on cortical neurons at DIV10. They were treated for 60 min with 5 mg/ml BFA or with 100 nM wortmannin before washing, fixation and immunostaining.

Hippocampal neurons plated on coverslips were transfected at P8 or P9 by the Calcium-Phosphate method. Conditioned culture medium was removed and saved. The cells were incubated for 15-30 min in 2 ml neurobasal, 0.5 mM glutamine, 100 U/ml penicillin and 100 mg/ml streptomycin (wash medium). 4 μg for single or double, or 4.5 μg of DNA for triple transfection per each 35mm dish were mixed with 200 mM $CaCl_2$ in a final volume of 60 μl and added very gently to the same volume of HBS 2X pH 7.07-7.12 (274 mM NaCl, 10 mM KCl, 1.4 mM Na_2HPO_4, 15 mM D-Glucose, 42 mM HEPES pH7.4). The mix was then incubated at RT for 30-40 min until a DNA-calcium phosphate precipitate formed. Then it was added drop-wise to each 35 mm-diameter plate. Plates were then returned to the incubator for 30 min. The incubation was stopped by « shocking » the cells for 1 min with Glycerol shock solution (HBS 1X, 10 mM $MgCl_2$ in 5 mM HEPES pH7.5, 5% glycerol). Cells were then rinsed 3 times with 2 ml wash medium. The saved conditioned medium was added back to each plate, and the cells were returned to the incubator.

II.4 Immunocytochemistry

For immunocytochemistry, cells were briefly washed twice in PBS 1X and fixed in 4% paraformaldehyd/4% Sucrose for 10 min. After fixation cells were rinsed 3 times in MTBS buffer (66 mM NaCl, 100 mM Tris-HCl, pH7.4). Cells were incubated with primary antibodies diluted in MTBS containing 20% goat serum, 20% horse serum and 0.3% Triton X-100, 2 h at RT. After rinsing 3 times with MTBS, cells were incubated with either Cy3- or Cy5- or Oregon green-conjugated goat anti-mouse or goat anti-rabbit secondary antibodies for 30 min at RT. Cells were extensively washed and mounted using Vectashield mounting medium (Vector). Immunostained cells were analyzed on a Leica TCSNT confocal microscope or a Leica TCS-AOBS SP2 confocal microscope (Leica).

II.5 Assays

II.5.1 Topology of NEEP21

Non-transfected or transfected PC12 cells with full length NEEP21, or pcDNA3-NH_2-terminus or pcDNA3-COOH-terminus of NEEP21 were plated in 35mm dishes (2 dishes per transfection). After 2 days, PC12 cells were first washed 2 times with 1ml PBS 1X and detached from the dish with a cell scraper. Dishes were washed with 1 ml PBS 1X and the cell supsension was centrifuged at 1000 g for 3 min. Cell pellet was resuspended in 200 μl PBS 1X and homogenized by seven passages through a 25-G needle, centrifuged at 1000 g for 5 min. The supernatant (40 μg) was incubated for 1 h either without additions, or with 4 μg trypsin, or with trypsin and 0.5% T, followed by Western blot. All preparations were done at 4°C.

II.5.2 Transferrin Internalization Assay

PC12 cells, plated on coverslips, were transfected with pcDNA3-hTfR. After 2 days of differentiation, cells were washed once with wash medium and incubated for 10 min at 4°C to stop constitutive receptor internalization. 25 μg/ml of either Oregon green-, FITC- or TRITC-conjugated human Tf diluted in wash medium were added to the cells for 25 min at 4°C which allows the attachment of the Tf to its receptor. Cells were washed twice with 1 ml wash medium and transferred to the incubator, and finally fixed at the indicated times. Immunocytochemistry was then performed for endogenous NEEP21.

II.5.3 Transferrin Cycling Assay

PC12 cells, plated on coverslips, were cotransfected with pcDNA3-hTfR and either pcDNA3-NEEP21-EE, pcDNA3-NEEP21-antisense, or pcDNA3-GFP. After 2 days of differentiation, cells were first washed once with 1 ml wash medium and incubated for 10 min at 4°C and then for 30 min in the presence of 25 μg/ml TRITC-conjugated human Tf in wash medium. Cells were then rinsed twice with 1 ml wash medium and transferred to the incubator for the indicated times. Cells were rinsed twice with 1 ml PBS 1X/30mM Glycine, pH 2.5, to remove all the TRITC-conjugated human Tf linked to its receptor on the plasma membrane and twice with 1 ml PBS 1X before fixation. Cells were then immunostained for endogenous NEEP21.
For hippocampal neuron, the protocol was carried out with the following modifications : cells, plated on coverslips at DIV8, transfected with pcDNA3-hTfR and either with pcDNA3-GFP or pcDNA3-N129-165, were treated 2 days later as described before except that they were incubated with 50 μg/ml TRITC-conjugated human Tf in wash medium.

II.5.4 L1 Surface Labeling

PC12 cells were prepared and transfected as described above (section II.5.3). After 2 days of differentiation, cells were first washed with 1 ml wash medium and chilled for 10 min at 4°C. Cells were incubated for 1 h with an extracellularly binding anti-L1 antibody (dil. 1:2000), and then for 1 h with Cy5-conjugated secondary IgG (dil. 1:100) to block the preexisting cell surface L1 molecules. Then cells were washed 3 times with 1ml wash medium and shifted at 37°C for the indicated times, washed twice with 1 ml PBS 1X, fixed and incubated without detergent with anti-L1, and then with Cy3-conjugated secondary IgG. Cells were then immunostained with anti-EE antibody for NEEP21-EE in permeabilized conditions.

II.5.5 Labeling of Internalized GluR2

Hippocampal neurons after DIV8 were incubated for 1 h at 37°C with 2 mM TTX to block synaptic transmission and for 30 min at 37°C with monoclonal anti-GluR2 antibody against an extracellular epitope in wash medium/2 mM TTX (dil. 1:250). Cells were washed twice with 1 ml wash medium/2 μM TTX, and internalization of AMPARs were stimulated by 100 μM AMPA for 2 min, or 50 μM NMDA for 2 min, or with 500 nM insulin for 15 min (except for time point at 2 min) in wash medium/2 mM TTX. Cells were then further incubated at 37°C for the indicated times. Cells were fixed and Cy5-anti-mouse IgG was added for 30 min

without detergent (dil. 1:100), to block noninternalized GluR2. Then anti-NEEP21 was added with detergent for 2 h, followed by Cy3-anti-mouse IgG and Oregon Green-anti-rabbit IgG.

II.5.6 AMPA Receptor Cycling essay

Hippocampal neurons at DIV8 were transfected with either pcDNA3-GFP, pcDNA3-antisense, or pcDNA3-N129-165 to investigate the trafficking of endogenous AMPA receptor subunits GluR1 or GluR2. To study the trafficking of exogenous subunits, double transfections were done using 6WI-GluR2-HA-tagged, 6WI-GluR1-HA-tagged with the previously mentioned constructs. 2 days after transfection, cells were incubated for 1 h at 37°C with 2 μM TTX. Stimulation of the internal cycling of AMPARs was achieved by applying 50 μM NMDA for 2 min in wash medium/2 μM TTX. Cells were then rinsed twice with 1 ml wash medium/2 μM TTX, and further incubated at 37°C for the indicated time. Cells were then fixed 3 min and stained with either anti-GluR1 (dil. 1:10), or anti-GluR2 (dil. 1:200), or anti-Myc (dil. 1:10), or anti-HA (dil 1:1000), which recognized an extracellular epitope or tag, of teh respective subunits present at the cell surface, in nonpermeabilized condition. . Cy3-secondary antibody was succesively applied during 30 min in nonpermeabized conditions.

II.5.7 Quantification of Dendrite and Axon Length of Hippocampal Neurons

Hippocampal neurons were transfected at DIV10 with either pcDNA3-GFP and pcDNA3, or pcDNA3-EGFP and pcDNA3-HA-GluR2, or pcDNA3-N129-165 and pcDNA3 or pcDNA3-N129-165 and pcDNA3-HA-GluR2. Two days later, neurons were fixed in parafomaldehyde 4% during 12 min and rinsed and immediately mounted. Images of fluorescent cells were acquired using a Leica TCS-AOBS SP2 confocal microscope (Leica) with 20X objective with the same gain and offset parameters for all the different experiments. In addition the pinhole was completely open to increase the fluorescent intensity. In case of cells, whose dendritic arborization or axon extended out of the objective field, several images were made and the complete picture of the total length of dendrites and axon were reconstituted by Photoshop 7.0. Distinction between axons and dendrites were set up by morphological criteria. For all selected neurons, the thinnest and longest process was considered to be the axon. Neurons for which it was not possible to identify clearly the axon from dendrites were not considered. In addition immunostaining with dendritic (MAP2) and axonal (Tau) markers were performed to

clearly distinguish axons and dendrites. For each experiment, 30-50 cells were analyzed for each condition.

II.5.8 Secretion Assay

Secretion assays from PC12 cells were carried out according to (Holz et al., 1994) with modifications. PC12 cells were cotransfected by electroporation with 10 μg pcDNA3-hGH encoding human growth hormone and either 10 μg pcDNA3 (control), or 10 μg pcDNA3.1B-RTN1-C-EE, or pcDNA3.1B RTN1-C-1-41. Cells were then plated into 6 separate wells per condition. Three days after transfection cells were washed 3 times with basal solution K5 (128 mM NaCl, 5 mM KCl, 2.7 mM CaCl2, 10 mM Glucose, 20 mM HEPES pH7.4, 1 mM $MgCl_2$) and incubated in K5 for 30 min at 37°C. Half of the wells for each condition were incubated with basal solution and 0.1% BSA and the other half with stimulation solution (53 mM NaCl, 80 mM KCl, 2.7 mM $CaCl_2$, 10 mM Glucose, 20 mM HEPES pH7.4, 1 mM $MgCl_2$), which stimulated the regulated secretion, for another 10 min. Finally, aliquots of the media in each well were taken and hGH content measured by an ELISA system (Roche). Stimulation was calculated by averaging the 3 basal values (corresponding to 100%) and the 3 stimulated values. The values from 5 independent experiments were cumulated and analyzed by a Student t-test for significant differences.

II.6 Trafficking in Living Cells

Live imaging was achieved using a motorized inverted Zeiss 200M microscope coupled to a monochromator with a Xenon lamp (polychrom IV, Till Photonics) which allowed to select the wavelength of interest and to switch between them in 50-100 ms. Images were acquired with a CCD camera (Coolsnap FX, Visitron). The whole system was controled by Metamorph software (v. 4.1). The monochromator was switched on 2 hours before each experiment. Living transfected hippocampal neurons, plated on a 24-mm coverslips, were transferred into the chamber of the microscope at 37°C and with 7-9% CO_2.

For trafficking experiments, neurons transfected with NEEP21-CFP and syntaxin 13-YFP were incubated in wash medium. One image in the CFP (ex. 433 nm, em. 475 nm) and YFP (ex. 513 nm, em. 527 nm) channels were acquired every 30 sec.

II.7 Quantitative Image Analysis

All experiments were done at least 3 times. Quantification of antisense experiments and internalization of AMPARs were done as following : 3 confocal sections covering the whole thickness of the cell were acquired with identical parameters (power of lasers, PMT detection threshold), and in each case the middle section was used for quantification. For colocalization between NEEP21 and GluR2 staining, 2 separate confocal images for the red (1) and green (2) channels were acquired. The laser line corresponding to the channel in which no image was acquired was switched off to prevent no crosstalk. For image analysis, the threshold was set to reduce background and optimized to specific signal at a fixed value. The intersection image of the merged red and green channels were separated into red (3) and green (4) channels corresponding to the double-labeled pixels. The number of pixels and their intensity was calculated by NIH image software to obtain the mean pixel intensity and number of labeled pixels per image. The value of channels (1) and (2) were added (which correspond to the total fluorescence = 100%, pixels being red or green). The same was done with channel (3) and (4) (corresponding to the colocalization, pixels being red and green)). The value corresponding to the colocalization were then divided by the value corrresponding to the total fluorescence, ((3)+(4))/((1)+(2))*100 to determine the fraction of the total signal which was colocalized. For quantification of endogenous surface AMPA receptor labeling in antisense experiments, the threshold was set by NIH image software to a level that suppressed all noncellular signals to 2 pixels/cm2 (corresponding to 0.3% of all pixels) to have a minimal visual backround density. For experiments with N129-164, quantification was done using Metamorph software with the same parameters.

Quantification of dendrite and axon length of hippocampal neurons was achieved using NeuronJ software, a semiautomatic neurite tracing technique (Meijering et al., 2004) on fluorescent images. Briefly, each process was identified by clicking at its beginning and at its end. For each process, its identity (axon or dendrite) was set up manually. The software recognizes the cellular process and automatically calculates its length. For the cases of processes that physically overlap or ambiguous situations, the tracing was done manually.

III Results

III.1 Identification of Potential Syntaxin 13-interacting Proteins

In order to investigate the molecular mechanisms of the endocytic pathway during neuronal differentiation, we immunopurified syntaxin 13-binding proteins specifically enriched in developing brain. We prepared membrane protein extracts from postnatal day 3 (P3) and adult rat brain, and sequentially passed them over a non-specific IgG column and specific anti-syntaxin 13 column. Bound and eluted proteins were separated on SDS-PAGE and the gel stained with Coomassie Blue (Figure 6A). This allowed us to visualize and distinguish non-specific from specific syntaxin 13-binding proteins. Several proteins whcih bound non-specifically, including tubulin, appeared in the elutions which correspond to bands present in the IgG column as well as the specific columns (Figure 6A). On the other hand, elutions from P3 and adult brain extracts of both specific columns, showed many bands which corresponded to potential syntaxin 13-interacting proteins, since they were absent in the non-specific IgG columns. In aggreement with our previous finding(Hirling et al., 2000), we detected syntaxin 13 at 38 kDa with a lower intensity from adult than from P3 brain (Figure 1A and 1B). We verified the specificity of the two syntaxin 13 columns by doing Western blots using elutions of the non-specific and specific column, probed with anti-SNAP25 antibodies. SNAP-25 was shown to interact with syntaxin 13 to form SNARE complexes (Prekeris et al., 1998). We found that it was only detected in eluates from the specific column and never in these from the non-specific IgG columns (Figure 6B). This verified that even in the presence of a strong background, the syntaxin 13 columns can immunopurify specific syntaxin 13-contining protein complexes. We then concentrated our analysis on 3 bands specifically present in the syntaxin 13 column elutions from P3 brain membrane extracts (Figure 6A, N° 1-3). In addition, we also included in our analaysis a band present in both P3 and adult brain (Figure 6A, N° 4). In order to obtain enough material, seven such immunopurifications representing a total of 21 g of P3 and adult rat brains, were pooled together and loaded on a separate SDS-PAGE. After migration, the gel was coloured with amido-black and candidate bands were cut out from the gel and sent for microsequencing to the Institut Pasteur, Paris. We obtained single peptide sequences for the bands N° 1, 3, 4 and a major (2a) and a minor (2b) sequence for band N° 2 (Figure 6A). Data base searches revealed the identity of the proteins containing the microsequenced peptides: (1) FLVPDHVN, corresponding to microtubule-associated protein 1 light chain 3 (LC3) (Mann and Hammarback, 1994); (2a) SVSPWMSV,

corresponding to a brain-specific rat clone 1A75 (Sutcliffe et al., 1983) and a recently cloned mouse full-length cDNA 1A75/p21 (Saberan-Djoneidi et al., 1998); (2b) AYLELEIT, corresponding to Reticulon 1 (RTN1)/Neuroendocrine-Specific Protein (NSP) (van de Velde et al., 1994a); (3) SYQLRPGT, correpsonding to 4-nitrophenylphosphatase synaptosomal associated protein 1 (NIPSNAP1) (Seroussi et al., 1998); (4) NRLDYHIS, corresponding to mitochondrial ATP synthase β chain, (Boyer, 1997; Tsurumi et al., 1990). The characteristics of these different proteins will be described in the following paragraph.

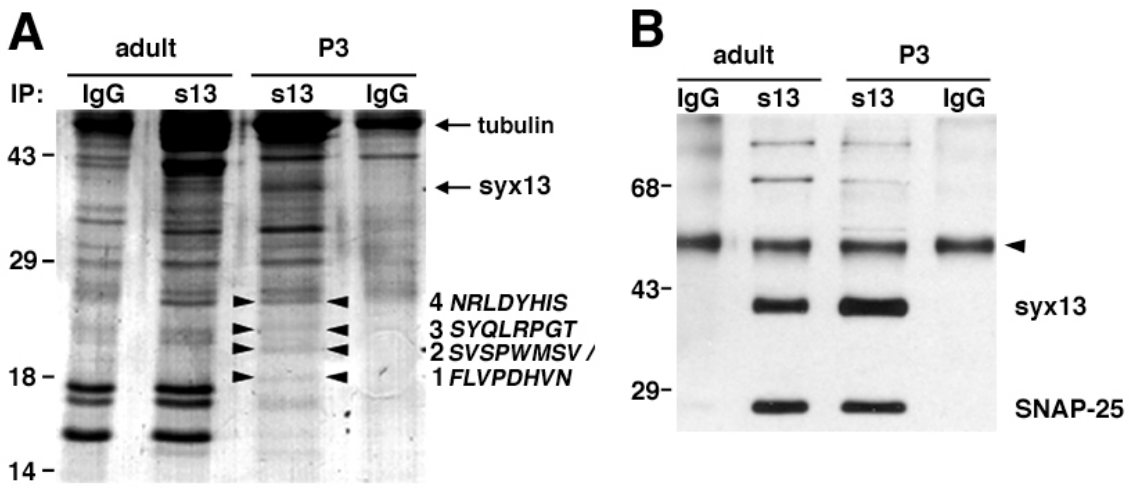

Figure 6. Identification of new syntaxin 13-binding proteins. (A) Membrane extracts from P3 and adult brains were sequentially passed over non-specific rabbit anti-IgG and anti-syntaxin 13 antibodies. Bound proteins were eluted and separated on SDS-PAGE and stained with Coomassie blue. The different bands chosen for purification and microsequencing are between arrowheads with their corresponding contained peptide sequences. (B) Immunoblot against SNAP-25 on the 4 different elutions, P3 and adult non-specific IgG elutions, P3 and adult specific syntaxin 13 elutions. The blot was probed with polyclonal anti-syntaxin 13 and monoclonal anti-SNAP-25 antibodies. Arrowhead shows crossreacting antibody heavy chains since we used the same anibodies (anti-syntaxin 13) for IP and blot. Molecular weights are in kDa (s13, anti-syntaxin 13 antibodies column ; syx13, syntaxin 13).

Light chain 3 (LC3)

Microtubule-associated protein 1A (MAP1A) and MAP1B are large proteins that co-purify with microtubules and are abundantly expressed only in the brain (Mann and Hammarback, 1994; Mann and Hammarback, 1996). MAP1A and MAP1B are composed of heavy and a combination of multiple light chains. Immunoprecipitation studies indicate that both the MAP1A and MAP1B heavy chains associate with light chain 1 (LC1) and LC3 (Kuznetsov and Gelfand, 1987). MAP1A and MAP1B are major components of the neuronal cytoskeleton

which are associated with microtubules. They are believed to regulate the organisation of microtubules in neurites and thus could play an important role in neuronal differentation, especially the extension of axons and dendrites (Gordon-Weeks and Fischer, 2000)

NEEP21(1A75/p21)

1A75/p21, that we propose to name NEEP21 (Neuron-Enriched Endosomal Protein of 21kDa) and the highly homologous p19 belong to a new family of proteins whose function had not been characterized (Saberan-Djoneidi et al., 1995; Saberan-Djoneidi et al., 1998). NEEP21 was described as being highly expressed in the brain and also present in germ cells (Saberan-Djoneidi et al., 1998). It was also postulated that NEEP21 is a type-I integral membrane protein with one transmembrane domain. Saberan-Djoneidi et al. associated NEEP21 with a Golgi-like staining pattern, and speculated that it might play a role in chemotaxis or respiratory activity (Saberan-Djoneidi et al., 1998).

Reticulon1-C (RTN1-C)/Neuroendocrine-Specific Protein-C (NSP-C)

Reticulons (RTN) are a family of membrane proteins localized primarily to the endoplasmic reticulum (ER) (Oertle and Schwab, 2003; van de Velde et al., 1994a). Among the 3 splice variants, RTN1-A/NSP-A, RTN1-B/NSP-B RTN1-C/NSP-C, the latter one, RTN1-C corresponds to the one identified by the syntaxin 13-immunoaffinity column. It had been shown to be expressed by neurons and cells of neuroendocrine tissue, and its expression is increased upon differentiation in PC12 cells and neuroblastoma cell lines (Hens et al., 1998). At this point no molecular function has been proven for RTN proteins belonging to the reticulon family.

4-nitrophenylphosphatase synaptosomal associated protein 1 (NIPSNAP1)

NIPSNAP1 and NIPSNAP2 were first identified during large-scale characterization of human genomic sequences from chromosome 22 (Seroussi et al., 1998). Recently it was shown that NIPSNAP1 was localized to the postsynaptic density of synapses (Satoh et al., 2002). NIPSNAP has been implicated in vesicular trafficking because its gene localizes in an operon encoding SNAP-25-like proteins in C. Elegans (Seroussi et al., 1998).

Mitochondrial ATP synthase β chain

The β-chain of the ATP synthase is a principal protein complex of the mitochondrial inner membrane (Boyer, 1997). This complex allows the coupling of the energy present in the

electrochemical proton gradient established across the mitochondrial membrane, to the formation of ATP from ADP and P_i (Leyva et al., 2003). More recently it was shown that β-chain of the ATP synthase was also present at the cell surface of hepatocyte and that it could play an essential role in cholesterol transport (Martinez et al., 2003).

At this stage we decided to characterize NEEP21 and RTN1-C, of these potential syntaxin 13-interacting proteins because the bands corresponding to NEEP21 and NSP were clear and easily identifiable, arguing for the strongest interactions that we have considered. In addition, NEEP21 was associated with Golgi-like structures and was postulated to play a role in trafficking, as for syntaxin 13. RTN-1/NSP overexpression in fibroblasts was shown to provoke formation and extension of processes (Senden et al., 1996); knowing that syntaxin 13 overexpresssion in PC12 cells increases the length of neurites (Hirling et al., 2000), we hypothesized that RTN1-C/NSP-C could share a common function with syntaxin 13. Because of the presence of a high proportion of tubulin in the purification we decided at first not to consider LC3, assuming that it could correspond to a non-specific interaction due to its association with microtubules. Concerning NIPSNAP1, the band was identified with difficulty and probably reflected a weak interaction. Finally we did not choose ATP synthase β chain because when we identifed it, the protein was known to be localized only on mitochondria (735), so we concluded that it was a non physiological interaction. Nevertheless, LC3, NIPSNAP1 and ATP synthase β chain will be investigated in the near future.

III.2 NEEP21 is Involved in Glutamate AMPA Receptor Cycling

III.2.1 Characterization of a Polyclonal NEEP21 Antibody

In order to study the endogenous NEEP21 protein, we raised a polyclonal antibody against a peptide spanning amino acids 7-23 with the commercial service Eurogentech. After peptide-affinity purification of the antibody we checked its specificity by Western blot using postnatal day 3 rat brain extracts (Figure 7A) and immunocytochemistry on hippocampal neuron cultures (Figure 7B). The anti-NEEP21 antibody recognized a single band at 21kDa, corresponding to the putative size of NEEP21 (Saberan-Djoneidi et al., 1998) (Figure 7A, lane b and c), which did not appear using the preimmune serum (lane a), or purified antibodies preblocked with the peptide (lane d). In hippocampal cultures, the anti-NEEP21

antibody revealed that NEEP21 is localized to round structures (puncta) present in the cell body and also along processes of the cells (Figure 7B, arrow). We also noted that NEEP21 is highly present in the perinuclear region (Figure 7B, arrowhead). These results indicate that polyclonal NEEP21 antibody is efficient by and specifically detects the endogenous NEEP21 protein.

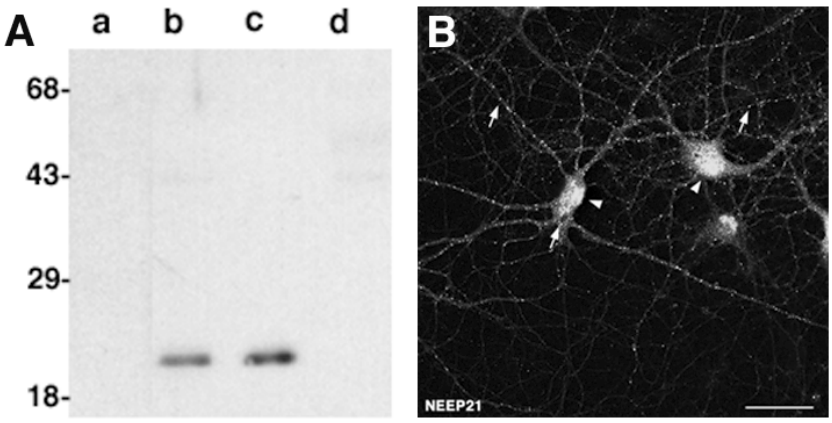

Figure 7. Characterization of polyclonal anti-NEEP21 antibody. (A) Immunoblot of P3 rat brain extract (30μg) using a polyclonal anti-NEEP21 antibody. Lane a, preimmune serum ; lane b, crude immune serum ; lane c, affinity-purified antibody ; lane d, purified antibody blocked by 50 ng of antigenic peptide. Molecular weights are in kDa (B) Hippocampal neurons at DIV 8 stained with anti-NEEP21 antibody. Arrows show NEEP21 present in punctate structures and arrowheads show enrichment of NEEP21 in cell body. Single confocal section is shown. Scale bar, 20 μm

III.2.2 NEEP21 Forms a Complex with Syntaxin 13

To obtain the cDNA of NEEP21, we amplified by PCR and subcloned it from mouse cDNA with the help of one of our technicians, Catherine Chevaley. The NEEP21 cDNA was then subcloned in a modified pCDNA3 vector containing the EE-tag. To verify that NEEP21 and syntaxin 13 could form a complex, we overexpressed EE-tagged NEEP21 and myc-tagged syntaxin 13 in a fibroblast cell line, COS-7 cells. NEEP21 appeared in the COS-7 cell extract as a major band at 21 kDa and syntaxin 13 at 38 kDa (Figure 8A). Both anti-myc and anti-EE antibodies coprecipitate myc-syntaxin 13 and NEEP21-EE in a specific manner; it was not possible to detect any corresponding bands in the non-specific IgG control immunoprecipitation (Figure 8A). We also tested whether the complex between NEEP21 and syntaxin 13 exists in brain preparations. We immunoprecipitated endogenous syntaxin 13 and NEEP21 from P3 rat brain membrane extract (Figure 8B). Anti-syntaxin 13 beads immunoprecipitates syntaxin 13 and coimmunoprecipitate NEEP21 and in the reverse

situation, anti-NEEP21 beads immunoprecipitates NEEP21 and coimmunoprecipitates syntaxin 13. Control non-specific IgG beads do not precipitate either protein, arguing for the specificity of the interaction between NEEP21 and syntaxin 13. The substoichiometric bands that we observed after coimmunprecipitations suggested that only a small fraction of both proteins are present in a complex at steady state. We originally identified syntaxin 13 in a complex with SNAP-25, another SNARE protein which participates in the formation of SNARE complexes, which might, among other fusion steps, be implicated in endosomal fusion (Prekeris et al., 1998; Sun et al., 2003). Therfore, we immunoprecipitated SNAP-25 to analyze whether NEEP21 could interact with SNAP-25 (Figure 8C). We immunoprecipiated SNAP-25 but did not coimmunoprecipitate NEEP21. These results show that NEEP21 and syntaxin 13 can form a complex which is different from the complex between syntaxin 13 and SNAP-25.

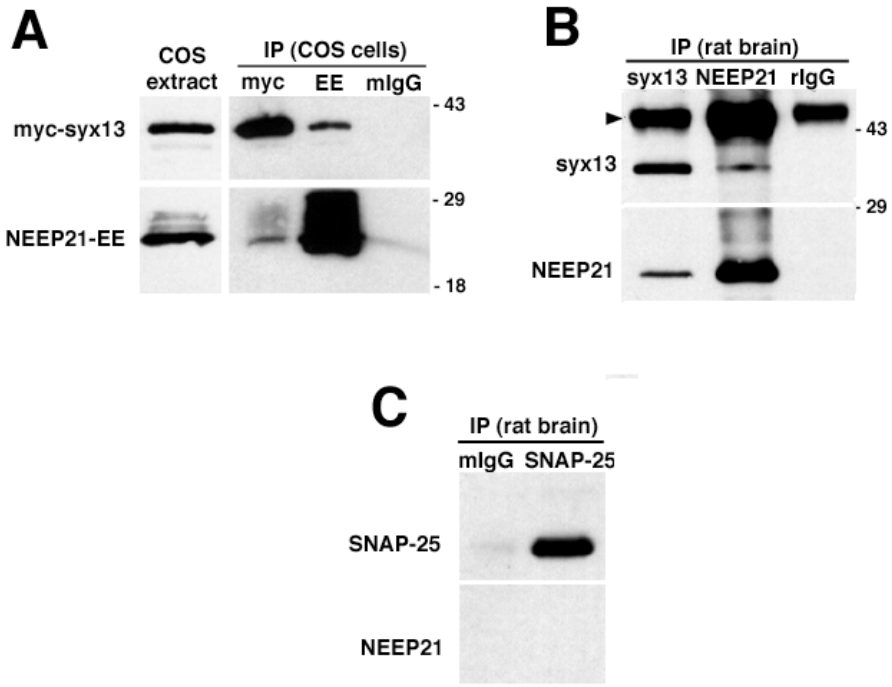

Figure 8. NEEP21 forms a complex with syntaxin 13. (A) Immunoprecipitation from COS-7 cells cotransfected with myc-tagged syntaxin 13 and EE-tagged NEEP21. COS extract and elutions for IP with monoclonal anti-myc, anti-EE or non-specific anti-IgG are shown. Detection on blots used anti-syntaxin 13 or anti-NEEP21 antibodies. (B) Immunoprecipitation from membrane extracts of P3 rat brain using polyclonal anti-syntaxin 13, anti-NEEP21, or rabbit non-specific IgG antibodies. There are crossreacting antibody heavy chains (arrowhead) as the same antibodies were used for IP and immunoblots. (C) As in B, but using monoclonal anti-SNAP-25 antibodies, mouse non-specific IgG for immunoprecipitation, and polyclonal anti-NEEP21 and monoclonal anti-SNAP25 antibodies for blot. Molecular weight are indicated in kDa.

III.2.3 NEEP21 is Strongly Expressed during Neuronal Maturation and Synapse Formation

Because we detected NEEP21 only from postnatal brain, we investigated the regulation of its expression during brain development. Previous Northern blot analysis characterized NEEP21 mRNA levels in rat cerebral hemispheres at different development stages from E14 to P21 (Saberan-Djoneidi et al., 1998), and found that NEEP21 mRNA was present as early as embryonic day 14. Its expression increased during embryognenesis to reach its maximum level of expression around embryonic day 20 and its expression faded afterward to reach adult levels at postnatal day 15. In agreement with this study and our affinity purification, NEEP21 was strongly detected by Western blot around birth, and then decreased at postnatal day 14 (Figure 9A). This pattern corresponds to that of syntaxin 13 (Hirling et al., 2000). In contrast, the level of synaptic vesicle protein 2 (SV2) is increased during the first 2 postnatal weeks and then is stabilized to reach a plateau around postnatal day 17 (Figure 9A). We also investigated the developmental expression profile of NEEP21 in dissociated cortical neuronal cultures at different stages (Figure 9B). As before, SV2 increased during the first 2 weeks of culture, whereas NEEP21 was already strongly expressed on day 2 and its level decreased at around day 14. Together these data confirmed that NEEP21 is developmentally regulated and its strongest level of expression correlates with neuronal maturation and synapse formation.

III.2.4 Membrane Topology of NEEP21

Analysis of the primary sequence of NEEP21 revealed that the NH_2-terminal domain (aa 1-84) and the COOH-terminal domain (aa 106-185) are hydrophilic and the intermediate domain (aa 85-103) corresponds to a transmembrane domain (Saberan-Djoneidi et al., 1998). To analyze the membrane orientation of NEEP21, we prepared membrane fractions of non-transfected or transfected PC12 cells with either full-length NEEP21-EE (aa 1-185), its NH_2 terminus (aa 1-106), or its COOH terminus (aa 77-185).

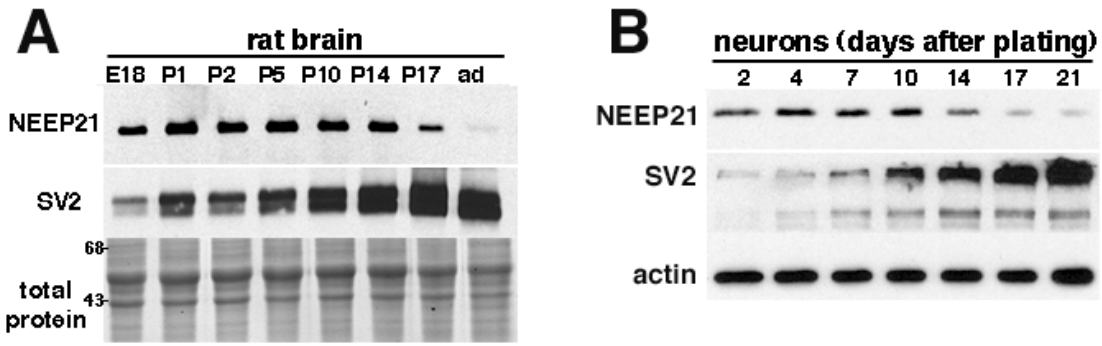

Figure 9. NEEP21 is strongly expressed during neuronal maturation and synapse formation. (A) Western blot of rat brain extracts (30μg) at different developmental stages (E, embryonic day ; ad, adult) probed with polyclonal anti-NEEP21 and monoclonal anti-SV2 antibodies. A parallel Coomassie blue-stained gel (total protein) indicates equal loading. (B) Immunoblot of extracts from rat cortical neuron cultures (30μg) at the indicated ages, probed with polyclonal anti-NEEP21, monoclonal anti-actin, or anti-SV2 antibodies. Molecular weights are indicated in kDa.

We treated membrane fractions with either trypsin alone, which digests all cytosolic proteins and domains of proteins present in the cytosol, or trypsin and detergent which permeabilise organelles and eradicates all proteins, and compared these to untreated membrane. We then analysed the presence of endogenous NEEP21 or transfected NEEP21 constructs with antibodies which recognized the NH_2- (anti-NEEP21) or COOH- (anti-EE) terminal domains (Figure 10A). Without trypsin digestion, anti-NEEP21 antibodies recognized endogenous NEEP21 (arrow) as well as transfected full-length protein NEEP21-EE (arrowhead) and the NH2 terminus (asterisk). In addition, anti-NEEP21 antibodies recognized a band around 17 kDa which is probably a product of degradation. Upon trypsin digestion, endogenous and full-length proteins were no longer detected by anti-NEEP21 antibodies, whereas the 17 kDa band and additional products of degradation appeared. In contrast, the NH_2 terminus was always detectable at the same size before and after trypsin digestion (asterisk). With trypsin treatment, the intensity of the band, corresponding to the NH_2 terminus, decreased, which could be explained by organelles that did not stay completely sealed during treatment and thus allowed the degradation of a fraction of NH_2 terminus no more protected. Trypsin incubation in the presence of detergent degraded every protein (Figure 10A). These data indicated that the NH_2 terminus of NEEP21 is protected by membrane during trypsin treatment. In cells overexpressing full-length NEEP21-EE (arrowhead) or the COOH terminus (circle), anti-EE antibodies recognized both proteins, but after trypsin digestion with or without addition of detergent, it was no longer possible to detect the corresponding band (Figure 10A). Taken

together theses results demonstrated that the COOH terminus of NEEP21 is oriented toward the cytoplasm, whereas the NH_2 terminus is localized in the lumen of the organelles (Figure 10B). Because we did not observe labeling in anti-NEEP21 immunostaining on PC12 cells in the absence of detergent (data not shown), it is unlikely that NEEP21 is present at the plasma membrane at steady state.

Since the COOH terminus of NEEP21 is localized in the cytosol of PC12, we postulated that this domain would interact with syntaxin 13. COS-7 cells were cotransfected with myc-syntaxin 13 and either the full-length NEEP21-EE (aa 1-185) or the COOH terminus of NEEP21 (aa 77-185). The anti-EE antibody immunoprecipitated the exogenous full-length and the COOH terminus of NEEP21 speciesand coimmunorpecipitated myc-syntaxin 13 in both situations (Figure 10C). These results shows that the COOH terminus of NEEP21 is sufficient to form a complex with myc-syntaxin 13 in COS-7 cells.

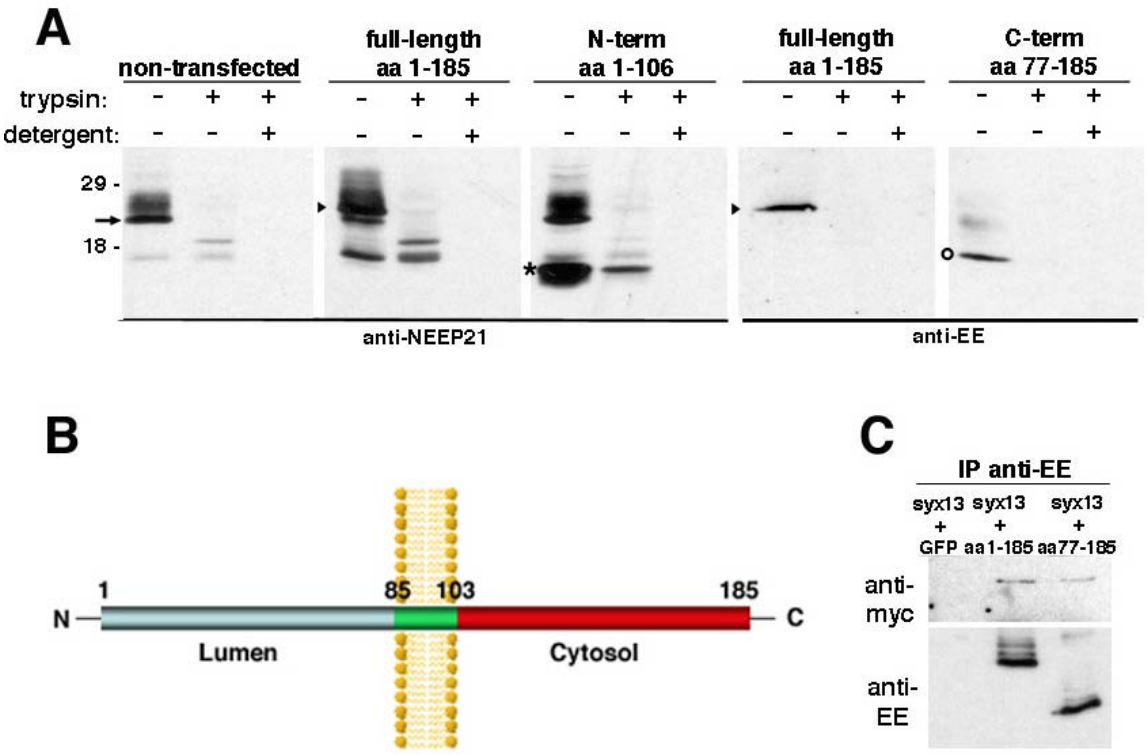

Figure 10. Membrane topology of NEEP21. (A) Membrane fractions (40 μg of proteins) of non-transfected PC12 cells, or cells transfected with full length NEEP21-EE (aa 1-185 ; arrowhead), its NH_2 terminus (aa 1-106, asterisk), or its COOH terminus (aa 77-185, circle) were incubated without or with 4 μg trypsin and 0.5% Triton X-100. They were then immunoblotted with anti-NEEP21 antibodies recognizing the NH2 terminus or with anti-EE antibodies recognizing the COOH terminus. (B) Model of NEEP21 topology with its NH_2 terminus in the lumen of organelles, and its COOH terminus in the cytosol. Note the presence of a transmembrane domain spanning aa 85-103. (C)

Immunoprecipitation with anti-myc antibodies using extracts of COS cells transfected with myc-tagged syntaxin 13, and either GFP, or the full length NEEP21-EE, or COOH terminus domain. Blots were probed with anti-myc and anti-EE antibodies. Molecular weights are in kDa.

III.2.5 NEEP21 is Localized Along the Early Endosomal Pathway

Due to its interaction with syntaxin 13, which is localized mainly onto the recycling endosome (Prekeris et al., 1998), we asked wether NEEP21 would be localized along the early endosomal pathway. To answer this question, we performed immunofluorescence on PC12 cells and primary cortical neuron cultures using combinations of markers for different vesicular compartments, and drugs which affect their morphology.

We examined the localization of endogenous NEEP21 and transfected NEEP21-EE in differentiated PC12 cells. We found in both cases that NEEP21 was present, as in Figure 7B, in the cell body and along the neurites of PC12 cells on round structures or puncta (Figure 12). When we compared the staining corresponding to NEEP21 and myc-syntaxin 13, we observed that NEEP21 staining was partially colocalized with the less regularly shaped myc-syntaxin 13-labeled organelles (Figure 12A-C, and compare inserts in A-C). NEEP21 was originally thought to be localized on Golgi-like structures (Saberan-Djoneidi et al., 1998). Therefore, we verified whether NEEP21 would be colocalized with a marker of the trans-Golgi network, TGN38 (trans-Golgi network of 38 kDa) (Lee and Banting, 2002; Luzio et al., 1990). Overlap between transfected NEEP21-EE (Figure 12D) and endogenous TGN38 (Figure 12E) was limited to the perinuclear region, but we did not see a clear colocalization between the well defined NEEP21-EE puncta and TGN38 structures.

Since it coprecipitates with syntaxin 13, we tested whether NEEP21 is present along the endosomal pathway. One of the most studied markers for the early endosomal pathway is the transferrin receptor (Buckley et al., 2000; Gruenberg and Maxfield, 1995). The transferrin (Tf)-transferrin receptor (TfR) system is reponsible for iron uptake from the extracellular medium into the cell (Richardson and Ponka, 1997). Iron-bound Tf in the extracellular medium delivers iron to cells by binding to TfR present at the cell surface. The iron-Tf-TfR complex is internalized into endocytic clathrin-coated vesicles which fuse then with sorting endosomes where iron is released due to acidic pH (Figure 11). A small fraction of Tf-TfR complexes is then recycled directly to the plasma membrane, while the majority of Tf-TfR complexes traffick through the recycling endosome before reaching the plasma membrane, (Figure 11). The time-course of the trafficking through the early endosmal pathway of Tt-Tf

receptor complex in fibroblast is well known (Figure 11) (Buckley et al., 2000; Gruenberg and Maxfield, 1995) : The complex enters the sorting endosome with a $t_{1/2}$ of 1.5-3 min then exits this compartment with a $t_{1/2}$ of 7 min to reach the recycling endosome. The final recycling step of the complex is relatively slow with a $t_{1/2}$ of 12 min.

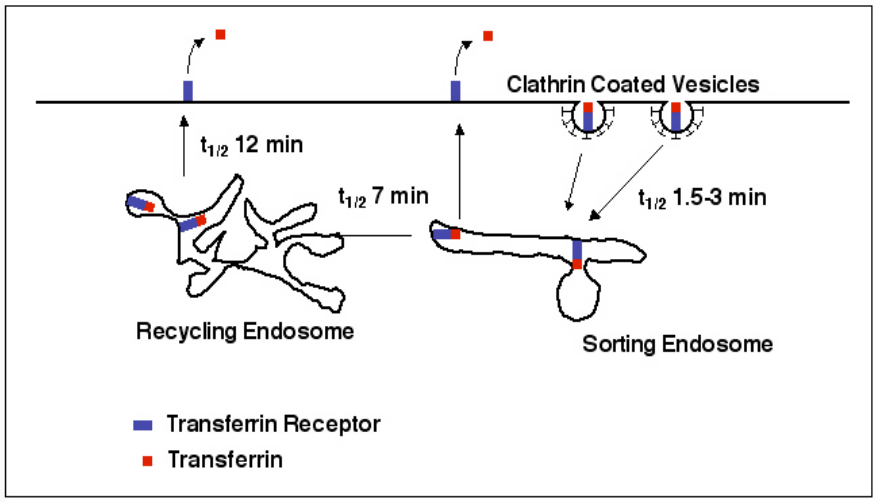

Figure 11. Scheme showing the Transferrin Receptor trafficking through the early endosomal pathway. Transferrin (Tf)-Transferrin Receptor (TfR) complex is responsible for iron delivery to cells. Iron bound to the Tf-TfR complex is internalized into endocytic clathrin-coated vesicles which fuse with sorting endosomes with a $t_{1/2}$ 1.5-3 min. Iron is released inside sorting endosomes and a small fraction of the Tf-TfR complex is recycled directly to the plasma membrane. The majority of Tf-TfR complexes trafficks through recycling endosomes in $t_{1/2}$ of 7 min. The final step of recycling between recycling endosomes and the plasma membrane is relatively slow with a $t_{1/2}$ of 12 min. Once the Tf-TfR complex is back to the plasma membrane Tf detached from TfR and is ready to bind iron and starts a new cycle.

We thus internalized Tf to demarcate the early endosomal pathway. PC12 cells with prebound surface FITC-labeled Tf were incubated for 3 or 15 min at 37°C to allow Tf endocytosis and trafficking through the early endosomal pathway (Figure 12H and K). At 3 min, endosomal compartments positive for FITC-Tf rarely colocalized with endogenous NEEP21 (Figure 12G, overlay in I), whereas at 15 min, the majority of both signals are colocalized (Figure 12J, K, overlay in L). Because at 3 min, Tf should localize to endocytic vesicles transported to or fusing with sorting endosomes (Figure 11), we conclude that NEEP21 is primarily associated with Tf-postivie compartments beyond the transport to sorting endosomes.

We also analyzed whether NEEP21 could be present along the degradation pathway. We costained PC12 cells for NEEP21 and lysobiphosphatidic acid (LBPA) (Figure 12N and

overlay in O), a phospholipid enriched in late endosomes (Kobayashi et al., 1998). We did not observed any significant colocalization, ruling out a late endosomal localization of NEEP21. These results indicate that NEEP21 localizes along the early endosomal pathway between the sorting and the recycling endosomes (Gruenberg and Maxfield, 1995).

III.2.6 NEEP21 Is Detected in Wortmannin-Sensitive Endosomes

We also analyzed the localization of NEEP21 in cortical neurons. Similar to immunostainings carried out in PC12 cells, NEEP21 is localized to distinct puncta (Figure 13A, D, and G), which colocalized partially with transfected myc-syntaxin 13 (Figure 13B and overlap in C). We also verified by costaining for the endogenous TfR that NEEP21 colocalizes in cortical neurons with TfR-positive endosomes. We found that NEEP21 puncta overlapped (Figure 13I, arrow) or were in close apposition with TfR-positive endosomes (Figure 13I, enlarged area). TfR-positive organelles correspond either to sorting or recycling endosome. To distinguish whether NEEP21 is selectively present on one of these 2 compartments, we applied brefeldin A (BFA) and wortmannin. BFA inactivates various Arf GTPases, inhibits the transport between the Golgi appartus and the ER (Chardin and McCormick, 1999; Klausner et al., 1992) and causes tubulation of TfR-positive organelles (Lippincott-Schwartz et al., 1991). More specifically, BFA was shown to affect endosomal compartments which correspond mainly to recycling endosomes (Sonnichsen et al., 2000). When we treated cortical neurons with BFA, TfR is observed in a tubule-like staining pattern (Figure 13K) compared with control cells (Figure 13E and H). The staining corresponding to NEEP21 (Figure 13J) is slightly more diffuse and NEEP21-positive organelles appeared smaller compared to control, but rarely colocalized with TfR (Figure 13, compare L and F). This suggests that NEEP21 is present on BFA-insensitive endosomes. Wortmannin is an inhibitor of the phosphatidylinositol-3-kinase (PI3K) (Vanhaesebroeck et al., 2001) which provokes an enlargement of TfR-positive structures (Malide and Cushman, 1997; Stenmark et al., 1994) corresponding to an early or intermediate recycling step, implicating the sorting endosomes (Sonnichsen et al., 2000). In cortical neurons treated with wortmannin, TfR is detected in patchy disk-like structures (Figure 13, N). NEEP21 localized to enlarged irregular puncta (Figure 13, M) that overlapped strongly with the TfR-positive patches (Figure 13, O). Altogether, these results show that NEEP21 localizes to a wortmannin-sensitive endosomal compartments which presumably corresponds to sorting endosomes

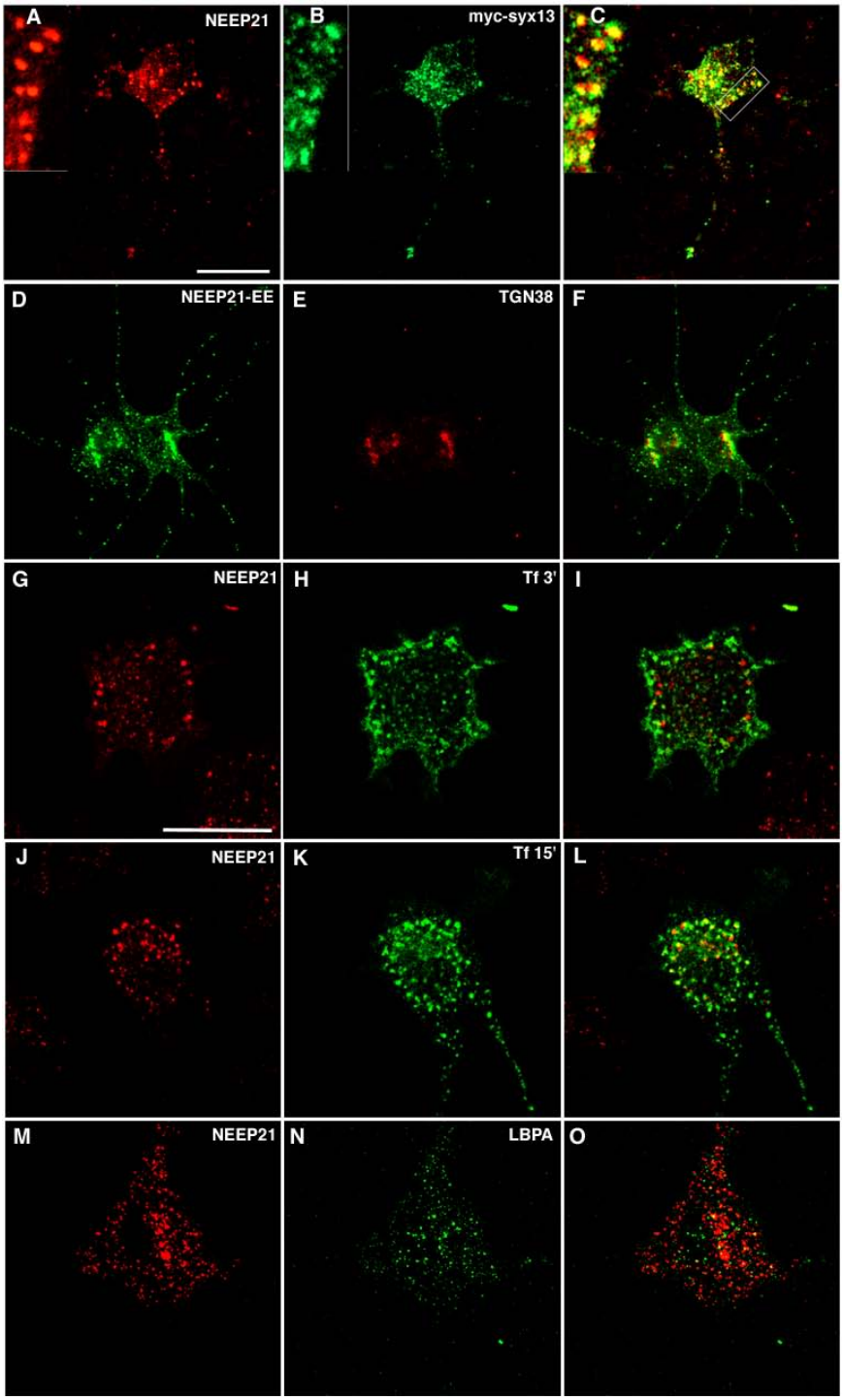

Figure 12. NEEP21 localizes along the early endosomal pathway in PC12 cells. (A-F) PC12 cells were transfected with myc-tagged syntaxin 13 (A-C) or EE-tagged NEEP21 (D-F) followed by NGF differentiation for 2 days and immunostained with antibodies against NEEP21 (A), Myc (B), EE (D), TGN38 (E). Note partial colocalization of NEEP21 with myc-syntaxin 13 in inserts of A-C. (G-L) PC12 cells transfected with human TfR were incubated on ice with human FITC-conjugated Tf, and subsequently at 37°C without Tf for 3 (H) or 15 min (K), and immunostained for NEEP21 (G and J). (M-O) PC12 cells were immunolabeled for NEEP21 (M) and the late endosomal marker LBPA (N). Scale bars, 20 μm. Single confocal sections are presented. Overlays are on the right panel.

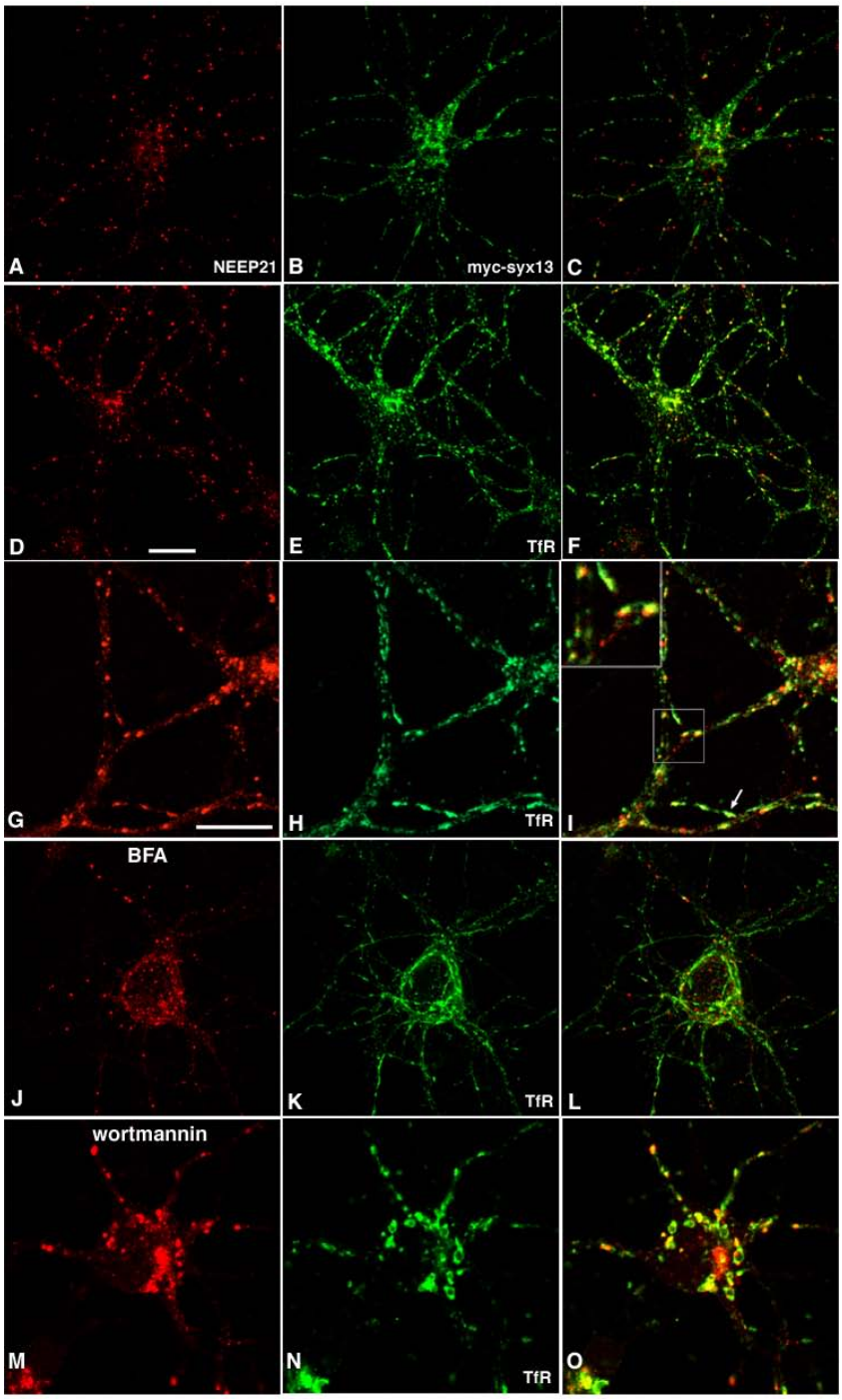

Figure 13. Localization of NEEP21 in neurons and redistribution by BFA and wortmanin. (A-C) Cortical neurons transfected with myc-syntaxin 13 were immunostained at DIV 10 using anti-NEEP21 (A) and anti-myc antibodies (B, overlay in C). (D-O) Untreated coritical neurons (D-I) or treated for 60 min with 5 μg/ml BFA (J-L) or with 100 nM wortmannin (M-O) were immunostained using anti-NEEP21 (D, G, J, and M) and anti-TfR antibodies (E, H, K, and N). Single confocal sections are shown. Scale bars 20 μm. Overlays in F, I, L, O.

III.2.7 NEEP21 is Present in a Rab4-Positive Compartment

To localize NEEP21 along the early endosomal pathway, we checked for colocalization between NEEP21 and myc-Rab5, endogenous Rab4, Rab11, and EEA1 in PC12 cells. Rab proteins are small GTPases which have multiple functions, ranging from organelle motility (Lebrand et al., 2002), membrane budding (mclauchlan, 1997) or docking (Christoforidis et al., 1999) to interactions with the cytoskeleton (Nielsen et al., 1999). In addition, EEA1 was shown to be a docking factor involved in endosomal fusion (McBride et al., 1999; Mills et al., 2001). All of them are associated preferentially with distinct compartments along the early endosomal pathway (Sonnichsen et al., 2000; Zerial and McBride, 2001) (Figure 14). Rab5 and EEA1 are involved in an early step of trafficking associated with sorting endosomes (Christoforidis et al., 1999; Gorvel et al., 1991; Simonsen et al., 1998). Rab4 is present in an intermediate step of trafficking between sorting and recycling endosomes (Daro et al., 1996; van der Sluijs et al., 1992), and Rab11 is known to be involved in the control of fusion processes between recycling endosomes, the plasma membrane and the trans-Golgi network (Ullrich et al., 1996; Wilcke et al., 2000). Rab7 was identified along the late endosomal pathway and was shown to be necessary for correct fusion processes associated with late endosomes and lysosomes (Feng et al., 1995; Meresse et al., 1995).

Immunostainings against Rab4, Rab5, Rab11, EEA1 annd NEEP21 in PC12 cells show that the discrete NEEP21 puncta (Figure 15, left) rarely colocalized with compartments positive for myc-Rab5 (Figure 15B, and overlay in C). In contrast there is a strong colocalization between NEEP21 and Rab4 (Figure 15, D-F). In immunostaining for NEEP21 and Rab11, a few colocalizing signals were observed (Figure 15G-I). We also overexpressed in PC12 cells a dominant negative mutant of Rab5, Rab5-Q79L which causes an enlargment of sorting endosomes due to an increased fusion of endocytic vesicles (Stenmark et al., 1994).

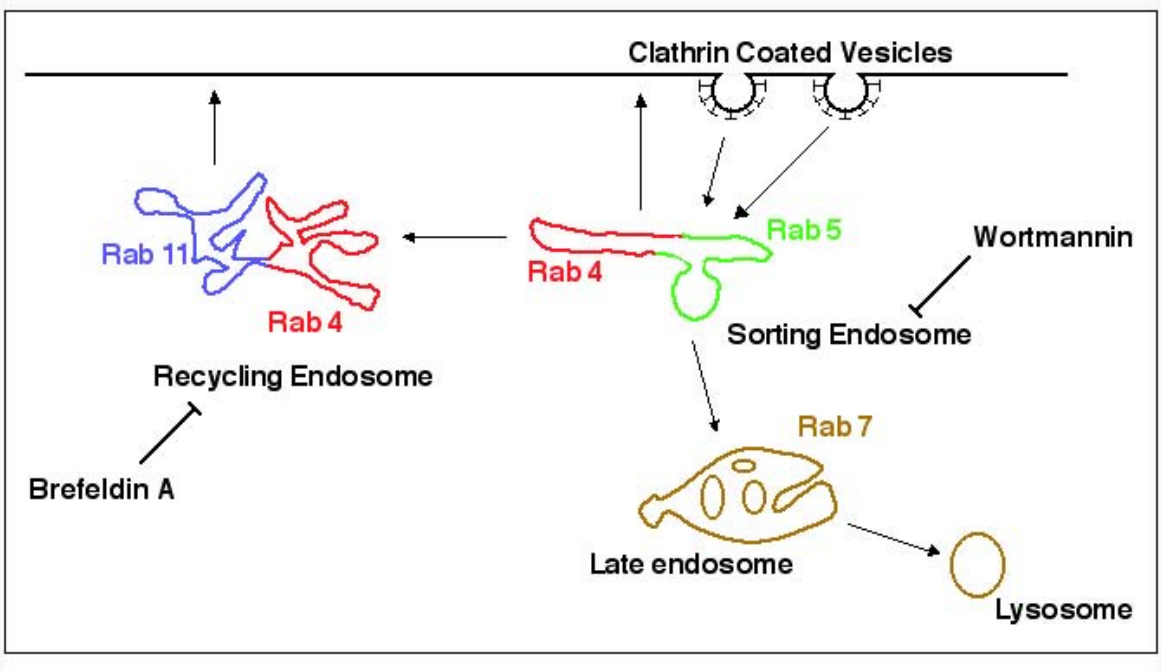

Figure 14. Model of subdomain organization along the endosomal pathway. The domain distribution of Rab4, Rab5, EEA1, Rab11 and Rab7 present onto sorting, recycling and late endosomes is depicted in red, green, blue and brown. Arrows indicated directions of trafficking through the different compartments. Cargo which enters into cells via clahrin-dependent pathway are mainly Rab5-containing structures. Fast recycling is achieved by rapid sorting from Rab5 into Rab4-positive domains on the same endosome. Recycling slows down once molecules enter pericentriolar membranes dominated by Rab4 and Rab11 domains. Wortmanin affects specifically the morphology of sorting endosomes while BFA disturbs recycling endosomes. (Adapted from (Sonnichsen et al., 2000; van der Goot and Gruenberg, 2002).

We found a complete overlap between endogenous NEEP21 (Figure 15J) and transfected Rab5-Q79L (Figure 15K and overlay in L). Little colocalizing signals were observed between NEEP21 (Figure 15M) and EEA1 (Figure 15N) confirming the results obtained with transfected myc-Rab5. Taken together, these immunocytochemistry data in PC12 cells and in primary neuronal cultures, showed that: (1) NEEP21 localizes mainly to the sorting endosomes ; (2) NEEP21 is present into the domain of sorting endosomes enriched with Rab4, which is known to be involved in the decision-making of receptor sorting between sorting endosomes, recycling endosomes, late endosomse and the plasma membrane (Cormont et al., 2001; Sonnichsen et al., 2000; Spiro et al., 1996; van der Sluijs et al., 1992) (Figure 16).

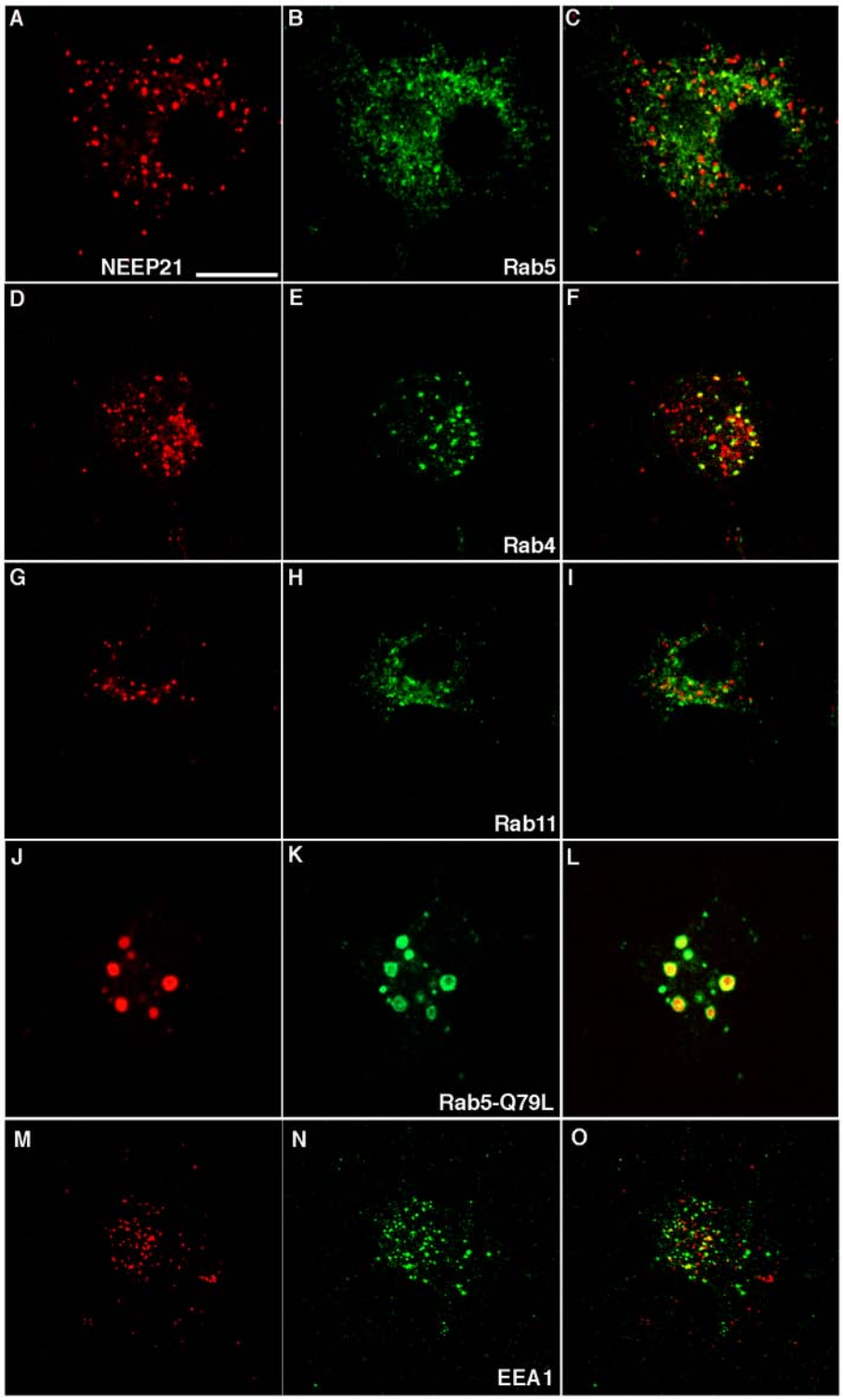

Figure 15. NEEP21 colocalizes with Rab4 and Rab5Q79L, but rarely with wild-type Rab5, Rab11, and EEA1. PC12 cells, transfected with myc-tagged wild type Rab5 (A-C), RabQ79L (J-L), or non-transfected PC12 cells (D-I and M-O) were labeled with anti-NEEP21 (left) and either anti-myc (B and K), -Rab4 (E), -Rab11 (H), or -EEA1 (N) antibodies. Single confocal sections are shown. Overlays on the right panel. Scale Bar, 10 μm.

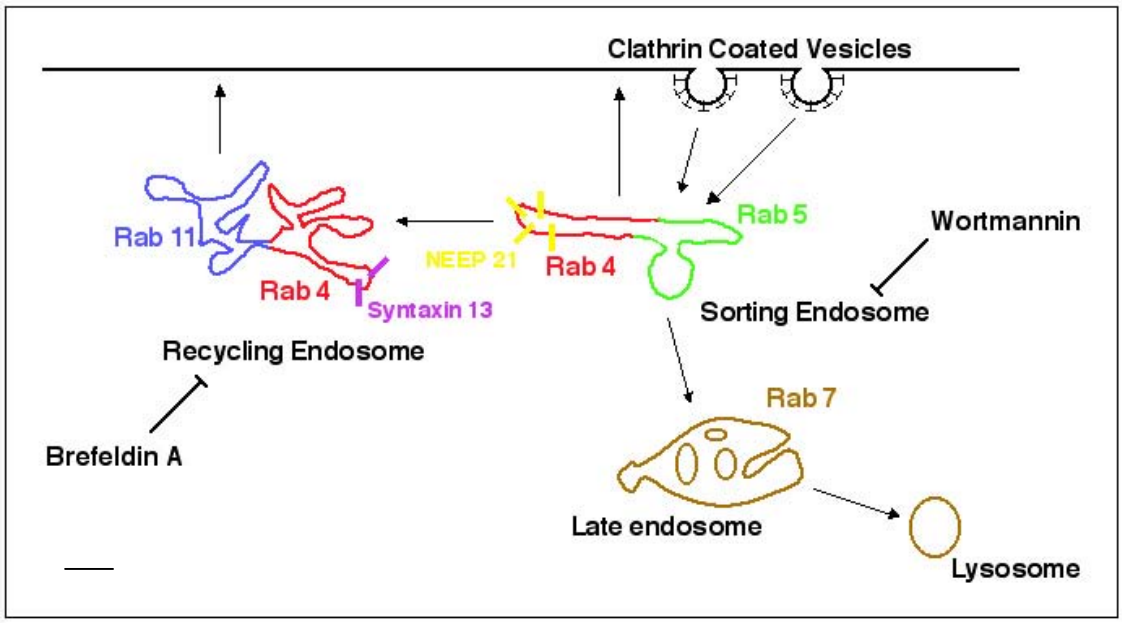

Figure 16. NEEP21 is localized on the subdomain of sorting endosomes enriched in Rab4. NEEP21 (yellow) is present on wortmannin-sensitive endosomes corresponding to sorting endosomes. It is principally present on a subdomain which is enriched in Rab4 and known to be necessary for correct sorting of molecules. Syntaxin 13 (purple) is enriched on recycling endosomes and is crucial for correct recycling of molecules. (Adapted from (Sonnichsen et al., 2000; van der Goot and Gruenberg, 2002).

III.2.8 Trafficking of NEEP21 in Living Hippocampal Neurons

Our data concerning the localization of NEEP21 showed that it was localized mainly on an endosomal compartment which differs from syntaxin 13-positive endosomes. Because we also found that both proteins form a complex, we investigated their behaviour using Green Fluorescent Protein (GFP) technology in living hippocampal neurons. GFP originally isolated from jellyfish *Aequorea victoria* (Prasher et al., 1992; Shimomura et al., 1962) , has been extensively used as a genetic fusion partner of host proteins to monitor their localization and fate in living cells or organisms (Tsien, 1998). The cDNA encoding a GFP is fused in frame with the cDNA encoding the endogenous protein and the resulting chimera is expressed in the cell or organism of interest. The ideal result is a fusion protein that maintains the normal functions and localizations of the host protein but is now fluorescent. We fused to the carboxyl terminal of NEEP21 a mutant of GFP, cyan fluorescent protein (CFP) and to the carboxyl terminal of syntaxin 13 another mutant of GFP, yellow fluorescent protein (YFP) (Heim and Tsien, 1996). Coexpression of these 2 fusion proteins in hippocampal neurons

allowed us to follow the trafficking of NEEP21-CFP and syntaxin 13-YFP after proper illuminations corresponding to CFP (excitation :430 nm, emission : 475 nm) and YFP (excitation :495 nm, emission : 527 nm). Because the excitation and emission of CFP and YFP are distinct, it is possible to clearly identify the compartments positive for NEEP21-CFP and syntaxin 13-YFP at the same time (Figure 17). We used a CCD camera to take pictures of NEEP21-CFP and syntaxin 13-YFP every 30 sec, to follow their trafficking. NEEP21-CFP was present in puncta which are relatively stationary and whose shape remains constant along time (Figure 17A, enlarged area in D). Syntaxin 13-YFP was detected in tubule-like organelles which are dynamic structures, moving constantly compared to NEEP21-CFP-positive organelles (Figure 17B, enlarged area in E). In addition, their shape is continually changing. We did not observe a significant colocalization between NEEP21-CFP and syntaxin 13-YFP signals, suggesting that NEEP21-CFP and syntaxin 13-YFP are present on different endosomal compartments, but we noted that NEEP21-CFP- and syntaxin 13-YFP are often in close apposition (Figure 17C, overlays, enlarged area in F). These data showed that NEEP21 is present in punctate structures in living hippocampal neurons confirming our immunostaining experiments achieved on fixed PC12 cells and primary neurons. They also showed that syntaxin 13 is preferentially found on tubular organelles as previously described (Prekeris et al., 1998). Moreover, the absence of colocalization but the close apposition of NEEP21-CFP and syntaxin 13-YFP organelles suggest that the interaction between both proteins could happen at the interface of these structures.

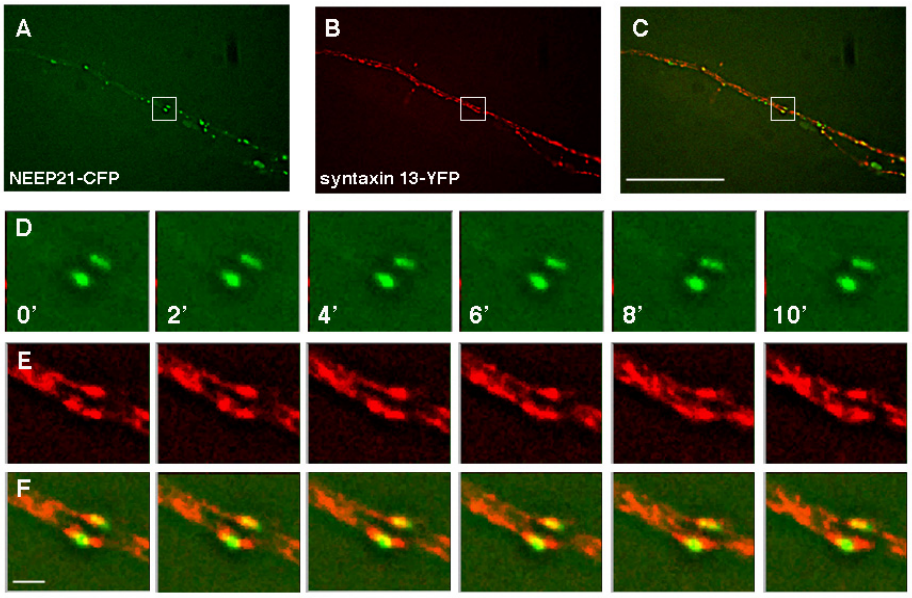

Figure 17. Trafficking of NEEP21-CFP and syntaxin 13-YFP in living hippocampal neurons. Transfected hippocampal neurons (DIV 11) with NEEP21-CFP and syntaxin 13-

YFP, kept at 37°C and 5% CO_2, were illuminated at 430 nm (CFP) and 495 nm (YFP). Pictures of NEEP21-CFP and syntaxin 13-YFP were taken every 30 sec with a CCD camera, to follow the trafficking of both chimeric proteins. (A-B, overlay in C) Process of neuronal cells overexpressing NEEP21-CFP and syntaxin 13-YFP. Scale bar 25μm. (D) Higher magnification shows that NEEP21-CFP is present on puncta which are relatively stable while (E) syntaxin 13-YFP positive structures correspond to tubules which are highly dynamic. (overlay in F) Note the absence of complete colocalization between NEEP21-CFP and syntaxin 13-YFP-positive structures. Images were acquired using a bright field microscope and monochromator illumination. Scale bar 2 μm.

III.2.9 Downregulation of NEEP21 Expression using Antisense Techonology

Due to NEEP21 localization in a domain of the early endosomal pathway which is crucial for receptor sorting, and because it interacts with syntaxin 13 which is necessary for correct Tf-TfR recycling (Prekeris et al., 1998), we hypothezised that NEEP21 could be involved in receptor cycling. We tested whether changing NEEP21 expression affects receptor cycling. Our strategy to downregulate its expression was to construct a plasmid carrying the NEEP21 cDNA in reverse direction, downstream of the green fluorescent protein (GFP) open-reading frame. This yields a RNA whose first part will allow GFP translation and the second part will hybridize to endogenous NEEP21-coding RNA (Figure 18A). We verified that the NEEP21-antisense construct could downregulate NEEP21 expression by doing immunocytochemistry in hippocampal neurons and Western blot in COS-7 cells (Figure 18B and C). When transfected into hippocampal neurons, NEEP21 staining (Figure 18B, middle) is clearly decreased in NEEP21-antisense-positive cells (top and middle rows) compared with the GFP-transfected cell (bottom row). Staining for MAP2 was indistinguishable (right) showing that NEEP21 downregulation did not affect the gross morphology of dendritic arborization. Because Western blotting in hippocampal neurons or PC12 cells was not possible due to the low transfection efficiency, we used transfected COS-7 cells. Cotransfection of NEEP21-EE and GFP yielded a strong NEEP21-EE expression (Figure 18, C, right lane). In contrast, upon cotransfection of NEEP21-EE and NEEP21-antisense, NEEP21 expression was specifically downregulated (Figure 18C, middle lane), whereas nonrelated EEA1, actin, αSNAP, Rab11, and Rab4 were not affected. These results show that NEEP21-antisense is powerful to

downregulate NEEP21 expression. Therefore, we used the NEEP21-antisense plasmid to analyze the effect of NEEP21 suppression on receptor cycling.

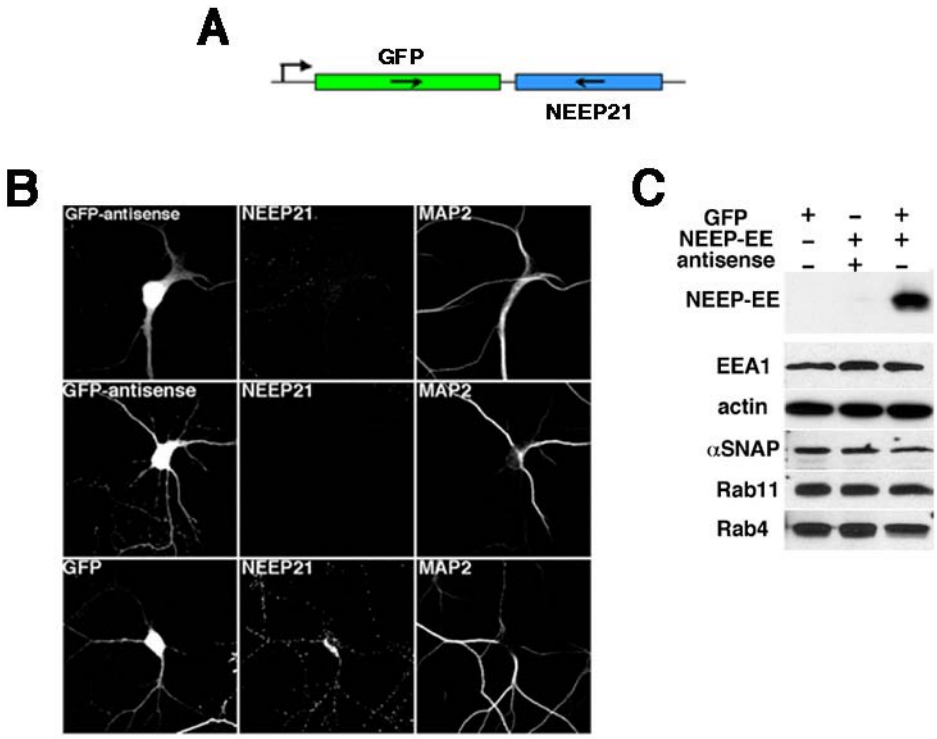

Figure 18. NEEP21-antisense construct downregulates specifically NEEP21 expression. (A) NEEP21-antisense design : subcloning of NEEP21 cDNA (blue) in reverse direction, downstream of the GFP open-reading frame (green). (B) NEEP21-antisense (top and middle row), or GFP alone (bottom row) were transfected into hippocamppal neurons. NEEP21 staining (middle) is strongly reduced in NEEP21-antisense-transfected cell ; MAP2 staining on the right panel. Single confocal sections are shown (C) Western blot from COS-7 cells cotransfected with the indicated cDNAs. Antisense abolishes NEEP21 expression, while endogenous nonrelated proteins, indicated on the left of the figure are not affected.

III.2.10 Overexpression or Suppression of NEEP21 Modulates Transferrin Receptor and L1 Cycling in PC12 Cells

To analyze whether changing NEEP21 expression level affects receptor cycling, we used the cycling of Tf-TfR as a model. As described before, the time course of internalization and recycling of Tf-TfR is well known (Buckley et al., 2000; Gruenberg and Maxfield, 1995). Moreover its trafficking through the early endosomal pathway is precisely described (Gruenberg and Maxfield, 1995). Therefore, we overexpressed the human TfR and either GFP (control), NEEP21-antisense (suppression), or NEEP21-EE (overexpression) in PC12 cells to

test the modulation of NEEP21 expression on TfR cycling (Figure 19A-B). Two days after transfection, PC12 cells were preincubated on ice with rhodamin-conjugated human Tf, followed by incubation at 37°C without Tf, which provokes the internalization of the rhodamin-conjugated Tf-TfR into the cells. External Tf was removed by acid stripping and then cells were fixed at different time to follow its trafficking along the early endosomal pathway. Suppression or overexperession of NEEP21 was verified by immunocytochemistry. Fluorescence of internalized Tf was quantified on confocal sections. Tf labeling of GFP-transfected cells corresponds to a typical time course of Tf internalization/recycling : the fluorescence intensity increases up to 15 min, corresponding to the internalization of the Tf, with a maximal internal accumulation. Then it decreases progressively reflecting the recycling of the Tf (Figure 19A, black bars). Suppression of NEEP21 had no effect up to 15 min, but then strongly delayed the decrease of internal Tf (white bars, $P < 0.01$) compared to the control. Even after 2 h, 46% of the 15 min maximal fluorescence remained ($P < 0.01$). Figure 19B shows an antisense-transfected cell that is Tf-positive (left), which illustrates the delay in the reycling of Tf, and a GFP-transfected cell that is Tf-negative at 60 min. The absence of endogenous NEEP21 verified the downregulation of its expression (bottom row). In contrast, overexpression of NEEP21-EE resulted in a significant increase of the internalization of Tf at 3 and 5 min ($P < 0.01$), and a more rapid recycling at 30 and 60 min ($P < 0.01$). (Figure 19A, grey bars). In an equivalent assay using peroxidase-conjugated Tf, we confirmed that NEEP21-EE overexpression accelerated internalization of Tf (Steiner et al., 2002a). In all conditions, the same maximal internalization was observed at 15 min.

To verify whether cycling of another, unrelated membrane protein is also modulated in PC12 by NEEP21, we tested recycling of the endogenous neuronal adhesion molecule L1 (Figure 19C-D). The cell adhesion molecule (CAM) L1 of the immunoglobulin superfamily plays a crucial role in axon growth and guidance during development (Kenwrick and Doherty, 1998). It was shown that L1, during axonal growth, was internalized into the early endosomal pathway and then recycled to plasma membrane, a process which was demonstrated to be fundamental for correct axon elongation (Kamiguchi and Lemmon, 2000). Costaining shows significant colocalization of internal L1 in NEEP21-positive endosomes (Figure 19C, arrowhead), suggesting that a fraction of L1 trafficks through endosomes which contain NEEP21. By surface labeling using an extracellularly binding anti-L1 antibody (kindly provided by Lemmon, V) on PC12 cells (preblocked at 0-min time point), we found that NEEP21 antisense transfection (Figure 19D, white bars) significantly retarded reinsertion of L1 into the plasma membrane compared with GFP transfection at 45, 60 and 120 min (black

bars, P < 0.01). NEEP21-EE overexpresssion accelerated the internalization of L1, but to a smaller extent (Figure 19D, gray bars, P < 0.02). These results showed that NEEP21 is essential for correct receptor cycling in PC12 cells. Furthermore, it also suggests that NEEP21 acts on a large range of different receptors and could be an essential component of trafficking along the early endosomal pathway.

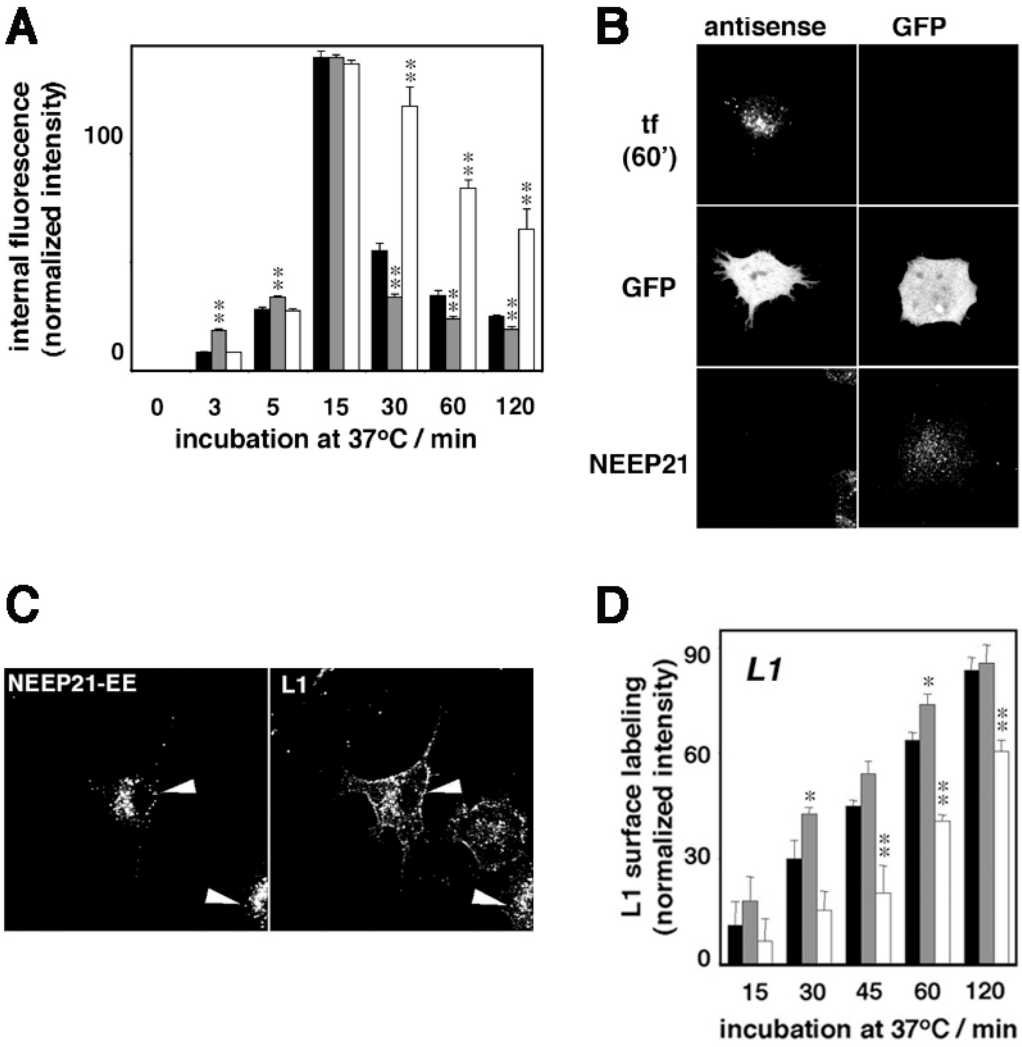

Figure 19. NEEP21 modulates Tf and L1 cycling. (A) PC12 cells, cotransfected with human TfR and either GFP (black bars), NEEP21-EE (gray bars), or NEEP21-antisense (white bars), were incubated on ice with rhodamin-Tf, and subsequently at 37°C without Tf for the indicated times. Acid washed cells were immunolabeled for NEEP21. Tf fluorescence on confocal images was quantified. Significant differences by NEEP21 overexpression or suppression compared with GFP are indicated by double asterisks (P < 0.01). Error bars indicate SEM. (B) Typical cells transfected with NEEP21-antisense (left) or GFP (right) as in A at 60 min. Single confocal sections are shown. (C) Colocalization of NEEP21 with L1 ; double-labeled structures are indictated by arrowheads. Single confocal sections are shown. (D) PC12 cells, transfected as in A (without hTfR), were surface labeled at 0 min using an anti-L1 antibody against an extracellular epitope and Cy5 secondary IgG antibody,

and then incubated for the indicated times. Cells were fixed and again surface labeled for L1 and Cy3 secondary IgG antibody to label newly inserted L1. Significant effects compared with controls are indicated with single ($P < 0.02$) or double ($P < 0.01$) asterisks. Error bars indicate SEM.

III.2.11 NEEP21 Localizes to the Somatodendritic Domain of Neurons

We next analyzed the localization of NEEP21 to specific neuronal domains. Neurons possess polarized discrete functional domains (Horton and Ehlers, 2003b). During their development, neurons proceed to develop axonal and somatodendritic domains which are distinct on a morphological and molecular bases (Craig and Banker, 1994; Winckler et al., 1999). We investigated whether NEEP21 has a preferential localization using markers of the somatodendritic compartment (MAP2), axons (Tau, SNAP-25), and of synaptic vesicles (SVs) (SV2, synaptophysin) in hippocampal neurons. NEEP21-positive puncta were present in the cell body and processes (Figure 20A, D, G, J, and M), which in all cases where positive for MAP2 (Figure 20B and overlay in C). In contrast, fibers outlined by Tau (Figure 20E) and SNAP-25 (Figure 20 H) did not overlap with NEEP21. These results show that NEEP21 is present in the somatodendritic domain of neurons.

To rule out that NEEP21-labeled structures were presynaptic boutons, we costained for SV2 (Figure 20K) and synaptophysin (Figure 20N). SV2 and synaptophysin staining revealed round puncta corresponding to the presynaptic part of synapses. We did not observe a significant overlap between NEEP21, SV2 or synaptophysin stainings. Moreover, signals were clearly separated. Nevertheless, the processes positive for NEEP21 were often surrounded by the synaptic vesicle markers. This is evident in the selected areas of Figure 20J and K, and M and N, which are enlarged overlays, L and O, respectively. This suggests that NEEP21-endosomes are not present in the presynaptic part of synapses. In addition, it also means that there are synapses onto NEEP21-containing dendrites.

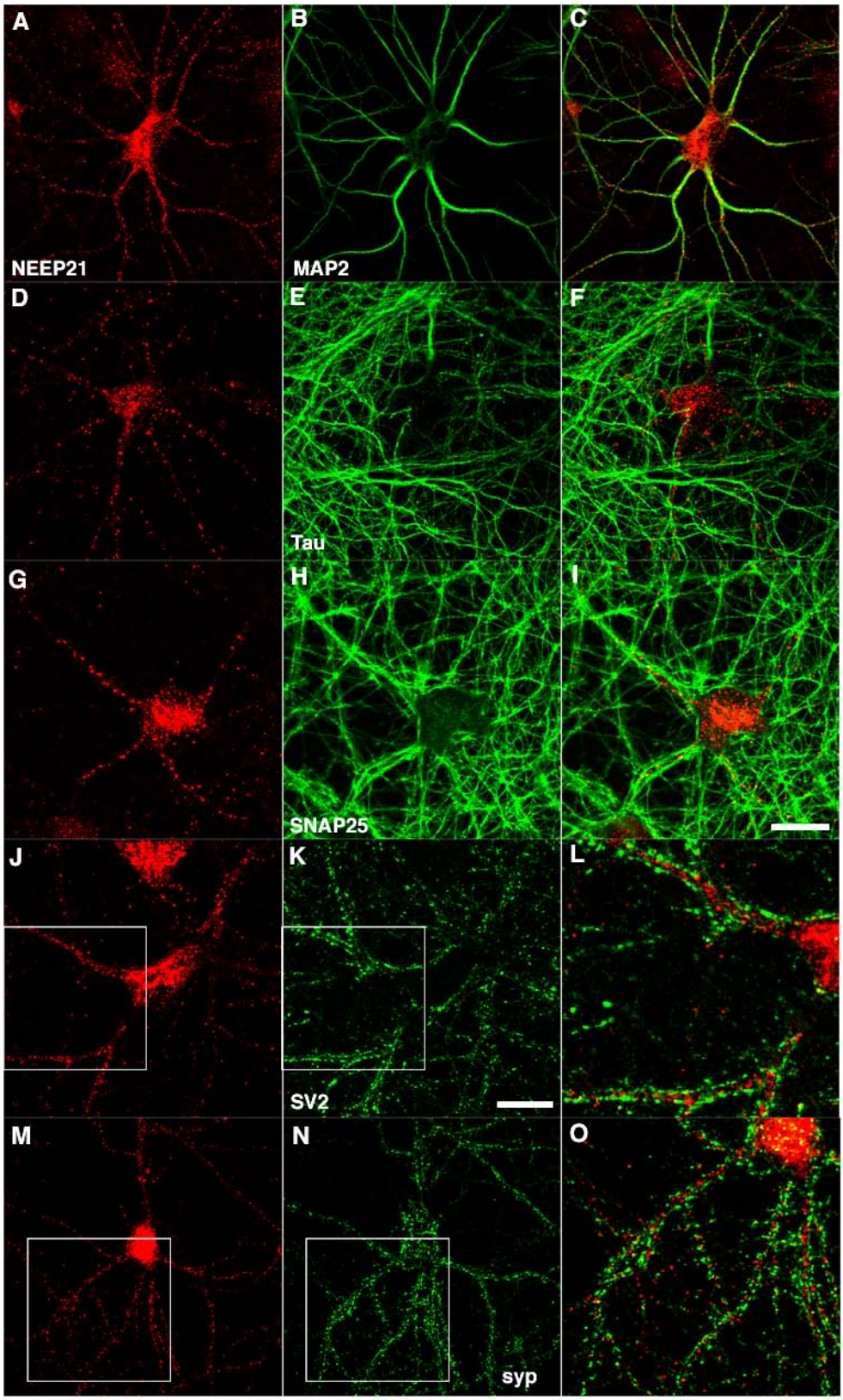

Figure 20. NEEP21 localizes to the somatodendritic domain of hippocampal neurons. Hipppocampal neurons at DIV 10 were double labeled using antibodies against NEEP21 (A, D, G, J), and MAP2 (B), Tau (E), SNAP-25 (H), SV2 (K), or synaptophysin (N). Overlays on the right panel.

Marked areas in J, K, and M, and N are enlarged in L and O, respectively. Single confocal sections are shown. Scale bars are 20 μm.

III.2.12 AMPA Receptors Traffick Through NEEP21-Positive Endosomes

Given the implication of NEEP21 in cycling of receptors in PC12 cells and its somatodendritic localization in hippocampal neurons, we asked whether NEEP21 is important for trafficking of neuronal receptors. AMPA (alpha-amino-3-hydroxy-5-methyl-4-isoxazolepropionate) receptors, which are constituted of 4 different subunits (GluR1-4), are the most abundant glutamate receptor found in excitatory neurons of the CNS and mediate the postsynaptic depolarization that initiates neuronal firing (Kauer et al., 1988; Muller et al., 1988). Their internalization into endosomal compartments is thought to be tightly regulated and crucial for synaptic strength (Beattie et al., 2000; Carroll et al., 1999b; Ehlers, 2000; Lin et al., 2000). In addition they are enriched in the somatodendrtitic domains of neurons. Therefore, we decided to analyze the effect of NEEP21 suppression in hippocampal neurons on trafficking of AMPA receptors.

The first step was to control that internalized AMPA receptors traffick through NEEP21-positive endosomes (Figure 21). We chose to analyze the trafficking of GluR2 AMPA receptor subunit. It has been suggested that AMPA receptors take different trafficking routes depending on the stimulus (Ehlers 2000 ; Lin, Ju et al. 2000) : stimulation with AMPA seems to direct these receptors into the degradative pathway (Ehlers 2000 ; Beattie, Carroll et al. 2000 but see also Lin, Ju et al. 2000), while NMDA application leads to their recycling (Ehlers 2000). It was also demonstrated that insulin can stimulate the internalization of AMPA receptor, but trafficking steps following their internalization are not known, (Lin, Ju et al. 2000 ; Beattie, Carroll et al. 2000). We first verified that NMDA, AMPA and insulin can provoke the internalization of GluR2 in our hippocampal cultures (Figure 21A). Therefore, we prebound the anti-GluR2 antibody to hippocampal neurons, which recognizes the extracellular part of GluR2, and then stimulated their internalization with NMDA or AMPA for 2 min or insulin for 15 min (except time point at 2 min). Cells were then fixed at the indicated times and immunostained under non-permeabilizing conditions using Cy5-coupled secondary antibodies which recognize non-internalized GluR2/anti-GluR2 complexes. Then we permeabilized the cells and added Cy3-coupled secondary antibodies, which stain the

fraction of the GluR2/anti-GluR2 complex which were internalized. We quantified specifically the fluorescence intensity corresponding to internalized GluR2. We observed that all 3 stimuli caused a steady increase in internal GluR2 staining, verifying efficient stimulations of internalization (Figure 21A). Internalization occurred after approximaly 5 min for the 3 stimuli and reaches its maximal level after 20-30 min.

We then verified for each different stimulus whether AMPA receptor GluR2 subunit trafficks through NEEP21-positive endosomes. Therefore, we applied the same experimental protocol as before, but in addition we also immunostained neurons with anti-NEEP21 antibodies and secondary antibodies which recognize either anti-NEEP21 or internalized anti-GluR2. Figure 21B illustrates typical cells after 2 min (left row) and 15 min of stimulation with the indicated stimuli (right row). Figure 21C shows quantification of colocalization between NEEP21 and GluR2, representing 10 cells at each point. At 2 min there was only 5.1 and 4.9% colocalization upon NMDA and insulin stimulation, respectively, whereas AMPA caused 14.8% colocalization, probably because AMPA binds directly to AMPA receptor. At later time points, colocalization after NMDA treatment increased strongly to 39.5% at 15 min and 38.6% at 30 min, whereas colocalization after AMPA or insulin stimulation remained < 20%.

These results show that a significant fraction of AMPA receptors traffick through NEEP21-positive endosomes after NMDA stimulation. It also argues for a potential role of NEEP21 in the sorting and recycling of AMPA receptors.

III.2.13 NEEP21 Is Involved in AMPA Receptor Recycling

The GluR2 subunit of AMPA receptors pass through a NEEP21-positive endosome in PC12 cells when the receptor is directed to the recycling pathway (NMDA stimulation). We therefore tested whether NEEP21 suppression affects cycling of 2 different AMPA receptor subunits GluR1 and GluR2, after NMDA stimulation of hippocampal cultures (Figure 22). We decided to analyze 2 different subunits because it was previously shown that GluR1 trafficking and exocytosis was regulated, whereas GluR2 subunit trafficking was faster and constitutive (Passafaro et al., 2001; Shi et al., 2001). Cells transfected with either GFP (control) or NEEP21-antisense (suppression) were fixed at different times after stimulation of receptor internalization with NMDA. Surface AMPA receptors were stained without permeabilization using an antibody against the extracellular domain of GluR1 or GluR2 (Figure 22 A and B).

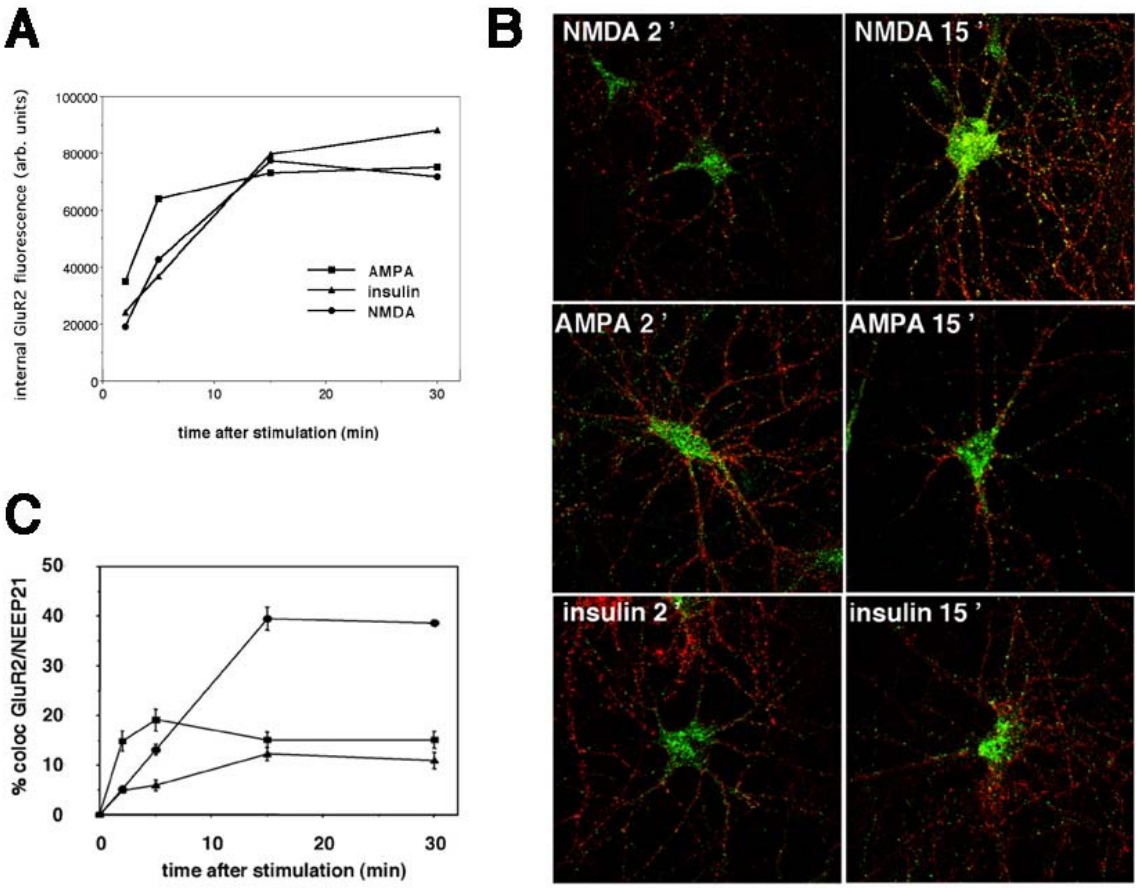

Figure 21. AMPA receptors are internalized in NEEP21-positive compartments after NMDA stimulation. (A) Hippocampal neurons were incubated with an antibody against an extracellular epitope of GluR2, and fixed (time 0) or incubated with either 50 μM NMDA, 100 μM AMPA (both 2 min), or 500 nM insulin (15 min) and further incubated for the indicated times at 37°C, before fixation. Neurons were then labeled with Cy3 secondary IgG antibodies without detergent (GluR2 ext) or with Cy5 secondary IgG antibodies without detergent and then Cy3 secondary IgG with deteregent (GluR2 int). Specific signals corresponding to internalized GluR2 of confocal images were then quantified by the NIH image software. (B) Typical confocal section of stainings corresponding to NEEP21 (green) and to internalized GluR2 after 2 min (left row), or after 15 min of either NMDA, AMPA, or insulin stimulation (right row). (C) Quantification of colocalization between NEEP21 and internalized GluR2 using NIH image software on confocal section as in A and B (NMDA, circle; AMPA, square ; insulin, triangle).

We then quantified specifically the fluorescence corresponding to the receptors which are present at the cell surface. Zero time-points represent the fraction of the receptors at the surface before stimulation. Fluorescence intensities were equal for both transfections before stimulation (100%). For GluR1, after stimulation the signal (fluorescence intensity) decreased

at 10 min to 22.2 (Figure 22A, GFP control, black bar) and 21.1% (Figure 22A, NEEP21-antisense, gray bars), reflecting equal receptor internalization, and remained low until 30 min (32.4 and 22.3%). Surface labeling in NEEP21 antisense-transfected cells remained significantly lower ($P < 0.01$) at 60 (2.6%) and 120 min (12.7%). When performing the equivalent experiment for GluR2 (Figure 22B) we observed in control cells a faster cycling than for GluR1 (Figure 22, compare A and B, 30 min time-points), in agreement with their reported time courses (Passafaro et al., 2001). Upon suppression of NEEP21, recycling of GluR2 was retarded at 30 min (40.8%) compared with control cells (63.3%, $P < 0.02$). These results indicate that NEEP21 down-regulation retards the recycling of both GluR1 and GluR2 subunits, indicating that NEEP21 is necessary for correct cycling of AMPA receptors.

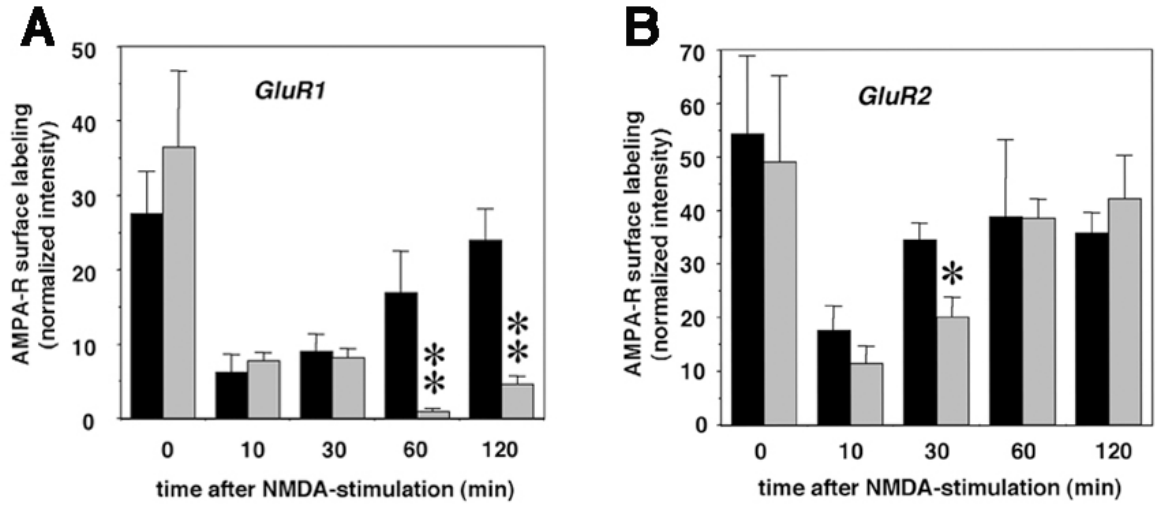

Figure 22. NEEP21 is involved in AMPA receptor recycling. (A) Downregulation of NEEP21 retards GluR1 recycling. Hippocampal neurons (DIV 10) transfected with either GFP (black bars) or NEEP21-antisense (gray bars) constructs were stimulated for 2 min with NMDA, and were further incubated for the indicated times before fixation and surface labeling using an anti-GluR1 antibody against the extracellular domain of AMPA receptors. Fluorescence intensity was quantified. (B) GluR2 cycling was analyzed as in A. Typical experiments out of three are shown in A and B, and 5-10 cells per condition were analyzed by a Student t test. Significant differences at $P < 0.01$ (double asterisks) and at $P < 0.02$ (single asterisk) are indicated. Error bars are SEM.

III.3 How Does NEEP21 Act on AMPA Receptor Cycling ?

III.3.1 NEEP21 Interacts with GRIP and the AMPA Receptor Subunit GluR2

In order to elucidate the molecular mechanisms which implicate NEEP21 in the cycling of AMPA receptors, we asked whether NEEP21 could be present in protein complexes containing AMPA receptor subunits and partners known to be necessary in the correct trafficking of these receptors. We performed immunoprecipitation using anti-NEEP21 antibodies and anti-syntaxin 13 antibodies. We chose to immunoprecipitate NEEP21 and syntaxin 13 from membrane extracts of postnatal day 8 rat brain (Figure 23). At this stage, NEEP21 and syntaxin 13 are expressed at high levels and intensive AMPA receptor trafficking takes place during the maturation of synapses (Kumar et al., 2002; Malinow and Malenka, 2002; Pickard et al., 2000; Zhu et al., 2000). Immunoblots for immunoprecipitation experiments with anti-NEEP21 antibody revealed the presence of the group II PDZ-protein GRIP (Glutamate receptor interacting protein) (130 kDA) (Figure 23A) in a complex with NEEP21. GRIP is a scaffolding molecule thought to be crucial for correct trafficking of several receptors (Sheng and Sala, 2001). It was further demonstrated that GRIP interacts specifically with GluR2 and GluR3 and participates in their delivery and/or stabilization at the cell surface (Dong et al., 1997; Dong et al., 1999; Seidenman et al., 2003; Shi et al., 2001). When immunprecipitations were carried out with anti-syntaxin 13 antibodies, we also detected GRIP specifically, since it was not coprecipated with non-specific control rabbit or mouse IgG (Figure 23A). As shown above (see Figure 7A), anti-NEEP21 antibody coprecipitates syntaxin 13 and anti-syntaxin 13 antibody coprecipitates NEEP21 (Figure 23A). We were not able to obtain NEEP21 or syntaxin 13 in precipitate using the available moncolonal commercial anti-GRIP antibody (Figure 23B). A possible explanation could be that the interaction between GRIP and NEEP21 or syntaxin 13 involves a domain recognized by this anti-GRIP antibody.

Due to its interaction with GRIP we also tested whether GluR2/3immunoreactivity would be coprecipitated with anti-NEEP21 antibodies. Indeed, on Figure 23C, a faint but specific band corresponding to GluR2/3 (102k Da) was present in the anti-NEEP21 immunoprecipation, while none was detected in the control IgG. We also checked for the presence of the group I SAP-97, which is involved in trafficking of GluR1. While SAP97 appeared in the input extract as a band at 140 kDa with a proteolysed form at 90 kDa (Muller et al., 1995), no signal

was detected either in the specific anti-NEEP21 immunoprecipitation or in the non-specific polyclonal IgG (Figure 23C). This strongly suggests that NEEP21 does not act via SAP-97. Given the reported interaction between GluR2 and NSF/αSNAP/βSNAP (Noel et al., 1999; Osten et al., 1998), we also blotted for coprecipitation with αSNAP (Figure 23C). The protein was not detected, suggesting that the complex formed between NEEP21 and GluR2 is different from the GluR2/NSF/αSNAP complex. We detected none of these proteins in the control non specific IgG (Figure 23 C).

These results demonstrate that NEEP21 is present in a molecular complex with GRIP, GluR2 and syntaxin 13. In addition, these interactions define new complexes which are different from the previously identified GluR2/NSF/αSNAP/βSNAP complex.

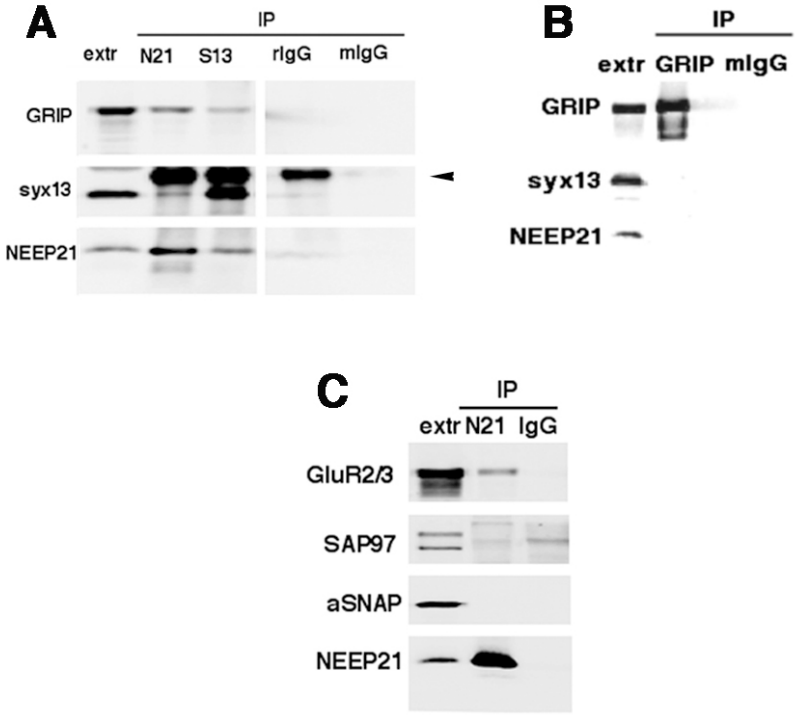

Figure 23. NEEP21 interacts with GRIP, GluR2 but not SAP97 and αSNAP. (A). Immunoprecipitation (IP) using anti-NEEP21 (N21), anti-syntaxin 13 (S13) and non-specific anti-rabbit (rIgG) and anti-mouse IgG (mIgG) antibodies on rat brain postnatal day 11 membrane extracts (1 g). Glycine-eluted proteins and crude extracts (extr) were analysed by Western blotting for NEEP21, syntaxin 13 (syx13) and GRIP. Arrowhead shows crossreacting heavy chain antibody since polyclonal antibodies were used for IP and western blot. (B) Immunoprecipitation as in A using anti-GRIP and non-specific mouse IgG antibodies. Western blots of elutions and crude extract are shown for GRIP, syntaxin 13 (syx13), and NEEP21. (C) Immunoprecipitation as in A and B using anti-NEEP21 and non-specific anti-rabbit IgG antibodies. Western blot of elutions and crude extract are shown for GluR2/3, SAP97, αSNAP, and NEEP21.

III.3.2 NEEP21 Interaction with PICK1 And Syntaxin 7

We also investigated whether NEEP21 can bind another member of the syntaxin family, syntaxin 7. Syntaxin 7, like syntaxin 13, was identified on endosomal compartments, and was suggested to be involved in the trafficking linked to late endosomes (Nakamura et al., 2000; Wong et al., 1998). Since NEEP21 is involved in recycling of receptors, syntaxin 7 would be a good candidate to test and verifiy whether NEEP21 would also be implicated in a molecular mechanism linked to the degradative pathway. Indeed, immunoprecipitation showed that syntaxin 7 (39 kDa) was specifically coprecipitated with NEEP21 using anti-NEEP21 antibodies since it was not present in control IgG antibodies (Figure 24A). This shows that NEEP21 forms a complex with syntaxin 7, suggesting that NEEP21 could be linked to many different sorting pathways.

In addition to GRIP and NSF, it has also been shown that the carboxy terminal domain of GluR2 binds PICK1 (Protein Interacting with C Kinase 1) (Staudinger et al., 1995; Xia et al., 1999). PICK1 is a postsynaptic scaffold protein that interacts with several glutanate receptor related proteins and it has been proposed that PICK1 either primes the receptor for internalization, or alternatively, it binds to internalized AMPA GluR2 and prevent their reinsertion to the plasma membrane (Xia et al., 2000). We thus tested whether we could coimmunoprecipitate PICK1 from brain membrane extracts with anti-NEEP21 (Figure 24B). Immunoprecipitation experiments showed that the anti-NEEP21 antibody precipitates NEEP21 and also coprecipitates PICK1 (55kDa) (Figure 24B). This interaction is specific since no corresponding signal is detected with non-specific IgG antibodies. These data show that NEEP21 is present in a complex which contains PICK1.

Figure 24. NEEP21 interacts with syntaxin 7 and PICK1. (A) Immunoprecipitation using anti-NEEP21 (N21) and non-specific rabbit (rIgG) antibodies on rat brain postnatal day 11 membrane

extracts (1 g). Western blot was achieved on glycine-eluted proteins and crude extracts for syntaxin 7 (syx7) and NEEP21. There are crossreacting antibody heavy chains (arrowhead) since polyclonal antibodies were used for IP and immunoblots. (B) Immunoprecipitation as in A. Shown is Western blot on elutions and crude extracts using anti-PICK1, -NEEP21 and non-specific rabbit IgG antibodies to detect the presence of corresponding proteins. Molecular weights are in kDa

---

III.3.3 Modulation of NEEP21-GRIP Interaction by NMDA Stimulation.

In order to get insight into the functional significance of the observed interaction between NEEP21 and GRIP, we asked whether it was sensitive to NMDA stimulation. It has previously been described that NMDA application to hippocampal and cortical cultures provokes the internalization and the recycling of AMPA receptors (Ehlers, 2000) and we have shown that suppression of NEEP21 strongly delays NMDA-induced AMPA receptor recycling, (Steiner et al., 2002a). Furthermore, it was also demonstrated that the association of GluR2 and GRIP is essential for AMPA receptor surface accumulation at synapses, possibly either by limiting their endocytosis or promoting their insertion into the plasma membrane, thus controling the cycling of the receptors (Osten et al., 1998; Seidenman et al., 2003). We performed anti-NEEP21 immunoprecipitation experiments from NMDA-stimulated hippocampal neurons. In control experiments (unstimulated), we observed, that anti-NEEP21 antibodies coimmunoprecipitate GRIP with NEEP21 (Figure 25), as shown from rat brain membrane extracts (see Figure 23A). When we stimulated neurons with 2 min NMDA and incubated them for 2 additional minutes to allow internalization of AMPA receptors, we observed a clear increase in the signal corresponding to GRIP (Figure 25A). Quantification of the bands from 6 independent experiments yielded a significant increase of 2.13 fold for coprecipitated GRIP from unstimulated to stimulated neurons (Figure 25B) ; ($P < 0.01$). This result shows that the NEEP21-GRIP interaction exists in living hippocampal neurons and is increased following NMDA stimulation. It also suggests that the formation of this complex is enhanced during NMDA-induced AMPA receptor cycling.

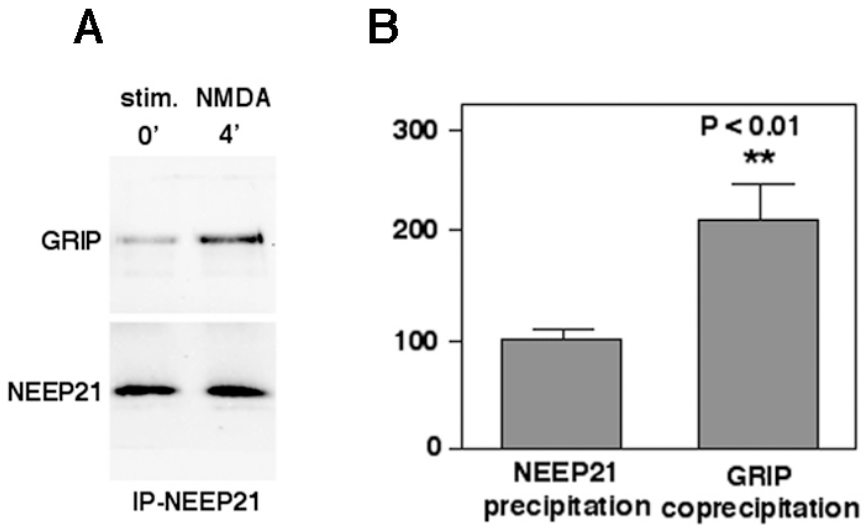

Figure 25. NEEP21-GRIP interaction is enhanced after NMDA-stimulation in hippocampal cultures. (A) Hippocampal cultures (DIV 11), preincubated with TTX, were either left unstimulated or stimulated for 2 min with 50 μM NMDA and further incubated for 2 min at 37°C in the absence of NMDA. Neurons were then lysed and subjected to immunoprecipitation using anti-NEEP21 antibodies crosslinked to protein-A beads. Shown is a Western blot for immunopellets without stimulation (time 0') or with NMDA-stimualtion (time 4') for NEEP21 and GRIP. (B) Quantifications of bands corresponding to NEEP21 and GRIP without or with stimulation. Pixel intensities of NEEP21 and GRIP bands from 6 experiments as described in A were quantified using NIH image software. Graph indicates the relative amount of coprecipitated GRIP. 100% corresponds to intensity from unstimulated cells, and values were normalized to precipitated NEEP21. There is a significant increase in GRIP coprecipitation ($P < 0.01$).

III.3.4 NEEP21 Amino Acids 129-165 Are Sufficient to Interact with GRIP

In a next step we wanted to elucidate which domains of NEEP21 are responsible for its interaction with GRIP. To this end we carried out pull-down experiments using rat brain membrane extracts at postnatal day 11 and recombinant fusion proteins between immobilized glutathione-S-transferase and different fragments of the carboxyterminus of NEEP21 (Figure 26A). We considered only the COOH terminus of NEEP21, because we had previously shown that it is present in the cytosol while its NH_2 terminus is in the lumen of organelles. (see Figure 10). As expected, the complete carboxyterminal domain representing aa 104-185 was able to pull down GRIP (Figure 26B). Likewise, a shorter fragment containing aa 104-165

also interacted with GRIP, while the extreme carboxyterminal fragment aa 164-185 as well as the aa 104-134 did not show any significant interaction with GRIP. The strongest signal corresponding to GRIP was obtained using a minimal fragment aa 129-165 (Figure 26). When we repeated the same experiments for GluR2/3, and discovered that the same fragments which pull-down GRIP, also pull-down GluR2/3 (Figure 26B). The specificity of these pull-down assays was revealed by the lack of signal for any of all proteins using the control immobilized glutathione-S-transferase (Figure 26B).

Altogether, these results verified by an independent technique for the existence of a NEEP21-GRIP-GluR2/3 interaction, and point to a 36 aa fragment containing the domain of NEEP21 which is responsible for its presence in a complex with GRIP and GluR2/3.

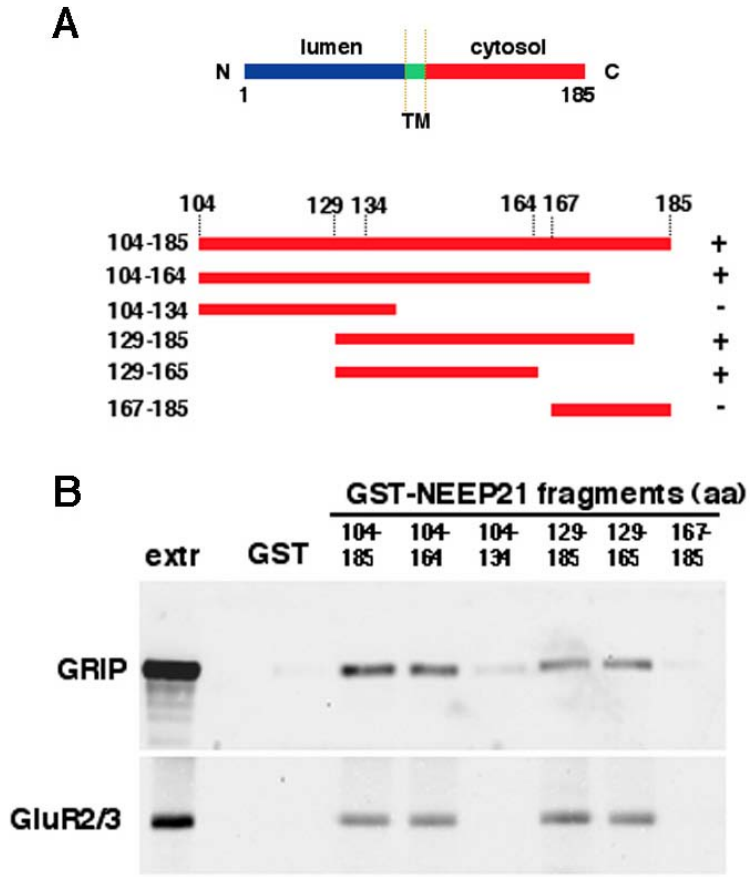

Figure 26. NEEP21 amino acids 129-165 are sufficient to interact with GRIP. (A) Scheme of different carboxyterminal fragments of NEEP21 expressed as GST fusion proteins. TM, transmembrane region. (B) aa 129-165 is the minimal NEEP21 fragment which binds to GRIP. Immobilized GST or fusion protein between GST and the indicated fragments of the carboxyterminal of NEEP21 were incubated with rat brain membrane extracts (P11). Bound proteins were analyzed by Western blot for GRIP and GluR2/3.

III.3.5 NEEP21 Amino Acids 129-165 Affects Dendrite Morphology

Having identified of the NEEP21 fragment implicated in the interaction with GRIP and GluR2, we postulated that it could act as a dominant-negative mutant in AMPA receptor trafficking. Therefore, we transfected hippocampal neurons with this fragment fused to GFP (N129-165), or with GFP alone as a control. The first observation that we noted was a shrinkage of the dendrites of the neurons overexpressing N129-165 after 2 days of transfection compared to the control GFP (Figure 27A). After 2 days of transfection, overexpression of the fragment specifically affects dendrite morphology, because, only the processes positive for MAP2 staining are affected, while those positive for neural cell adhesion molecule L1, a marker for the axonal domain, are not altered and present the typical axonal morphology (Figure 27A). The shorter dendrites of N129-165 transfected neurons also contain varicositiy-like structures not present in the control situation (Figure 27A). Quantification of the total axon length and dendrite length showed that the axon length is not significantly different (Figure 27B), while the dendrite length is strongly reduced in neurons overexpressing N129-165, compared to control (Figure 27C, $P < 0.01$). Recently, it was shown that overexpression of HA-tagged GluR2 increases the number of spines along dendrites, due to its presence at the cell surface of neurons (Passafaro et al., 2003). Reasoning that the fragment N129-165 binds GRIP and GluR2 and could potentially affect the trafficking of GluR2, we asked whether overexpression of HA-GluR2 would influence the morphological effect observed with N129-165. To this purpose, we cotransfected N129-165 or GFP with HA-GluR2. Indeed, we found that overexpression of HA-tagged GluR2 compensates modestly but significantly for the decrease of dendritic length caused by N129-165 (Figure 27C, $P < 0.02$). Overexpression of HA-GluR2 had no significant effect on dendrite length when coexpressed with GFP (Figure 27C) compared to GFP alone and we did not observe any effect of its expression on axon length (Figure 27B). When neurons were analyzed 7 days after transfection, we also noted a drastic effect of N129-165 expression on dendrite length compared to control (Figure 27E, $P < 0.01$). In addition, cotransfection of HA-GluR2 did no longer compensated for this effect (Figure 27E, $P < 0.09$). The length of axons of cells which overexpressed N129-165 alone or in combination with HA-GluR2 were also altered (Figure 27D, $P < 0.01$).

These results shows that the fragment aa 129-165 of NEEP21 affects specifically the morphology of neuronal dendritic arbor as an immediate effect, possibly by interferring with

receptors trafficking including GluR2. They also suggest that the specific dendritic effect is generalized to all processes including axons after long term overexpression of the fragment aa 129-165 of NEEP21.

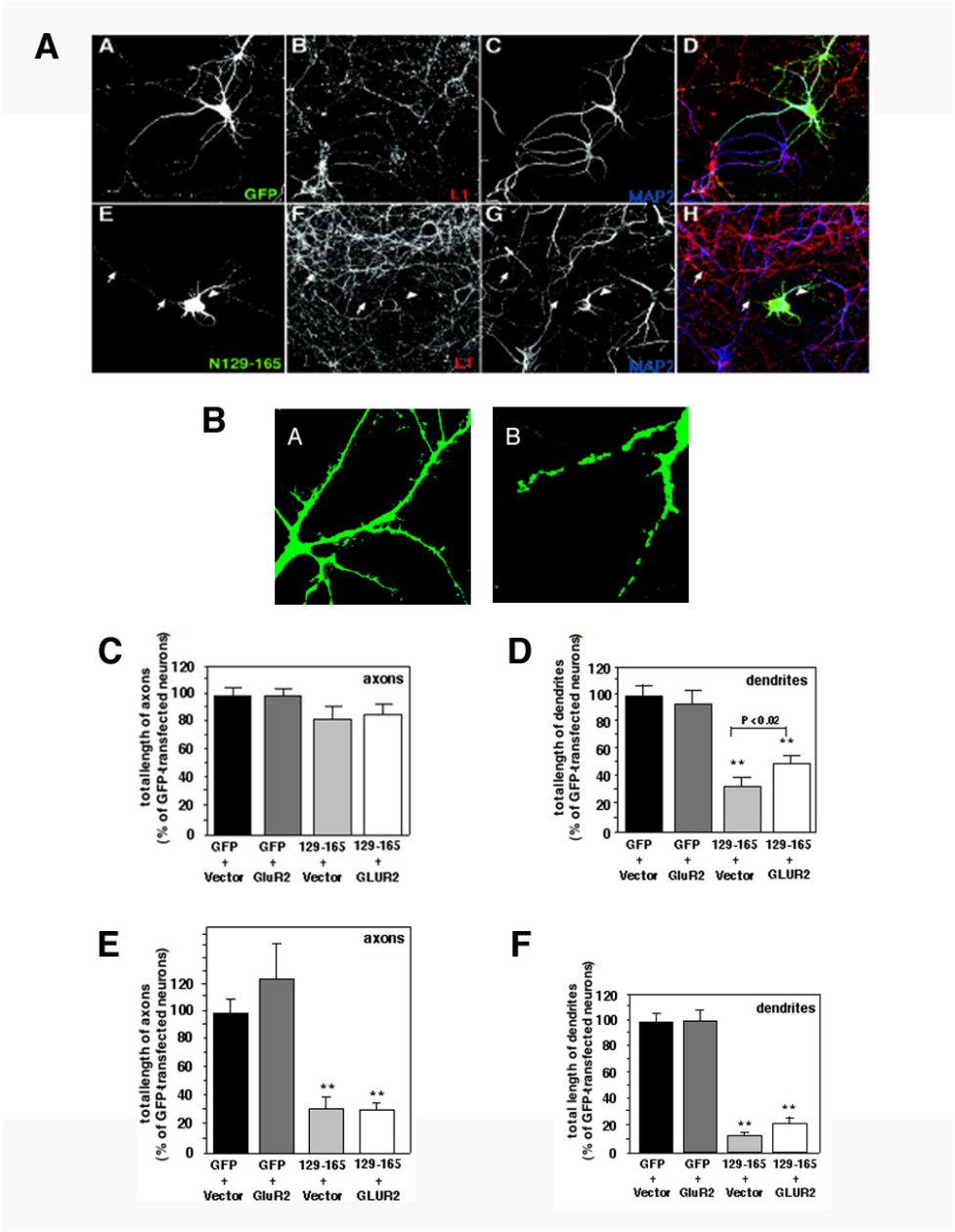

Figure 27. NEEP21 amino acids 129-165 alters dendrite morphology. (A) Hippocampal neurons at DIV 8 were transfected with either GFP (AA-AD) or GFP-NEEP21aa129-165 (N129-165) (AE-AH). After 2 days of transfection, neurons were stained with L1, an axonal marker (AB, AF) or MAP2, a dendritic marker (AC, AG). GFP-labeling is shown in AA and AE. Overlays in AD and AH. Note that axons are not affected (arrow) while dendrites are shorter (arrowhead) for neurons overexpressing N129-165. (B) Hippocampal neurons at DIV 10 were transfected with either GFP (BA) or GFP-NEEP21aa129-165 (BB) and fixed after 2 days of transfection. Images were acquired with a zoom of 4X. Note the presence of varicosities along neurites in GFP-NEEP21 aa129-165 transfected cells (BB).

Single confocal sections are shown, (C-F) Hippocampal neurons at DIV 10 transfected with either GFP and pcDNA3, or GFP and HA-GluR2, or N129-165 and pcDNA3 or N129-165 and HA-GluR2. Cells were fixed after 2 days (C-D) or 7 days (E-F) of transfection, and total length of axons and dendrites were measured. Note that N129-165, while having no effect on axon length, strongly reduced dendrite length after 2 days of transfection. This effect is at least partially compensated when N129-165 was cotransfected with HA-GluR2. After 7 seven days of transfection, both axon and dendrite lengths were affected by overexpression of N129-165.

III.3.6 NEEP21 Amino Acids 129-165 Impairs Correct Recycling of GluR2

We tested directly the effect of GFP-N129-165 on the trafficking of endogenous AMPA receptors subunits GluR2 and GluR1. We transfected hippocampal neurons either with GFP as a control, or with N129-165. Two days after transfection we performed immunolabelling of surface receptors following NMDA-stimulation. In good agreement with our previous results and recent studies (Ehlers, 2000; Lin et al., 2000), quantification of fluorescence intensity revealed that GluR2 and GluR1 were internalized into intracellular compartments after 2 min of NMDA stimulation, reaching a maximum of internalization at 10 min (Figure 28). 60 min after NMDA applications both subunits reappear at the plasma membrane of neurons transfected with GFP (Figure 28, black bars). In neurons expressing N129-165 we found that ever at steady-state (before stimulation), there was a significant decrease in the GluR2 signal at the cell surface compared to the control (Figure 28A, white bars, $P < 0.01$). At 60 min, we observed a strong decrease in the reappearance of GluR2 at the cell surface for GFP-N129-165-transfected neurons (Figure 28A, double atseriks $P < 0.01$). This suggests that internalized GluR2 is not properly recycled in neurons overexpressing N129-165. When we quantified the of GluR1 present at the cell surface, we only observed a statistical difference after 60 min of NMDA stimulation for neurons transfected with N129-165 and compared to GFP transfection (Figure 28B, $P < 0.01$). We did not observe any effect at steady state between GFP and N129-165 (Figure 28B). Moreover, we did not see any statistical difference comparing levels of GluR1 at 0 min and 60 min time-points for N129-165 and GFP transfected neurons (Figure 28B, pound sign, $P < 0.03$), on the contrary of GluR2 (Figure 28A, $P < 0.01$, pound sign).

We also analyzed in the same manner surface appearance of exogenous HA-tagged GluR2 and HA-tagged GluR1 overexpressed in neurons. For HA-GluR2, we did not see any

difference at steady state, probably due to the overexpression of this subunit in neurons (Figure 28C). 10 min after NMDA stimulation, HA-GluR2 was decreased equally in N129-165 and GFP transfected cells reflecting the internalization of subunits (Figure 28C), though to a lesser extent than measured for endogenous GluR2. At 60 min, HA-GluR2 recycling was significantly decreased for neurons expressing N129-165 compared to the control (Figure 28C), as it was the case for the endogenous subunit (Figure 28A). Concerning HA-GluR1, neither its steady-state level not its internalization and recycling due to NMDA stimulation was not different between N129-165 and GFP transfected cells (Figure 28D). Taken together, these results showed that NEEP21 aa 129-165 disturbs trafficking of GluR2, probably by interferring with NEEP21-GRIP-GluR2 complex formation.

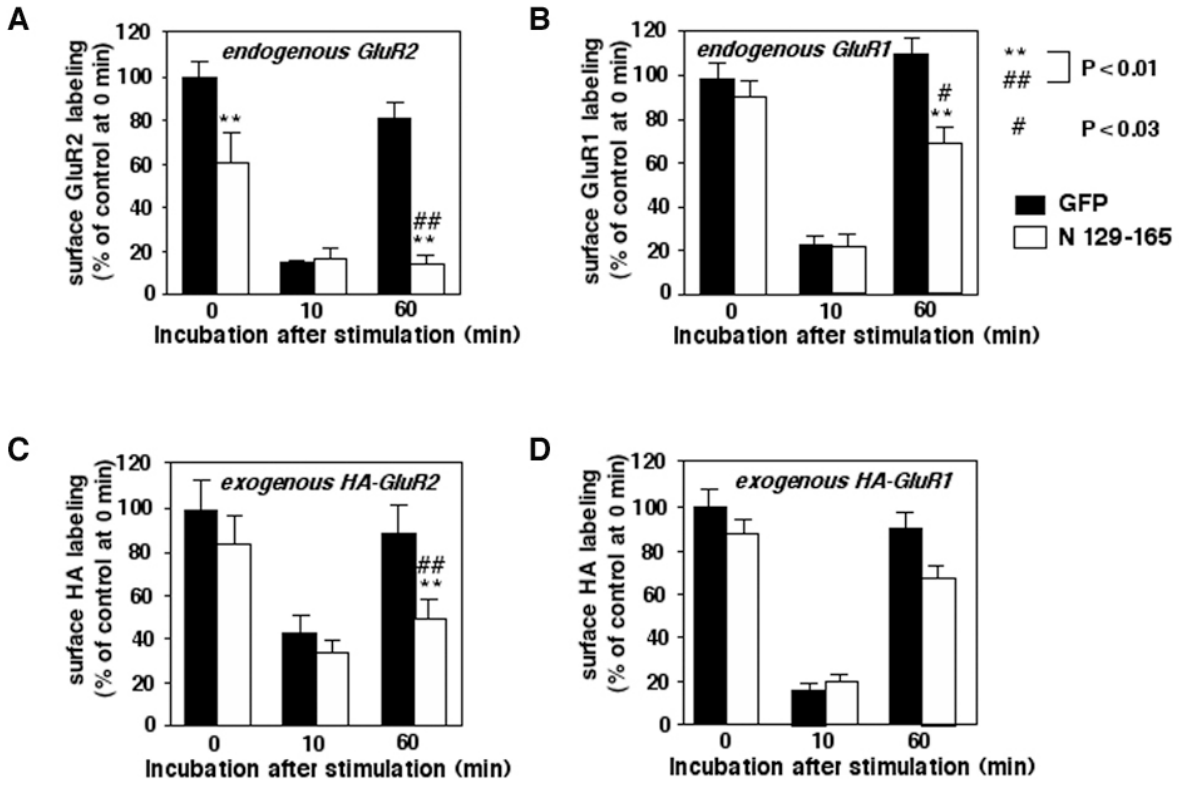

Figure 28. A fragment of NEEP21 (amino acids 129-165) delays recycling of endogenous GluR2 and exogenous HA-GluR2 in hippocampal neurons. (A, B) Hippocampal neurons at DIV 8 were transfected with GFP (black bars) or N129-165 (white bars). At DIV 10 cells were either fixed or stimulated for 2 min with 50 μM NMDA at 37°C and further incubated for 10 or 60 min before fixation. Then they were stained with anti-GluR2 (A) or-GluR1 (B) antibodies which recognize an extracellular domain of GluR2 or GluR1 in non-permeabilized condition to label receptors present at the cell surface. Fluorescence was quantified on confocal sections by Metamorph software. 100% corresponds to fluorescence intensity of GFP transfected cells at 0 min. (C, D) As in A and B except that neurons were cotransfected with HA-tagged GluR2 (C) or HA-tagged GluR1 (D) and anti-HA antibodies were used for surface labeling of exogenous receptors. Double asterisks and double pound

signs indicate significant differences ($P < 0.01$), while single pound sign indicates marginal significance ($P < 0.03$). Asterisks compare black bars and white bars at given time point, while pound signs compare white bars (N129-165) between 0 min and 60 min.

III.3.7 NEEP21 Amino Acids 129-165 Does Not Affect Transferrin Receptors Cycling

Due to the strong effect of NEEP21 aa 129-165 on GluR2 trafficking and on the morphology of dendrites, we verified that general trafficking through the early endosomal pathway was not affected. We thus analyzed the cycling of rhodamin-hTf-hTfR complex in hippocampal neurons overexpressing N129-165 or GFP in combination with the human TfR plasmid. Rhodamin-Tf signal quantification into neurons showed that it was internalized at 5 and 15 min and then recycled at 60 and 240 min in GFP and N129-165 transfected neurons (Figure 29, GFP black bars, N129-165 white bars). We did not see any statistical difference between GFP and N129-165, which indicates that the expression of GFP-N129-165 does not cause a general alteration of the clathrin-coated receptor cycling pathway.

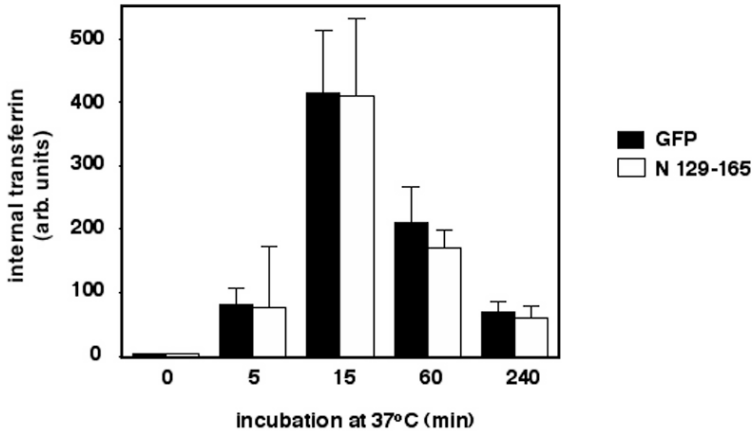

Figure 29. NEEP21 fragment aa 129-165 does not disturb Transferrin Receptors cycling. Hippocampal neurons at DIV 8 were cotransfected for human Transferrin Receptor (hTfR) and either GFP (black bars) or N129-165 (white bars). At DIV 10, rhodamin-Tf were added during 20 min at 4°C to allow rhodamin-Tf binding to TfR at the cell surface and then transferred to 37°C for the indicated time. Acid washed neurons were then fixed and fluorescence intensity corresponding to internalized rhodamin-Tf was quantified on confocal sections.

III.4 RTN1-C Interacts with SNARE Proteins and Is Involved in Regulated Secretion Mechanisms

III.4.1 Characterization of a Polyclonal RTN1-C Antibody

In order to characterize RTN1-C, we raised a polyclonal antiserum against a peptide (aa 5 to 20) of the RTN1-C primary sequence with the commercial service Eurogentech. Affinity-purified RTN1-C antibodies recognized a single specific band at about 23 kDa corresponding to the size of RTN1-C (Figure 30A, lane 3, arrow), and a very faint band around 50 kDa. The 23 kDa band was also detected by crude immune serum (Figure 30A, lane 2) but we observed it neither in preimmune serum nor in purified antibody preblocked with antigenic peptide (Figure 30A, lane 1 and 4). In hippocampal cultures at DIV 10, this antibody detected RTN1-C along neurites and in the cell body, localized to tubule-like structures (Figure 30B, white arrowhead) but also to puncta (Figure 30B, yellow arrowhead). In addition we noted that RTN1-C was enriched in the tips of neurites (Figure 30B, arrow). These data showed that our anti-RTN1-C detects RTN1-C by Western blot and immunofluorescence.

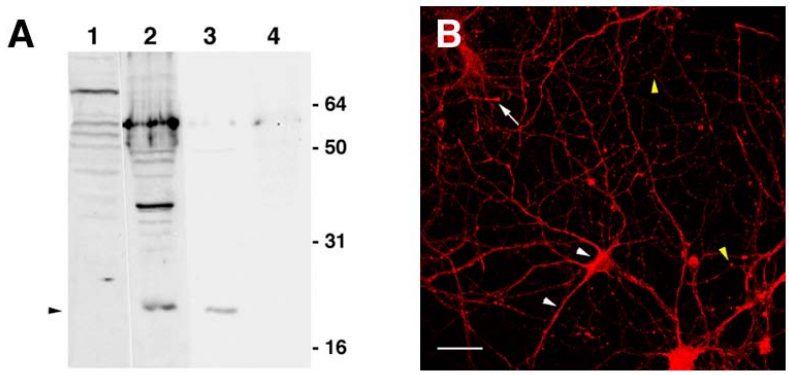

Figure 30. Characterization of polyclonal anti-RTN1-C antibody. (A) Immunoblot of P3 rat brain extract (30 μg) using a polyclonal anti-RTN1-C antibody. Lane 1, preimmune serum ; lane 2, crude immune serum ; lane 3, affinity-purified antibody ; lane 4, purified antibody blocked with 50 ng of antigenic peptide. RTN1-C is detected around 23 kDa (arrow) Molecular weights are indicated in kDa. (B) Hippocampal neurons (P8) stained with anti-RTN1-C antibody. White arrowheads show that RTN1-C is present on tubule-like structure along neurites and in the cell body. Yellow arrowheads show that RTN1-C is localized to puncta. In addition, arrow shows that RTN1-C was enriched in the tip of neurites. Single confocal section is shown. Scale bar is 20 μm.

III.4.2 Syntaxin 13 Forms a Complex with RTN1-C

We verified the existence of a complex containing syntaxin 13 and RTN1-C by immunoprecipitation using anti-syntaxin 13 or anti-RTN1-C antibodies. Figure 31A, 1st and 2nd rows shows that the anti-RTN1-C antibody precipitates RTN1-C and specifically coprecipitate syntaxin 13, since no corresponding signals appear using the non-specific polyclonal IgG antibodies for immunoprecipitation. These results show that syntaxin 13 forms a complex with RTN1-C and confirms our initial observation from anti-syntaxin 13 immunoaffinity chromatography (Figure 6). We then asked whether RTN1-C could be present in complexes containing other SNARE proteins. We analyzed anti-RTN1-C immunoprecipitations by Western blots using antibodies against the SNARE proteins, syntaxin 1, syntaxin 7, VAMP2/synaptobrevin, VAMP1, VAMP3/cellubrevin, and SNAP-25 (Figure 31A). Interestingly, we found that syntaxin 1 (Figure 31A, 3rd row), syntaxin 7 (Figure 31, 4th row) and VAMP2 (Figure 31A, 5th row), were also coprecipitates with anti-RTN1-C antibodies. Syntaxin 1 was recognized as a double band by monoclonal HPC1 antibodies corresponding to syntaxin 1A and syntaxin 1B (Foletti et al., 2000); both isoforms were present in the immunopellet. In contrast, VAMP1 (Figure 31A, 6th row) and VAMP3 (Figure 31A, 7th row) were never detected in complexes with RTN1-C. In addition, SNAP-25, a peripheral SNARE protein was not coprecipitated with anti-RTN1-C antibodies (Figure 31, 8th row). To control further the specificity of these interactions, we also tested for the presence of unrelated integral membrane proteins Na/K-ATPase and synaptophysin. Neither of these proteins were found to be coprecipitated with RTN1-C (Figure 31A, 9th and 10th row). None of the analysed proteins we detected in immunoprecipitates using polyclonal non-specific IgG antibodies (Figure 31, A).

In the reverse situation, immunoprecipitation using antibodies against syntaxin 13 (Figure 31B), syntaxin 1 (Figure 31C) and VAMP2 (Figure 31D), showed that in every case RTN1-C was coprecipitated with these different SNAREs respectively. This verified that RTN1-C exists in complexes with syntaxin 1, syntaxin 13, syntaxin 7 and VAMP2 and excluded artefactual coimmunoprecipitations which would be due to anti-RTN1-C antibodies. In all the cases, only a fraction of the different SNARE proteins and RTN1-C precipitates together,which means that only subpopulations of these proteins are complexed to each other. These results show that RTN1-C is a new syntaxin- and VAMP2-interacting protein.

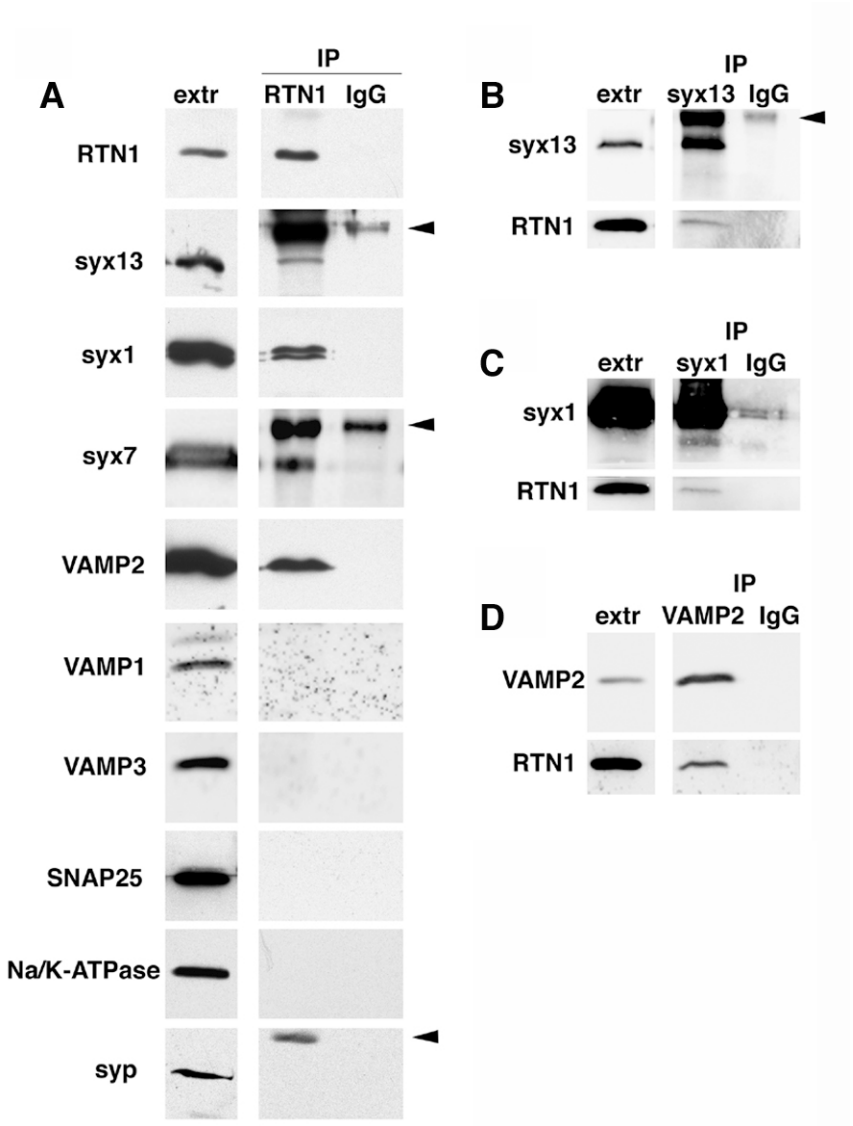

Figure 31. RTN1-C interacts with SNARE proteins. (A) Postnatal day 3 rat brain membrane extracts were incubated with protein-A sepharose beads coupled to polyclonal anti-RTN1-C or non-specific anti-rabbit IgG antibodies. Western blots were done on crude extracts (extr) or glycine-eluted proteins (IP) and probed with antibodies against the indicated proteins on the left of the figure (syx, syntaxin ; syp, synaptophhysin). (B-D) Reciprocal immunoprecipitations using the following antibodies crosslinked to beads : (B) polyclonal anti-syntaxin 13 antibody, (C) monoclonal anti-syntaxin 1 antibody, and (D) monoclonal anti-VAMP2 antibody. Shown are Western blots carried out on crude extract (ext) or glycine-eluted proteins (IP) and probed with the indicated protein on the left. Arrowheads point to crossreaction of rabbit heavy chains from IP antibodies.

III.4.3 RTN1-C Is Localized to a Nocodazole-sensitive, SERCA-2-positive Domain of the Endoplasmic Reticulum

RTN/NSP proteins have been shown to be localized to the endoplasmic reticulum (Senden et al., 1996; van de Velde et al., 1994b). We verified that the encoded protein of the RTN1-C cDNA that was amplified by PCR from a mouse cDNA bank with the help of our technician Catherine Chevaley yields a similar localization. We overexpressed EE-tagged RTN1-C in COS-7 fibroblasts which are devoided of endogenous RTN1-C and immunolabeled them using anti-RTN1-C antibodies (Figure 32A) and anti-ER-calcium pump SERCA2 antibodies (Figure 32B). Both proteins were strongly colocalized with RTN1-C as previously described (Senden et al., 1996), verifying an ER localization of RTN1-C. We also used an antibody recognizing calreticulin, an ER-calcium-binding protein (Figure 32D), which is present on domains of the ER different than SERCA2-positive domains (Michalak et al., 2002) (Figure 32C). We did not observe significant colocalization between RTN1-C-EE (Figure 32C) and calreticulin (Figure 32D). We confirmed this differential localization by treating COS-7 cells with the microtubule-destabilizing drug nocodazole. RTN1-C (Figure 32E, G), as well as SERCA2 (Figure 32F) appeared in patchy aggregates present preferentially in the perinuclear region, while the localization of calreticulin was not affected by nocodazole treatment (Figure 32H). These data show that RTN1-C is present on a domain of the ER which is SERCA2-positive, calreticulin-negative, and whose integrity is microtubule dependent.

III.4.4 RTN1-C Colocalizes Partially With SNARE Proteins and SV2

RTN1-C is a protein which is specifically expressed in neuroendocrine cells and neurons (Hens et al., 1998; Ninkina et al., 1997). We investigated the subcellular localization of endogenous RTN1-C (Figure 33D, G, J) and exogenous RTN1-C-EE (Figure 33A) in hippocampal cultures. Endogenous and exogenous RTN1-C were shown to be present in tubular and punctate structures distributed in the cell body and along processes (Figure 33A, D, G, J). We also noted that RTN1-C was present in the tips of processes in bulb-like structures (Figure 33D, G, J, arrow) as already shown in Figure 30.

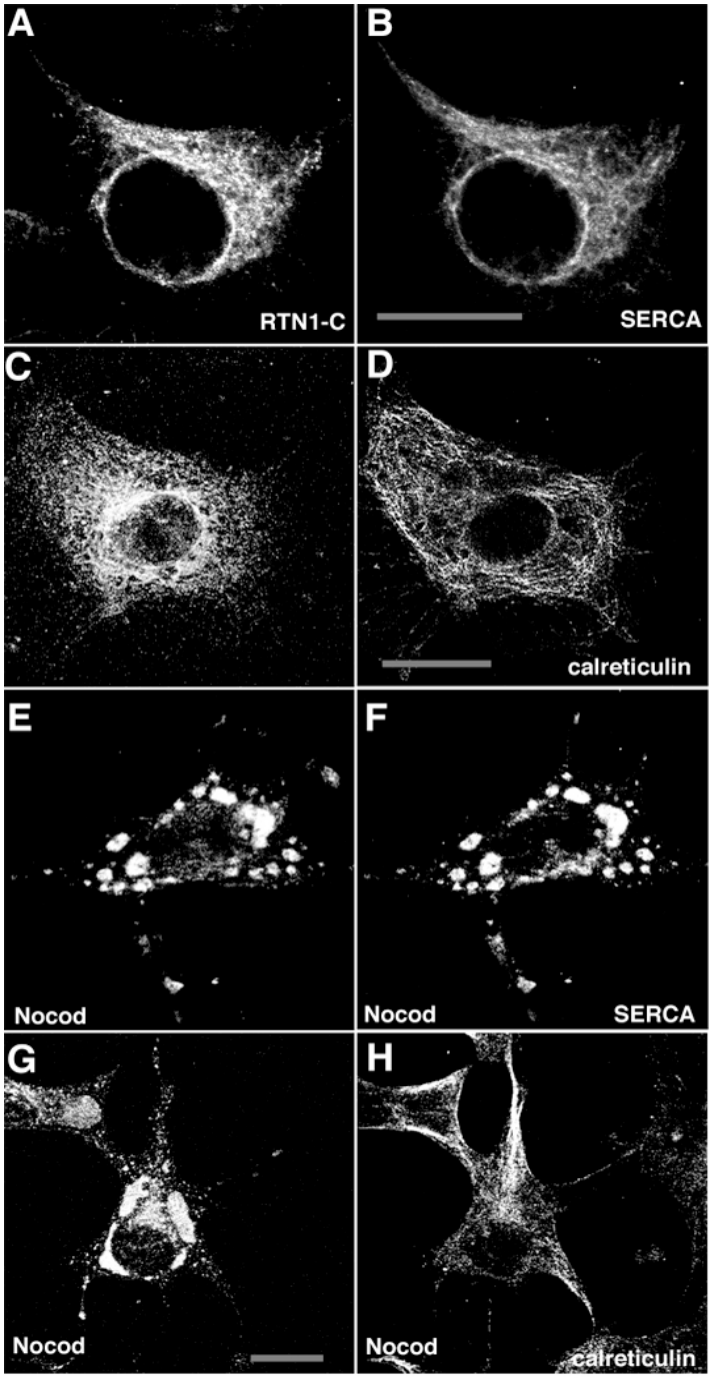

Figure 32. ER localization of RTN1-C in COS-7 cells. COS-7 cells were transfected with RTN1-EE, and either not treated (A-D), or treated with 10 μM nocodazole for 30 minutes (E-H). Cells were fixed and immunostained using polyclonal anti-RTN1-C (A, E), monclonal anti-SERCA2 (B, F), monoclonal anti-EE (C, G) or polyclonal anti-calreticulin (D-H) antibodies. Single confocal sections are shown. Scale bars are 10 μm.

Because RTN1-C interacts with different SNARE proteins, we compared the localization of RTN1-C with that of syntaxin 1, syntaxin 13, and VAMP2 by double-immunostainings. Due to the lack of availability of antibodies, we overexpressed RTN1-C-EE in order to compare its staining with endogenous syntaxin 13 (Figure 33B). We also compared endogenous RTN1-C staining (Figure 33D, G. J) with the one corresponding to endogenous syntaxin 1 (Figure 33E), and endogenous VAMP2 (Figure 33H). In the three different cases, we observed that RTN1-C staining usually did not overlap with the staining of syntaxin 1, syntaxin 13 or VAMP2 (Figure 33, overlays in C, F, I). Nevertheless, it was possible to identify clear structures which were strongly labeled at the same time for RTN1-C and the three different SNARE proteins. A few examples are indicated by arrowheads in Figure 33. We also compared the localization of endogenous RTN1-C and SV2, a classical marker for presynaptic boutons. As before, both stainings were clearly distinct but some SV2-positive puncta overlap strongly with RTN1-C staining (Figure 33J-L, arrowheads).

We next analyzed the localization of RTN1-C to specific neuronal domains in hippocampal cultures using a marker of the somatodendritic domain, MAP2, and of the axonal domain, Tau. RTN1-C-positive structures present in the cell body and processes (Figure 34A) were postitive for MAP2 (Figure 34C, overlay in E), indicating for the presence of RTN1-C in the somatodendritic domain of neurons. In addition, many processes which were labeled with anti-Tau antibodies (Figure 34D) were also stained by the anti-RTN1-C antibody (Figure 34B arrows, overlay in F), which shows that RTN1-C is also present in the axonal domain of neurons.

Altogether these data demonstrate that RTN1-C is present in tubules and puncta in the somatodendritic and axonal domains of hippocampal neurons. It also shows that subfractions of RTN1-C can be at a common subcellular locations with SNAREs and in the presynaptic part of synapses, while most of these SNARE proteins are present in RTN1-C-negative compartments. The latter observation is not suprising, regarding the common location of syntaxin 13 (Hirling et al., 2000; Prekeris et al., 1998), syntaxin 1 (Bennett et al., 1992; Garcia et al., 1995), and VAMP2 (Baumert et al., 1989).

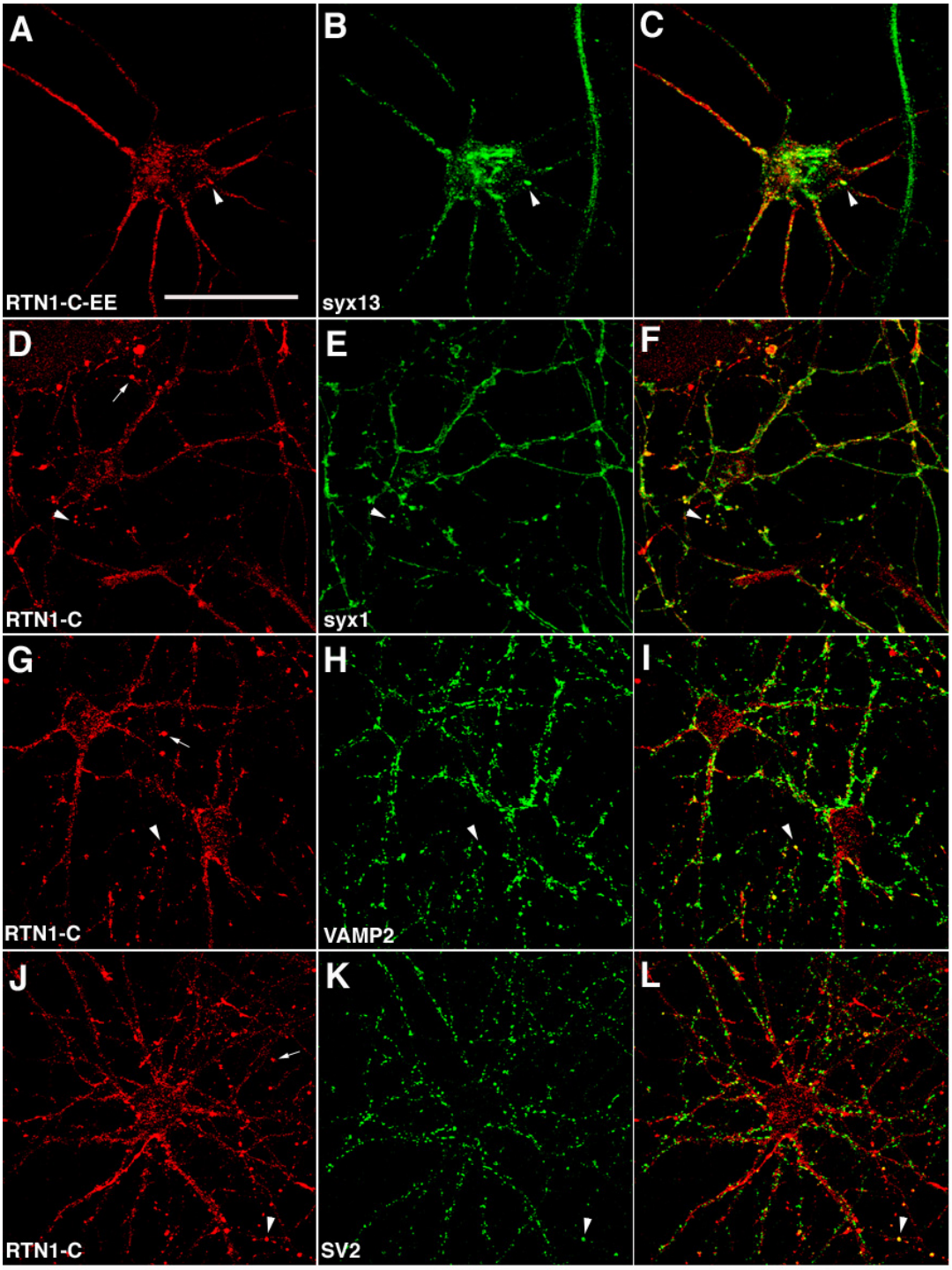

Figure 33. **RTN1-C is partially colocalized with SNARE proteins and SV2 in hippocampal neurons.** Hippocampal neurons at DIV 10 were fixed and immostained using anti-EE (A), anti-syntaxin 13 (B), anti-RTN1-C (D, G, J), anti-syntaxin 1 (E), anti-VAMP2 (H), or anti-SV2 (K) antibodies. Due to available monoclonal and polyclonal antibodies, neurons in A to C were transfected at DIV 8 with EE-tagged RTN1-C. Overlays are shown on the right panel. Arrows indicate bulb-like RTN1-C-positive structures, and arrowheads indicate strongly overlapping puncta. Single confocal sections are shown. Scale bar is 10 μm.

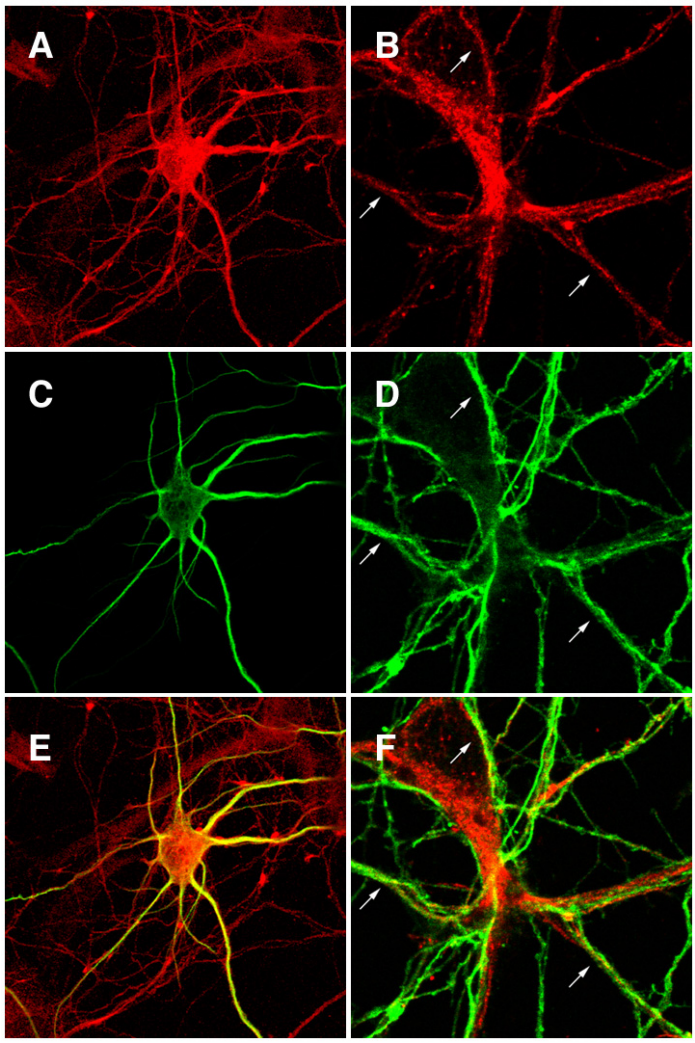

Figure 34. **Localization of RTN1-C in somatodenritic and axonal domains of hippocampal neurons**. Hippocampal neurons at DIV 13 were double-labeled using antibodies against RTN1-C (A, B), MAP2 (C), or Tau (D). In D, arrows show processes positive for RTN1-C (B) and Tau (D). Single confocal sections are shown. Overlays are on E and F.

III.4.5 RTN1-C Is Implicated in Secretion in PC12 Cells

RTN1-C is most highly expressed in neuroendocrine cells (Hens et al., 1998), suggesting that RTN1-C function could be linked to secretion mechanism. Due to the presence of RTN1-C in complexes with syntaxin 1 and VAMP2, two SNAREs necessary for mechanisms of regulated secretion (Jahn and Sudhof, 1999), we asked whether overexpression of RTN1-C or its first aa 1-41, which was shown to be sufficient for its interaction with syntaxin 1 and VAMP2 (Steiner et al., 2004), could affect basal or stimulated secretion. To test this possibility, PC12 cells were cotransfected with plasmids encoding human growth hormone (hGH) and either no exogenous protein (vector) or full length RTN1-C or RTN1-C aa 1-41 (Figure 35). Three days

after transfection, secretion from these PC12 cells was either not stimulated and incubated in 5 mM potassium or stimulated with 80 mM potassium to evoke hGH release. Measurement of basal secretion was not significantly different between control (vector) and RTN1-C or RTN1-C aa 1-41 (Figure 35A, $P < 0.5$), suggesting that RTN1-C or RTN1-C aa1-41 have no influence on secretion at steady state. On the other hand, stimulated secretion (Figure 35B) was significantly increased by a factor of 1.75 for cells overexpressing RTN1-C aa 1-41 (5.23 fold stimulation over basal) compared to the control (3.08 fold stimulation over basal; $P < 0.01$). Stimulation of cells which overexpress RTN1-C full length was not affected compared to cells which were transfected with the empty vector (2.91 fold stimulation over basal, $P < 0.7$). These data indicate that RTN1-C is directly or indirectly involved in regulated secretion and suggest that the observed protein complexes between RTN1-C and exocytic SNAREs have functional implications.

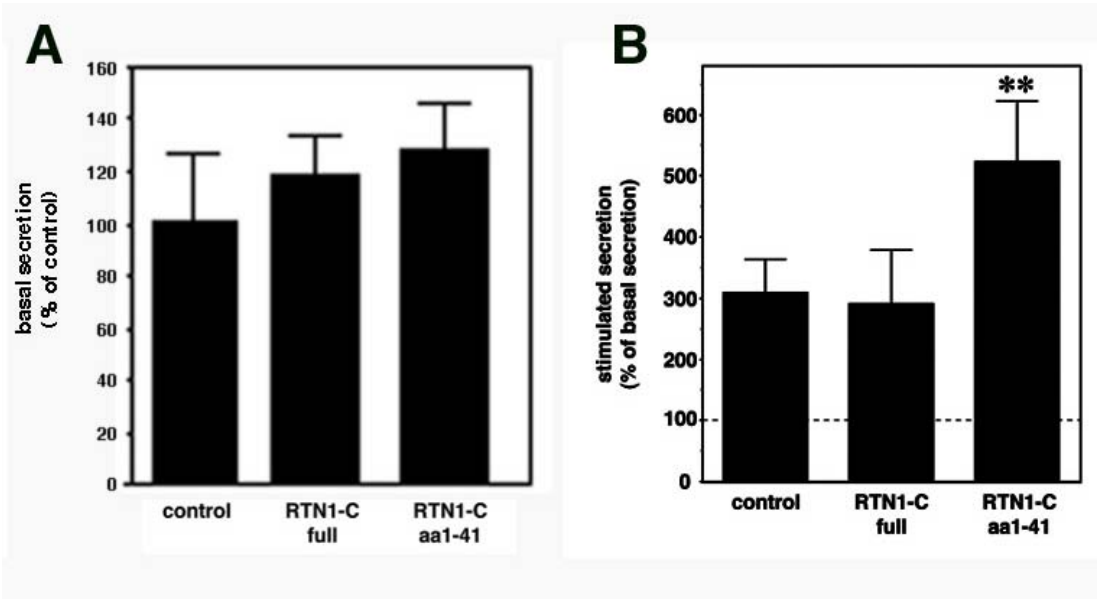

Figure 35. RTN1-C aa1-41 expression stimulates regulated secretion. (A,B) PC12 cells were cotransfected with plasmids coding for human growth hormone and either GFP (control), or full length RTN1-C (RTN1-C full), or RTN1-C aa1-41-EE (RTN1-C aa1-41). After 3 days of transfection cells were either incubated with basal solution (5 mM KCl) or stimulated secretion solution (80 mM KCl), and secreted hGH were measured in the medium for cells in basal condition (A) and in stimulated condition (B). Average stimulation from 4 independent experiments is shown. Error bars indicate standard deviation. No statistical difference was observed for basal secretion while stimulated GH-release is significantly different between control and RTN1-C aa1-41 overexpression (double asterisks ; $P< 0.01$).

IV Discussion

Correct functionning of the mammalian central nervous system relies on precise synaptic circuits. These circuits are assembled during development by the formation of synaptic connections between millions of neurons. It is believed that the construction of functional neuronal circuits requires 2 general processes (Goodman and Shatz, 1993). The initial rough neuronal diagram of connectivity is established in absence of neuronal electrical activity. After these initial events, synapses are extensively remodeled to establish precise functional connections (Katz and Shatz, 1996) and neuronal activity seems to be crucial in this process. In addition, it has been shown that mechanisms underlying synaptic plasticity, like information processing (learning) and storage (memory), also contribute to the activity-dependent formation and refinement of neuronal circuits during development (Zhu et al., 2000).

Recently, it has been shown that correct trafficking of neuronal plasma membrane receptors along the endosomal pathway is directly implicated in molecular mechanisms underlying synaptic plasticity and is fundamental for proper neuronal communication (Buckley et al., 2000). In order to gain insight into endosomal protein trafficking implicated in synapse maturation and synaptic function, we used syntaxin 13, a neuron-enriched endosomal SNARE protein (Hirling et al., 2000), as a bait to immunopurify complexes from new born rat brain membrane extracts, which corresponds to stage of synapse maturation. Among the 5 new syntaxin 13-interacting proteins that we identified, the presented work focused on the characterization of 2 of them, NEEP21 and RTN1-C.

IV.1 NEEP21, a Key Actor of Synapse Maturation and Synaptic Plasticity

IV.1.1 NEEP21 Belongs to a New Family of Proteins Recently Identified

A mRNA, named p1A75, which contained a part of NEEP21 reading frame, had been isolated from adult rat brain in a differential screen for brain-specific genes (Sutcliffe et al., 1983). Its corresponding protein was shown to be expressed in the whole brain and PC12 cells; it was

postulated that the protein was cytoplasmic, enriched in the somtodendritic domain of neurons and could play a role in export of proteins into dendrites (Sutcliffe et al., 1983). In 1996, Carlock et al. described the molecular characterization of human (D4S234 locus) and mouse (m234) homologues, which were mapped near the Huntington gene region whose transcripts are 93% identical to p1A75 (Carlock et al., 1996). They also found that they share 65% DNA sequence identity with p19, a 19-kDa protein, expressed specifically in neurons and neuroendocrine cells, and localized to Golgi-like structures (Saberan-Djoneidi et al., 1995). However, non conservative sequence differences suggested that these genes are independent members of a multigene family. 3 years later, the same group isolated a full length murine clone corresponding to the rat neuronal p1A75 partial cDNA (Saberan-Djoneidi et al., 1998). In addition, they showed that it encodes a 185-residue polypeptide containing a transmembrane domain that displays 56% identity with p19. Using an antibody directed against the recombinant polypeptide, the authors demonstrate the existence of the native 21-kDa protein (p21) corresponding to NEEP21. All these studies identified NEEP21, in those previous studies called 1A75, p21 or D4S234/m234, as a protein enriched in neurons, which belongs to the same new family as the p19 protein (Saberan-Djoneidi et al., 1998) of so far unknown function. A third protein, called calcyon (Lezcano et al., 2000) was identified recently and appeared to be the most highly diverged member of this family with 37% identity to NEEP21/p21. Calcyon interacts with D1 dopamine receptor and seems to regulate the signaling of this receptor through an unknown mechanism (Lezcano et al., 2000).

A remarkable aspect of NEEP21 is the high sequence conservation between homologues of several different species : NEEP21 is 98.4% identical between mouse and human, and 99.5% between rat and mouse. EST sequences (AJ394144, AJ393704, AY394975 and AF543538) indicate the existence of chicken and fish homologues 88% and 50% identical to human NEEP21 respectively. This suggests that NEEP21 but also p19 are subjected to strong selection pressure, arguing for a fundamental role of these proteins in brain development and function during evolution of vertebrates, since no related sequences were identified in any non vertebrate animal.

IV.1.2 NEEP21 Is a Type I Integral Membrane Protein

Analysis of NEEP21 primary aa sequence suggested that its NH2- and COOH-terminal domains are hydrophilic and separated by a transmembrane domain (Saberan-Djoneidi et al.,

1998), allowing the incorporation of the protein into lipid bilayers of organelles and/or plasma membrane. In our study, we investigated the topography of NEEP21 and demonstrated that its COOH-terminal domain was present in the cytosol while its NH2-terminal domain was restricted to the lumen of organelles, as described for type I integral membrane proteins (High, 1997; Rapoport et al., 1996). Moreover, we found that the COOH-terminus of NEEP21 was responsible for its interaction with syntaxin 13. We thus focused on its COOH-terminus to characterize molecular interactions involving cytoplasmic proteins.

IV.1.3 NEEP21 Is Localized to the Sorting Domain of Endosome

Many aspects of neuronal function are apt to be regulated by protein trafficking through the endocytic endosomal pathway. This includes targeting of proteins to specific pre- and post-synaptic domains in response to activation of signal transduction pathways by extracellular stimuli (Buckley et al., 2000). Many aspects of the molecular endosomal machinery and the different domains of the endosomal pathways necessary for correct spatial and temporal targeting of lipids and proteins are well characterized in fibroblasts (Gruenberg, 2001; Pfeffer, 2003; Zerial and McBride, 2001). In contrast, little is known about those implicated in trafficking events in neurons. Because we found that NEEP21 interacts with syntaxin 13, we hypothezised that it is present along the endosomal pathway. Indeed, NEEP21 colocalized strongly with internalized Tf and TfR, typical markers for early endosomes, and partially with syntaxin 13. In contrast, no colocalization was found with LBPA, a marker of late endosomes. Colocalization of NEEP21 with TGN38 showed a clear overlap between both proteins in the perinuclear region. This may reflect NEEP21 during biosynthesis, or its presence in perinuclear endosomes close to Golgi compartments (Gruenberg, 2001; Gruenberg and Maxfield, 1995), or a subpopulation of NEEP21 localized to TGN. We concluded that NEEP21 is present along the early endosomal pathway. Previous studies of NEEP21/p21 localization argued that it was expressed strongly in the juxtanuclear region of neurons and germ cells in a punctate staining (Saberan-Djoneidi et al., 1998). Although double labeling was not performed, the authors interpreted the NEEP21 staining as Golgi complex.

Since the function of NEEP21 and its homologues has been completely unknown, a precise identification of the endosomal subdomain containing NEEP21 would give clues about the function of NEEP21. Early endosomes contain at least 3 functionally distinct elements that are needed for the processes of receptor sorting, receptor recycling, and receptor degradation

(Pfeffer, 2003; Zerial and McBride, 2001). They were identified by visualization of endosomal protein segregation using live cell video microscopy to simultaneously follow multiple Rab GTPases (de Renzis et al., 2002; Sonnichsen et al., 2000). Distinct Rabs localize to the surface of distinct membrane-bound endosomes: it is possible to distinguish along the early endosomal pathway a wortmannin-sensitive Rab5/Rab4 domain and a BFA-sensitive Rab4/Rab11 domain (see figure 14). Rab5 is involved in endocytosis (mclauchlan, 1998) and vesicle fusion on early endosomes (Gorvel et al., 1991) ; Rab4 in the trafficking from early endosomes to the plasma membrane (van der Sluijs et al., 1992), to recycling endosomes (Nagelkerken et al., 2000) or to late endosomes (McCaffrey et al., 2001), suggesting a role in the sorting of proteins and lipids. Finally, Rab11 was shown to be involved in trafficking through recycling endosomes (Ullrich et al., 1996). We found here that NEEP21 colocalized significantly with Rab4-positive endosomes, whereas little overlap was observed with Rab5-, EEA1- and Rab11-positive endosomes in PC12 cells. In addition, wortmannin, which affects sorting endosomes, but not BFA, which affects recycling endosomes, relocalized NEEP21 together with TfR in primary neurons. We thus concluded that NEEP21 is localized to a domain of sorting endosomes enriched in Rab4. Such a domain has been postulated to be crucial for the sorting into distinct pathway of internalized lipids and proteins (McCaffrey et al., 2001; van der Sluijs et al., 1992; Zerial and McBride, 2001). In addition, when we overexpressed in PC12 cells a mutant of Rab5, Rab5Q79L, which causes an enlargment of sorting endosomes by increased fusion of endocytosed vesicles, NEEP21 localized to Rab5Q79L-positive structures, confirming the presence of NEEP21 on sorting endosomes.

Syntaxin 13 was detected mainly on tubular recycling endosome (Prekeris et al., 1998), with a small fraction present in Rab5-positive endosomes (McBride et al., 1999; Trischler et al., 1999). Therefore syntaxin 13 might act on recycling or sorting endosomes, where it could interact with NEEP21. Using video microscopy to follow the trafficking of NEEP21-CFP and syntaxin 13-YFP in living hippocampal neurons, we noted that syntaxin 13-YFP is present on tubular organelles which were highly mobile was previously described (Prekeris et al., 1999a) and thus confirmed that syntaxin 13 is enriched on recycling endosomes. In contrast, we observed that NEEP21-CFP is present on punctate structures which are less dynamic than syntaxin 13-positive organelles. We did not detected any significant colocalization but both organelles were, in some cases, in apposition to each other. We thus postulate that NEEP21 and syntaxin 13 are present on separate endosome populations (see figure 16). Their interaction would happen when NEEP21- and syntaxin 13-positive endosomes are

temporarily in contact and would fuse following a kiss-and-run mechanism that would allow the exchange of lipids and molecules.

Altogether these data showed that NEEP21 is present on endosomes, which are known to be crucial for trafficking of proteins. In addition, we managed to identify the NEEP21-enriched subdomain, which is involved in the sorting of lipids and receptors. We thus focused our work to investigate whether NEEP21 would participate in the trafficking of receptors.

IV.1.4 NEEP21 is Essential for Correct Protein Cycling in PC12 Cells

We used an antisense strategy to inhibit NEEP21 expression or exogenous NEEP21 overexpression to assess its role in receptor cycling in PC12 cells. We first chose Tf-TfR because it is well established that it trafficks along the early endosomal pathway in a precisely characterized time-course (Buckley et al., 2000; Gruenberg and Maxfield, 1995) (see figure 11). We found that exogenous overexpression of NEEP21 not only accelerates internalization of rhodamin-Tf but also its recycling, demonstrating that NEEP21 could act in the coupling of exo-and endocytosis mechanisms through the regulation of endosomal trafficking of TfR. In light of the described NEEP21 localization, faster decrease of internal Tf upon NEEP21 overexpression is most probably due to an accelerated recycling of Tf to recycling endosome or to plasma membrane. This could indirectly stimulate earlier steps of the cycle causing faster intenalization. When we downregulated NEEP21 expression TfR internalization was not affected while a strong delay in its recycling was observed. This might reflect the correct internalization of TfR into sorting endosomes, but an inhibited transport to the plasma membrane or to the recycling endosomes due to its retention for longer time in endosomal compartments. NEEP21 is thus necessary to link the trafficking of TfR between different early endosomes and/or between early endosomes and the plasma membrane.

We also demonstrated that modulation of NEEP21 expression by overexpression or downregulation affects the correct cycling of L1 in PC12 cells. L1 is a cell adhesion molecule expressed in the axonal domain of neurons. In axonal growth cone, L1 is internalized at the central domain into early endosomes and is then recycled to growth cone peripehry (Kamiguchi and Lemmon, 2000). Because, TfR and L1 are rather divergent plasma membrane proteins, NEEP21 probably acts on a large range of receptors at least in PC12 cells. This means that, first, a general molecular mechanism exists for sorting and trafficking along the

early endosomal pathway in PC12 cells, and, second, that NEEP21 is an important constituent of this mechanism.

IV.1.5 NEEP21 Interacts With Syntaxin 13 and Syntaxin 7

We isolated NEEP21 as a new syntaxin 13-interacting protein. Syntaxin 13 was first described as a SNARE protein localized to the recycling endosomes and found to be developmentally regulated and enriched in the brain (Advani et al., 1998; Hirling et al., 2000; Tang et al., 1998). Antibodies against syntaxin 13 combined with a TfR recycling assay in permeablized PC12 cells inhibited TfR recycling, demonstrating its direct link to receptor recycling from endocytosis to the plasma membrane (Prekeris et al., 1998). In addition, syntaxin 13 has been identified in a complex with the Rab5-effectors Rabaptin-5 and EEA1 necessary for homotypic early endosomal fusion in vitro (McBride et al., 1999). More recently, Sun W. et al. confirmed a role for syntaxin 13 and established a role for SNAP-25 and VAMP2 in endosome fusion (Sun et al., 2003). NEEP21 interaction with syntaxin 13 gives it a direct link with the endosomal molecular machinery and renforces the notion that NEEP21 is involved in the correct cycling of membrane proteins, even if the exact molecular details are just beginning to be understood.

We also found that NEEP21 interacts with syntaxin 7. Syntaxin 7 is a membrer of the SNARE syntaxin family which was first localized to the early endosomal pathway (Advani et al., 1998). It was shown that it was present on vacuolar early endosomes and at the plasma membrane (Prekeris et al., 1999b). However, recently, syntaxin 7 was identified on the late endosomes and required for the fusion of late endosomes and lysosomes in vitro (Mullock et al., 2000). Moreover, syntaxin 7 interacts with vti1b, syntaxin 8 and VAMP8, 3 other late endosomal SNARE proteins to form an atypical core complex, which promotes homotypic fusion of late endosomes in vitro (Antonin et al., 2002; Antonin et al., 2000). The interaction between NEEP21 and syntaxin 7 suggests that NEEP21 is not only connected to the machinery of trafficking through the recycling pathway but is also linked to the degradation pathway. These findings argue for a model in which NEEP21 could be a molecular switch between the recycling and the degradation pathway. Moreover NEEP21 is the first molecule known to be coupled at the same time with the recycling and the degradation endosomal pathways.

IV.1.6 NEEP21 is Involved in AMPA Receptors Cycling

In contrast to other known endosomal proteins, NEEP21 is strongly enriched in neurons and, to a lesser extent, in germ cells (Saberan-Djoneidi et al., 1998; Sutcliffe et al., 1983). Therefore, it is probably not engaged in ubiquitous endosomal trafficking. In primary neurons, NEEP21 localizes to processes positive for a dendritic marker, but negative for axonal markers. Consequently, the function of NEEP21 must be specific to endosomal trafficking of somatodendritic membrane proteins of neurons. Recent studies have proven the importance of AMPA receptor internalization and trafficking through the endosomal pathway for the expression of long term potentiation (LTP) and long term depression (LTD), 2 forms of synaptic plasticity, which are believed to underlie the formation of memories (Beattie et al., 2000; Carroll et al., 1999b; Shi et al., 2001). Endocytosed AMPA receptors are internalized in syntaxin 13- (Lee et al., 2001; Lin et al., 2000) and Rab4-positive compartments (Ehlers, 2000). In addition the type of AMPA receptor trafficking is dictated by the type of stimulus : AMPA stimulation leads to the degradation pathway (late endosomal pathway), NMDA to the recycling pathway (early endosomal pathway) and insulin stimulation provokes the internalization of receptors in an undefined pathway (Ehlers, 2000; Lin et al., 2000). We found here that among the 3 stimuli, NMDA resulted in the strongest colocalization between the AMPA receptor subunit GluR2 and NEEP21, confirming the presence of NEEP21 along the recycling endosomal pathway. In addition, antisense-mediated down-regulation of NEEP21 retarded recycling of GluR1 and to a lesser extent of GluR2, after NMDA application. These results indicate that NEEP21 is an important component of the machinery necessary for AMPA receptor recycling. We did not observe any effect of NEEP21 down-regulation on the presence of AMPA receptors at the plasma membrane either at steady state (absence of stimulation) or after 10 min of stimulation (internalization). This demonstrates that constitutive cycling of AMPA receptors happens in the presence of spontaneous activity (Passafaro et al., 2001; Piccini and Malinow, 2002; Shi et al., 2001).

IV.1.7 Deciphering NEEP21 Function in AMPA Receptor Trafficking Through its Interaction with GRIP and GluR2

Mechanisms linked to the internalization of AMPA receptors into endocytic vesicles are starting to be elucitated (Lee et al., 2002; Lin and Sheng, 1998), while the molecular components which are involved in the trafficking of AMPA receptors through the endosomal

pathway are definitely not clear (Buckley et al., 2000). Our findings that NEEP21, an endosomal protein, is necessary for correct AMPA receptor trafficking, prompted us to define the molecular context for NEEP21 in AMPA receptor cycling. We thus tested whether NEEP21 could interact with molecules known to be linked to AMPA receptor trafficking.

We identified NEEP21 in complexes with GRIP, PICK1, GluR2, and syntaxin 13 but not with SAP97. GRIP binds to the C-terminus of GluR2 and GluR3 through its PDZ domains 4 and 5. This interaction is necessary for maintaining the accumulation of GluR2/3 receptors at the plasma membrane and/or for its correct delivery from an endosomal compartment to the synapse (Daw et al., 2000; Dong et al., 1997; Osten et al., 2000; Seidenman et al., 2003; Shi et al., 2001). In transfected hippocampal neurons, a GluR2 mutant lacking the PDZ binding site is transiently transported to the synaptic surface but does not accumulate at the plasma membrane (Osten et al., 2000). On the other hand, loading CA1 pyramidal cells in slices with a peptide that distrupts the GluR2/3-GRIP interaction caused an increase in synaptic currents and prevented the generation of LTD (Daw et al., 2000). Even if the precise role of the interaction between GluR2/3 receptors and GRIP is not clear, it is conceivable that GRIP subserve essential functions in the delivery, stabilization, and endocytosis of synaptic AMPA receptors. PICK1, like GRIP was found to bind the extreme C-terminal PDZ-binding domain of GluR2/3 receptors (Xia et al., 1999). PICK1 was first described as protein that interacts with the catalytic subunit of PKCα (Staudinger et al., 1995). Phosphorylation of serine 880 by PKC in the PDZ-binding domain of GluR2 greatly decreases the affinity of GluR2/3 receptors for GRIP but not for PICK1 (Chung et al., 2000), leading to the destabilization of the phosphorylated GluR2/3 receptors in the plasma membrane and to their internalization. On this basis, it was proposed that PICK1 could target PKC to GluR2/3, in order to phosphorylate serine 880, which eventually releases it from GRIP. They are thus internalized, enter the recycling pathway, and finally reinserted into the plasma membrane (Collingridge and Isaac, 2003). The complexes between NEEP21, GRIP, GluR2 and PICK1 that we identified likely occurs most probably along the early endosomal pathway, since we never detected NEEP21 at the plasma membrane. Subsequent work has shown that GRIP is colocalized with GluR2/3 at intracellular dendritic locations, which is fully consistent with this hypothesis (Burette et al., 2001). These results suggest that the action of NEEP21 on GluR2 trafficking, that we discovered, takes place through its interaction with GRIP, GluR2/3 and PICK1. We did not manage to coimmunoprecipitate NEEP21 with monoclonal anti-GRIP antibodies and

coimmunostaining with anti-NEEP21 and the same monoclonal anti-GRIP antibodies revealed an apparent absence of colocalization between both proteins (data not shown). This was suprising regarding the quantity of GRIP which was coimmunoprecipitated with anti-NEEP21 antibodies. One possibility would be that the monoclonal anti-GRIP antibody recognizes an epitope on GRIP which is implicated in the interaction with NEEP21, and thus would not detect GRIP being complexed with NEEP21.

We also found that syntaxin 13 interacts with GRIP. Due to the role of syntaxin 13 as a constituent of the SNARE core complex necessary for endosomal fusion, it is tempting to speculate that this interaction reflects the first link between GluR2 trafficking and the fusion machinery necessary to move from one compartment to another along the reycling pathway.

PDZ domain 2 of SAP97 interacts with the C-terminus of GluR1 and is the only PDZ protein currently known to interact directly with GluR1 (Leonard et al., 1998). In dissociated neuronal cultures, transfected SAP97 concentrates at postsynaptic sites and increases synaptic AMPA receptor density (Rumbaugh et al., 2003). Deletion of the last 4 residues of GluR1 which prevent interaction between GluR1 and SAP97 results in a drastic loss of GluR1 surface delivery (Passafaro et al., 2001). However, overexpression of SAP97 into hippocampal slice cultures failed to detect a change in the magnitude of AMPA receptor EPSCs, suggesting that SAP-97 is not important for GluR1 insertion into the synaptic plasma membrane (Schnell et al., 2002). A recent report has also suggested that interaction involving SAP97 and GluR1 occurs early in the secretory pathway, while the receptors are still in the endoplasmic reticulum or cis-Golgi (Sans et al., 2001). In addition, few synaptic GluR1-containing receptors were found to associate with SAP97. Taken together, the role of SAP97 in regulating AMPA receptors remains contreversial. Nevertheless, SAP97 is a potential candidate in the control of GluR1 trafficking. Using anti-NEEP21 as bait for immunoprecipitation, we did not detect any interaction between NEEP21 and SAP97. Since we found that NEEP21 suppression delays strongly the recycling of GluR1, it means that the implication of NEEP21 related to the trafficking of GluR1 is not connected to the SAP97-GluR1 complex. In addition we did not find a clear interaction between GluR1 and NEEP21 by immunoprecipitation (experiments performed by Liliane Glauser, a technician in our group), suggesting that modulation of GluR1 trafficking by NEEP21, happens through an indirect mechanism. The majority of AMPA receptors are of 2 different subunits combinations namely GluR1/2 or GluR2/3 receptors (Bredt and Nicoll, 2003). Because we did not specifically immunoprecipitated GluR1, which should be associated with GluR2, NEEP21 probably interacts with GluR2/3 receptors and not GluR1/2 receptors.

IV.1.8 Modulation of NEEP21-GRIP Interaction by NMDA

The mechanisms underlying NMDA stimulation which provokes internalization of AMPA receptors and targeting to recycling pathway, was postulated to be dependent on NMDA receptor activation and phosphorylation of the C-terminus of AMPA receptors (Ehlers, 2000). Following activation of NMDA receptors, GluR1 and GluR2 are phosphorylated on Serine 845 (Lee et al., 2000) and 880 respectively (Kim et al., 2001). For GluR1, it was then demonstrated in culture that entry of calcium through NMDA receptors was accompanied by activation of phosphatases, which leads to the dephosphorylation of GluR1 and provokes its recycling (Ehlers, 2000). In the absence of dephosphorylation, which happens with AMPA stimulation, receptors are transported to late endosomes and then to lysosomes for degradation. Endocytosis entry into different AMPA receptor routes is thus regulated by differentiated phosphorylation/dephosphorylation cycles. As mentioned above, in slices, these cycles control the rate of association between GluR2 and scaffolding proteins GRIP or PICK1. In this context, we found that after NMDA stimulation, the level of NEEP21-GRIP interaction was increased by a factor of 2. This means that during recycling of AMPA receptors, this interaction is regulated, and suggests a functional link between its formation and the trafficking of GluR2/3 receptors along the early endosomal pathway.

IV.1.9 Dendritic Morphology and NEEP21-GRIP Interaction

We have shown that the COOH-terminal domain of NEEP21 is oriented towards the cytosol, and is responsible for the interaction with syntaxin 13. We thus produced differents fragments of its COOH-terminal domain, and identified that the NEEP21 fragment aa 129-165 is sufficient to interact with GRIP and GluR2. We reasoned that overexpression of this fragment in neurons might act in a dominant-negative manner by competing with endogenous NEEP21-GRIP interaction, which could elucidate the functional importance of this interaction during AMPA receptor trafficking. Overexpression of fragment aa 129-165 provoked a strong inhibition of dendritic outgrowth after 2 days of transfection, while their axon remains intact. At 7 days, we found that the length of axons was also reduced. Specific changes in dendritic morphology after 2 days of transfection suggests that the NEEP21 fragment aa 129-165 impairs some mechanisms linked to dendritic structural plasticity. It is known that activity can

affect the number and the shape of synapses, in vivo and in vitro (Grutzendler et al., 2002; Knott et al., 2002; Toni et al., 1999; Trachtenberg et al., 2002). Morover, it was shown that modulation of NMDA and AMPA receptor activity in hippocampal slices affects the density of spines and the number of synapses (Luthi et al., 2001; McKinney et al., 1999). These authors showed that the chronical blockade of AMPA receptors provokes a strong decrease in the density of spines and conclude that AMPA receptor activation is sufficient to maintain dendritic spines (McKinney et al., 1999). They also demonstrated that activation of NMDA receptors limits the number of synaptic connections during hippocampal development (Luthi et al., 2001).

At the same time, under pathological conditions of excessive synaptic activation of glutamate receptors, dendrites undergo functional and morphological changes. Indeed, pathomorphological studies identified a common feature of dendritic injury, which is the formation of varicosity along the dentritic arbor in vivo (Matesic and Lin, 1994) and in vitro (Al-Noori and Swann, 2000), which resembles the type of varicosities that appeared along dendrites during NEEP21 fragment aa 129-165 overexpression. Varicosity formation occurs even after brief sublethal excitotoxicity exposure, and thereafter recuperates spontaneously (Hasbani et al., 2001). In addition, varicosity formation was shown to be accompanied by AMPA receptor internalization which could be a self protective response against excitotoxicity (Ikegaya et al., 2001). These studies show that glutamate receptor activity is tightly associated with structural modification of dendritic arborization of glutamatergic neurons. More recently, Passafaro et al. found that overexepression of exogenous HA-GluR2 in hippocampal neurons induces denditritic spines formation (Passafaro et al., 2003), suggesting that in addition to their activation, the number of AMPAR receptors present at the cell surface is crucial for the control of dendritic structure. In this sense, overexpression of NEEP21 fragment aa 129-165 could disturb NEEP21-GRIP interaction and consequently impair correct trafficking of GluR2 (see below) which would affect dendrites morphology. Indeed, we found that coexpression of fragment aa 129-165 and exogenous HA-GluR2 slighly compensates shrinkage of dendrites, suggesting that the observed dentritic swelling, is linked, at least in a part, to GluR2 trafficking.

Since overexpression of HA-GluR2 did not compensate fully the morphological effect due to NEEP21 fragment aa 129-165 overexpression, further target of GRIP different from GluR2 might also be affected. GRIP interacts with several other proteins through its seven PDZ domains (Sheng and Sala, 2001). GRIP may thus function as a scaffold for multiprotein complexes. In particular, GRIP binds to molecules which are clearly important for dendritic

shape and synapse formation. Its PDZ 6 and 7 are known to be responsible for its interaction with Eph-receptors and their membrane-bound ligands, the ephrins (Bruckner et al., 1999; Contractor et al., 2002; Torres et al., 1998). It is believed that interactions between Eph-receptors and their ligands located on adjacent cells are important for processes involved in neurite extension, axonal guidance and dendritic spine formation (Henkemeyer et al., 2003; Himanen and Nikolov, 2003). It was further demonstrated that GRIP-ephrins interaction was necessary in the clustering of ephrins and important for signal transduction (Bruckner et al., 1999). GRIP also interacts with the liprin-α family of proteins through its PDZ 6. Liprin-α promotes surface expression and clustering of AMPA receptors (Wyszynski et al., 2002). Liprin-α in turn interacts with GRK interactor 1 (GIT1), a multidomain protein, that regulates membrane trafficking, the actin cytoskeleton and synapse formation (Ko et al., 2003; Zhang et al., 2003). It was postulated that GRIP could be important to couple different pathways together, like dendritic morphology and activity-dependent AMPA receptor trafficking. It is thus possible that NEEP21 fragment aa 129-165 overexpression disturbs the formation of molecular complexes between GRIP and molecules involved in the maintenance of dendrites arborization. Another possibility would be that it impairs the correct localization of GRIP and its assocation with its partner, avoiding the formation of such molecular complex. This would be a simple sequestration of GRIP, independent of a NEEP21 role.

A third possibility would be that overexpression of NEEP21 fragment aa 129-165 is deleterious for dendrites because it would disturb molecular mechanisms which would be important for dendritic shape determination. This scenario is relatively impropable, because if the fragment has a toxic effect, it would affect dendrites and axons to the same extent. Since we observed that dendrites shrink early and axons only after one week of transfection, it is more plausible that the fragment affects specifically dendritic morphology, impairing functions of GRIP in AMPA receptor trafficking and in formation of molecular complexes implicated in the architecture of dendritic arborization.

IV.1.10 GRIP-NEEP21 Interaction is Implicated in Constitutive and Regulated GluR2 Trafficking

Overexpression of the NEEP21 fragment aa 129-165 in hippocampal neurons impairs correct regulated and constitutive trafficking of GluR2 but not of GluR1. Indeed, we found that following NMDA stimulation, endogenous GluR2 and exogenous HA-GluR2 were correctly internalized but failed to recycled properly to the cell surface. It demonstrates that the link

between NEEP21 and GluR2 trafficking is due to its interaction with GRIP. In addition, we also found that the fragment affects constitutive delivery of endogenous GluR2. This points out that the interaction of NEEP21 with GRIP is important for the constitutive cycling of GluR2/3 receptors. Constitutive cycling of exogenous HA-GluR2 are not affected probably due to its overexpression. These data emphasize the role of NEEP21 in trafficking of GluR2/3 receptors. Furthermore, they established for the first time the molecular link between AMPA receptors and the endosomal machinery through GRIP-NEEP21 and probably syntaxin 13 interactions. Since NEEP21 interacts with 2 different syntaxins, syntaxin 13 belonging to the fusion machinery of recycling pathway, and syntaxin 7 to the degradation pathway, it is possible that NEEP21 is necessary to couple « physically » GluR2/3 receptors to the recycling pathway or the degradation pathway, depending on the type of external stimulations (see below). Suprisingly, we found that the NEEP21 fragment disturbs the constitutive cycling of AMPA receptors, while GluR2 COOH-terminal mutants defective in PDZ-binding are targeted to the dendritic spine (Piccini and Malinow, 2002) and the neuronal surface (Passafaro et al., 2001), but fail to be detected electrophiosologically in the synapse (Shi et al., 2001). It is thus possible that GluR2/3 receptors which do not bind to GRIP or PICK1, could traffick internally and bypass the « classical » pathway containing NEEP21 and GRIP, which thus would lead to a normal constitutive cycling of receptors. But once receptors are bound to GRIP, this complex has to be linked to NEEP21 to find the proper way of trafficking from internal compartments to the cell surface. Interfering with NEEP21-GRIP interaction would thus lead to the missorting or receptors, which will never go back to the cell surface. This reenforces the idea that NEEP21 could be the molecular switch which control the fate of GluR2/3 receptors, and by this way could modulate synaptic plasticity.

We found that in NEEP21 fragment aa 129-165 transfected neurons, endogenous GluR1 recycling was slightly delayed after its NMDA-induced internalization. But we noted that there was no significant difference in signal intensity corresponding to the number of GluR1/2 receptors at steady state and after 60 minutes of stimulation. We thus conclude that the difference in recycling observed between cells overexpressing GFP or the fragment did not reflect a specific effect of the NEEP21 fragment aa 129-165 on cycling of GluR1/2 receptors. In addition, we did not found any effect of the fragment on exogenous HA-GluR1 cycling. We concluded that the interaction between NEEP21 and GRIP is important for GluR2/3 receptor trafficking but does not affect or control trafficking steps of GluR1/2 receptors. It is known that the molecular machinery and molecular events that control the trafficking steps of GluR1/2 receptors are different from those of GluR2/3 receptors (Passafaro et al., 2001; Shi et

al., 2001). Surface delivery of GluR1/2 in dendrites is slow under basal condition but inducible over a timescale of minutes by NMDA receptor activation, whereas exocytosis of GluR2/3 is constitutive and rapid, and continually replace synaptic GluR2/3 receptors. The distinct trafficking behaviors of GluR1 and GluR2 are determined by their C-terminal cytoplasmic tails, and in heteromeric GluR1/2 receptors, the behavior of GluR1 is « dominant » over GluR2 in terms of exocytosis to the neuronal surface (Passafaro et al., 2001). It is thus probable that the route of trafficking and the molecular machinery of GluR1/2 and GluR2/3 are different. Since GluR1 does not interact with GRIP and since NEEP21 interacts with GRIP and GluR2, it is not suprising that disturbing NEEP21-GRIP interaction affects the trafficking of GluR2/3 receptors but not GluR1/2 receptors. Suppression of NEEP21 delays the recycling of endogenous GluR1/2 receptors. This suggests that NEEP21 would also be linked to the molecular machinery responsible for GluR1 trafficking through a mechanims which remains to be identified. Since we did not find an interaction with SAP97 or GluR1, but with syntaxin 13 involved in the general mechanisms of endosomal fusion, another possibility would be that suppression of NEEP21 would disturb formation of complexes involved in fusion processes along the early endosomal pathway and thus would retard the delivery of GluR1 at the cell surface after its internalization.

NEEP21 fragment aa 129-165 affects the trafficking of GluR2/3 receptors but not of GluR1/2, which demonstrates the specificity of the action of the fragment on receptor trafficking. But because the fragment provokes such a dramatic effect on dendrite morphology, we checked whether cycling of TfR as an unregulated receptor would be also affected. We found that TfR cycling in hippocampal neurons which overexpressed NEEP21 fragment aa 129-165, was indistinguishable from control. This demonstrates that the NEEP21 fragment aa 129-165 disturbs cycling of receptors regulated by GRIP, including GluR2/3.

IV.1.11 NEEP21, a New Protagonist of Synaptic Plasticity

For more than a century it has been suggested that information storage in the brain involves alteration in the strength of synaptic communication between neurons. Such a cellular mechanism requires that synapses show activity-dependent long-lasting changes (Kandel, 2001). The most thoroughly characterized examples of such synaptic plasticity in the mammalian nervous system are long-term potentiation (LTP) and long-term depression (LTD). Since the discovery that rapid delivery of AMPA receptors from nonsynaptic sites to

the synapses could explain, at least in part, the change of synaptic strength during LTP or LTD, strong motivation and efforts were developped to understand the molecular mechanisms implicated in AMPA receptors trafficking (Malinow and Malenka, 2002). The mechanisms which allow the internalization of AMPA receptors following NMDA stimulation had received intense attention and many studies identified important constituents of this process. On the other hand, the different step following their internalization and their trafficking along endosomal pathways are almost unknown.

In this study, we discovered a new syntaxin 13-interacting protein, NEEP21, which is localized to the sorting endosomes and interacts with GluR2, as well as GRIP and PICK1, which are major actors in the control of delivery and/or stabilization of AMPA receptors. In addition we showed that this interaction is necessary for correct cycling of GluR2 during the constitutive and the NMDA-dependent cycling of GluR2/3 receptors. Based on these results, we can generate a tentative model for the role of NEEP21 regarding the trafficking of GluR2 along the endosomal pathway (Figure 36). In this model (Figure 36A), GluR2/3 receptors are tethered to the synaptic membrane via a scaffolding protein, such as a palmitoylated long form of ABP (an homologue of GRIP) (DeSouza et al., 2002) or of an N-terminal isoform of GRIP, GRIP1b (Yamazaki et al., 2001), which binds to the extreme C-terminus of GluR2. NSF, a multimeric ATPase that plays an essential role in membrane fusion (Jahn and Sudhof, 1999) is also bound to GluR2 and was shown to participate in the stabilization of GluR2/3 receptors at the plasma membrane (Noel et al., 1999). In response to glutamate release from the presynaptic terminus, calcium enters via activated NMDA receptors, leading to phosphorylation of serine 880 on GluR2, which induces dissociation of GRIP1b/ABP. AP2, a clathrin adaptator which links membrane proteins to clathrin and promotes assembly of clathrin coats, then exchanges with NSF to initiate clathrin-dependent endocytosis (Lee et al., 2002). The NMDA receptor-dependent calcium influx also initiates the activation of phosphatases (Ehlers, 2000) which cause dephosphorylation of serine 880 on GluR2, which then allows internalized AMPA receptors to be « gripped », by intracellular GRIP. This intracellular GRIP-GluR2 complex is then bound to NEEP21 on the sorting endosomes in the shaft of dendrites, which makes the link with the recycling fusion machinery through its interaction with syntaxin 13. PKC is then activated and targeted by PICK1, phosphorylates serine 880 of GluR2 (Henley, 2003). GluR2/3 receptor is then re-inserted into the plasma membrane and re-associated with ABP/GRIP1b and NSF after receptor dephosphorylation. In contrast, AMPA receptors activated in the absence of NMDA receptor activity (Figure 36B), are internalized as before. Dephosphorylation of serine 880 could be achieved via activation

of phosphatases due to calcium entry through an NMDA-independent mechanism (Beattie et al., 2000; Lin et al., 2000). GluR2/3 receptor will then form a complex with GRIP and NEEP21 which will coupled them to the degradation pathway through its interaction with syntaxin 7. The switch of the interaction between NEEP21 and syntaxin 13 or syntaxin 7 which directs the receptor to the recycling or degradation pathway could be regulated by the state of phosphorylation of AMPA receptors or GRIP itself (Bruckner et al., 1999). Indeed, it is known that differential calcium elevation, depending on the level of activity, can lead to phosphorylation/dephosphorylation of AMPA receptor subunits and promotes the induction of LTP or LTD (D'Alcantara et al., 2003; Malinow and Malenka, 2002). Controling the degree of AMPA receptor recycling and degradation through the formation of complexes with NEEP21 and different syntaxins, may ensure the maintenance or elimination of AMPA receptors at a given synapse, with its particular state of activation.

Expression of NEEP21 mRNA (Saberan-Djoneidi et al., 1998; Sutcliffe et al., 1983) and protein (Steiner et al., 2002a) is highest during the first postnatal week. AMPA receptors are recruited into NMDA receptor-containing synapses during postnatal development, with a subsequent switch of receptor subunits (Pickard et al., 2000; Zhu et al., 2000). Most excitatory synapses initially have only NMDA receptors and such synapses transmit little electrophysiological information at resting membrane potentials. During development, these silent synapses acquire AMPA receptors and can transmit faithfully. This functional transformation is due to the delivery of GluR4-containing AMPA receptors which only necessitates spontaneous activity to traffick from internal stores to synapses (Zhu et al., 2000).

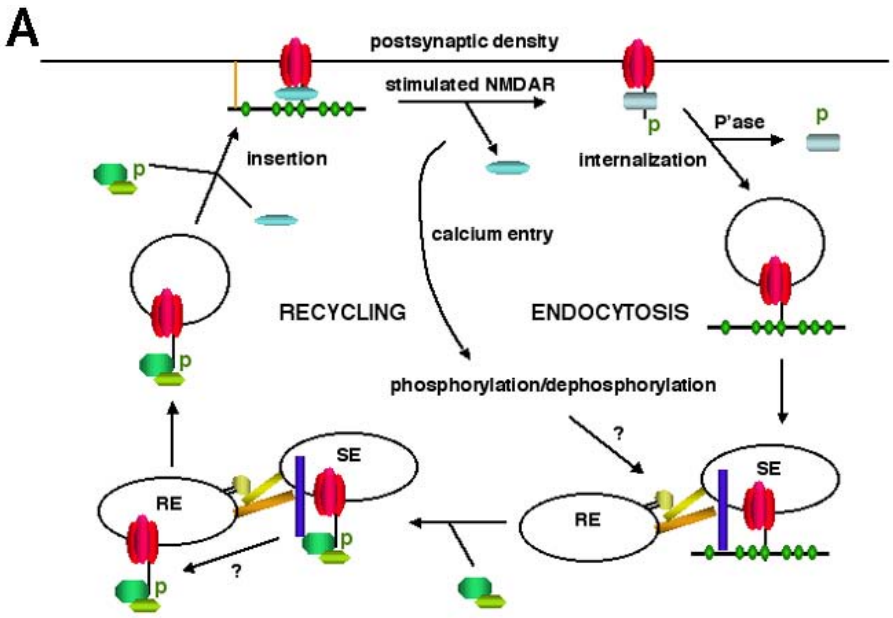

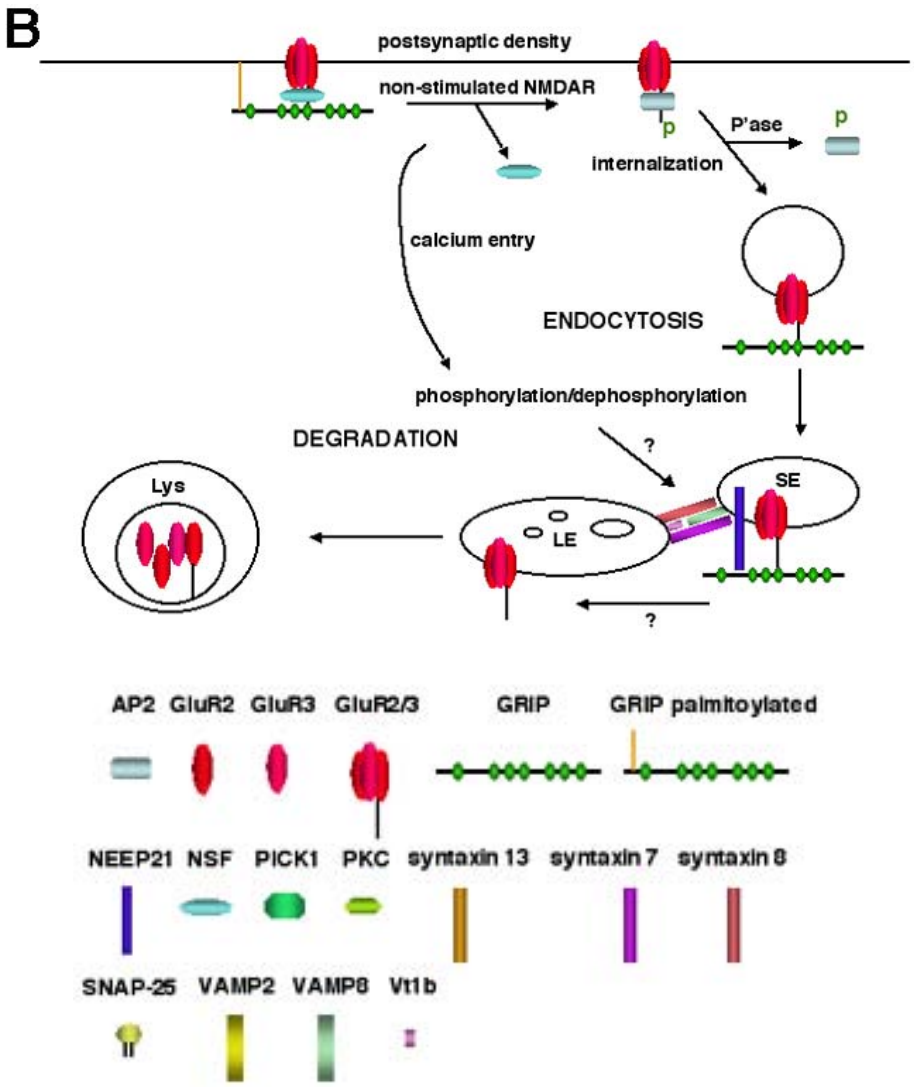

Figure 36. A model for the possible role of NEEP21 in recycling and degradation of AMPA GluR2/3 receptors. (A) role of NEEP21 during GluR2/3 recycling. (B) Role of NEEP21 during GluR2/3 degradation. See text for details. LE, late endosome ; Lys, lysosome ; NMDAR, NMDA receptor ; P'ase, phosphatase ; RE, recycling endosome ; SE, sorting endosome.

This is in contrast to GluR1/2 receptors which need high-frequency stimulation. Indeed, GluR4 is strongly expressed during the first postnatal week and synapses, potentiated by transient delivery of GluR4-containing AMPA receptors, maintain their strength over this period (Zhu et al., 2000). This delivery allowed non-functional connections to transmit at resting potentials. The delivered receptors were then exchange with non-synaptic GluR2/3 receptors in a manner that required little neuronal activity. This occurs over the course of days after the activity-driven delivery of GluR4-containing receptors. This step may be crucial for

the maturation of glutamatergic synapses and be important for maintaining synaptic strength despite protein turnover. Strong expression of NEEP21 during this period could thus be necessary to promote subunit exchange during synaptogenesis in modulating alternatively the degradation of GluR4-containing AMPA receptor and promoting the recycling and delivery of GluR2/3 AMPA receptors. This would contribute to the formation and maintenance of synapses and thus the establishment of the neural circuits which are the basis of brain activity.

IV.1.12 Future Directions

Future experiments will adress mainly the issues related to the mechanism that control the formation of the complex of NEEP21-GRIP-GluR2 and will highlight the role of NEEP21 in the reycling versus the degradation pathway. The first step will be to identify whether NEEP21 binds directly GRIP or GluR2 and what are the minimal domains of these proteins necessary to interact with each other. This will be achieved by in vitro binding assays using recombinant proteins or AFM technology. Recently we have shown that it was possible to reconstitute the molecular interactions between proteins in an AFM chamber (Yersin et al., 2003). It is thus planed to use this technology to decipher the details of the formation of the NEEP21-GRIP-GluR2 complex. Isolation of specific domains involved in their interaction will give us the possibility to raise peptides that we could inject in hippocampal slices and record then their putative effect on synaptic strength. The potential phosphorylation of NEEP21 and its role on the formation of the NEEP21-GRIP-GluR2 complex will be investigated. Treatment of dissociated primary hippocampal neurons, with activators and inhibitors of kinases and phosphatases followed by pull-down experiments, should revealed, first, the importance of phosphorylation, and, second which kinases and/or phosphatases are implicated. Double-immunostaining will be perfomed to determine in which compartment GluR2/3 receptors accumulate, in neurons overexpressing the NEEP21 fragment aa 129-165, after NMDA stimulation. The role of NEEP21 related to the degradation pathway will be asked using video microscopy, and living hippocampal neurons loaded with Cy5-coupled dextran which accumulates in late endosomes and lysosomes. NEEP21 trafficking in neurons transfected with NEEP21-antisense or different fragments of NEEP21 will be investigated to determine whether it will affect its accumulation along the degradation pathway. It will be also useful to characterize p19 which has the highest homology with NEEP21 among the different members of this family. Since p19 has not the same pattern of mRNA expression in

the brain compared to NEEP21 (Saberan-Djoneidi et al., 1995; Saberan-Djoneidi et al., 1998), it will be interesting to investigate the role of p19 compared to NEEP21. Finally, it did not escape to our attention that at this step, it will be important to adress the role of NEEP21 in the developing nervous system. It will be thus important to generate and analyse genetically-modified mice, in which the gene encoding NEEP21 has been disrupted (« knock-out approach »).

IV.2 RTN1-C Is a New SNARE-interacting Protein Involved in Regulated Secretion

IV.2.1 RTN1-C Belongs to the Reticulon Family of Proteins

Reticulons (RTNs) are an eukaryotic gene family with unknown functions but a broad expression. RTNs are widely distributed in plants, yeast and animals (Oertle and Schwab, 2003). Over 300 family members sharing homologies within the C-terminal region of 200 aa are known in a variety of organisms (Oertle and Schwab, 2003). There are 4 mammalian reticulon genes (RTN1, RTN2, RTN3, RTN4), each of them can give rise to a range of alternative transcripts. The first members, the RTN1s, were identified from small lung carcinoma cells and neuroendocrine tissues (Roebroek et al., 1993). These are alternatively spliced variants from the single RTN1 gene, which was previously named NSP-A, NSP-B and NSP-C due to their neuroendocrine-specific expression (Roebroek et al., 1996) and are now called RTN1-A, RTN1-B, and RTN1-C. RTN1-C is expressed by neurons and cells of neuroendocrine tissue, and its expression is increased upon PC12 cells and neuroblastoma cell lines differentiation (Hens et al., 1998). It has also been proposed to be a marker of neuronal differentiation that is reduced in temporal cortices of Down's syndrome patients and in Alzheimer disease (Kim et al., 2000).

As all reticulons, RTN1-C is associated with membranes of the endoplasmic reticulum (van de Velde et al., 1994a). Because all RTNs lack a canonical leader peptide at their N-termini, translocation into the ER is assumed to be directed by internal signals (transmembrane domains). Alternatively, the ER association could be independent of signal-recognition particle and thus occur post-translationally (Oertle and Schwab, 2003). The membrane topology of RTNs is of specific interest, since they have a large putative transmembrane domains. Indeed the RTN1-C aa sequence of 208 aa possesses 2 putative transmembrane

domains between aa 41-57 and aa 140-162. Computer analysis predicts the most aminoterminal domain, (aa 1-41) as well as the carboxyterminal part, aa 163-208 to be cytosolic, while the central hydrophilic domain, aa (58-139), appears to be lumenal/extracellular. This gives the protein a horse-shoe-like orientation in the membrane. This membrane topology is consistent with the one which has been proposed for other reticulons (GrandPre et al., 2000).

During the past 4 years, the reticulon family has attracted considerable interest since one member, RTN4-A/Nogo-A was found to be an inhibitor of axon regeneration (Chen et al., 2000; GrandPre et al., 2000; Prinjha et al., 2000). Another member, RTN4-B1/Nogo-B has been implicated in the induction of apoptosis, specifically in cancer cells (Li et al., 2001). In addition, the recently identified RTN-$_{XS}$ has been shown to reduce apoptosis in a fibroblast cell line (Tagami et al., 2000). Several studies have concentrated on Nogo and its possible clinical implications (Brittis and Flanagan, 2001), but the rest of the RTN familiy has received little attention. In addition, despite these interesting findings the molecular functions of RTN family members are very little understood.

IV.2.2 RTN1-C Interacts with SNARE Proteins

SNARE proteins are composed of the 3 different families of proteins, SNAP-25 and its related isoforms, VAMPs and syntaxins. They form the core complex necessary to promote docking and fusion between donor and target membranes (Jahn et al., 2003). We found that RTN1-C forms a protein complex with several SNARE proteins. Indeed we found that RTN1-C interacts specifically with 3 different members of the syntaxin family, syntaxin 1, syntaxin 7, and syntaxin 13 and with one member of the VAMP family, VAMP2. In addition these interacting molecules are present in substoichiometric ratios in the complexes, because only a minor fraction of a given protein is coprecipitated with the precipitated protein. This suggests that at a given time only a small fraction of RTN1-C, syntaxin 1, syntaxin 7, syntaxin 13 or VAMP2 are complexed. When we tested for RTN1-C interaction with other SNAREs, we did not detect significant interactions neither with VAMP1 or VAMP3/cellubrevin, nor with SNAP25. It thus seems that RTN1-C is not a partner of the SNARE SNAP-25 family. However, it might be that certain other SNARE proteins of the syntaxin and VAMP family would also interact with RTN1-C.

In hippocampal cultures, RTN1-C appeared to be present on tubular structures in the cell body and along processes. In addition, we also noted there are labeled bulb-like structures at the distal part of processes. We also found that RTN1-C is present in the somatodendritic and axonal domains of neurons. Double-immunolabeling with RTN1-C and syntaxin 1, syntaxin 13 and VAMP2 showed that RTN1-C and SNARE proteins rarely colocalized. Nevertheless, there were round small structures which were clearly positive for RTN1-C and the different SNAREs. Furthermore, colocalization between RTN1-C and SV2, a synaptic vesicle marker, exhibits the same pattern. This result is not surprising since RTN1-C is localized to the ER, which the different SNARE protein are mainly localized to non-ER positive structures.

IV.2.5 RTN1-C is Involved in Regulated Secretion in PC12

We found that overexpression of RTN1-C did not affect basal secretion or regulated secretion in PC12 cells. On the contrary, overexpression of the RTN1-C fragment aa 1-41 significantly enhanced regulated secretion. In our laboratory, Karina Kulangara has recently shown, by pull-down assay, that this fragment is sufficient to bind syntaxin 1 and VAMP2 from brain extracts. This suggests that this fragment competes for the interaction between endogenous RTN1-C and SNARE proteins and moreover that RTN1-C-SNAREs interaction would limit the formation of the SNARE complex necessary for vesicle fusion with the plasma membrane. In other words, this interaction might, therefore, have an inhibitory action on secretion, in which RTN1-C is not limiting, and, in consequence, overexpression of full-length RTN1-C would not have any effect on secretion. These data suggest that RTN1-C is involved in vesicle events including secretion.

IV.2.6 Proposed Functions of RTN1-C

Due to the interaction of RTN1-C with SNAREs , its localization on the ER and its implication on regulated secretion in PC12 cells, we propose 2 different functions for RTN1-C which are not exclusive.

RTN1-C Is Involved in SNAREs Trafficking

Syntaxin 1 is localized at the plasma membrane and involved fusion processes between secretory vesicle and the cell membrane during regulated secretion (Jahn et al., 2003); syntaxin 13 is found along the early endosmal pathway and is involved in membrane fusion

process between endocytic vesicles and early endosomes (McBride et al., 1999); syntaxin 7 is present on late endosome and is linked to fusion events between early endosomes, late endosomes and lysosomes (Nakamura et al., 2000); VAMP2 is a component of the SNARE core complexes which take place during regulated secretory pathway and also between endosomes (Jahn et al., 2003; Prekeris et al., 1998; Sun et al., 2003). Since RTN1-C is associated with SNAREs which participate in membrane fusion in different pathways, it suggests that RTN1-C could be involved in a general mechanism related to SNARE proteins. RTN1-C could be involved in the biosynthesis or taregting of new SNARE molecules. Indeed, it is still not completely understood how SNAREs are incorporated into the secretory pathway that brings them to their final destination. SNARE proteins like syntaxins or VAMPs, do not possess a signal sequence, and contain a single hydrophobic segment close to their C-terminus, leaving most of the polypeptide chain in the cytoplasm (tail anchored) (Kutay et al., 1995). Membrane insertion of their transmembrane domain will thus not occur via a Signal-Recognition-Particle-dependent process. It was shown that in PC12 cells VAMP2 is not directly incorporated into target organelles, but was first inserted into the endoplasmic reticulum. Its insertion into the ER membrane in vitro occurs post-translationally, is dependent on ATP and requires ER protein(s) different from the translocation components needed for proteins with signal sequences (Kutay et al., 1995). RTN1-C which is localized to the ER and binds VAMP2 could be one of the components involved in VAMP2 insertion into ER. Moreover, a minimal endoplasmic reticulum targeting domain to the transmembrane area of VAMP2 has been recently identified as being sufficient to confer receptor-mediated, ATP-dependent, binding of a heterelogous protein to membranes (Kim et al., 1999). Previous attempts to identify VAMP2-interacting protein using the hydrophilic part of VAMP2, probably missed RTN1-C because we found that the transmembrane domain could be important for interaction (Steiner et al., 2004). The VAMP3/cellubrevin-interacting protein BAP31 has been identified by GST-pull-down with the full-length VAMP3. Deletion of the transmembrane domain of VAMP3 impaired its interaction with BAP31, arguing for the importance of the transmembrane domain of VAMPs. Like RTN1-C, BAP31 was also shown to be localized to a microtubulue-dependent compartment of the ER (see below), and only very little overlapping with VAMP3. The authors also demonstrated that BAP31 is implicated in exit of VAMP3 from the ER (Annaert et al., 1997). It is thus possbible that RTN1-C, similar to BAP31 could promote the exit of different SNAREs.

In addition, we found that RTN1-C is present on a nocodazole-sensitive ER. Nocodazole, a microtubule-destabilizing drug has been shown to affect the retrograde transport between the

Golgi appartus, an intermediate compartment and the ER (Lippincott-Schwartz et al., 1990). Moreover, it has been shown that this intermediate compartment, named ER-Golgi intermediate compartment (ERGIC) communicates with the Golgi in a microtubule-dependent manner and is important for vesicular transport between ER and Golgi (Hammond and Glick, 2000). This renforces the idea that RTN1-C could play a role in exit mechanisms from the ER. RTN1-C could be thus a good candidate, as an ER resident to assume a function during SNAREs biosynthesis and trafficking.

Another possibility would be that RTN1-C would target SNARE proteins to their final destination. However, RTN1-C molecules which escort the SNAREs would have to be retrieved to the ER. Given the fact that syntaxin 1, syntaxin 7, syntaxin 13 and VAMP2 have very different locations, it would be surprising that a single protein could manage the different sorting routes which correspond to these proteins.

RTN1-C Is Involved in the Regulation of Membrane Fusion by Intracellular Calcium

Endoplasmic reticulum is a multifaceted organelle that regulates protein synthesis and trafficking, cellular responses to stress, and intracellular calcium levels. In neurons, it is distributed between the cellular compartments that regulate plasticity and survival, including dendrites and dendritic spines, axons and presynaptic terminals, and growth cone (Dailey and Bridgman, 1989; Lysakowski et al., 1999; Mattson et al., 2000). In addition, ER is highly motile, rapidly extending into and retracting from distal regions of growth cones (Dailey and Bridgman, 1989). Microtubules and actin filaments appear to have key roles in controlling ER motility, as well as in its structure and function (Bannai et al., 2004; Tabb et al., 1998). Recent studies suggests that ER controls calcium homeostasis which could contribute to neuronal plasticity. Under resting conditions the concentration of calcium in the ER is considerably higher (10-100 μM) than the calcium concentration in the cytoplasm (100-300 nM). This calcium gradient is maintained by SERCA, an ATP-dependent pump, in the smooth ER membrane (Mattson et al., 2000).

We found that RTN1-C localizes to a nocodazole-sensitive domain of the ER. RTN1-C was present in tubule-like compartments which seem to be interconnected with each others. Morover, RTN1-C differentially colocalized with the ER-calcium pump SERCA2 (smooth ER calcium ATPase), but not with the ER-calcium-binding protein calreticulin. This indicates that RTN1-C is localized to a particular domain of the ER and is not distributed throughout

the whole ER. Indeed, It has been shown that SERCA and calreticulin are present on separate domains of the ER, which represent different calcium store compartments (Johnson et al., 1993). It is thus tempting to postulate that RTN1-C, due to its localization, could be associated with ion channels in the ER membrane. The ion flows through such channels might be involved in membrane fusion processes like calcium regulation from or into ER stores.

The ER has important roles in both presynaptic and postsynaptic processes associated with synaptic transmission and plasticity. It was shown that calcium release from ER store contributes to evoked neurotransmitter release at basket cell-Purkinje cell synapses by increasing the basal level of cytosolic calcium concentration in the vicinity of release sites (Galante and Marty, 2003). Emptage et al. monitored calcium transients in axons and presynaptic terminals of hippocampal slice cultures and found that calcium release from internal store influences the frequency of spontanenous transmitter release and short-term plasticity (Emptage et al., 2001). Recent studies also demonstrated that depletion of intracellular calcium stores blocks the induction of LTD in hipppocampal slices, without affecting basal synaptic transmission (Reyes and Stanton, 1996). Knock-out mice for ryanodine receptor 3 (RyR3), one of the channels responsible for calcium release from ER, exhibited facilitated LTP in hippocampus, suggesting that calcium release from ER might inhibit hippocampal LTP and spatial learning (Futatsugi et al., 1999). These examples assess the role of calcium stores in synaptic plasticity but the exact molecular mechanism is currently unknown. It is thus possible that the interaction between RTN1-C and SNAREs are under the control of calcium release from the ER which could via RTN1-C influence SNARE core complex formation and promote or inhibit neurotransmitters release. We also found that RTN1-C is present in the somatodendritic domain of neurons. Because LTP is also dependent of a postsynaptic SNARE-dependent exocytosis (Lledo et al., 1998), it is also possible that the control of addition of AMPA receptors during LTP will be controled in part by calcium release from ER through the RTN1-C-SNAREs interaction. Moreover, our studies provide evidence that RTN1-C interacts with syntaxin 13, an endosomal SNARE involved in the recycling of receptors. Since we also demonstrated that syntaxin 13 forms a complex with NEEP21, GRIP and GluR2 which is crucial for the regulation of AMPA receptors trafficking, it is tempting to speculate that the molecular link between LTP, LTD and calcium stores would take place through the regulation of the interaction between RTN1-C and syntaxin 13. The role of RTN1-C in the recycling process is supported by a recent study in C. elegans which documented a direct binding between a C. elegans reticulon and RME-1 (Iwahashi et

al., 2002). This factor is implicated, as syntaxin 13, in the endosomal recycling pathway (Grant et al., 2001; Lin et al., 2001).

ER has been demonstrated to be present in axons, terminal filopodia and growth cone of developing central and peripheral neurons (Bouchard et al., 2003). Calcium has been established as a key second messenger that is capable of mediating the response of growth cones to environmental signals. It is widely believed that calcium may be an important intracellular regulator of neurite elongation and growth cone guidance and motility. For example, the speed and direction of neurite outgrowth depends on changes in internal calcium concentration (Meldolesi, 2001), and dysregulation of internal calcium concentration can lead to growth cone collapse and arrest of neurite elongation (Gu and Spitzer, 1997). SNARE proteins were shown to be important for neurite outgrowth and transformation of the growth cone into mature synapses (Catsicas et al., 1994; Hepp and Langley, 2001). Syntaxin 1 and SNAP-25 was shown to be necessary for axonal elongation, since it was inhibited by SNAP-25 antisense oligonucleotides and treatments by botulinic neurotoxin which specifically cleaved SNAP-25 and syntaxin 1 in neurons (Osen-Sand et al., 1993; Osen-Sand et al., 1996). Futhermore, overexpression of syntaxin 13 in PC12 enhanced neurite outgrowth of these cells (Hirling et al., 2000). Expression of RTN1-C increased during differentiation of PC12 and neuroblastoma cell lines (Hens et al., 1998), suggesting RTN1-C should be important for neurite elongation. In a similar manner than before, RTN1-C could couple calcium homeostasis during neuronal development and the different SNARE

IV.2.7 Future Directions

A remaining question is to whether other reticulon proteins can also form complexes with SNAREs. According to our pull-down experiments, the first 41 aa of RTN1-C are sufficient for syntaxin 1-binding, though it does not rule out that other domains are also involved. This sequence of 41 aa contains a unique stretch from aa 1 to aa 20, while the following 20 aa contain a domain which is highly conserved between RTN1-C, RTN1-A, RTN1-B, RTN2 and RTN4/Nogo. It will be thus important to test whether these other RTNs could also interact with SNAREs. In the reverse situation, it will be interesting to check whether RTN1-C could interact with other SNAREs. The ER is composed of many different compartments. It will be useful to obtain a precise localization of RTN1-C. To this purpose, RTN1-C will be colocalized with different markers of the different subcompartments of the ER, like ERGIC-

53 which is a marker of the intermediate compartment or Sec13, a marker for the transitional ER. The trafficking of YFP/CFP-tagged RTN1-C in association with different YFP/CFP-tagged SNAREs will be investigated in living hipocampal neurons by time-lapse video microscopy. In addition using different drugs, like BFA, nocodazole or cytochalasin which affect the structure of the ER, will be used to modulate their trafficking. Finally the same experiments will be performed after neuronal depolarization to see whether it affects the trafficking of the different proteins of interest. Since RTN1-C interacts with syntaxin 13, overexpression of RTN1-C fragment aa 1-41 will be carry out to establish its potential relationship wiith the recycling of TfR and also the trafficking of AMPA receptors.

V Bibliography

Advani, R. J., Bae, H. R., Bock, J. B., Chao, D. S., Doung, Y. C., Prekeris, R., Yoo, J. S., and Scheller, R. H. (1998). Seven novel mammalian SNARE proteins localize to distinct membrane compartments. J Biol Chem *273*, 10317-10324.

Ahmari, S. E., Buchanan, J., and Smith, S. J. (2000). Assembly of presynaptic active zones from cytoplasmic transport packets. Nat Neurosci *3*, 445-451.

Al-Noori, S., and Swann, J. W. (2000). A role for sodium and chloride in kainic acid-induced beading of inhibitory interneuron dendrites. Neuroscience *101*, 337-348.

Annaert, W. G., Becker, B., Kistner, U., Reth, M., and Jahn, R. (1997). Export of cellubrevin from the endoplasmic reticulum is controlled by BAP31. J Cell Biol *139*, 1397-1410.

Antonin, W., Fasshauer, D., Becker, S., Jahn, R., and Schneider, T. R. (2002). Crystal structure of the endosomal SNARE complex reveals common structural principles of all SNAREs. Nat Struct Biol *9*, 107-111.

Antonin, W., Holroyd, C., Tikkanen, R., Honing, S., and Jahn, R. (2000). The R-SNARE endobrevin/VAMP-8 mediates homotypic fusion of early endosomes and late endosomes. Mol Biol Cell *11*, 3289-3298.

Bannai, H., Inoue, T., Nakayama, T., Hattori, M., and Mikoshiba, K. (2004). Kinesin dependent, rapid, bi-directional transport of ER sub-compartment in dendrites of hippocampal neurons. J Cell Sci *117*, 163-175.

Barria, A., Muller, D., Derkach, V., Griffith, L. C., and Soderling, T. R. (1997). Regulatory phosphorylation of AMPA-type glutamate receptors by CaM-KII during long-term potentiation. Science *276*, 2042-2045.

Barry, M. F., and Ziff, E. B. (2002). Receptor trafficking and the plasticity of excitatory synapses. Curr Opin Neurobiol *12*, 279-286.

Baumert, M., Maycox, P. R., Navone, F., De Camilli, P., and Jahn, R. (1989). Synaptobrevin: an integral membrane protein of 18,000 daltons present in small synaptic vesicles of rat brain. Embo J *8*, 379-384.

Beattie, E. C., Carroll, R. C., Yu, X., Morishita, W., Yasuda, H., von Zastrow, M., and Malenka, R. C. (2000). Regulation of AMPA receptor endocytosis by a signaling mechanism shared with LTD. Nat Neurosci *3*, 1291-1300.

Bennett, M. K., Calakos, N., and Scheller, R. H. (1992). Syntaxin: a synaptic protein implicated in docking of synaptic vesicles at presynaptic active zones. Science *257*, 255-259.

Bennett, M. V. (2000). Seeing is relieving: electrical synapses between visualized neurons. Nat Neurosci *3*, 7-9.

Bi, G., and Poo, M. (2001). Synaptic modification by correlated activity: Hebb's postulate revisited. Annu Rev Neurosci *24*, 139-166.

Bianchi, M. T., Song, L., Zhang, H., and Macdonald, R. L. (2002). Two different mechanisms of disinhibition produced by GABAA receptor mutations linked to epilepsy in humans. J Neurosci *22*, 5321-5327.

Bliss, T. V., and Gardner-Medwin, A. R. (1973). Long-lasting potentiation of synaptic transmission in the dentate area of the unanaestetized rabbit following stimulation of the perforant path. J Physiol *232*, 357-374.

Bliss, T. V., and Lomo, T. (1973). Long-lasting potentiation of synaptic transmission in the dentate area of the anaesthetized rabbit following stimulation of the perforant path. J Physiol *232*, 331-356.

Blue, M. E., and Parnavelas, J. G. (1983a). The formation and maturation of synapses in the visual cortex of the rat. I. Qualitative analysis. J Neurocytol *12*, 599-616.

Blue, M. E., and Parnavelas, J. G. (1983b). The formation and maturation of synapses in the visual cortex of the rat. II. Quantitative analysis. J Neurocytol *12*, 697-712.

Boschert, U., O'Shaughnessy, C., Dickinson, R., Tessari, M., Bendotti, C., Catsicas, S., and Pich, E. M. (1996). Developmental and plasticity-related differential expression of two SNAP-25 isoforms in the rat brain. J Comp Neurol *367*, 177-193.

Bouchard, R., Pattarini, R., and Geiger, J. D. (2003). Presence and functional significance of presynaptic ryanodine receptors. Prog Neurobiol *69*, 391-418.

Boyer, P. D. (1997). The ATP synthase--a splendid molecular machine. Annu Rev Biochem *66*, 717-749.

Braun, A. P., and Schulman, H. (1995). The multifunctional calcium/calmodulin-dependent protein kinase: from form to function. Annu Rev Physiol *57*, 417-445.

Bredt, D. S., and Nicoll, R. A. (2003). AMPA receptor trafficking at excitatory synapses. Neuron *40*, 361-379.

Brittis, P. A., and Flanagan, J. G. (2001). Nogo domains and a Nogo receptor: implications for axon regeneration. Neuron *30*, 11-14.

Bruckner, K., Pablo Labrador, J., Scheiffele, P., Herb, A., Seeburg, P. H., and Klein, R. (1999). EphrinB ligands recruit GRIP family PDZ adaptor proteins into raft membrane microdomains. Neuron *22*, 511-524.

Buckley, K. M., Melikian, H. E., Provoda, C. J., and Waring, M. T. (2000). Regulation of neuronal function by protein trafficking: a role for the endosomal pathway. J Physiol *525 Pt 1*, 11-19.

Burette, A., Khatri, L., Wyszynski, M., Sheng, M., Ziff, E. B., and Weinberg, R. J. (2001). Differential cellular and subcellular localization of ampa receptor-binding protein and glutamate receptor-interacting protein. J Neurosci *21*, 495-503.

Carlock, L., Vo, T., Lorincz, M., Walker, P. D., Bessert, D., Wisniewski, D., and Dunbar, J. C. (1996). Variable subcellular localization of a neuron-specific protein during NTera 2 differentiation into post-mitotic human neurons. Brain Res Mol Brain Res *42*, 202-212.

Carroll, R. C., Beattie, E. C., Xia, H., Luscher, C., Altschuler, Y., Nicoll, R. A., Malenka, R. C., and von Zastrow, M. (1999a). Dynamin-dependent endocytosis of ionotropic glutamate receptors. Proc Natl Acad Sci U S A *96*, 14112-14117.

Carroll, R. C., Lissin, D. V., von Zastrow, M., Nicoll, R. A., and Malenka, R. C. (1999b). Rapid redistribution of glutamate receptors contributes to long-term depression in hippocampal cultures. Nat Neurosci *2*, 454-460.

Catsicas, S., Berbel, P. J., and Innocenti, G. M. (1986). A combination of Golgi impregnation and fluorescent retrograde labeling. J Neurosci Methods *18*, 325-332.

Catsicas, S., Grenningloh, G., and Pich, E. M. (1994). Nerve-terminal proteins: to fuse to learn. Trends Neurosci *17*, 368-373.

Catsicas, S., Larhammar, D., Blomqvist, A., Sanna, P. P., Milner, R. J., and Wilson, M. C. (1991). Expression of a conserved cell-type-specific protein in nerve terminals coincides with synaptogenesis. Proc Natl Acad Sci U S A *88*, 785-789.

Chardin, P., and McCormick, F. (1999). Brefeldin A: the advantage of being uncompetitive. Cell *97*, 153-155.

Chen, M. S., Huber, A. B., van der Haar, M. E., Frank, M., Schnell, L., Spillmann, A. A., Christ, F., and Schwab, M. E. (2000). Nogo-A is a myelin-associated neurite outgrowth inhibitor and an antigen for monoclonal antibody IN-1. Nature *403*, 434-439.

Chen, Y. A., and Scheller, R. H. (2001). SNARE-mediated membrane fusion. Nat Rev Mol Cell Biol *2*, 98-106.

Christoforidis, S., McBride, H. M., Burgoyne, R. D., and Zerial, M. (1999). The Rab5 effector EEA1 is a core component of endosome docking. Nature *397*, 621-625.

Chung, H. J., Xia, J., Scannevin, R. H., Zhang, X., and Huganir, R. L. (2000). Phosphorylation of the AMPA receptor subunit GluR2 differentially regulates its interaction with PDZ domain-containing proteins. J Neurosci *20*, 7258-7267.

Cline, H. T. (2001). Dendritic arbor development and synaptogenesis. Curr Opin Neurobiol *11*, 118-126.

Collingridge, G. L., and Isaac, J. T. (2003). Functional roles of protein interactions with AMPA and kainate receptors. Neurosci Res *47*, 3-15.

Contractor, A., Rogers, C., Maron, C., Henkemeyer, M., Swanson, G. T., and Heinemann, S. F. (2002). Trans-synaptic Eph receptor-ephrin signaling in hippocampal mossy fiber LTP. Science *296*, 1864-1869.

Cooney, J. R., Hurlburt, J. L., Selig, D. K., Harris, K. M., and Fiala, J. C. (2002). Endosomal compartments serve multiple hippocampal dendritic spines from a widespread rather than a local store of recycling membrane. J Neurosci *22*, 2215-2224.

Cormont, M., Mari, M., Galmiche, A., Hofman, P., and Le Marchand-Brustel, Y. (2001). A FYVE-finger-containing protein, Rabip4, is a Rab4 effector involved in early endosomal traffic. Proc Natl Acad Sci U S A *98*, 1637-1642.

Cowan, W. M., Südhof, T. C., Stevens, C. F. (2001). Synapses, The John Hopkins University Press edn (Baltimore and London, The John Hopkins University Press).

Craig, A. M., and Banker, G. (1994). Neuronal polarity. Annu Rev Neurosci *17*, 267-310.

Craig, A. M., and Boudin, H. (2001). Molecular heterogeneity of central synapses: afferent and target regulation. Nat Neurosci *4*, 569-578.

D'Alcantara, P., Schiffmann, S. N., and Swillens, S. (2003). Bidirectional synaptic plasticity as a consequence of interdependent Ca2+-controlled phosphorylation and dephosphorylation pathways. Eur J Neurosci *17*, 2521-2528.

Dailey, M. E., and Bridgman, P. C. (1989). Dynamics of the endoplasmic reticulum and other membranous organelles in growth cones of cultured neurons. J Neurosci *9*, 1897-1909.

Dalva, M. B., Takasu, M. A., Lin, M. Z., Shamah, S. M., Hu, L., Gale, N. W., and Greenberg, M. E. (2000). EphB receptors interact with NMDA receptors and regulate excitatory synapse formation. Cell *103*, 945-956.

Daro, E., van der Sluijs, P., Galli, T., and Mellman, I. (1996). Rab4 and cellubrevin define different early endosome populations on the pathway of transferrin receptor recycling. Proc Natl Acad Sci U S A *93*, 9559-9564.

Daw, M. I., Chittajallu, R., Bortolotto, Z. A., Dev, K. K., Duprat, F., Henley, J. M., Collingridge, G. L., and Isaac, J. T. (2000). PDZ proteins interacting with C-terminal GluR2/3 are involved in a PKC-dependent regulation of AMPA receptors at hippocampal synapses. Neuron *28*, 873-886.

De Paola, V., Arber, S., and Caroni, P. (2003). AMPA receptors regulate dynamic equilibrium of presynaptic terminals in mature hippocampal networks. Nat Neurosci *6*, 491-500.

de Renzis, S., Sonnichsen, B., and Zerial, M. (2002). Divalent Rab effectors regulate the sub-compartmental organization and sorting of early endosomes. Nat Cell Biol *4*, 124-133.

Delcroix, J. D., Valletta, J. S., Wu, C., Hunt, S. J., Kowal, A. S., and Mobley, W. C. (2003). NGF signaling in sensory neurons: evidence that early endosomes carry NGF retrograde signals. Neuron *39*, 69-84.

DeSouza, S., Fu, J., States, B. A., and Ziff, E. B. (2002). Differential palmitoylation directs the AMPA receptor-binding protein ABP to spines or to intracellular clusters. J Neurosci *22*, 3493-3503.

Dityatev, A., Dityateva, G., and Schachner, M. (2000). Synaptic strength as a function of post- versus presynaptic expression of the neural cell adhesion molecule NCAM. Neuron *26*, 207-217.

Dong, H., O'Brien, R. J., Fung, E. T., Lanahan, A. A., Worley, P. F., and Huganir, R. L. (1997). GRIP: a synaptic PDZ domain-containing protein that interacts with AMPA receptors. Nature *386*, 279-284.

Dong, H., Zhang, P., Song, I., Petralia, R. S., Liao, D., and Huganir, R. L. (1999). Characterization of the glutamate receptor-interacting proteins GRIP1 and GRIP2. J Neurosci *19*, 6930-6941.

Ehlers, M. D. (2000). Reinsertion or degradation of AMPA receptors determined by activity-dependent endocytic sorting. Neuron *28*, 511-525.

Emptage, N. J., Reid, C. A., and Fine, A. (2001). Calcium stores in hippocampal synaptic boutons mediate short-term plasticity, store-operated Ca2+ entry, and spontaneous transmitter release. Neuron *29*, 197-208.

Engert, F., and Bonhoeffer, T. (1999). Dendritic spine changes associated with hippocampal long-term synaptic plasticity. Nature *399*, 66-70.

Feldman, D. E. (2000). Timing-based LTP and LTD at vertical inputs to layer II/III pyramidal cells in rat barrel cortex. Neuron *27*, 45-56.

Feng, Y., Press, B., and Wandinger-Ness, A. (1995). Rab 7: an important regulator of late endocytic membrane traffic. J Cell Biol *131*, 1435-1452.

Fiala, J. C., Feinberg, M., Popov, V., and Harris, K. M. (1998). Synaptogenesis via dendritic filopodia in developing hippocampal area CA1. J Neurosci *18*, 8900-8911.

Firsov, D., Schild, L., Gautschi, I., Merillat, A. M., Schneeberger, E., and Rossier, B. C. (1996). Cell surface expression of the epithelial Na channel and a mutant causing Liddle syndrome: a quantitative approach. Proc Natl Acad Sci U S A *93*, 15370-15375.

Fischer, M., Kaech, S., Wagner, U., Brinkhaus, H., and Matus, A. (2000). Glutamate receptors regulate actin-based plasticity in dendritic spines. Nat Neurosci *3*, 887-894.

Foletti, D. L., Lin, R., Finley, M. A., and Scheller, R. H. (2000). Phosphorylated syntaxin 1 is localized to discrete domains along a subset of axons. J Neurosci *20*, 4535-4544.

Friedman, H. V., Bresler, T., Garner, C. C., and Ziv, N. E. (2000). Assembly of new individual excitatory synapses: time course and temporal order of synaptic molecule recruitment. Neuron *27*, 57-69.

Futatsugi, A., Kato, K., Ogura, H., Li, S. T., Nagata, E., Kuwajima, G., Tanaka, K., Itohara, S., and Mikoshiba, K. (1999). Facilitation of NMDAR-independent LTP and spatial learning in mutant mice lacking ryanodine receptor type 3. Neuron *24*, 701-713.

Galante, M., and Marty, A. (2003). Presynaptic ryanodine-sensitive calcium stores contribute to evoked neurotransmitter release at the basket cell-Purkinje cell synapse. J Neurosci *23*, 11229-11234.

Garcia, E. P., McPherson, P. S., Chilcote, T. J., Takei, K., and De Camilli, P. (1995). rbSec1A and B colocalize with syntaxin 1 and SNAP-25 throughout the axon, but are not in a stable complex with syntaxin. J Cell Biol *129*, 105-120.

Goda, Y., and Davis, G. W. (2003). Mechanisms of synapse assembly and disassembly. Neuron *40*, 243-264.

Goodman, C. S., and Shatz, C. J. (1993). Developmental mechanisms that generate precise patterns of neuronal connectivity. Cell *72 Suppl*, 77-98.

Gordon-Weeks, P. R., and Fischer, I. (2000). MAP1B expression and microtubule stability in growing and regenerating axons. Microsc Res Tech *48*, 63-74.

Gorvel, J. P., Chavrier, P., Zerial, M., and Gruenberg, J. (1991). rab5 controls early endosome fusion in vitro. Cell *64*, 915-925.

GrandPre, T., Nakamura, F., Vartanian, T., and Strittmatter, S. M. (2000). Identification of the Nogo inhibitor of axon regeneration as a Reticulon protein. Nature *403*, 439-444.

Grant, B., Zhang, Y., Paupard, M. C., Lin, S. X., Hall, D. H., and Hirsh, D. (2001). Evidence that RME-1, a conserved C. elegans EH-domain protein, functions in endocytic recycling. Nat Cell Biol *3*, 573-579.

Greene, L. A., and Tischler, A. S. (1976). Establishment of a noradrenergic clonal line of rat adrenal pheochromocytoma cells which respond to nerve growth factor. Proc Natl Acad Sci U S A *73*, 2424-2428.

Grimes, M. L., Zhou, J., Beattie, E. C., Yuen, E. C., Hall, D. E., Valletta, J. S., Topp, K. S., LaVail, J. H., Bunnett, N. W., and Mobley, W. C. (1996). Endocytosis of activated TrkA: evidence that nerve growth factor induces formation of signaling endosomes. J Neurosci *16*, 7950-7964.

Gruenberg, J. (2001). The endocytic pathway: a mosaic of domains. Nat Rev Mol Cell Biol *2*, 721-730.

Gruenberg, J., and Maxfield, F. R. (1995). Membrane transport in the endocytic pathway. Curr Opin Cell Biol *7*, 552-563.

Grussenmeyer, T., Scheidtmann, K. H., Hutchinson, M. A., Eckhart, W., and Walter, G. (1985). Complexes of polyoma virus medium T antigen and cellular proteins. Proc Natl Acad Sci U S A *82*, 7952-7954.

Grutzendler, J., Kasthuri, N., and Gan, W. B. (2002). Long-term dendritic spine stability in the adult cortex. Nature *420*, 812-816.

Gu, X., and Spitzer, N. C. (1997). Breaking the code: regulation of neuronal differentiation by spontaneous calcium transients. Dev Neurosci *19*, 33-41.

Hammond, A. T., and Glick, B. S. (2000). Dynamics of transitional endoplasmic reticulum sites in vertebrate cells. Mol Biol Cell *11*, 3013-3030.

Hasbani, M. J., Schlief, M. L., Fisher, D. A., and Goldberg, M. P. (2001). Dendritic spines lost during glutamate receptor activation reemerge at original sites of synaptic contact. J Neurosci *21*, 2393-2403.

Hayashi, Y., Shi, S. H., Esteban, J. A., Piccini, A., Poncer, J. C., and Malinow, R. (2000). Driving AMPA receptors into synapses by LTP and CaMKII: requirement for GluR1 and PDZ domain interaction. Science *287*, 2262-2267.

Hebb, D. (1949). The Organization of behavior (New York, Wiley).

Heim, R., and Tsien, R. Y. (1996). Engineering green fluorescent protein for improved brightness, longer wavelengths and fluorescence resonance energy transfer. Curr Biol *6*, 178-182.

Henkemeyer, M., Itkis, O. S., Ngo, M., Hickmott, P. W., and Ethell, I. M. (2003). Multiple EphB receptor tyrosine kinases shape dendritic spines in the hippocampus. J Cell Biol *163*, 1313-1326.

Henley, J. M. (2003). Proteins interactions implicated in AMPA receptor trafficking: a clear destination and an improving route map. Neurosci Res *45*, 243-254.

Hens, J., Nuydens, R., Geerts, H., Senden, N. H., Van de Ven, W. J., Roebroek, A. J., van de Velde, H. J., Ramaekers, F. C., and Broers, J. L. (1998). Neuronal differentiation is accompanied by NSP-C expression. Cell Tissue Res *292*, 229-237.

Hepp, R., and Langley, K. (2001). SNAREs during development. Cell Tissue Res *305*, 247-253.

High, S. a. L., V (1997). membrane protein biosynthesis - all swen up? Trends Cell Biol *7*, 206-210.

Himanen, J. P., and Nikolov, D. B. (2003). Eph signaling: a structural view. Trends Neurosci *26*, 46-51.

Hirling, H., Steiner, P., Chaperon, C., Marsault, R., Regazzi, R., and Catsicas, S. (2000). Syntaxin 13 is a developmentally regulated SNARE involved in neurite outgrowth and endosomal trafficking. Eur J Neurosci *12*, 1913-1923.

Holz, R. W., Brondyk, W. H., Senter, R. A., Kuizon, L., and Macara, I. G. (1994). Evidence for the involvement of Rab3A in Ca(2+)-dependent exocytosis from adrenal chromaffin cells. J Biol Chem *269*, 10229-10234.

Horton, A. C., and Ehlers, M. D. (2003a). Dual modes of endoplasmic reticulum-to-Golgi transport in dendrites revealed by live-cell imaging. J Neurosci *23*, 6188-6199.

Horton, A. C., and Ehlers, M. D. (2003b). Neuronal polarity and trafficking. Neuron *40*, 277-295.

Hu, C., Ahmed, M., Melia, T. J., Sollner, T. H., Mayer, T., and Rothman, J. E. (2003). Fusion of cells by flipped SNAREs. Science *300*, 1745-1749.

Huber, A. B., Kolodkin, A. L., Ginty, D. D., and Cloutier, J. F. (2003). Signaling at the growth cone: ligand-receptor complexes and the control of axon growth and guidance. Annu Rev Neurosci *26*, 509-563.

Ikegaya, Y., Kim, J. A., Baba, M., Iwatsubo, T., Nishiyama, N., and Matsuki, N. (2001). Rapid and reversible changes in dendrite morphology and synaptic efficacy following NMDA receptor activation: implication for a cellular defense against excitotoxicity. J Cell Sci *114*, 4083-4093.

Isaac, J. T., Crair, M. C., Nicoll, R. A., and Malenka, R. C. (1997). Silent synapses during development of thalamocortical inputs. Neuron *18*, 269-280.

Iwahashi, J., Kawasaki, I., Kohara, Y., Gengyo-Ando, K., Mitani, S., Ohshima, Y., Hamada, N., Hara, K., Kashiwagi, T., and Toyoda, T. (2002). Caenorhabditis elegans reticulon interacts with RME-1 during embryogenesis. Biochem Biophys Res Commun *293*, 698-704.

Jahn, R., Lang, T., and Sudhof, T. C. (2003). Membrane fusion. Cell *112*, 519-533.

Jahn, R., and Sudhof, T. C. (1999). Membrane fusion and exocytosis. Annu Rev Biochem *68*, 863-911.

Jensen, V., Kaiser, K. M., Borchardt, T., Adelmann, G., Rozov, A., Burnashev, N., Brix, C., Frotscher, M., Andersen, P., Hvalby, O., *et al.* (2003). A juvenile form of postsynaptic hippocampal long-term potentiation in mice deficient for the AMPA receptor subunit GluR-A. J Physiol *553*, 843-856.

Jia, Z., Agopyan, N., Miu, P., Xiong, Z., Henderson, J., Gerlai, R., Taverna, F. A., Velumian, A., MacDonald, J., Carlen, P., *et al.* (1996). Enhanced LTP in mice deficient in the AMPA receptor GluR2. Neuron *17*, 945-956.

Johnson, R. J., Pyun, H. Y., Lytton, J., and Fine, R. E. (1993). Differences in the subcellular localization of calreticulin and organellar Ca(2+)-ATPase in neurons. Brain Res Mol Brain Res *17*, 9-16.

Jontes, J. D., and Smith, S. J. (2000). Filopodia, spines, and the generation of synaptic diversity. Neuron *27*, 11-14.

Jovanovic, J. N., Czernik, A. J., Fienberg, A. A., Greengard, P., and Sihra, T. S. (2000). Synapsins as mediators of BDNF-enhanced neurotransmitter release. Nat Neurosci *3*, 323-329.

Kamiguchi, H., and Lemmon, V. (2000). Recycling of the cell adhesion molecule L1 in axonal growth cones. J Neurosci *20*, 3676-3686.

Kandel, E. R. (2001). The molecular biology of memory storage: a dialogue between genes and synapses. Science *294*, 1030-1038.

Katz, L. C., and Shatz, C. J. (1996). Synaptic activity and the construction of cortical circuits. Science *274*, 1133-1138.

Kauer, J. A., Malenka, R. C., and Nicoll, R. A. (1988). A persistent postsynaptic modification mediates long-term potentiation in the hippocampus. Neuron *1*, 911-917.

Kennedy, M. B. (2000). Signal-processing machines at the postsynaptic density. Science *290*, 750-754.

Kenwrick, S., and Doherty, P. (1998). Neural cell adhesion molecule L1: relating disease to function. Bioessays *20*, 668-675.

Kim, C. H., Chung, H. J., Lee, H. K., and Huganir, R. L. (2001). Interaction of the AMPA receptor subunit GluR2/3 with PDZ domains regulates hippocampal long-term depression. Proc Natl Acad Sci U S A *98*, 11725-11730.

Kim, P. K., Hollerbach, C., Trimble, W. S., Leber, B., and Andrews, D. W. (1999). Identification of the endoplasmic reticulum targeting signal in vesicle-associated membrane proteins. J Biol Chem *274*, 36876-36882.

Kim, S. H., Yoo, B. C., Broers, J. L., Cairns, N., and Lubec, G. (2000). Neuroendocrine-specific protein C, a marker of neuronal differentiation, is reduced in brain of patients with Down syndrome and Alzheimer's disease. Biochem Biophys Res Commun *276*, 329-334.

Kirkwood, A., Rioult, M. C., and Bear, M. F. (1996). Experience-dependent modification of synaptic plasticity in visual cortex. Nature *381*, 526-528.

Klausner, R. D., Donaldson, J. G., and Lippincott-Schwartz, J. (1992). Brefeldin A: insights into the control of membrane traffic and organelle structure. J Cell Biol *116*, 1071-1080.

Knott, G. W., Quairiaux, C., Genoud, C., and Welker, E. (2002). Formation of dendritic spines with GABAergic synapses induced by whisker stimulation in adult mice. Neuron *34*, 265-273.

Ko, J., Kim, S., Valtschanoff, J. G., Shin, H., Lee, J. R., Sheng, M., Premont, R. T., Weinberg, R. J., and Kim, E. (2003). Interaction between liprin-alpha and GIT1 is required for AMPA receptor targeting. J Neurosci *23*, 1667-1677.

Kobayashi, T., Stang, E., Fang, K. S., de Moerloose, P., Parton, R. G., and Gruenberg, J. (1998). A lipid associated with the antiphospholipid syndrome regulates endosome structure and function. Nature *392*, 193-197.

Kolleker, A., Zhu, J. J., Schupp, B. J., Qin, Y., Mack, V., Borchardt, T., Kohr, G., Malinow, R., Seeburg, P. H., and Osten, P. (2003). Glutamatergic plasticity by synaptic delivery of GluR-B(long)-containing AMPA receptors. Neuron *40*, 1199-1212.

Korte, M., Carroll, P., Wolf, E., Brem, G., Thoenen, H., and Bonhoeffer, T. (1995). Hippocampal long-term potentiation is impaired in mice lacking brain-derived neurotrophic factor. Proc Natl Acad Sci U S A *92*, 8856-8860.

Kovalchuk, Y., Hanse, E., Kafitz, K. W., and Konnerth, A. (2002). Postsynaptic Induction of BDNF-Mediated Long-Term Potentiation. Science *295*, 1729-1734.

Kullmann, D. M., and Siegelbaum, S. A. (1995). The site of expression of NMDA receptor-dependent LTP: new fuel for an old fire. Neuron *15*, 997-1002.

Kumar, S. S., Bacci, A., Kharazia, V., and Huguenard, J. R. (2002). A developmental switch of AMPA receptor subunits in neocortical pyramidal neurons. J Neurosci *22*, 3005-3015.

Kutay, U., Ahnert-Hilger, G., Hartmann, E., Wiedenmann, B., and Rapoport, T. A. (1995). Transport route for synaptobrevin via a novel pathway of insertion into the endoplasmic reticulum membrane. Embo J *14*, 217-223.

Kuznetsov, S. A., and Gelfand, V. I. (1987). 18 kDa microtubule-associated protein: identification as a new light chain (LC-3) of microtubule-associated protein 1 (MAP-1). FEBS Lett *212*, 145-148.

Lebrand, C., Corti, M., Goodson, H., Cosson, P., Cavalli, V., Mayran, N., Faure, J., and Gruenberg, J. (2002). Late endosome motility depends on lipids via the small GTPase Rab7. Embo J *21*, 1289-1300.

Lee, H. K., Barbarosie, M., Kameyama, K., Bear, M. F., and Huganir, R. L. (2000). Regulation of distinct AMPA receptor phosphorylation sites during bidirectional synaptic plasticity. Nature *405*, 955-959.

Lee, S. H., Liu, L., Wang, Y. T., and Sheng, M. (2002). Clathrin adaptor AP2 and NSF interact with overlapping sites of GluR2 and play distinct roles in AMPA receptor trafficking and hippocampal LTD. Neuron *36*, 661-674.

Lee, S. H., Valtschanoff, J. G., Kharazia, V. N., Weinberg, R., and Sheng, M. (2001). Biochemical and morphological characterization of an intracellular membrane compartment containing AMPA receptors. Neuropharmacology *41*, 680-692.

Lee, S. S., and Banting, G. (2002). Characterisation of the lumenal domain of TGN38 and effects of elevated expression of TGN38 on glycoprotein secretion. Eur J Cell Biol *81*, 609-621.

Lee, W. C., Yoshihara, M., and Littleton, J. T. (2004). Cytoplasmic aggregates trap polyglutamine-containing proteins and block axonal transport in a Drosophila model of Huntington's disease. Proc Natl Acad Sci U S A *101*, 3224-3229.

Lendvai, B., Stern, E. A., Chen, B., and Svoboda, K. (2000). Experience-dependent plasticity of dendritic spines in the developing rat barrel cortex in vivo. Nature *404*, 876-881.

Leonard, A. S., Davare, M. A., Horne, M. C., Garner, C. C., and Hell, J. W. (1998). SAP97 is associated with the alpha-amino-3-hydroxy-5-methylisoxazole-4-propionic acid receptor GluR1 subunit. J Biol Chem *273*, 19518-19524.

Leuner, B., Falduto, J., and Shors, T. J. (2003). Associative memory formation increases the observation of dendritic spines in the hippocampus. J Neurosci *23*, 659-665.

Levine, E. S., Crozier, R. A., Black, I. B., and Plummer, M. R. (1998). Brain-derived neurotrophic factor modulates hippocampal synaptic transmission by increasing N-methyl-D-aspartic acid receptor activity. Proc Natl Acad Sci U S A *95*, 10235-10239.

Leyva, J. A., Bianchet, M. A., and Amzel, L. M. (2003). Understanding ATP synthesis: structure and mechanism of the F1-ATPase (Review). Mol Membr Biol *20*, 27-33.

Lezcano, N., Mrzljak, L., Eubanks, S., Levenson, R., Goldman-Rakic, P., and Bergson, C. (2000). Dual signaling regulated by calcyon, a D1 dopamine receptor interacting protein. Science *287*, 1660-1664.

Li, Q., Qi, B., Oka, K., Shimakage, M., Yoshioka, N., Inoue, H., Hakura, A., Kodama, K., Stanbridge, E. J., and Yutsudo, M. (2001). Link of a new type of apoptosis-inducing gene ASY/Nogo-B to human cancer. Oncogene *20*, 3929-3936.

Liao, D., Hessler, N. A., and Malinow, R. (1995). Activation of postsynaptically silent synapses during pairing-induced LTP in CA1 region of hippocampal slice. Nature *375*, 400-404.

Liao, D., Zhang, X., O'Brien, R., Ehlers, M. D., and Huganir, R. L. (1999). Regulation of morphological postsynaptic silent synapses in developing hippocampal neurons. Nat Neurosci *2*, 37-43.

Lin, J. W., Ju, W., Foster, K., Lee, S. H., Ahmadian, G., Wyszynski, M., Wang, Y. T., and Sheng, M. (2000). Distinct molecular mechanisms and divergent endocytotic pathways of AMPA receptor internalization. Nat Neurosci *3*, 1282-1290.

Lin, J. W., and Sheng, M. (1998). NSF and AMPA receptors get physical. Neuron *21*, 267-270.

Lin, R. C., and Scheller, R. H. (1997). Structural organization of the synaptic exocytosis core complex. Neuron *19*, 1087-1094.

Lin, S. X., Grant, B., Hirsh, D., and Maxfield, F. R. (2001). Rme-1 regulates the distribution and function of the endocytic recycling compartment in mammalian cells. Nat Cell Biol *3*, 567-572.

Lippincott-Schwartz, J., Donaldson, J. G., Schweizer, A., Berger, E. G., Hauri, H. P., Yuan, L. C., and Klausner, R. D. (1990). Microtubule-dependent retrograde transport of proteins into the ER in the presence of brefeldin A suggests an ER recycling pathway. Cell *60*, 821-836.

Lippincott-Schwartz, J., Yuan, L., Tipper, C., Amherdt, M., Orci, L., and Klausner, R. D. (1991). Brefeldin A's effects on endosomes, lysosomes, and the TGN suggest a general mechanism for regulating organelle structure and membrane traffic. Cell *67*, 601-616.

Lissin, D. V., Carroll, R. C., Nicoll, R. A., Malenka, R. C., and von Zastrow, M. (1999). Rapid, activation-induced redistribution of ionotropic glutamate receptors in cultured hippocampal neurons. J Neurosci *19*, 1263-1272.

Lledo, P. M., Zhang, X., Sudhof, T. C., Malenka, R. C., and Nicoll, R. A. (1998). Postsynaptic membrane fusion and long-term potentiation. Science *279*, 399-403.

Lu, B. (2003). BDNF and activity-dependent synaptic modulation. Learn Mem *10*, 86-98.

Luscher, C., Xia, H., Beattie, E. C., Carroll, R. C., von Zastrow, M., Malenka, R. C., and Nicoll, R. A. (1999). Role of AMPA receptor cycling in synaptic transmission and plasticity. Neuron *24*, 649-658.

Luthi, A., Schwyzer, L., Mateos, J. M., Gahwiler, B. H., and McKinney, R. A. (2001). NMDA receptor activation limits the number of synaptic connections during hippocampal development. Nat Neurosci *4*, 1102-1107.

Luzio, J. P., Brake, B., Banting, G., Howell, K. E., Braghetta, P., and Stanley, K. K. (1990). Identification, sequencing and expression of an integral membrane protein of the trans-Golgi network (TGN38). Biochem J *270*, 97-102.

Lysakowski, A., Figueras, H., Price, S. D., and Peng, Y. Y. (1999). Dense-cored vesicles, smooth endoplasmic reticulum, and mitochondria are closely associated with non-specialized parts of plasma membrane of nerve terminals: implications for exocytosis and calcium buffering by intraterminal organelles. J Comp Neurol *403*, 378-390.

Malenka, R. C., Kauer, J. A., Perkel, D. J., Mauk, M. D., Kelly, P. T., Nicoll, R. A., and Waxham, M. N. (1989). An essential role for postsynaptic calmodulin and protein kinase activity in long-term potentiation. Nature *340*, 554-557.

Malenka, R. C., and Nicoll, R. A. (1999). Long-term potentiation--a decade of progress? Science *285*, 1870-1874.

Maletic-Savatic, M., Koothan, T., and Malinow, R. (1998). Calcium-evoked dendritic exocytosis in cultured hippocampal neurons. Part II: mediation by calcium/calmodulin-dependent protein kinase II. J Neurosci *18*, 6814-6821.

Maletic-Savatic, M., and Malinow, R. (1998). Calcium-evoked dendritic exocytosis in cultured hippocampal neurons. Part I: trans-Golgi network-derived organelles undergo regulated exocytosis. J Neurosci *18*, 6803-6813.

Maletic-Savatic, M., Malinow, R., and Svoboda, K. (1999). Rapid dendritic morphogenesis in CA1 hippocampal dendrites induced by synaptic activity. Science *283*, 1923-1927.

Malide, D., and Cushman, S. W. (1997). Morphological effects of wortmannin on the endosomal system and GLUT4-containing compartments in rat adipose cells. J Cell Sci *110 (Pt 22)*, 2795-2806.

Malinow, R., and Malenka, R. C. (2002). AMPA receptor trafficking and synaptic plasticity. Annu Rev Neurosci *25*, 103-126.

Man, H. Y., Lin, J. W., Ju, W. H., Ahmadian, G., Liu, L., Becker, L. E., Sheng, M., and Wang, Y. T. (2000). Regulation of AMPA receptor-mediated synaptic transmission by clathrin-dependent receptor internalization. Neuron *25*, 649-662.

Mann, S. S., and Hammarback, J. A. (1994). Molecular characterization of light chain 3. A microtubule binding subunit of MAP1A and MAP1B. J Biol Chem *269*, 11492-11497.

Mann, S. S., and Hammarback, J. A. (1996). Gene localization and developmental expression of light chain 3: a common subunit of microtubule-associated protein 1A(MAP1A) and MAP1B. J Neurosci Res *43*, 535-544.

Marrs, G. S., Green, S. H., and Dailey, M. E. (2001). Rapid formation and remodeling of postsynaptic densities in developing dendrites. Nat Neurosci *4*, 1006-1013.

Martin, K. C., Barad, M., and Kandel, E. R. (2000a). Local protein synthesis and its role in synapse-specific plasticity. Curr Opin Neurobiol *10*, 587-592.

Martin, S. J., Grimwood, P. D., and Morris, R. G. (2000b). Synaptic plasticity and memory: an evaluation of the hypothesis. Annu Rev Neurosci *23*, 649-711.

Martinez, L. O., Jacquet, S., Esteve, J. P., Rolland, C., Cabezon, E., Champagne, E., Pineau, T., Georgeaud, V., Walker, J. E., Terce, F.*, et al.* (2003). Ectopic beta-chain of ATP synthase is an apolipoprotein A-I receptor in hepatic HDL endocytosis. Nature *421*, 75-79.

Matesic, D. F., and Lin, R. C. (1994). Microtubule-associated protein 2 as an early indicator of ischemia-induced neurodegeneration in the gerbil forebrain. J Neurochem *63*, 1012-1020.

Matsuzaki, M., Ellis-Davies, G. C., Nemoto, T., Miyashita, Y., Iino, M., and Kasai, H. (2001). Dendritic spine geometry is critical for AMPA receptor expression in hippocampal CA1 pyramidal neurons. Nat Neurosci *4*, 1086-1092.

Mattson, M. P., LaFerla, F. M., Chan, S. L., Leissring, M. A., Shepel, P. N., and Geiger, J. D. (2000). Calcium signaling in the ER: its role in neuronal plasticity and neurodegenerative disorders. Trends Neurosci *23*, 222-229.

Mayor, S., Presley, J. F., and Maxfield, F. R. (1993). Sorting of membrane components from endosomes and subsequent recycling to the cell surface occurs by a bulk flow process. J Cell Biol *121*, 1257-1269.

McAllister, A. K., Katz, L. C., and Lo, D. C. (1999). Neurotrophins and synaptic plasticity. Annu Rev Neurosci *22*, 295-318.

McBride, H. M., Rybin, V., Murphy, C., Giner, A., Teasdale, R., and Zerial, M. (1999). Oligomeric complexes link Rab5 effectors with NSF and drive membrane fusion via interactions between EEA1 and syntaxin 13. Cell *98*, 377-386.

McCaffrey, M. W., Bielli, A., Cantalupo, G., Mora, S., Roberti, V., Santillo, M., Drummond, F., and Bucci, C. (2001). Rab4 affects both recycling and degradative endosomal trafficking. FEBS Lett *495*, 21-30.

McKinney, R. A., Capogna, M., Durr, R., Gahwiler, B. H., and Thompson, S. M. (1999). Miniature synaptic events maintain dendritic spines via AMPA receptor activation. Nat Neurosci *2*, 44-49.

mclauchlan, h., newell, j, morrice, n, osborne, a, west, m, and smythe, e (1997). a novel role for rab5-GDI in lignad sequestration into clathrin-coated pits. current biology *8*, 34-85.

mclauchlan, h., newell, j, morrice, n, osborne, a, west, m, and smythe, e (1998). a novel role for rab5-GDI in ligand sequestration into clathrin-coated pits. current biology *8*, 34-85.

McNew, J. A., Parlati, F., Fukuda, R., Johnston, R. J., Paz, K., Paumet, F., Sollner, T. H., and Rothman, J. E. (2000). Compartmental specificity of cellular membrane fusion encoded in SNARE proteins. Nature *407*, 153-159.

Meijering, E., Jacob, M., Sarria, J. C., Steiner, P., Hirling, H., and Unser, M. (2004). Design and validation of a tool for neurite tracing and analysis in fluorescence microscopy images. Cytometry *58A*, 167-176.

Meldolesi, J. (2001). Rapidly exchanging Ca2+ stores in neurons: molecular, structural and functional properties. Prog Neurobiol *65*, 309-338.

Meresse, S., Gorvel, J. P., and Chavrier, P. (1995). The rab7 GTPase resides on a vesicular compartment connected to lysosomes. J Cell Sci *108 (Pt 11)*, 3349-3358.

Michalak, M., Robert Parker, J. M., and Opas, M. (2002). Ca2+ signaling and calcium binding chaperones of the endoplasmic reticulum. Cell Calcium *32*, 269-278.

Mills, I. G., Urbe, S., and Clague, M. J. (2001). Relationships between EEA1 binding partners and their role in endosome fusion. J Cell Sci *114*, 1959-1965.

Muller, B. M., Kistner, U., Veh, R. W., Cases-Langhoff, C., Becker, B., Gundelfinger, E. D., and Garner, C. C. (1995). Molecular characterization and spatial distribution of SAP97, a novel presynaptic protein homologous to SAP90 and the Drosophila discs-large tumor suppressor protein. J Neurosci *15*, 2354-2366.

Muller, D., Joly, M., and Lynch, G. (1988). Contributions of quisqualate and NMDA receptors to the induction and expression of LTP. Science *242*, 1694-1697.

Mullock, B. M., Smith, C. W., Ihrke, G., Bright, N. A., Lindsay, M., Parkinson, E. J., Brooks, D. A., Parton, R. G., James, D. E., Luzio, J. P., and Piper, R. C. (2000). Syntaxin 7 is localized to late endosome compartments, associates with Vamp 8, and Is required for late endosome-lysosome fusion. Mol Biol Cell *11*, 3137-3153.

Nagelkerken, B., Van Anken, E., Van Raak, M., Gerez, L., Mohrmann, K., Van Uden, N., Holthuizen, J., Pelkmans, L., and Van Der Sluijs, P. (2000). Rabaptin4, a novel effector of the small GTPase rab4a, is recruited to perinuclear recycling vesicles. Biochem J *346 Pt 3*, 593-601.

Nakamura, N., Yamamoto, A., Wada, Y., and Futai, M. (2000). Syntaxin 7 mediates endocytic trafficking to late endosomes. J Biol Chem *275*, 6523-6529.

Nicoll, R. A., and Malenka, R. C. (1995). Contrasting properties of two forms of long-term potentiation in the hippocampus. Nature *377*, 115-118.

Nielsen, E., Severin, F., Backer, J. M., Hyman, A. A., and Zerial, M. (1999). Rab5 regulates motility of early endosomes on microtubules. Nat Cell Biol *1*, 376-382.

Nikonenko, I., Jourdain, P., Alberi, S., Toni, N., and Muller, D. (2002). Activity-induced changes of spine morphology. Hippocampus *12*, 585-591.

Nimchinsky, E. A., Sabatini, B. L., and Svoboda, K. (2002). Structure and function of dendritic spines. Annu Rev Physiol *64*, 313-353.

Ninkina, N. N., Baka, I. D., and Buchman, V. L. (1997). Rat and chicken s-rex/NSP mRNA: nucleotide sequence of main transcripts and expression of splice variants in rat tissues. Gene *184*, 205-210.

Nishimune, A., Isaac, J. T., Molnar, E., Noel, J., Nash, S. R., Tagaya, M., Collingridge, G. L., Nakanishi, S., and Henley, J. M. (1998). NSF binding to GluR2 regulates synaptic transmission. Neuron *21*, 87-97.

Noel, J., Ralph, G. S., Pickard, L., Williams, J., Molnar, E., Uney, J. B., Collingridge, G. L., and Henley, J. M. (1999). Surface expression of AMPA receptors in hippocampal neurons is regulated by an NSF-dependent mechanism. Neuron *23*, 365-376.

O'Brien, R., Xu, D., Mi, R., Tang, X., Hopf, C., and Worley, P. (2002). Synaptically targeted narp plays an essential role in the aggregation of AMPA receptors at excitatory synapses in cultured spinal neurons. J Neurosci *22*, 4487-4498.

O'Brien, R. J., Xu, D., Petralia, R. S., Steward, O., Huganir, R. L., and Worley, P. (1999). Synaptic clustering of AMPA receptors by the extracellular immediate-early gene product Narp. Neuron *23*, 309-323.

Oertle, T., and Schwab, M. E. (2003). Nogo and its paRTNers. Trends Cell Biol *13*, 187-194.

Okabe, S., Miwa, A., and Okado, H. (2001). Spine formation and correlated assembly of presynaptic and postsynaptic molecules. J Neurosci *21*, 6105-6114.

Osen-Sand, A., Catsicas, M., Staple, J. K., Jones, K. A., Ayala, G., Knowles, J., Grenningloh, G., and Catsicas, S. (1993). Inhibition of axonal growth by SNAP-25 antisense oligonucleotides in vitro and in vivo. Nature *364*, 445-448.

Osen-Sand, A., Staple, J. K., Naldi, E., Schiavo, G., Rossetto, O., Petitpierre, S., Malgaroli, A., Montecucco, C., and Catsicas, S. (1996). Common and distinct fusion proteins in axonal growth and transmitter release. J Comp Neurol *367*, 222-234.

Osten, P., Khatri, L., Perez, J. L., Kohr, G., Giese, G., Daly, C., Schulz, T. W., Wensky, A., Lee, L. M., and Ziff, E. B. (2000). Mutagenesis reveals a role for ABP/GRIP binding to GluR2 in synaptic surface accumulation of the AMPA receptor. Neuron *27*, 313-325.

Osten, P., Srivastava, S., Inman, G. J., Vilim, F. S., Khatri, L., Lee, L. M., States, B. A., Einheber, S., Milner, T. A., Hanson, P. I., and Ziff, E. B. (1998). The AMPA receptor GluR2 C terminus can mediate a reversible, ATP-dependent interaction with NSF and alpha- and beta-SNAPs. Neuron *21*, 99-110.

Ostroff, L. E., Fiala, J. C., Allwardt, B., and Harris, K. M. (2002). Polyribosomes redistribute from dendritic shafts into spines with enlarged synapses during LTP in developing rat hippocampal slices. Neuron *35*, 535-545.

Oyler, G. A., Polli, J. W., Wilson, M. C., and Billingsley, M. L. (1991). Developmental expression of the 25-kDa synaptosomal-associated protein (SNAP-25) in rat brain. Proc Natl Acad Sci U S A *88*, 5247-5251.

Palade, G. (1975). Intracellular aspects of the process of protein synthesis. Science *189*, 347-358.

Passafaro, M., Nakagawa, T., Sala, C., and Sheng, M. (2003). Induction of dendritic spines by an extracellular domain of AMPA receptor subunit GluR2. Nature *424*, 677-681.

Passafaro, M., Piech, V., and Sheng, M. (2001). Subunit-specific temporal and spatial patterns of AMPA receptor exocytosis in hippocampal neurons. Nat Neurosci *4*, 917-926.

Petralia, R. S., Esteban, J. A., Wang, Y. X., Partridge, J. G., Zhao, H. M., Wenthold, R. J., and Malinow, R. (1999). Selective acquisition of AMPA receptors over postnatal development suggests a molecular basis for silent synapses. Nat Neurosci *2*, 31-36.

Pfeffer, S. (2003). Membrane domains in the secretory and endocytic pathways. Cell *112*, 507-517.

Philpot, B. D., Sekhar, A. K., Shouval, H. Z., and Bear, M. F. (2001). Visual experience and deprivation bidirectionally modify the composition and function of NMDA receptors in visual cortex. Neuron *29*, 157-169.

Piccini, A., and Malinow, R. (2002). Critical postsynaptic density 95/disc large/zonula occludens-1 interactions by glutamate receptor 1 (GluR1) and GluR2 required at different subcellular sites. J Neurosci *22*, 5387-5392.

Pickard, L., Noel, J., Henley, J. M., Collingridge, G. L., and Molnar, E. (2000). Developmental changes in synaptic AMPA and NMDA receptor distribution and AMPA receptor subunit composition in living hippocampal neurons. J Neurosci *20*, 7922-7931.

Prasher, D. C., Eckenrode, V. K., Ward, W. W., Prendergast, F. G., and Cormier, M. J. (1992). Primary structure of the Aequorea victoria green-fluorescent protein. Gene *111*, 229-233.

Prekeris, R., Foletti, D. L., and Scheller, R. H. (1999a). Dynamics of tubulovesicular recycling endosomes in hippocampal neurons. J Neurosci *19*, 10324-10337.

Prekeris, R., Klumperman, J., Chen, Y. A., and Scheller, R. H. (1998). Syntaxin 13 mediates cycling of plasma membrane proteins via tubulovesicular recycling endosomes. J Cell Biol *143*, 957-971.

Prekeris, R., Yang, B., Oorschot, V., Klumperman, J., and Scheller, R. H. (1999b). Differential roles of syntaxin 7 and syntaxin 8 in endosomal trafficking. Mol Biol Cell *10*, 3891-3908.

Prinjha, R., Moore, S. E., Vinson, M., Blake, S., Morrow, R., Christie, G., Michalovich, D., Simmons, D. L., and Walsh, F. S. (2000). Inhibitor of neurite outgrowth in humans. Nature *403*, 383-384.

Rapoport, T. A., Jungnickel, B., and Kutay, U. (1996). Protein transport across the eukaryotic endoplasmic reticulum and bacterial inner membranes. Annu Rev Biochem *65*, 271-303.

Reyes, M., and Stanton, P. K. (1996). Induction of hippocampal long-term depression requires release of Ca2+ from separate presynaptic and postsynaptic intracellular stores. J Neurosci *16*, 5951-5960.

Richardson, D. R., and Ponka, P. (1997). The molecular mechanisms of the metabolism and transport of iron in normal and neoplastic cells. Biochim Biophys Acta *1331*, 1-40.

Roebroek, A. J., Ayoubi, T. A., Van de Velde, H. J., Schoenmakers, E. F., Pauli, I. G., and Van de Ven, W. J. (1996). Genomic organization of the human NSP gene, prototype of a novel gene family encoding reticulons. Genomics *32*, 191-199.

Roebroek, A. J., van de Velde, H. J., Van Bokhoven, A., Broers, J. L., Ramaekers, F. C., and Van de Ven, W. J. (1993). Cloning and expression of alternative transcripts of a novel neuroendocrine-specific gene and identification of its 135-kDa translational product. J Biol Chem *268*, 13439-13447.

Rothman, J. E. (1994). Mechanisms of intracellular protein transport. Nature *372*, 55-63.

Rumbaugh, G., Sia, G. M., Garner, C. C., and Huganir, R. L. (2003). Synapse-associated protein-97 isoform-specific regulation of surface AMPA receptors and synaptic function in cultured neurons. J Neurosci *23*, 4567-4576.

Sabatini, B. L., Maravall, M., and Svoboda, K. (2001). Ca(2+) signaling in dendritic spines. Curr Opin Neurobiol *11*, 349-356.

Saberan-Djoneidi, D., Marey-Semper, I., Picart, R., Studler, J. M., Tougard, C., Glowinski, J., and Levi-Strauss, M. (1995). A 19-kDa protein belonging to a new family is expressed in the Golgi apparatus of neural cells. J Biol Chem *270*, 1888-1893.

Saberan-Djoneidi, D., Picart, R., Escalier, D., Gelman, M., Barret, A., Tougard, C., Glowinski, J., and Levi-Strauss, M. (1998). A 21-kDa polypeptide belonging to a new family of proteins is expressed in the Golgi apparatus of neural and germ cells. J Biol Chem *273*, 3909-3914.

Salin, P. A., Malenka, R. C., and Nicoll, R. A. (1996). Cyclic AMP mediates a presynaptic form of LTP at cerebellar parallel fiber synapses. Neuron *16*, 797-803.

Salinas, P. C. (2003). Synaptogenesis: Wnt and TGF-beta take centre stage. Curr Biol *13*, R60-62.

Sans, N., Racca, C., Petralia, R. S., Wang, Y. X., McCallum, J., and Wenthold, R. J. (2001). Synapse-associated protein 97 selectively associates with a subset of AMPA receptors early in their biosynthetic pathway. J Neurosci *21*, 7506-7516.

Satoh, K., Takeuchi, M., Oda, Y., Deguchi-Tawarada, M., Sakamoto, Y., Matsubara, K., Nagasu, T., and Takai, Y. (2002). Identification of activity-regulated proteins in the postsynaptic density fraction. Genes Cells *7*, 187-197.

Scheiffele, P. (2003). Cell-cell signaling during synapse formation in the CNS. Annu Rev Neurosci *26*, 485-508.

Scheiffele, P., Fan, J., Choih, J., Fetter, R., and Serafini, T. (2000). Neuroligin expressed in nonneuronal cells triggers presynaptic development in contacting axons. Cell *101*, 657-669.

Scheller, R. H. (1995). Membrane trafficking in the presynaptic nerve terminal. Neuron *14*, 893-897.

Schnell, E., Sizemore, M., Karimzadegan, S., Chen, L., Bredt, D. S., and Nicoll, R. A. (2002). Direct interactions between PSD-95 and stargazin control synaptic AMPA receptor number. Proc Natl Acad Sci U S A *99*, 13902-13907.

Seidenman, K. J., Steinberg, J. P., Huganir, R., and Malinow, R. (2003). Glutamate receptor subunit 2 Serine 880 phosphorylation modulates synaptic transmission and mediates plasticity in CA1 pyramidal cells. J Neurosci *23*, 9220-9228.

Senden, N. H., Timmer, E. D., Boers, J. E., van de Velde, H. J., Roebroek, A. J., Van de Ven, W. J., Broers, J. L., and Ramaekers, F. C. (1996). Neuroendocrine-specific protein C (NSP-C): subcellular localization and differential expression in relation to NSP-A. Eur J Cell Biol *69*, 197-213.

Seroussi, E., Pan, H. Q., Kedra, D., Roe, B. A., and Dumanski, J. P. (1998). Characterization of the human NIPSNAP1 gene from 22q12: a member of a novel gene family. Gene *212*, 13-20.

Sheng, M., and Sala, C. (2001). PDZ domains and the organization of supramolecular complexes. Annu Rev Neurosci *24*, 1-29.

Shi, S., Hayashi, Y., Esteban, J. A., and Malinow, R. (2001). Subunit-specific rules governing AMPA receptor trafficking to synapses in hippocampal pyramidal neurons. Cell *105*, 331-343.

Shi, S. H., Hayashi, Y., Petralia, R. S., Zaman, S. H., Wenthold, R. J., Svoboda, K., and Malinow, R. (1999). Rapid spine delivery and redistribution of AMPA receptors after synaptic NMDA receptor activation. Science *284*, 1811-1816.

Shi, S. H., Jan, L. Y., and Jan, Y. N. (2003). Hippocampal neuronal polarity specified by spatially localized mPar3/mPar6 and PI 3-kinase activity. Cell *112*, 63-75.

Shimomura, O., Johnson, F. H., and Saiga, Y. (1962). Extraction, purification and properties of aequorin, a bioluminescent protein from the luminous hydromedusan, Aequorea. J Cell Comp Physiol *59*, 223-239.

Shirasu, M., Kimura, K., Kataoka, M., Takahashi, M., Okajima, S., Kawaguchi, S., Hirasawa, Y., Ide, C., and Mizoguchi, A. (2000). VAMP-2 promotes neurite elongation and SNAP-25A increases neurite sprouting in PC12 cells. Neurosci Res *37*, 265-275.

Simonsen, A., Lippe, R., Christoforidis, S., Gaullier, J. M., Brech, A., Callaghan, J., Toh, B. H., Murphy, C., Zerial, M., and Stenmark, H. (1998). EEA1 links PI(3)K function to Rab5 regulation of endosome fusion. Nature *394*, 494-498.

Song, I., Kamboj, S., Xia, J., Dong, H., Liao, D., and Huganir, R. L. (1998). Interaction of the N-ethylmaleimide-sensitive factor with AMPA receptors. Neuron *21*, 393-400.

Sonnichsen, B., De Renzis, S., Nielsen, E., Rietdorf, J., and Zerial, M. (2000). Distinct membrane domains on endosomes in the recycling pathway visualized by multicolor imaging of Rab4, Rab5, and Rab11. J Cell Biol *149*, 901-914.

Spiro, D. J., Boll, W., Kirchhausen, T., and Wessling-Resnick, M. (1996). Wortmannin alters the transferrin receptor endocytic pathway in vivo and in vitro. Mol Biol Cell *7*, 355-367.

Staudinger, J., Zhou, J., Burgess, R., Elledge, S. J., and Olson, E. N. (1995). PICK1: a perinuclear binding protein and substrate for protein kinase C isolated by the yeast two-hybrid system. J Cell Biol *128*, 263-271.

Steiner, P., Kulangara, K., Sarria, J. C., Glauser, L., Regazzi, R., and Hirling, H. (2004). Reticulon 1-C/neuroendocrine-specific protein-C interacts with SNARE proteins. J Neurochem *89*, 569-580.

Steiner, P., Sarria, J. C., Glauser, L., Magnin, S., Catsicas, S., and Hirling, H. (2002a). Modulation of receptor cycling by neuron-enriched endosomal protein of 21 kD. J Cell Biol *157*, 1197-1209.

Steiner, P., Sarria, J. C., Huni, B., Marsault, R., Catsicas, S., and Hirling, H. (2002b). Overexpression of neuronal Sec1 enhances axonal branching in hippocampal neurons. Neuroscience *113*, 893-905.

Stenmark, H., Parton, R. G., Steele-Mortimer, O., Lutcke, A., Gruenberg, J., and Zerial, M. (1994). Inhibition of rab5 GTPase activity stimulates membrane fusion in endocytosis. Embo J *13*, 1287-1296.

Stevens, C. F. (1998). A million dollar question: does LTP = memory? Neuron *20*, 1-2.

Stevens, C. F., and Sullivan, J. (1998). Synaptic plasticity. Curr Biol *8*, R151-153.

Sun, W., Yan, Q., Vida, T. A., and Bean, A. J. (2003). Hrs regulates early endosome fusion by inhibiting formation of an endosomal SNARE complex. J Cell Biol *162*, 125-137.

Sutcliffe, J. G., Milner, R. J., Shinnick, T. M., and Bloom, F. E. (1983). Identifying the protein products of brain-specific genes with antibodies to chemically synthesized peptides. Cell *33*, 671-682.

Sytnyk, V., Leshchyns'ka, I., Delling, M., Dityateva, G., Dityatev, A., and Schachner, M. (2002). Neural cell adhesion molecule promotes accumulation of TGN organelles at sites of neuron-to-neuron contacts. J Cell Biol *159*, 649-661.

Sytnyk, V., Leshchyns'ka, I., Dityatev, A., and Schachner, M. (2004). Trans-Golgi network delivery of synaptic proteins in synaptogenesis. J Cell Sci *117*, 381-388.

Tabb, J. S., Molyneaux, B. J., Cohen, D. L., Kuznetsov, S. A., and Langford, G. M. (1998). Transport of ER vesicles on actin filaments in neurons by myosin V. J Cell Sci *111 (Pt 21)*, 3221-3234.

Tagami, S., Eguchi, Y., Kinoshita, M., Takeda, M., and Tsujimoto, Y. (2000). A novel protein, RTN-XS, interacts with both Bcl-XL and Bcl-2 on endoplasmic reticulum and reduces their anti-apoptotic activity. Oncogene *19*, 5736-5746.

Tang, B. L., Tan, A. E., Lim, L. K., Lee, S. S., Low, D. Y., and Hong, W. (1998). Syntaxin 12, a member of the syntaxin family localized to the endosome. J Biol Chem *273*, 6944-6950.

Tashiro, A., Dunaevsky, A., Blazeski, R., Mason, C. A., and Yuste, R. (2003). Bidirectional regulation of hippocampal mossy fiber filopodial motility by kainate receptors: a two-step model of synaptogenesis. Neuron *38*, 773-784.

Tessier-Lavigne, M., and Goodman, C. S. (1996). The molecular biology of axon guidance. Science *274*, 1123-1133.

Toni, N., Buchs, P. A., Nikonenko, I., Bron, C. R., and Muller, D. (1999). LTP promotes formation of multiple spine synapses between a single axon terminal and a dendrite. Nature *402*, 421-425.

Tooze, J., and Hollinshead, M. (1991). Tubular early endosomal networks in AtT20 and other cells. J Cell Biol *115*, 635-653.

Torres, R., Firestein, B. L., Dong, H., Staudinger, J., Olson, E. N., Huganir, R. L., Bredt, D. S., Gale, N. W., and Yancopoulos, G. D. (1998). PDZ proteins bind, cluster, and synaptically colocalize with Eph receptors and their ephrin ligands. Neuron *21*, 1453-1463.

Trachtenberg, J. T., Chen, B. E., Knott, G. W., Feng, G., Sanes, J. R., Welker, E., and Svoboda, K. (2002). Long-term in vivo imaging of experience-dependent synaptic plasticity in adult cortex. Nature *420*, 788-794.

Trischler, M., Stoorvogel, W., and Ullrich, O. (1999). Biochemical analysis of distinct Rab5- and Rab11-positive endosomes along the transferrin pathway. J Cell Sci *112 (Pt 24)*, 4773-4783.

Trudeau, M. C., and Zagotta, W. N. (2002). An intersubunit interaction regulates trafficking of rod cyclic nucleotide-gated channels and is disrupted in an inherited form of blindness. Neuron *34*, 197-207.

Tsien, R. Y. (1998). The green fluorescent protein. Annu Rev Biochem *67*, 509-544.

Tsui, C. C., Copeland, N. G., Gilbert, D. J., Jenkins, N. A., Barnes, C., and Worley, P. F. (1996). Narp, a novel member of the pentraxin family, promotes neurite outgrowth and is dynamically regulated by neuronal activity. J Neurosci *16*, 2463-2478.

Tsurumi, C., Yoshihara, Y., Osaka, F., Yamada, F., Tani, I., Higuti, T., Shimizu, M., Oeda, K., Ohkawa, H., Toda, H., and et al. (1990). cDNA cloning and sequencing for the import

precursor of subunit B in H(+)-ATP synthase from rat mitochondria. Biochem Biophys Res Commun *169*, 136-142.

Ullrich, O., Reinsch, S., Urbe, S., Zerial, M., and Parton, R. G. (1996). Rab11 regulates recycling through the pericentriolar recycling endosome. J Cell Biol *135*, 913-924.

van de Velde, H. J., Roebroek, A. J., Senden, N. H., Ramaekers, F. C., and Van de Ven, W. J. (1994a). NSP-encoded reticulons, neuroendocrine proteins of a novel gene family associated with membranes of the endoplasmic reticulum. J Cell Sci *107 (Pt 9)*, 2403-2416.

van de Velde, H. J., Roebroek, A. J., van Leeuwen, F. W., and Van de Ven, W. J. (1994b). Molecular analysis of expression in rat brain of NSP-A, a novel neuroendocrine-specific protein of the endoplasmic reticulum. Brain Res Mol Brain Res *23*, 81-92.

van der Goot, F. G., and Gruenberg, J. (2002). Oiling the wheels of the endocytic pathway. Trends Cell Biol *12*, 296-299.

van der Sluijs, P., Hull, M., Webster, P., Male, P., Goud, B., and Mellman, I. (1992). The small GTP-binding protein rab4 controls an early sorting event on the endocytic pathway. Cell *70*, 729-740.

Vanhaesebroeck, B., Leevers, S. J., Ahmadi, K., Timms, J., Katso, R., Driscoll, P. C., Woscholski, R., Parker, P. J., and Waterfield, M. D. (2001). Synthesis and function of 3-phosphorylated inositol lipids. Annu Rev Biochem *70*, 535-602.

Verhage, M., Maia, A. S., Plomp, J. J., Brussaard, A. B., Heeroma, J. H., Vermeer, H., Toonen, R. F., Hammer, R. E., van den Berg, T. K., Missler, M., *et al.* (2000). Synaptic assembly of the brain in the absence of neurotransmitter secretion. Science *287*, 864-869.

Voronin, L. L., and Cherubini, E. (2003). "Presynaptic silence" may be golden. Neuropharmacology *45*, 439-449.

Wan, Q., Xiong, Z. G., Man, H. Y., Ackerley, C. A., Braunton, J., Lu, W. Y., Becker, L. E., MacDonald, J. F., and Wang, Y. T. (1997). Recruitment of functional GABA(A) receptors to postsynaptic domains by insulin. Nature *388*, 686-690.

Washbourne, P., Bennett, J. E., and McAllister, A. K. (2002). Rapid recruitment of NMDA receptor transport packets to nascent synapses. Nat Neurosci *5*, 751-759.

Wenthold, R. J., Petralia, R. S., Blahos, J., II, and Niedzielski, A. S. (1996). Evidence for multiple AMPA receptor complexes in hippocampal CA1/CA2 neurons. J Neurosci *16*, 1982-1989.

Wilcke, M., Johannes, L., Galli, T., Mayau, V., Goud, B., and Salamero, J. (2000). Rab11 regulates the compartmentalization of early endosomes required for efficient transport from early endosomes to the trans-golgi network. J Cell Biol *151*, 1207-1220.

Winckler, B., Forscher, P., and Mellman, I. (1999). A diffusion barrier maintains distribution of membrane proteins in polarized neurons. Nature *397*, 698-701.

Wong, S. H., Xu, Y., Zhang, T., and Hong, W. (1998). Syntaxin 7, a novel syntaxin member associated with the early endosomal compartment. J Biol Chem *273*, 375-380.

Wu, G., Malinow, R., and Cline, H. T. (1996). Maturation of a central glutamatergic synapse. Science *274*, 972-976.

Wyszynski, M., Kim, E., Dunah, A. W., Passafaro, M., Valtschanoff, J. G., Serra-Pages, C., Streuli, M., Weinberg, R. J., and Sheng, M. (2002). Interaction between GRIP and liprin-alpha/SYD2 is required for AMPA receptor targeting. Neuron *34*, 39-52.

Xia, J., Chung, H. J., Wihler, C., Huganir, R. L., and Linden, D. J. (2000). Cerebellar long-term depression requires PKC-regulated interactions between GluR2/3 and PDZ domain-containing proteins. Neuron *28*, 499-510.

Xia, J., Zhang, X., Staudinger, J., and Huganir, R. L. (1999). Clustering of AMPA receptors by the synaptic PDZ domain-containing protein PICK1. Neuron *22*, 179-187.

Yamazaki, M., Fukaya, M., Abe, M., Ikeno, K., Kakizaki, T., Watanabe, M., and Sakimura, K. (2001). Differential palmitoylation of two mouse glutamate receptor interacting protein 1 forms with different N-terminal sequences. Neurosci Lett *304*, 81-84.

Yersin, A., Hirling, H., Steiner, P., Magnin, S., Regazzi, R., Huni, B., Huguenot, P., De los Rios, P., Dietler, G., Catsicas, S., and Kasas, S. (2003). Interactions between synaptic vesicle fusion proteins explored by atomic force microscopy. Proc Natl Acad Sci U S A *100*, 8736-8741.

Yu, R. C., Jahn, R., and Brunger, A. T. (1999). NSF N-terminal domain crystal structure: models of NSF function. Mol Cell *4*, 97-107.

Zamanillo, D., Sprengel, R., Hvalby, O., Jensen, V., Burnashev, N., Rozov, A., Kaiser, K. M., Koster, H. J., Borchardt, T., Worley, P., *et al*. (1999). Importance of AMPA receptors for hippocampal synaptic plasticity but not for spatial learning. Science *284*, 1805-1811.

Zerial, M., and McBride, H. (2001). Rab proteins as membrane organizers. Nat Rev Mol Cell Biol *2*, 107-117.

Zhai, R. G., Vardinon-Friedman, H., Cases-Langhoff, C., Becker, B., Gundelfinger, E. D., Ziv, N. E., and Garner, C. C. (2001). Assembling the presynaptic active zone: a characterization of an active one precursor vesicle. Neuron *29*, 131-143.

Zhang, H., Webb, D. J., Asmussen, H., and Horwitz, A. F. (2003). Synapse formation is regulated by the signaling adaptor GIT1. J Cell Biol *161*, 131-142.

Zhang, L. I., Tao, H. W., and Poo, M. (2000). Visual input induces long-term potentiation of developing retinotectal synapses. Nat Neurosci *3*, 708-715.

Zhu, J. J., Esteban, J. A., Hayashi, Y., and Malinow, R. (2000). Postnatal synaptic potentiation: delivery of GluR4-containing AMPA receptors by spontaneous activity. Nat Neurosci *3*, 1098-1106.

Ziv, N. E., and Smith, S. J. (1996). Evidence for a role of dendritic filopodia in synaptogenesis and spine formation. Neuron *17*, 91-102.

Curriculum Vitae

Pascal Steiner

Address : Swiss Federal Institute of Technology (EPFL)
School of Life Sciences
The Laboratory of Cellular Neurobiology
CH-1015 Lausanne
Switzerland
Phone : + 41 21 693 95 24
E-mail : pascal.steiner@epfl.ch

Personal information :

30 years old
Swiss nationality
single

Objective

After completing my PhD in neuroscience inthe fall of 2004, I would like to apply my scientific backround and enlarge my knowledge and technical skills by doing a postdoctoral research stay in a neurobiology laboratory working on synaptic plasticity.

Education and Scientific Formation

PhD student

Since 01/ 2002: Institute of Neurosciences (Laboratories of Prof. S. Catsicas and Dr H. Hirling), Swiss Federal Institute of Technology of Lausanne (EPFL)

1999-2001 : Institute of Cellular Biology and Morphology (IBCM), (Group of Prof. S. Catsicas and Dr H. Hirling), University of Lausanne

University degrees (obtained at the University of Lausanne)

12/1998 Diploma in Neurosciences. Supervisor : S. Catsicas, IBCM
Specialization in molecular and cellular neurobiology

06/1997 Licence in Biology :
Certificate of Neurosciences and Endocrinology (06/1997)
Certificate of Human Physiology (03/1997)
Certificate of Molecular Biology (10/1996)
2nd Propaedeutics in Biology (06/1995)
1st Propaedeutics in Biology (10/1994)

Training course

03-07/2002 Certificate of Technology, Innovation and Leadership (TIL). Prof. William W. George (Medtronic).

Publications

- Debaigt, C., Hirling, H., Steiner, P., Vincent, J.-P., and Mazella, J. Crucial role of neuron-enriched endosomal protein of 21 kD in sorting between degradation and recycling of internalized G-protein coupled receptors. *J. Biol. Chem. In Press.*
- Steiner, P., Kulangara, K, Glauser, L., and Hirling, H. Reticulon 1-C/Neuroendocrine-Specific Protein-C interacts with SNARE proteins. (2004). *J. Neurochem.*, 89, 569-80.
- Meijering, E., Jacob, M., Sarria, J.-C., F., Steiner, P., Hirling, H., and Unser, M. Design and validation of a tool for neurite tracing and analysis in fluorescence microscopy images. (2004). *Cytometry,* 58A, 167-76.

- Uldry, M., Steiner, P., Zürich-Graf, M.-G., Béguin, P., Hirling, H., Honneger, P., Dolci, W., and Thorens B. (2004). Regulated exocytosis of a H^+/*myo*-inositol symporter at synapses and growth cones. *EMBO J.*, 23, 531-40
- Yersin, A., Kasas, S., Hilring, H., Steiner, P., and Catsicas, S. (2003) Linking functional genomics and screening for new drugs. *Laborwelt*. 4, 26-27.
- Yersin, A., Hirling, H., Steiner, P., Hugenot, P., Huni, B., Magnin, S., Wang, X., Dietler G., Catsicas, S., and Kasas, S. (2003) Interactions between synaptic vesicle fusion protein explored by atomic force microscopy. *Proc. Natl. Acd. Sci.*, 100, 8736-41.
- Voutsinos-Porche, B., Bonvento, G., Tanaka, K., Steiner, P., Welker, E., Chatton, J.-Y., Magistretti, P.J. and Pellerin, L. (2003) Glial glutamate transporters mediate a functional metabolic crosstalk between neurons and astrocytes in the mouse developing cortex. *Neuron,* 37, 275-286.
- Yersin,A., Hirling, H, Steiner, P, Dietler, G., Catsicas, S., and Kasas, S. (2002). Multilayer Protein Film Deposition on AFM Tip. *Single Mol.*, 162, 2-3.
- Steiner, P., Sarria, J.-C., F., Glauser, L., Magnin, S., Catsicas, S., and Hirling, H. (2002a). Modulation of receptor cycling by neuron-enriched endosomal protein of 21 kDa. *J. Cell Biol.*, 157, 1197-209.
- Steiner, P., Huni, B., Marsault, R., Catsicas, S., and Hirling, H. (2002b). Overexpression of neuronal Sec1 enhances axonal branching in hippocampal neurons. *Neuroscience*, 113, 893-905.
- Hirling, H., Steiner, P., Chaperon, C., Marsault, R., Regazzi, R., and Catsicas, S. (2000). Syntaxin 13 is a developmentally regulated SNARE involved in neurite outgrowth and endosomal trafficking. *Eur. J. Neurosci.*, 12, 1913-1923.

Conferences

- P. Steiner, J.-C. F. Sarria, L. Glauser, S. Catsicas and H. HirlingNeuron-Enriched Endosomal Protein of 21 kDa (NEEP21) interacts with syntaxin 13 and modulates cycling of membrane receptors (poster presentation). *Annual Meeting of the Society for Neuroscience, Orlando, Nov. 2nd-7th, 2002*
- P. Steiner, J.-C. Sarria, L. Glauser, S. Magnin, S. Catsicas, and H. Hirling. Neuron-Specific Early Endosomal Protein of 21 kDa (NEEP21) interacts with syntaxin 13 and regulates cycling of membrane receptors (poster presentation*). The Federation of European Neuroscience Societies, FENS meeting, Paris, July 13th-17th, 2002*
- C., Quairiaux, P. Steiner, G., Knott, H., Hirling, S., Catsicas, and E., Welker. Glutamate transporters GLT1 and GLAST expression is modulated by neuronal activity in adult mouse somatosensory system (poster presentation). *The Federation of European Neuroscience Societies, FENS meeting, Paris, July 13th-17th, 2002.*
- P. Steiner, J.-C. Sarria, L. Glauser, S. Magnin, S. Catsicas, and H. Hirling. Neuron-enriched endosomal protein of 21 kDa (NEEP21) interacts with syntaxin 13 and regulates cycling of membrane receptors (poster presentation). *European Life Scientist Organization, ELSO meeting, Nice, June 29th-July 4th, 2002.*
- H. Hirling, P. Steiner, J.-C. Sarria, J.-P. Hornung, R. Regazzi, and S. Catsicas. Syntaxin 13 is developmentally regulated and enhances neurite outgrowth in PC12 cells (poster presentation). *Annual Meeting of the Society for Neuroscience, New Orleans, Nov. 4th-9th, 2000.*

Languages

French : mother tongue **English** : good knowledge **German** : basic

Computer Skills

Internet communication tools
Office 2000 (Word, Excel, Power Point)
Adobe Photoshop (image processing)
Metamorph (image analysis and acquisition)

NIH Image (image and blot quantification)

Personal Interests

Hobbies : sports (swimming, ski, biking, sailing), art exhibition & literature
Community involvement: participation in summer camps for children with physical and mental disabilities.

References

Prof. Stefan Catsicas, vice-president, Swiss Federal Institute of Technology, 1015 Lausanne, phone +41 21 693 70 11, VPR@epfl.ch

Dr Harald Hirling, group leader, Institute of Neurosciences, Swiss Federal Institute of Technology, 1015 Lausanne, phone +41 21 693 53 63, harald.hirling@epfl.ch

Prof. Egbert Welker, director, Institut de Biologie Cellulaire et Morphologie (IBCM), University of Lausanne, phone + 41 21 692 51 25, egbert.welker@ibcm.unil.ch

Technical Skills

- **Molecular Biology**
  PCR, primer design, plasmid constructs.
- **Biochemistry**
  antibody purification, immunopurification, immunoprecipitation, GST-binding essay, ELISA, Western blotting.
- **Cell biology**
  Culture of cell lines, preparation of dissociated primary neuron cultures, different transfection methods of cell lines and primary neurons, immunocytochemistry, imaging-based receptor cycling assays.
- **Microscopy**
  Confocal microscopy, video microscopy on living neurons using GFP technology, atomic force microscopy
- **Data analysis**
  Image processing, fluorescence quantification.
- **Teaching**
  Human histology to medical students.

Research Activities for Diploma Work and Doctoral Thesis

I gained my first research experience as a diploma student in the laboratories of Prof. Stefan Catsicas, and Dr Harald Hirling, University of Lausanne, Switzerland. During my diploma work I analyzed nSec1/Munc18a during axonal growth. NSec1 is a syntaxin 1-binding protein, proposed to regulate SNARE complex formation in neurotransmitter release. I found that overexpression of nSec1/Munc18a, but not of the ubiquitous isoform Munc18b, enhances axonal sprouting by increasing the number of axonal branch points. In addition, I demonstrated by immunocytochemistry and living imaging techniques that nSec1 accumulates in the growth cones of cellular processes (Steiner et al., 2002b).

For my PhD thesis I continue to work in the same laboratories which moved to the EPFL in the beginning of 2002. My PhD project consists in identifying new protein interactions during brain development. Using immunoaffinity purification, I identified a previously cloned protein of unknown function in a complex

with the endosomal SNARE protein syntaxin 13. We characterized and named it Neuron-Enriched Endosomal Protein of 21 kDa (NEEP21). Our work revealed that NEEP21 is expressed by neurons and it is detected on early endosomes exclusively in the somatodentritic compartment. Furthermore, it is essential for correct recycling of internalized surface receptor. Reinsertion of AMPA-receptors was perturbed in the absence of NEEP21 (Steiner et al., 2002a). In addition, we recently identified the molecular mechanism which links NEEP21 to AMPA-receptors trafficking (manuscript in preparation). We found that NEEP21 forms a complex with GRIP (Glutamate Receptor Interacting Protein) and AMPA-receptors. Expression of the NEEP21 binding site for GRIP has drastic effects on AMPA-receptors cycling. Moreover, the morphology of dendrites is dramatically altered. Based on the recent findings of the importance of AMPA-receptor trafficking between internal stores and the cell membrane during synaptic structural and functional plasticity, we hypothesize that NEEP21 could modulate synaptic strength.